Investigation of the roles of the actin cytoskeleton remodelling proteins coronin and CAP1 in platelet function

David R J Riley

PhD in Medical Sciences

The University of Hull and the University of York

Hull York Medical School

June 2020

Abstract

Platelets undergo profound rapid F-actin cytoskeleton remodeling and experience morphological and functional changes in response to receptor-mediated signaling from damaged blood vessel walls. The evolutionarily conserved proteins coronin 1 and adenylyl cyclase-associated protein 1 (CAP1) regulate the F-actin cytoskeleton and participate in signaling events. They are abundant in platelets but until recently their roles were poorly understood. Subcellular fractionation found coronin 1 is mainly cytosolic, but a significant amount associates with membranes in an actin-independent manner and does not translocate to or from the membrane upon platelet stimulation or inhibition. Coronin 1, 2 and 3 associate with the Triton insoluble cytoskeleton upon platelet stimulation. Immunostainings of spread platelets revealed that coronin 1, 2 and 3 demonstrate strong accumulation at F-actin nodules and display diffuse cytoplasmic localisation with discontinuous accumulation at the cell cortex. This is consistent with the role of coronins as integrators of extracellular signals with actin remodeling. Ablation of coronin 1 in platelets is associated with impaired translocation of integrin β2 to the cell surface upon stimulation with thrombin. However, morphological and functional defects are absent including Arp2/3 complex translocation, VASP phosphorylation, spreading ability, secretion, basal receptor levels, αIIbβ3 activation and haemostasis. While integrin β2 translocation appears specifically or predominantly dependent on coronin 1, the lack of other phenotypes suggests a high extent of functional overlap and redundancy among coronins 1, 2 and 3 in platelets. Subcellular fractionation found that ~20% of CAP1 is membrane-associated in an F-actin independent manner. Immunostainings demonstrated that in basal platelets CAP1 is mostly cortical whereas stimulation results in translocation to the cytosol in a significant proportion of platelets which can be inhibited by prostacyclin or nitric oxide. This places CAP1 at a crossroad of signalling pathways that controls platelet activation by contributing to actin remodelling at the cell cortex and actin nodules during platelet spreading.

List of contents

List of Figures

11

List of Tables

Abbreviations

AC	Adenylyl cyclase / adenylate cyclase
ACD	Acid citrate dextrose
ADF	Actin depolymerising factor
ADP	Adenosine diphosphate
ANO6	Anoctamin-6
APC	Allophycocyanin
APS	Ammonium persulphate
ARHGEF	Rac/CDC42 guanine nucleotide exchange factor
Arp	Actin-related proteins
ATP	Adenosine triphosphate
bFGF	Basic fibroblast growth factor
BSA	Bovine serum albumin
CAD	Chronic arterial disease
cAK	cAMP-dependent kinase
CalDAG-GEFI	Calcium and diacylglyc- erol-regulated guanine nucleotide exchange factor I
cAMP	Cyclic adenosine monophosphate
CAP	Cyclase-associated protein
CARMIL	Capping protein ARP2/3 and myosin I linker
CARP	Cyclase-associated protein and retinitis pigmentosa 2
CK2	Casein kinase II
CD	Cluster of differentiation
CD2AP	CD2-associated protein
CD40L	CD40 ligand
CDC	Cell division control protein

CDK	Cell division protein kinase
cGK	cGMP-dependent kinase
cGMP	Cyclic guanosine monophosphate
CRIB	Cell division control protein 42 (CDC42) and Rac-interactive binding
CRISPR	Clustered regularly interspaced short palindromic repeats
CRP-XL	Collagen related peptide – cross linked
COX	Cyclooxygenase
DAG	Diacylglycerol
Dock	Dedicator of cytokinesis
DTS	Dense tubular system
DTT	Dithiothreitol
EDTA	Ethylenediaminetetraacetic acid
EGTA	Ethylene glycol-bis(β-aminoethyl ether)-N,N,N′,N′-tetraacetic acid
ENA/VASP	Enabled/vasodilator-stimulated phosphoprotein
Epac	Exchange proteins directly activated by cAMP
Eps8	Epidermal growth factor receptor pathway substrate 8
FACS	Fluorescence activated cell sorting
FcR	Fc receptor
FITC	Fluorescein isothiocyanate
FSC	Forward scatter
GAP	GTPase-activating protein
Gαs	Gs alpha subunit
GAPDH	Glyceraldehyde 3-phosphate dehydrogenase

CCL19	Chemokine (C-C motif) ligand 19
GDI	Guanine nucleotide dissociation inhibitor
GEF	Guanine nucleotide exchange factor
GSK3	Glycogen synthase kinase 3
GSNO	S-Nitrosoglutathione
GP	Glycoprotein
GTP	Guanosine triphosphate
HDL	High-density lipoprotein
HEK	Human embryonic kidney
HRP	Horse radish peroxidase
Hs	Homo sapiens
HS	High speed
ICAM1	Intercellular adhesion molecule 1
IF	Immunofluorescence
IP	Immunoprecipitation
IP3	Inositol 1,4,5-trisphosphate
ITAM	Immunoreceptor tyrosine–based activation motif
KO	Knock out
LARG	Leukemia-associated Rho guanine-nucleotide exchange factor
LDL	Low-density lipoprotein
LFA-1	Lymphocyte functions associated antigen-1
LIMK	LIM-kinase
LS	Low speed
MLC	Myosin light chain
MLCK	Myosin light chain kinases
Mm	*Mus musculus* (mouse)

MMP	Metalloproteinase
MTB	Modified Tyrode's buffer
NMII	Non-muscle myosin II
OPHN1	Oligophrenin1
PBG	Phosphate buffer saline fish gelatin
PBS	Phosphate buffered saline
PDK1	3-phosphoinositide-dependent protein kinase 1
PE	Phycoerythrin
PF4	Platelet-factor 4
PFA	Paraformaldehyde
PGE_2	Prostaglandin E_2
PGI_2	Prostacyclin (Prostaglandin I_2)
PGH_2	Prostaglandin H_2
PIP_2	Phosphatidylinositol 4,5-bisphosphate
PKA	Protein kinase A
PKC	Protein kinase C
PKG	Protein kinase G
PNC	Platelet-neutrophil complexes
PLCγ2	Phospholipase Cγ2
PMSF	Phenylmethylsulfonyl fluoride
PPP	Platelet poor plasma
PRex1	Phosphatidylinositol-3,4,5-trisphosphate dependent Rac exchange factor 1
PROTAC	Proteolysis-targeting chimera
PRP	Platelet rich plasma
PSGL-1	P-selectin glycoprotein ligand-1
PtdSer	Phosphatidylserine
PVDF	Polyvinylidene difluoride

Rap1B	Ras related protein 1B
Rb	Rabbit
RCC2	Regulator of chromosome condensation 2
RhoA	Ras homolog gene family, member A
RPM	Revolutions per minute
SCID	Severe combined immunodeficiency
SDS	Sodium dodecyl sulphate
SD	Standard deviation
SDS-PAGE	Sodium dodecyl sulphate polyacrylamide gel electrophoresis
SEM	Standard error of the mean
SFK	Src family tyrosine kinase
SGR	Small G protein regulator
SLP-76	Src-homology leucocyte protein 76
SNAP	Soluble N-ethylmaleimide-sensitive factor attachment proteins
SNARE	Soluble N-ethylmaleimide-sensitive factor attachment proteins receptors
SPR	Surface plasmon resonance
SH3	Src homology 3
SSC	Side scatter
TBS-T	Tris buffered saline Tween
TEMED	Tetramethylethylenediamine
TIMP 1	Tissue inhibitor of metalloproteinase
TRITC	Tetramethylrhodamine isothiocyanate
VEGF	Vascular endothelial growth factor
WAS	Wiskott–Aldrich syndrome
WASP	Wiskott–Aldrich Syndrome protein
WB	Western blot

WBC	White blood cells
WH2	Wiscott Aldrich syndrome protein homology 2
WT	Wild type

Acknowledgements

Author's declaration

I confirm that this work is original and that if any passage(s) or diagram(s) have been copied from academic papers, books, the internet or any other sources these are clearly identified by the use of quotation marks and the reference(s) is fully cited. I certify that, other than where indicated, this is my own work and does not breach the regulations of HYMS, the University of Hull or the University of York regarding plagiarism or academic conduct in examinations. I have read the HYMS Code of Practice on Academic Misconduct, and state that this piece of work is my own and does not contain any unacknowledged work from any other source.

Published contributions from this thesis

Riley, D.R., Khalil, J.S., Naseem, K.M. and Rivero, F. (2020). Biochemical and immunocytochemical characterization of coronins in platelets. *Platelets*, **31**. 913-924.

Riley, D. R. J., Khalil, J. S., Pieters, J., Naseem, K. M. & Rivero, F. (2020). Coronin 1 is required for integrin β2 translocation in platelets. *International Journal of Molecular Sciences*. **21**. 356.

Joshi, P., Riley, D.R.J., Khalil, J.S., Xiong, H., Ji, W. & Rivero, F. (2018). The membrane-associated fraction of cyclase associate protein 1 translocates to the cytosol upon platelet stimulation. *Scientific. Reports*. **8**. 10804.

Other publication

Berger, M., Riley, D. R. J., Lutz, J., Khalil, J . S., Aburima, A., Naseem, K. M. & RIvero, F. (2019). Alterations in platel*et al*pha-granule secretion and adhesion on collagen under flow in mice lacking the atypical Rho GTPase RhoBTB3. *Cells*. **8**. 149.

1 Introduction

1.1 Platelets

Humans have nearly a trillion platelets in circulation which have a lifespan of around 6-10 days. They are anucleate discoid cells, around 2-3 µm in diameter, derived from megakaryocytes that regulate haemostasis upon vessel damage (Thon & Italiano, 2012). Platelet activation results in the secretion of alpha and dense granules and changes platelets into a flat and spread shape, resulting in a larger surface area. This process allows platelets to adhere to damaged blood vessel walls, transitioning from a spheroid to a flat shape by extending filopodia and lamellipodia (Poulter *et al.*, 2015). This is a very complex process involving many signalling pathways and proteins. During this process the platelet actin cytoskeleton is remodelled (Aslan *et al.*, 2012). Many factors are important for actin remodelling including CAP1 (Joshi *et al.*, 2018) and Coronin 1 (Gandhi & Goode, 2008) which were the focus of this thesis. Platelets also have roles in immunity, infection, inflammation (Klinger & Jelkmann, 2002), tissue regeneration (Nurden, 2011) and cancer (Nash *et al.*, 2002).

1.1.1 Platelet formation

Platelets are produced from mature megakaryocytes which are predominantly present in bone marrow by a process called thrombopoiesis (Thon & Italiano, 2012). Megakaryotes are produced from differentiated hematopoietic stem cells. They are multinucleate and as they mature they undergo repeated rounds of endomitosis (Bluteau *et al.*, 2009). Maturing megakaryocytes migrate from the osteoblastic niche towards the vascular niche of the bone marrow which is proximal to blood vessels (Thon & Italiano, 2012). Once mature, megakaryocytes extend long slender microtubular structures called proplatelets which have the appearance of beads linked by narrow cytoplasmic strands (Italiano *et al.*, 1999). The mature megakaryocyte contains an extensive internal labyrinth of membrane which is

22

continuous with the plasma membrane and is termed the invaginated membrane system or the demarcation membrane system which provides membranes for the proplatelets to form (Ghalloussi *et al.*, 2019). The proplatelets elongate, thin and bifurcate to form pseudopodia ribbons before becoming dissociated from the megakaryocyte. Dissociated proplatelets can resemble barbell structures and retain their ability to form platelets, doing so at both ends (Italiano *et al.*, 2007).

1.1.2 Platelet organelles

Platelet organelles include α-granules, dense granules (Flaumenhaft & Sharda, 2019), lysosomes (Ciferri *et al.*, 2000), mitochondria (Verhoeven *et al.*, 1984), ribosomes (Zimmerman & Weyrich, 2008), a dense tubular system (DTS) (Harper & Sage, 2017), an open canalicular system (Escolar & White, J., 1991) and residual Golgi (Yadav *et al.*, 2017) (**Figure 1.1**).

The α-granules are far more numerous than dense granules, lysosomes or mitochondria and comprise around 10% of the total platelet volume (Flaumenhaft & Sharda, 2019). They contain over 300 proteins which are both membrane-bound and soluble proteins including integrins αIIb and β3 as well as glycoprotein (GP) VI, von Willebrand factor (vWF), P-selectin and thrombospondin which are secreted or exposed upon platelet activation to contribute towards the activation cascade and platelet aggregation (Burkhart *et al.*, 2014).

The contents of dense granules include cations including very high levels of Ca^{2+}, lower levels of Mg^{2+} (Ruiz *et al.*, 2004) and high concentrations of nucleotides such as ~650 mM ADP and ~440 mM ATP. Their pH is maintained at around 5.4 by a H^+-ATPase (proton pump). Upon platelet activation, the dense granule contents are released, which again contribute towards the platelet activation cascade and aggregation (Flaumenhaft & Sharda, 2019).

The contents of lysosomes are very similar to other cell types and include enzymes involved in degradation including collagenases, glycohydrolases and phosphatases. The main role of the platelet lysosomes is to degrade proteins

23

(Coughlin, 2000). They are also released upon platelet activation (Ciferri *et al.*, 2000), possibly contributing to thrombus remodeling (Falet, 2017).

Platelets have only a few mitochondria which contribute to energy metabolism (Verhoeven *et al.*, 1984). Platelets retain mRNA transcripts from megakaryocytes (Rowley *et al.*, 2011) and have ribosomes which have a limited ability to contribute to protein synthesis which can rapidly increase in response to activation (Zimmerman & Weyrich, 2008). Platelets also contain fragments of the Golgi apparatus, scattered around the platelet which may contribute towards protein synthesis (Yadav *et al.*, 2017).

The platelet DTS contains a high concentration of Ca^{2+} which is maintained by sarco/endoplasmic reticulum Ca^{2+}-ATPase 2b (Harper & Sage, 2017) of which platelets contain an estimated 9,000 copies per cell. Sarco/endoplasmic reticulum Ca^{2+}-ATPase 3 is more abundant at over 16,000 copies per cell (Burkhart, *et al.*, 2012) and it pumps Ca^{2+} into the alpha granules and lysosomes, as does V-type H+-ATPase. Upon platelet activation, IP_3 binds to the IP_3 receptor enabling the release of Ca^{2+} from the DTS stores. The DTS also contains the transmembrane protein stromal interaction molecule 1 (STIM1) which binds calcium. When the DTS Ca^{2+} stores are depleted, it translocates to the platelet membrane and associates with Orai1 to contribute to calcium influx (Harper & Sage, 2017).

The platelet membrane, like in many cells, is a phospholipid bilayer embedded with cholesterol, glycolipids and glycoproteins. The membrane contains a tunneling network of tiny channels called the canalicular system which is a semi-selective and runs through the platelet which allows the passage of small molecules. It serves as a conduit for the passage of substances into the platelet and for the secretion of α-granules (**Figure 1.1**) (Escolar & White, 1991).
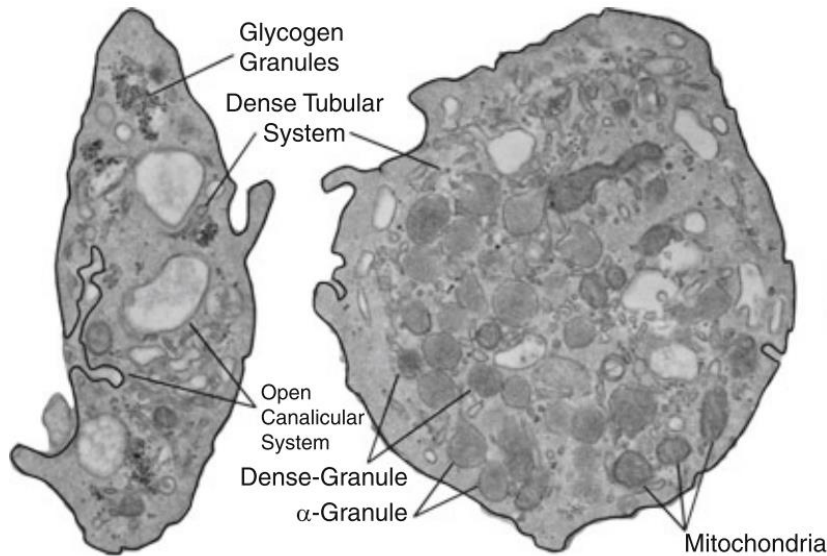
Figure 1.1 – Platelet organelles
A transmission electron micrograph (TEM) of a cross section of a platelet displaying the DTS, dense granules, α-granules, OCS, mitochondria and ribosomes. The Golgi apparatus fragments are not visible. Adapted from (Hartwig *et al.*, 1999; Thon & Italiano, 2012)

1.1.3 Platelet function

The primary function of platelets is to stop haemorrhage caused by vascular injury (Broos et al., 2011) Other functions of platelets include contributions to immunity, inflammation (Smyth *et al.*, 2009), vascular remodeling and cancer (Menter *et al.*, 2014).

1.1.3.1 Haemostasis

Haemostasis is the first function in which platelets were identified to participate. In a healthy uninjured individual, platelets would not normally adhere to the vasculature. However, upon vascular injury platelets respond by adhering to the subendothelial extracellular matrix, resulting in tethering to, rolling over, and eventually adherence to damaged vascular tissue. The platelet undergoes shape change which includes the formation of lamellipodia and filopodia (**Figure 1.2**). This forms a haemostatic clot, comprised of platelets, red blood cells and fibrin which ceases blood loss (**Figure 1.3**). The plug can also contain white blood cells (WBC)s can also be present in a platelet plug (not shown). Platelet adhesion is followed by tyrosine kinase and G-protein coupled receptor mediated signaling cascades, resulting in platelet activation and granule release, which triggers additional platelet recruitment

and activation. These platelets will produce a fibrin-rich haemostatic plug to stop haemorrhage and will also trigger endothelial cells to produce signaling molecules to limit thrombus formation (Broos *et al.*, 2011).

Figure 1.2 – Platelet spreading
Scanning electron micrographs showing the spreading stages of platelets. A resting platelet is shown on the left. Upon activation, platelets adhere to a surface and form filopodia. These then spread out and merge to form lamellipodia. Finally, a platelet is fully spread when the lamellipodia merge (White, 2013)
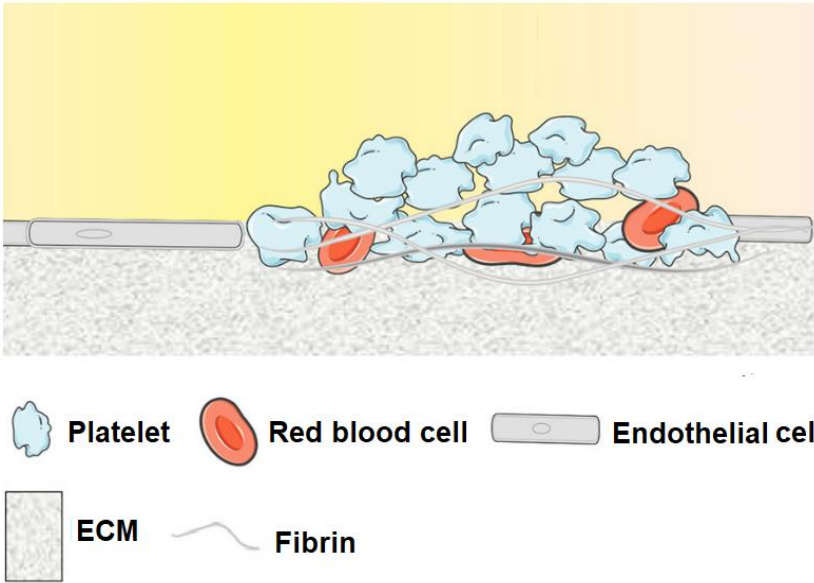
Figure 1.3 – Platelet plug
A platelet plug forms over damaged tissue which is comprised of red blood cells, platelets, and fibrin.

1.1.3.2 Platelets contribute to immunity, inflammation and wound healing

Platelets and WBCs have an ability to interact and bind together to form platelet-neutrophil complexes (PNC)s. Healthy individuals have ~25% of circulating neutrophils attached to platelets as PNCs (Page & Pitchford, 2013). The ability of platelets to form the complex leads to platelets contributing to immunological events including the response to microbial threats, WBC recruitment to sites of injury and the enhancement of immune responses (Smyth *et al.*, 2009). The formation of PNCs is required for their recruitment to inflamed tissue. Platelets 'prime' neutrophils for efficient adhesion to vascular tissue through up-regulation of integrins and enhanced responsiveness to chemokines. An increased number of PNCs is also associated with cardiovascular diseases such as atherosclerosis, unstable angina, and where the complexes may contribute the disease progression through thrombotic and inflammatory processes (Page & Pitchford, 2013).

The exposure of P-selectin on platelets is responsible for the interaction with leukocytes. The binding of P-selectin on platelets to P-selectin glycoprotein ligand (PSGL)-1 (CD162) on leukocytes leads to intracellular signals that contribute to integrin activation and platelet-neutrophil adhesion (McEver, 2002). In leukocytes, the cytoplasmic domain of PSGL-1 forms a constitutive complex with Nef-associated factor 1. Upon P-selectin binding, Src family tyrosine kinases (SFKs) phosphorylate Nef-associated factor 1 which recruits the phosphoinositide-3-OH kinase p85-p110δ heterodimer and results in activation of leukocyte integrins. Inhibition of this pathway has been found to diminish adhesion of leukocytes to capillary venules (Lam *et al.*, 2015). Platelets also express PSGL-1, albeit at levels 25-100 times lower than that of leukocytes (Frenette *et al.*, 2000), which binds to L-selectin on leukocytes (Bruehl *et al.*, 1996) to contribute to adhesion in the complexes (**Figure 1.4**).

Upon initial platelet-leukocyte tethering through selectin, the leukocyte will become activated. Leukocyte activation strengthens integrin bonds resulting in strong adhesion (Smyth *et al.*, 2009). Leukocytes express integrin α_M (CD11b) and integrin β2 (CD18) which form a complex (αMβ2) called macrophage-1 antigen

(Mac-1) receptor. This is the most abundant intgerin β2 complex (Wang *et al.*, 2017). and increases in expression upon selectin-binding-mediated leukocyte activation (Pitchford *et al.*, 2005). It contributes to platelet-leukocyte interactions by binding primarily to intercellular adhesion molecule 2 (ICAM-2), on platelets (Wang *et al.*, 2017). Although Mac-1 is a promiscuous receptor and also facilitates binding of WBCs to ICAM-1, iC3b and CD40 ligand (CD40L) (CD154) on other white blood cells (Simon, 2011) and also to GPIbα (Wang *et al.*, 2017) and CD40L on platelets (Henn *et al.*, 1998) (**Figure 1.4**). αMβ2 is required for the recruitment of neutrophils to adherent platelets and for the development of intimal hyperplasia (Smyth *et al.*, 2009). Leukocytes also contain Pyk2 which contributes to adhesion and sustains β2 activation. Pyk2 is phosphorylated upon adhesion to platelets and its inhibition is associated with a decrease in PNCs (Evangelista *et al.*, 2007). *Mac-1*$^{-/-}$ mice demonstrate delayed thrombosis after carotid artery and cremaster microvascular injury which is associated with a reduction in the accumulation of platelets at the site of injury (Wang *et al.*, 2017).

Integrin β2 can also interact with integrin α_L to form lymphocyte function associated antigen-1 (α_Lβ2) (LFA-1) on neutrophils (McCaffery & Berridge, 1986). ICAM-2 is expressed on platelets in an activation-independent manner and binds to LFA-1 (Diacovo *et al.*, 1994). Platelets also express integrin β2 and (Piguet *et al.*, 2001) LFA-1 (McCaffery & Berridge, 1986). LFA-1 is quite promiscuous in nature and has been reported to bind to ICAM-1, ICAM2 which are both present on WBC (de Fougerolles *et al.*, 1991) (**Figure 1.4**).

The binding of platelets to neutrophils 'primes' the neutrophils. Platelets then bind to exposed collagen and extracellular matrix proteins (e.g. laminin, fibronectin, vitronectin) in damaged vasculature and this contributes to the recruitment of neutrophils to damaged vasculature. Platelets bind to endothelial cells using several of the same proteins to which they bind to neutrophils including P-selectin and ICAM-1. Platelet activation (see **section 1.1.4.2**) recruits additional platelets to a site of injury (Page & Pitchford, 2013).
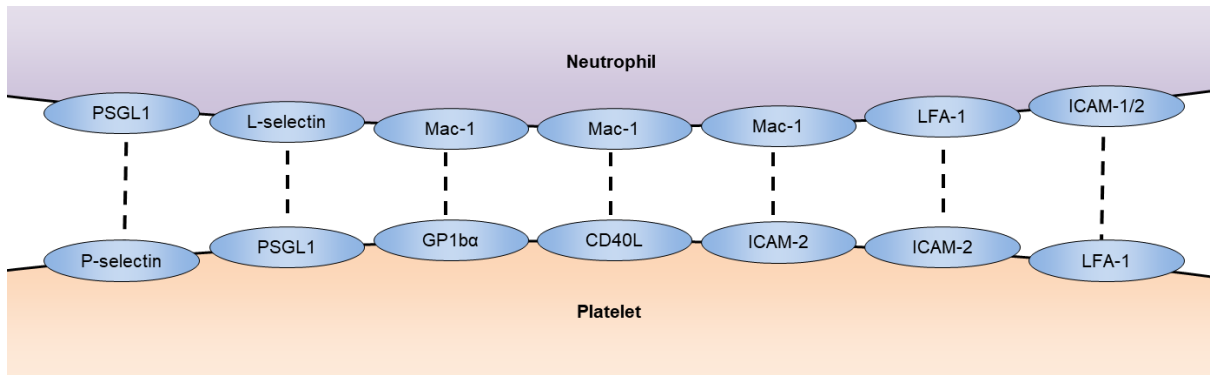
Figure 1.4 – Receptor-ligands implicated in platelet-neutrophil interactions
The surface of activated platelets express P-selectin, PSGL-1, ICAM-2 and LFA-1 which bind to PSGL-1, L-selectin, LFA-1 and ICAM-1 and 2 respectively, on the surface on neutrophils. Mac-1 on neutrophils is promiscuous and binds to GPIb α, CD40L and ICAM-2 on platelets. LFA-1 = $\alpha_L\beta2$ CD11a/CD18. Mac-1 = $\alpha_M\beta2$ = CD11b/CD18. Redrawn with modifications from (Page & Pitchford, 2013).

Platelets have also been implicated in wound healing. Upon injury, platelets are recruited in part due to exposure to collagen. They activate and spread and a platelet plug is formed that contains fibrin and acts as a scaffold for wound healing. Platelets and fibrin effectively act as chemoattractors for the recruitment of circulating macrophages, stromal cells, and endothelial cells to the site of injury (Nurden, 2011).

Activated platelets secrete from their α-granules, MIP-1 α, monocyte chemotactic protein-3 and RANTES which recruit and activate leukocytes. They also secrete PF4 and β-thromboglobulin which recruit neutrophils and suppress neutrophil apoptosis (Lam *et al.*, 2015).

Platelets also secrete wide range of growth factors, cytokines and chemokines that directly influence the reparative process such as vascular endothelial growth factor (VEGF), basic fibroblast growth factor (bFGF), and platelet-derived growth factor (PDGF) (Nurden, 2011).

1.1.3.3 Platelets contribute to cancer progression

As platelets contribute to hemostasis in the presence of cancer, they can initiate thrombotic events that facilitate the progression of cancer. Circulating tumour cells

adhere to platelets which they can use to mask their presence from the immune system. Tumour cells can also induce degranulation of platelets which generally leads to cancer progression. This includes the release of PDGF, TGFβ and VEGF from α-granules that stimulate tumor cell growth and angiogenesis. The release of platelet α-granules also includes proteins which stimulate tissue and vascular remodeling. These include matrix metalloproteinases including (MMP)-1, MMP-2, MMP-3, MMP-9, membrane type 1-MMP and MMP-14. Their inhibitors are also released including tissue inhibitor of metalloproteinase (TIMP)-1, TIMP-2, and TIMP-4. Also, a disintegrin and metalloproteinase (ADAM)-10, ADAM-17 and ADAM with thrombospondin motifs 13. The promotion of vascular remodeling by these proteins can lead to invasion at secondary metastatic sites. The release of dense granule contents such as ADP and calcium contribute to aggregation (Menter *et al.*, 2014).

1.1.4 Activatory and inhibitory signalling in platelets

Platelets maintain haemostasis and thrombosis by utilising an array of interconnected signaling networks. These can be divided into inhibitory and activatory pathways. Platelets experience multiple extracellular signals simultaneously and react to a plethora of primary and secondary activatory signals as well as to opposing inhibitory signals (Bye *et al.*, 2016).

Activatory signals originate from a site of vascular injury. They result in platelet activation and cause a signaling cascade that activates additional platelets and initiates thrombus formation.

The majority of platelets will spend their whole lifespan in a resting, inactive state. This is vital to prevent thrombotic events *in vivo*. This state is maintained by inhibitory signals which are released from healthy vasculature.

1.1.4.1 Platelet inhibition

Platelets are normally found *in* vivo in quiescence. In this state, healthy, intact vasculature release the inhibitory molecules prostacyclin/prostaglandin I_2 (PGI_2) and nitric oxide (NO) (Butt *et al.*, 1994). Endothelial CD39 degrades ATP and ADP to AMP and adenosine, the latter of which acts as a signalling molecule (Johnston-Cox & Ravid, 2011). Together, PGI_2, NO and adenosine inhibit platelets with PGI_2 the most potent (Johnston-Cox & Ravid, 2011). When platelets are in their resting state, phospholipase $C\gamma2$ ($PLC\gamma2$) will be inactive, myosin light chain kinase (MLCK) will maintain an inactive actin cytoskeleton, the granules will not secrete their contents, the microtubules and calcium stores will be stabilised (Menter *et al.*, 2014).

1.1.4.1.1 Prostacyclin

PGI_2 is the most potent natural platelet inhibitor in the body and it released from healthy vasculature rather than from platelets (Cheng *et al.*, 2002). Arachidonic acid is converted into prostaglandin H_2 (PGH_2) by cyclooxygenase 1 and 2. PG_H is then converted into PGI_2 by prostacyclin synthase (Gibbins & Mahaut-Smith, 2012). Circulating PGI_2 binds to the $G\alpha s$-protein coupled prostacyclin IP receptor on platelets and activates it. $G\alpha s$ then unbinds GDP and binds GTP instead and also dissociates from its β and γ subunits then binds to and activates adenyl cyclase (AC) (Sunahara & Insel, 2016). This can be reversed by regulator of G-protein signaling 2 which converts GTP to GDP. Activated AC in turn catalyses ATP conversion into cyclic adenosine monophosphate (cAMP) which activates protein kinase A (PKA). PKA in turn phosphorylates several other targets, resulting in platelet inhibition (**Figure 1.5**). PKA also activates phosphodiesterase 3 (PDE3) and 5 which degrade cAMP, acting as negative feedback loop (Smolenski, 2012). Prostacyclin receptor KO mice demonstrate an increase in susceptibility to thrombosis and demonstrate reduced inflammatory responses (Murata *et al.*, 1997).

1.1.4.1.2 Nitric oxide

NO is produced by endothelial nitric oxide synthase (eNOS) on intact endothelial cells. eNOS KO mice are hypertensive and demonstrate larger infarcts when subjected to focal ischemia (Huang, 1999) Circulating NO diffuses through the platelet membrane and binds to the heme component of soluble guanyl cyclase (GC), causing a conformational change that activates GC. GC then catalyses the conversion of GTP to cyclic guanosine monophosphate (cGMP) which in turn activates protein kinase G (PKG). Active PKG then proceeds to phosphorylate a range of proteins which results in platelet inhibition. cGMP also inhibits PDE3 by competing with its cAMP binding site. This prevents PDE3 from indirectly inhibiting the effects of cAMP and cGMP through hydrolysis (Smolenski, 2012) (**Figure 1.5**). However PDE2 and 5 are activated by cGMP and PKG, respectively, which degrade cAMP and cGMP and act as negative feedback (Menter *et al.*, 2014). NO also promotes MLC phosphatase activity and so prevents MLC phosphorylation and shape change (Aburima et al., 2017). PKG KO mice demonstrate prolonged bleeding times (Li, *et al.*, 2003).

1.1.4.1.3 Downstream PKA and PKG targets

The substrates targeted by PKA and PKG tend to converge. These kinases both phosphorylate VASP at S157, S239 and T278 which contributes to platelet inhibition (Cook & Haynes, 2007). Although KO models have demonstrated that VASP is not a major contributor to aggregation, thrombogenesis, haemostasis (Ito *et al.*, 2018) and shape change as it is dispensable (Eliautou *et al.*, 2009).

PKA and PKG also phosphorylate and inactivate several other targets which would otherwise be involved in a range of platelet activatory events (Smolenski, 2012). These targets include IP$_3$R which results in an inhibition of Ca^{2+} release (Tertyshnikova *et al.*, 1998); GPIbβ at S166 leading to a reduction in platelet adherence (Wardell *et al.*, 1989); and heat shock protein 27 at T143 which results in a reduction of F-actin polymerisation (Butt *et al.*, 2001).

Ras related protein 1b (Rap1b) is the most abundant GTPase in platelets (see Section 1.2.2.7), is mostly membrane-bound and is a potent regulator of integrin activity (Subramanian, *et al.*, 2013). Rap1b KO mice demonstrate defects in platelet aggregation and display prolonged bleeding times (Chrzanowska-Wodnicka *et al.*, 2005). PKA and PKG phosphorylation inhibit Rap1b induced platelet activation (Subramanian, *et al.*, 2013). One mechanism is through calcium and diacylglyc- erol-regulated guanine nucleotide exchange factor I (CalDAG-GEFI). Upon platelet activation CalDAG-GEFI translocates to the membrane and activates rap1b, this can be inhibited by phosphorylation of CalDAG-GEFI by PKA (Subramanian, *et al.*, 2013).

1.1.4.1.4 CD39

CD39, although probably not present in platelets (Burkhart *et al.*, 2012), is expressed on the endothelium and can degrade ATP and ADP to AMP and adenosine. Platelets express low levels of the Gαs-coupled receptors adenosine receptors (AR) A2A and A2B. Adenosine signals to these receptors to increase cAMP production through AC activation. This further contributes to platelet inhibition by degrading circulating agonists and stimulating the inhibitory pathway (Johnston-Cox & Ravid, 2011) (**Figure 1.5**). CD39 KO mice have been reported to demonstrate an increase in bleeding times (Enjyoji *et al.*, 1999).
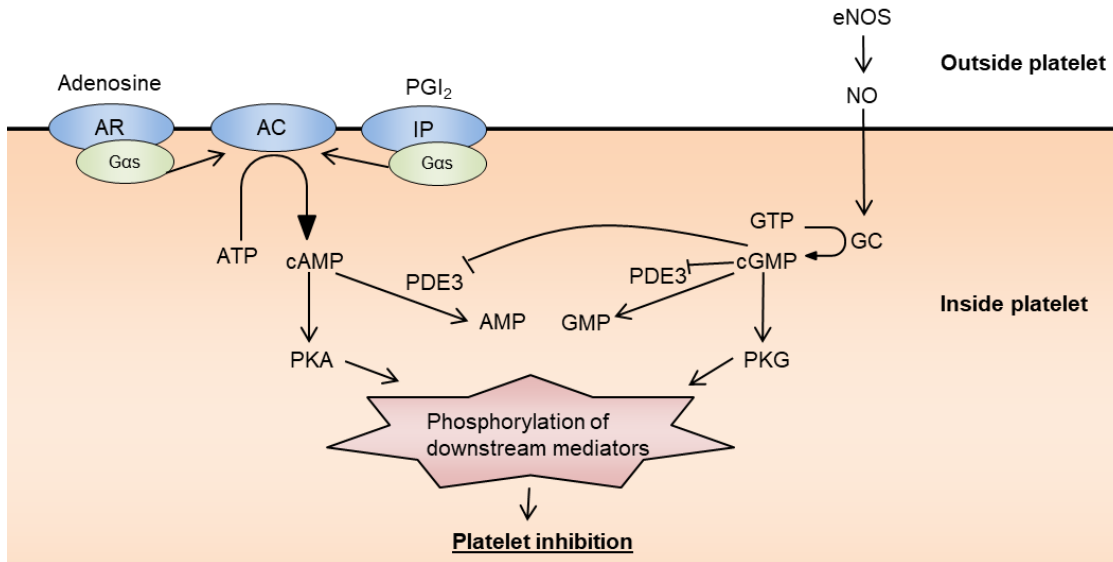
Figure 1.5 – Inhibitory signals in platelets
PGI_2 and NO are released from healthy endothelial cells. They signal to AC and GC to elevate levels of cAMP and cGMP which activate PKA and PKG, respectively. PKA and PKG in turn phosphorylate downstream mediators including VASP which results in platelet inhibition. Adenosine also activates AC through AR binding. cGMP also inhibits phosphodiesterase 3 (PDE3), preventing it from indirectly inhibiting the effects of cAMP through hydrolysis. Adapted from (Smolenski, 2012).

1.1.4.2 Platelet activation

Platelets can activate upon damage to the vascular tissue. There are far more different types of activatory molecules than inhibitory molecules. Exposure of blood platelets to the subendothelial matrix allows the binding of platelet surface receptors to ligands including VWF, laminin, fibronectin and thrombospondin, collagen. Several activatory molecules are also secreted by activated platelets including thromboxane, ADP and thrombin. Several of these agonists result in phosphorylation of Src family kinases, activation of small G protein regulators (SGR) and activation of PLCγ2 (Broos *et al.*, 2011). Activated PLCγ2 hydrolyses phosphatidylinositol 4,5-bisphosphate (PIP_2) into inositol 1,4,5-trisphosphate (IP_3) and diacylglycerol (DAG). IP_3 activates the Inositol trisphosphate receptor on the DTS resulting in Ca^{2+} release into the platelet. The subsequent lower Ca^{2+} levels results in stromal interaction molecule 1 (STIM1) leaving the DTS and activating the calcium ion channel moiety Orai1 on the membrane, enabling the influx of more

calcium to further activate the platelet. DAG activates protein kinase C (PKC) leading to granule secretion which leads to an activation cascade. The activation of several receptors including αIIbβ3 (GPIIb/IIIa) (CD41/CD61) by agonists is calcium concentration dependent with increased levels of calcium resulting in increased activation. Many of the signaling pathways interconnect and result in the activation of PLCγ2, an increase in calcium levels and ultimately platelet activation, shape change, granule release and activation (Gibbins, 2004) (**Figure 1.6**).

The secretion of granules requires their fusion with the plasma membrane in a process regulated by soluble N-ethylmaleimide-sensitive factor attachment proteins (SNAP) SNAP receptors (SNARE)s and connected regulatory proteins. Downstream of prolonged calcium signalling is phosphatidylserine (PtdSer) exposure and platelet ballooning which serves as a pro-coagulant surface. This occurs due to activation of the calcium-activated ion channel–phospholipid scramblase anoctamin-6 (ANO6), involves Cl^- influx and mediated by the intracellular protease calpain 2 (**Figure 1.6**) (van der Meijden & Heemskerk, 2019).

Platelet activation can be viewed as a weak, reversible activation followed by an irreversible, sustained activation which forms a stable platelet aggregate/clot. The reversible stage involves binding to agonists including fibrinogen and collagen. It also includes the release of soluble agonists including ADP and thromboxane. The irreversible stage of activation is characterised by an increase in calcium levels, sustained activatory signalling, thromboxane production by COX1 and release aswell as secretion the release of alpha and dense granules and the exposure of phosphatidylserine PtdSer (van der Meijden & Heemskerk, 2019). Rap1b activation is part of a tater stage of platelet activation and when Rap1b translocates to the cytoskeleton (Torti, *et al.*, 1999). Irreversible platelet activation also results in a stable spread shape (See section 1.2.2.8 and section 1.2.2.9) (Aslam, 2019)

1.1.4.2.1 Glycoprotein VI

The fibrillar collagens I, III and to a lesser extent the cross-linked collagen IV, are potent mediators of platelet adhesion (Boulaftali *et al.*, 2014). The platelet

receptor GPVI is the main receptor responsible for the interaction of collagen with platelets. Human GPVI is a 339 amino acid transmembrane complex. It consists of two extracellular immunoglobulin-like domains formed by disulphide bonds, a mucin-like stalk, a transmembrane region and a short 51 amino acid cytoplasmic tail (Nieswandt & Watson, 2003). GPVI is coupled with an Fc receptor (FcR) γ-chain that contains a tyrosine-based activation motif (ITAM). The cytosolic tail is required for intracellular signaling and contains a proline-rich motif that binds selectively to the Src homology 3 (SH3) domain of Fyn and Lyn (Berlanga *et al.*, 2002). Cross-linking of two GPVI complexes by collagen brings Fyn and Lyn to the FcR chain which allows them to phosphorylate the ITAM motif. Syk is then recruited and initiates a signalling cascade. The cascade involves the adaptor proteins includes Src-homology leucocyte protein 76 (SLP-76) and LAT (Watson *et al.*, 2010). The cascade leads to activation of serine/threonine-protein kinases (STKs), PLCγ2 phosphoinositide 3-kinases (PI3K). PLCγ2 then increases calcium levels (Nieswandt & Watson, 2003) and PI3K activation results in the production of PIP_3 which signals to Akt (Guidetti, *et al.*, 2015). Together, this results in platelet activation, granule release and aggregation (Nieswandt & Watson, 2003) (**Figure 1.6**).

The cytoplasmic tail of GPVI also interacts with calmodulin, regulating signalling and receptor shedding in a manner dependent on the binding of a ligand to GPVI and the binding of calcium to calmodulin (Gardiner *et al.*, 2005). GPVI activation results in Rac1 GTPase activation contributing to PLCγ2 activation, shape change and calcium mobilisation (Soulet *et al.*, 2001).

GPVI also has a binding affinity for laminin which is 10 times less strong than to collagen (Ozaki *et al.*, 2009). GPVI is less crucial for thrombus formation in mice than humans, possibly due to their lack of the equivalent to human FcRγ (McKenzie, 2002).

Gp6^{-/-} murine platelets fail to aggregate in response to collagen or the GPVI specific agonist convulxin. *Ex vivo* thrombus formation could also not occur on collagen. However the mice displayed no significant difference to the WT controls in tail bleeding assays (Kato *et al.*, 2003).

1.1.4.2.2 Integrin α2β1

Integrin α2β1 is a receptor for collagen types I, II, III and IV in a Mg^{2+} dependent manner. It consists of α2 and β1 integrins. α2β1 does not initiate a tyrosine kinase phosphorylation cascade itself but is thought to contribute to the effects of GPVI by binding collagen (Gibbins, 2004). This contributes both to adhesion and also aids the interaction of other receptors with the adjacent collagen (Varga-Szabo *et al.*, 2008). α2β1 also triggers contributes towards activation of αIIbβ3 through cross-talk with Rap1b (**Figure 1.6**) (Bernardi *et al.*, 2006)

1.1.4.2.3 Thrombin

Thrombin is a potent platelet activator and has an ability to polymerise fibrinogen into fibrin to contribute to the formation of a platelet plug. It signals through the membrane receptors protease-activated receptor 1 (PAR1) and PAR4 which are coupled to the G-proteins G_q, G_i, G_{12} and G_{13}. Activation of G12/13 leads to Ras homolog gene family (Rho) activation which goes on to contribute to myosin light chain phosphorylation, modification of the actin cytoskeleton and an induction of platelet shape change. Rho-associated coiled-coil-containing protein kinase (ROCK) is also activated. Rho signalling is discussed in **Section 1.2.2.7**. G_q stimulates PLCß2/3 which uses calcium as a cofactor calcium to convert PIP_2 to IP_3 and DAG leading to PKC activation, calcium mobilisation and platelet activation. The G_i subunit inhibits AC, leading to lower cAMP levels, and also stimulates PI3K which produces PIP_3. G_q is also bound to the 5HT2A receptor for serotonin which signals to activate PLCß2 (**Figure 1.6**) (Rivera *et al.*, 2009). It is worth noting that mice have differences in PARs. Humans have the PAR1 and PAR4 receptors whereas mice have PAR3 and PAR4 (French *et al.*, 2016).

1.1.4.2.4 Integrin αIIbβ3

Platelets express high levels of integrin αIIbβ3. Increased levels of calcium in activated platelets contribute towards activation of integrin αIIbβ3. A conformational change in the extracellular domain of integrin αIIbβ3 occurs as a result of the cytoplasmic tails becoming bound by talin and/or kindlin which triggers unclasping of the intracellular αIIbβ3 complex. This causes the receptor to have a high affinity for fibrinogen and fibrin to which it binds to contribute towards platelet adhesion. Conformational change also results in αIIbβ3 having a higher affinity for VWF and fibronectin (**Figure 1.6**) (Huang *et al.*, 2019). αIIbβ3 binds to the KQAGDV sequence of the fibrinogen γ-chain to cross-link platelets (Springer *et al.*, 2008). Clustering of active integrin αIIbβ3 molecules promotes activation of Src by autophosphorylation. Calpain then cleaves the cytoplasmic tail of integrin β3 which reduces its association to partially active Src. Src in turn activates a range of enzymes and signaling proteins including FAK, Syk kinase, SGRs, PI3K. talin, kindlin, which provide a link between the cytoplasmic tail of integrin β3 and the actin cytoskeleton. This leads to an intracellular signaling cascade that mediates irreversible stable adhesion, spreading, clot retraction, aggregation and cytoskeletal reorganisation of platelets (Huang *et al.*, 2019).

CalDAG-GEFI has been identified as an integrator of αIIbβ3 signalling and is required to mediate activation through targeting Rap1 (**Figure 1.6**). *CalDAG-GEFI$^{-/-}$* mice demonstrate severe aggregation defects in response to a range of agonists and demonstrate a significantly longer bleeding times in tail bleeding assays (Crittenden *et al.*, 2004).

1.1.4.2.5 Von Willebrand factor

VWF is a large multimeric adhesive protein produced by endothelial cells and megakaryocytes and is stored in alpha granules. VWF can bind to GP1b-V-IX on the platelet membrane, resulting in activation of several proteins including Rac1 and PLCγ2, leading to granule secretion. Binding of VWF to GP1b-V-IX also changes

αIIbβ3 from a low to high affinity receptor through Rap1 and PKC activation as well as from induction of calcium release through platelet activation which further enhances activation and subsequent adhesion and aggregation (**Figure 1.6**) (Bryckaert *et al*., 2015). VWF can also bind directly to αIIbβ3, resulting in adhesion (Roberts *et al*., 2009). Deficiencies of VWF lead to von Willebrand disease which in humans is the most common inherited bleeding disorder (De Meyer *et al*., 2009).

1.1.4.2.6 ADP and ATP

ADP binds to the $P2Y_1$ receptor which is coupled to G_q. Once activated, this activates PLCß2 leading to shape change which precedes aggregation. ADP also binds the P2Y12 receptor which is coupled to G_i. G_i activation inhibits AC and activates PI3K leading to increased PIP_3 levels and platelet activation. $P2Y_1$ and P2Y12 activation also lead to conversion of arachidonic acid to thromboxane. Binding of ATP to the ligand gated cation channel $P2X_1$ results in an influx of calcium which pushes platelets into a more active state (**Figure 1.6**) (Broos *et al*., 2011).

1.1.4.2.7 Thromboxane

Thromboxane receptor (TP) can occur as either the TPα or TPβ isoform which differ in the C-terminal and are spliced from the same gene. The isoform present in platelets is TPα (Habib *et al*., 1999). TP signals though its G_q coupled protein that signals to PLCß2/3 which results in an increase in calcium levels. G12/13 is also associated with TP which signals to ROCK which in turn phosphorylates and activates MLC and LIM-kinase (LIMK) to effect platelet shape change (**Figure 1.6**) (Menter *et al*., 2014).

Additional production of thromboxane can also occur downstream of PAR1/PAR4 activation by thrombin. Activation of the rate limiting factor, cytosolic phospholipase $A_{2\alpha}$ ($cPLA_{2\alpha}$), converts fatty acids into arachidonic acid. This is then

converted by COX1 and 2 into PGH2 which is in turn converted by thromboxane synthase into thromboxane (**Figure 1.6**) (Holinstat *et al*., 2011).

1.1.4.2.8 Podoplanin

Podoplanin signals through the receptor CLEC-2 which is one of the two ITAM receptors on platelets. The other is GPVI, discussed in **Section 1.1.4.2.1**. Binding of podoplanin to its receptor can also contribute to platelet activation and stable adhesion. CLEC-2 downstream mediators are the same as those of GPVI (**Figure 1.6**). *Clec2*$^{-/-}$ mice demonstrate significantly reduced abilities of platelets to prevent inflammation induced hemorrhage of skin lesions (Boulaftali *et al*., 2014).

1.1.4.2.9 Fibronectin, laminin and vitronectin

Upon vessel damage, laminin, fibronectin and vitronectin in the extracellular matrix are exposed to blood flow (Varga-Szabo *et al*., 2008). Laminin can bind to the receptor α6β1 to contribute to adhesion and activation of SGRs (van der Meijden & Heemskerk, 2019) (**Figure 1.6**). GPVI also has a binding affinity for laminin which is 10 times less strong than to collagen (Ozaki *et al*., 2009). Fibronectin and vitronectin bind to α5β1 and αvβ3, respectively, to contribute towards platelet adhesion and activation of PLCγ2 (Varga-Szabo *et al*., 2008).
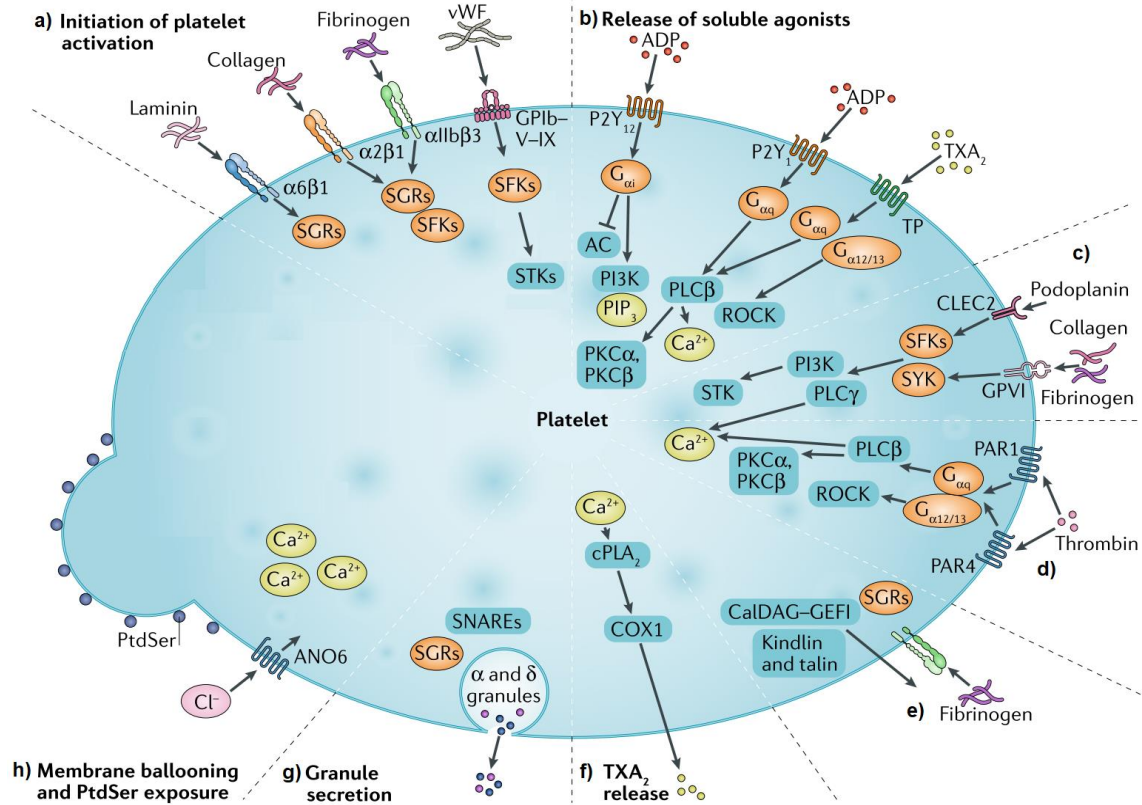
Figure 1.6 – Model of human platelet activatory signals and receptors

a) Platelet activation is initiated by the binding of ligands including laminin, collagen, fibrinogen and vWF.to receptors including integrins α6β1, α2β1, αIIbβ3, and GPIb–V–IX which signal through SGRs. **b**) Circulating agonists, released from platelets such as ADP and thromboxane lead to activation of P2Y12, P2Y1 and TP. P2Y12 acts through $G_{\alpha i}$ to inhibit AC and also stimulates PI3K to produce PIP_3. P2Y1 and TP signal through $G_{\alpha q}$ leading to PLCβ stimulation which increases calcium levels and activates PKC and further downstream events. TP activation also activates Gα12/13 which in turn activates ROCK, leading to platelet shape change and spreading. **c**) GPVI and CLEC2 induce strong signalling through Syk and SFK protein, leading to activation of PLCγ and PI3K which in turn raise Ca^{2+} and PIP_3 levels, respectively. **d**) Thrombin activates PAR1 and PAR4 leading to PLCβ stimulation, PKC activation, increased levels of calcium and ROCK activation. **e**) Increased intracellular calcium levels and platelet activation causes a conformational change in the shape of αIIbβ3. This involves the binding of talin and kindlin to the β3 cytoplasmic tail which results in a conformational change in the extracellular domain. This causes αIIbβ3 to have a high affinity for its ligand fibrinogen to contribute to platelet adhesion and cross-linking. Active CalDAG–GEFI and Rap1B are also required to mediate a signalling cascade that involves SFKs and contributes to platelet activation, secretion and aggregation. **f**) Platelet activation results in cPLA activation which results in thromboxane production. **g**) Activated platelets secrete α and dense (δ) granules mediated by SNAREs and SGRs. **h**) ANO6 is activated resulting in Cl⁻ influx, platelet ballooning and exposure of PtdSer. Adapted from van der Meijden & Heemskerk, 2019 with modifications.

41

1.1.5 Heterogeneity in platelets

Platelets do not represent a homogeneous population. This has been known for a long time as larger and denser platelets, isolated by density gradients, were found to be more metabolically active (Karpatkin & Charmate, 1969). Platelets can be heterogeneous with regards to intrinsic characteristics, e.g. structure, size, granule numbers, age, receptor expression and activation properties with consequences for their functions including activation, secretion, adhesion, spreading and aggregation (van der Meijden & Heemskerk, 2019).

During thrombosis, platelets will be exposed to different levels of agonists. Platelets will be heterogenic in response to the extrinsic factors they experience, for example the middle of a thrombus may consist of densely pack platelets which are highly activated by collagen and from the secretions from other platelets including thrombin and VWF. However, the periphery of a thrombus may consist of loosely adhered platelets with lower levels of activation which may experience inhibitory signals from PGI_2 and NO in the bloodstream which are released form healthy intact vasculature (van der Meijden & Heemskerk, 2019).

1.2 The cytoskeleton

The eukaryotic cytoskeleton maintains cell structure and is important for cytoplasmic mechanics (Guo *et al.*, 2013). The cytoskeleton comprises of three components: microfilaments, intermediate filaments and microtubules (Fischer & Fowler, 2015). It can be utilised for functions including migration, endocytosis and cytokinesis (Cai *et al.*, 2005).

The actin cytoskeleton is comprised of polymerised F-actin. It undergoes dynamic assembly and disassembly and it both spatially and temporally regulates cell protrusion, adhesion, contraction, and retraction from the front, middle and rear. This is the protein associated with coronin (Shina & Noegel, 2008) and CAP1 (Nancy L. Freeman & Field, 2000) which were investigated in the current project.

42

Intermediate filaments are predominantly located in the cell cytoplasm and provide mechanical and structural integrity. There are five types – I, II, III, IV and V. Type I and II comprise the epithelial keratins and trichocytic keratins, respectively. Type III includes desmins in muscle sarcomeres and vimentin which supports the membrane in many cell types. Type IV includes neurofilaments and syncoilin which binds to desmin. Type V are fibrous lamins which maintain the structure of the eukaryotic nucleus (Omary, 2009).

There are nine microtubule genes which encode variety of α and β tubulin isoforms. Microtubules are long, hollow cylinders consisting of α- and β-tubulin dimers. These bind back to front into proto-filaments which are heteropolymerised laterally with a helical pitch. Mictotubules are polar structures - the plus end is capable of rapid growth and the minus end slowly loses subunits if not stabilised. Mictotubule polymerisation can refer to either the growth of existing microtubules through addition of dimers or the spontaneous formation of new microtubules (Ghalloussi *et al.*, 2019). These combine to create hollow tubes approximately 25 nm in diameter. The functions of microtubules include mechanical support, organisation of the cytoplasm, transport, secretion, motility and chromosome segregation (Tang & Gerlach, 2017). Rho GTPases are important upstream proteins in the regulation of microtubule and actin cytoskeleton formation (Ghalloussi *et al.*, 2019). Rho GTPases will be explained in **Section 1.2.2.8** with regards to actin.

1.2.1 The Actin cytoskeleton

Actin is a highly conserved protein which is abundant in the cytosol and nucleus of almost all eukaryotic cells. Actin can contribute to a diverse range of regulatory and structural functions such as muscle contraction, cell motility, cell division and cytokinesis, vesicle and organelle movement and cell signaling. Actin can exist in α, β or γ isoforms (Yamin & Morgan, 2012). Actin is one of the most abundant proteins in many eukaryotic cells with concentrations over 100 µM (Millard *et al.*, 2004). Actin turnover is regulated by associated proteins including capping, severing, branching, cross-linking proteins as well as nucleotide exchange factors (Pollard, 2016). The

43

cytoskeleton can also form specialised structures such as lamellipodia and filopodia which are required for migration spreading (Fletcher & Mullins, 2010).

1.2.1.1 Actin polymerisation and depolymerisation

Monomeric actin, also known as G-actin, can polymerise into filamentous actin, also known as F-actin. Polymerisation of actin can be initiated by nucleation of a G-actin trimer. The F-actin network is in constant flux with polymerisation and depolymerisation. F-actin filaments have both slow growing pointed and fast growing barbed ends (Pollard & Borisy, 2003). Actin polymerisation is utilised by eukaryotic cells to alter their shape, for motility and to undertake the processes of phagocytosis and endocytosis (Linardopoulou *et al.*, 2007).

Formins are important initiators of actin polymerisation. They utilise free actin monomers to nucleate new F-actin filaments then remain bound to the barbed ends of these filaments as they polymerise. This increases new actin filaments much quickly than they would otherwise form spontaneously (A. S. Paul & Pollard, 2009).

The assembly and disassembly of actin filaments of the actin cytoskeleton is essential for the majority of aspects involving cell motility as well as cell migration, endocytosis/phagocytosis, cytokinesis and cell morphogenesis (Tojkander *et al.*, 2012) and host-pathogen interactions (Haglund & Welch, 2011). Motile cells extend a leading edge, rich in branched actin filaments, which push the cell forward, enabling motility (Pollard & Borisy, 2003). Reorganisation of the cytoskeleton is dynamic and involves the net addition of actin monomers at branched ends of actin filaments and the net removal of actin subunits at pointed ends. The addition of actin monomers is essential for maintaining the network and for producing force whereas the removal of subunits is important for sustaining plasticity and recycling actin. This is known as actin treadmilling. The remodeling of actin networks, in response to temporal spatial cues is tightly regulated by the combined effects of many different actin associated proteins (Tojkander *et al.*, 2012).

Both actin polymerisation and actin branching is dependent upon regulators including the Arp2/3 complex, Rho-GTPases, Wiskott–Aldrich

44

Syndrome protein (WASP) (Rybakin & Clemen, 2005), coronin and (Gandhi & Goode, 2008) CAP1 (Moriyama & Yahara, 2002). The diverse structure and functions of F-actin can be further modified by G-actin sequestering or associated, capping and severing, actin filament crosslinking and bundling, motor, or membrane anchoring proteins (Rybakin & Clemen, 2005).

1.2.1.2 Actin severing proteins

Actin severing proteins include cofilin and gelsolin and the formins FRL-α and INF-2. Cofilin binds to the barbed-end groove of actin filaments and inhibits nucleotide exchange. Cofilin also binds to the sides of filaments with a higher affinity for ADP-actin and severs the filament. Cofilin is inactivated by phosphorylation at S3 by LIMK. Phosphatases such as slingshot and chronophin can remove the phosphate group. The mammalian gelsolin family members consist of three or six gelsolin domains plus other domains. Gelsolin, like cofilin can sever filaments by binding to the barbed end. Gelsolin can also cap filaments which prevents their elongation. Gelsolin is activated by an increase in calcium levels (Pollard, 2016). Gelsolin KO mice demonstrate defects in platelet shape change and have prolonged bleeding times (Witke *et al.*, 1995).

1.2.1.3 Actin capping proteins

Actin capping proteins bind to the barbed end of actin filaments to 'cap' them which prevents nucleotide exchange and prevents further elongation. Examples of capping proteins include gelsolin, the capping protein and epidermal growth factor receptor pathway substrate 8 (Eps8). Gelsolin is activated upon calcium binding which causes a conformational change allowing it to interact with F-actin which it severs and caps (Menna *et al.*, 2011). The capping protein competes with other actin regulatory proteins such as formins and enabled/vasodilator-stimulated phosphoprotein (ENA/VASP) for binding to the barbed end of filaments. The capping protein is in turn regulated by molecules including myotrophin and

phospholipids which bind to it and block its function. It can also be recruited to specific subcellular locations to undergo its function by proteins including capping protein ARP2/3 and myosin I linker (CARMIL) and CD2-associated protein (CD2AP) (Edwards *et al.*, 2014). Eps8 is not regulated by calcium but rather through phosphorylation and interactions with other proteins. The capping domain of Eps8 resides in its C-terminal effector domain. Eps8 becomes active and can cap filaments upon binding to Abi1 (Roffers-Agarwal *et al.*, 2005). Eps8 can also bundle and cross-link actin filaments upon binding to insulin receptor tyrosine kinase substrate of 53 kDa (IRSp53) (Menna *et al.*, 2011). Together, these proteins contribute to creating and maintaining the integrity of actin structures.

1.2.1.4 Actin Structures

Actin structures include filopodia, lamellipodia and actin nodules(Svitkina, 2018). Actin nodules are explained with regards to platelets in **Section 1.2.2.3**.

Filopodia are slender protrusions which extend from cells. Filopodia contain parallel bundles of tightly cross-linked actin filaments due to proteins including fascin. Some of the filaments span the length of the filopodia. These filaments are uniformly organised with their growing barbed tip pointing towards the growing edge of the filopod. The tip of the filopod undergoes elongation and is protected from capping by ENA/VASP proteins and formins which are enriched at the tips filopodia partially buckle and retract after a period of elongation. Filopodia contribute to spreading, migration and sensing of chemoattractants (Svitkina, 2018).

Lamellipodia are protrusions from cells that are wider and flatter than filopods. They consist of highly branched actin filaments which are nucleated by Arp2/3. The actin filament barbed ends are pointed towards the edge of the cell. Lamellipodia, like filopods are also enriched in ENA/VASP proteins but they experience higher levels of filament severing, capping and actin turnover than with assembly and disassembly occurring constantly. Lamellipodia contribute to spreading, cell locomotion, exocytosis and sensing of chemoattractants (Svitkina, 2018). A

diagram of filopods and lamellipodia on platelets was presented previously (**Figure 1.2**).

.

1.2.1.5 Arp2/3 promotes F-actin branching

Actin filament nucleation is intrinsically suppressed by profilin and thymosin-b4. Cells utilise regulatory proteins to enable filament assembly in controlled ways (Pollard, 2016). Actin filament assembly is regulated by multiple distinct Arp2/3 complex variants (Rottner & Stradal, 2015). The Arp2/3 complex is essential for mammalian list and consists of 7 protein subunits: Arp2, Arp3 and ArpC1-5. The Arp2/3 complex is involved in the mediation of actin polymerisation (Millard *et al.*, 2004). The subunit composition can determine actin assembly efficiency and stability. ArpC1 and ArpC5 each have two isoforms with high and low levels of activity. The complex with lower activity is more stable than the complex with higher activity (Rottner & Stradal, 2015). The ratio of Arp2/3 complex variants in platelets is currently unclear.

Arp2/3 can associate with the side of a growing actin filament and can nucleate actin to enable the formation of a new actin filament at a 70° angle to the existing actin filament, producing a branched actin network (Linardopoulou *et al.*, 2007). Cortactin is thought to bind near the nucleation site and stabilise branches (Pollard, 2016). The activity of the Arp2/3 complex is influenced by several activators and inhibitors. WASP can stimulate actin assembly in response to extracellular signals. Arp2/3 activity is also regulated by suppressor of cyclic adenosine monophosphate (cAMP) receptor (SCAR) which is also known as WAVE (WASP family verprolin homologous protein). Both WASP and SCAR bind to Arp2/3 to stimulate actin assembly by nucleation (Millard *et al.*, 2004). The Wiskott-Aldrich syndrome protein and SCAR homologue (WASH) can also activate Arp2/3 and regulate the spatial–temporal formation of actin networks (Linardopoulou *et al.*, 2007).

47

The Arp2/3 complex can also nucleate a new actin filament independent of a preexisting one upon activation by Dip1 (Wagner *et al.*, 2013). Arpin is recruited at the tip of the lamellipodia by Rac to inhibit nucleation of actin filament branches by Arp2/3 complex (Dang *et al.*, 2013).

1.2.2 The platelet cytoskeleton

The platelets have a cytoskeleton that consists of a spectrin-based membrane skeleton, an actin-based cytoskeletal network and a peripheral band of microtubules (Thon & Italiano, 2012) (**Figure 1.7**).
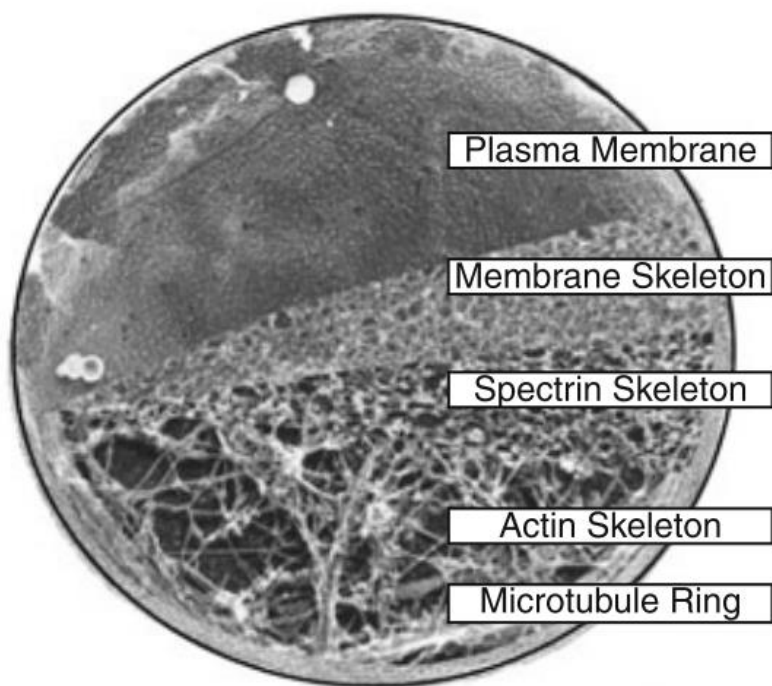
Figure 1.7 - Electron micrograph of a discoid platelet cut in an equatorial plane to reveal the cytoskeleton
Areas include the plasma membrane, membrane skeleton, spectrin cytoskeleton, actin skeleton and microtubule ring (Hartwig *et al.*, 1999; Jonathan N Thon & Italiano, 2012).

1.2.2.1 Spectrin based network

The spectrin network is required for platelet formation. The assembly of spectrin into tetramers is required for invaginated membrane system maturation and proplatelet extension. Spectrin tetramers stabilise the barbell shapes in the final stage of

platelet production and a tetramer-disrupting construct has beven reported to change these barbells into spheres (Patel-Hett *et al.*, 2011).

1.2.2.2 Platelet tubulin cytoskeleton

Platelets express several of these of α and β tubulin isoforms, with β1 tubulin the most important (Ghalloussi *et al.*, 2019). Rearrangement of the tubulin cytoskeleton of proplatelets is essential to the platelet development. Mice with hematopoietic-specific β1-tubulin knockout demonstrate severe thrombocytopenia and a defect in generating proplatelets (Schwer *et al.*, 2001). The cortex of a megakaryocyte is rich in microtubules parallel to the plasma membrane. Dyenin 'motors' cause the microtubules to slide and produce pseudopodia which narrow and elongate to become proplatelets. The microtubules taper towards the end of the proplatelets then perform a U-turn and re-enter the proplatelets shaft, producing a platelet structure. An actin-dependent reaction is utilised to bifurcate the proplatelets shaft, increasing the amount of proplatelet ends which allows more area for platelet formation (Italiano *et al.*, 2007).

1.2.2.3 Actin nodules

A proteomic study of human platelets identified that β-actin is the most abundant protein, followed by γ-actin then α-actin. In total, actin represents over 10% of the total platelet protein content by copy number (Burkhart *et al.*, 2012).

During spreading on certain matrices including fibrinogen and fibronectin, platelets demonstrate areas of rich F-actin staining. These have been called actin nodules and are rich in polyermised actin and are connected together by actin fibres. These are highly dynamic structures with the turnover rate of an individual nodule less than 1 minute. The nodules also contain a central core of tyrosine-phosphorylated proteins. The area immediately around the nodule consists of a ring rich in talin and vinculin which tether the actin cytoskeleton to the plasma membrane. The area of the platelet membrane closest to an actin nodule displays a greatly

reduced level of integrins compared to the surrounding area (Poulter *et al.*, 2015) (**Figure 1.8**).

The nodules tend to move towards and then away from the substrate on which they spread during their turnover which may be the reason for the lack of integrins. The formation of nodules is dependent upon Arp2/3 and WASP. In mice, only ~20% of WASP KO platelets have nodules compared to ~80% of WT when statically spread on fibrinogen. In human Wiskott–Aldrich syndrome (WAS) patients only about 10% of platelets had nodules compared to ~40% of platelets from unaffected donors. Platelets from WASP KO mice and WAS human patients spread over a slightly smaller area compared to healthy controls in static conditions. However, under flow conditions with a shear rate of 600^{-s} on fibrinogen, a large proportion of WASP KO platelets do not fully spread and there was a huge reduction in the proportion of platelets with lamellipodia (Poulter *et al.*, 2015).
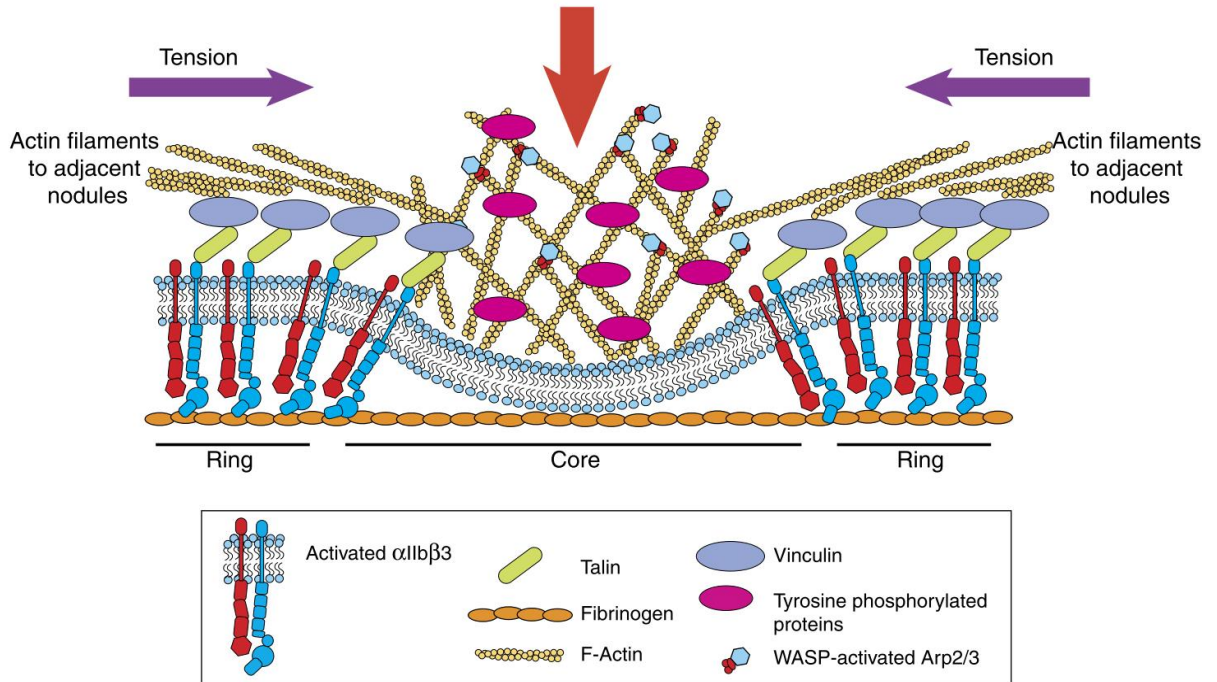
Figure 1.8 – Diagram of a platelet actin nodule
An actin nodule of a platelet spread on fibrinogen. The area of the nodules, indicated by the arrow, is rich in F-actin, tyrosine-phosphorylated proteins and WASP-activated Arp2/3 and has low levels of integrins. The ring immediately around the nodule is rich in vinculin and talin which link the F-actin cytoskeleton to the plasma membrane. Tension is created in a direction towards the nodules and additional nodules are linked by stress fibres. Adapted from (Poulter *et al.*, 2015).

1.2.2.4 The Arp2/3 complex in platelets

Arp2/3 is required for actin polymerisation, specifically branching, during platelet shape change. Blocking Arp2/3 using a specific inhibitor blocks the formation of filopodia and lamellipodia and inhibits the spreading of platelets (Li *et al*. 2012; Rondina *et al*. 2016). Cortactin is thought to bind near the nucleation site and stabilise branches (Pollard, 2016) but cortactin KO mice demonstrated it is dispensable for spreading and aggregation (Thomas et al., 2016).

Deletion of the Arp2/3 complex in megakaryocytes leads to microthrombocytopenia in mice. This is due to premature platelet release and

51

defects in survival of circulating platelet. The platelets have greatly impaired spreading abilities and display a mild defect in integrin activation and aggregation, although no significant differences in hemostasis are present. This phenotype resembles that (Paul *et al.*, 2017). Humans with a loss of the ARPC1B subunit of the Arp 2/3 complex also display microthrombocytopenia, impaired platelet spreading, and a largely intact hemostatic response (Kahr *et al.*, 2017). The precise mechanism is unclear but is hypothesised to be due to deficient WAVE1 or WAS signalling (Paul *et al.*, 2017).

1.2.2.5 Actin depolymerising protein family in platelets

The cofilin family of proteins, also called the actin depolymerising factor (ADF) family, consist of cofilin 1, cofilin 2 and ADF which is also called destrin (Bender *et al.*, 2010). Cofilin 1 and cofilin 2 and ADF are encoded for by COF1, COF2 and DEST and are abundant in human platelets, representing the 17th, 48th and 233rd most abundant proteins by copy number in a proteomic study (Burkhart *et al.*, 2012), with cofilin 1 is the most studied. Cofilin is a conserved, G- and F-actin binding protein which contributes to actin disassembly (Vartiainen *et al.*, 2002).

Cofilin severs actin filaments, with a preference for ADP-bound actin at the rear of the network. This recycles actin monomers for polymerisation and increases the rate (Kardos *et al.*, 2009). In mice, KO of *Cof1* is lethal due to impaired neural crest development and migration (Gurniak *et al.*, 2005). Megakaryocyte specific KO resulted in slightly reduced platelet numbers which were double the normal size but still functional (Bender *et al.*, 2010). Conditional KO from embryonic day 10.5 results in defects in cell cycle control and neuronal migration in the cerebral cortex (Bellenchi *et al.*, 2007). Cofilin is regulated by several proteins including coronin (Gandhi & Goode, 2008) and CAP1 (Moriyama & Yahara, 2002) as discussed in **Section 1.4**.

Actin depolymerising factor (ADF) is a conserved protein responsible for the severing and enhancement of depolymerisation of actin filaments. KO of the ADF gene, *Dest*, does not lead to developmental defects or obvious platelet defects but

results in epithelial hyperproliferation leading to cornea thickening and blindness. This has been attributed to aberrant cytoskeleton regulation as KO corneal cells demonstrated increased F-actin staining (Ikeda *et al.*, 2003).

In mice, megakaryocyte specific double KO of *Cof1* and *Dest* results in an inability to produce functional platelets. The mice had severe thrombocytopenia, the megakaryocytes displayed an aberrant accumulation of F-actin and the proplatelets were shorter and less complex with lower levels of F-actin. This demonstrates that *in vivo* dynamic actin turnover is important in the late stages of thrombopoiesis and that cofilin is critical for platelet size (Bender *et al.*, 2010).

1.2.2.6 Profilin and twinfilin in platelets

Profilin is a monomeric actin-binding protein with a preference for ATP-bound actin. Profilin promotes the incorporation of ATP-actin monomers into filaments at the barbed ends (Kardos *et al.*, 2009). Profilin is also involved with nucleotide exchange, effectively providing a phosphate group to convert ADP to ATP bound actin. This is regulated by proteins such as CAP1 as described later (Moriyama & Yahara, 2002).

Profilin is also capable of regulating the microtubule cytoskeleton. In mice, megakaryocyte-specific KO of the profilin gene, *Pfn1*, leads to microthrombocytopenia attributed to increased platelet turnover and premature release of platelets into the bone marrow. The *Pfn1*$^{-/-}$ platelets also displayed abnormally organised and hyperstable microtubules (Bender *et al.*, 2014).

Twinfilin is represented by two genes, *Twf1* and *Twf2*, the latter of which leads to *Twf2a* and *Twf2b* through alternative promoter usage (Nevalainen *et al.*, 2009). Human (Burkhart *et al.*, 2012) and murine platelets express *Twf1* and *Twf2* (Zeiler *et al.*, 2014)*,* although *Twf2b* is generally considered muscle specific (Nevalainen *et al.*, 2009). Twinfilins bind to ADP-bound G-actin and promoting sequestration. They also cap actin filaments to prevent barbed end growth and enhance barbed end depolymerisation (Stritt *et al.*, 2017).

In mice, constitutive *Twf2a* deletion resulted in mild macrothrombocytopenia due to accelerated platelet clearance in the spleen. *Twf2a* KO platelets presented generally prothrombotic phenotypes including increases in integrin activation and α-granule secretion in response to a range of agonists and larger surface area when spread on fibrinogen, shortened tail bleeding times and faster occlusive arterial thrombus formation. This was attributed to enhanced actin dynamics with increased activity of cofilin and profilin, resulting in a thickened cortical cytoskeleton and sustained integrin activation by limiting calpain mediated integrin inactivation (Stritt *et al.*, 2017). Interestingly *Twf1* appears redundant for platelet levels and reactivity (Becker *et al.*, 2020).

Double KO of *Twf1* and *Twf2* resulted in a very similar phenotype to the *Twf1* KO. This demonstrates the complex redundancies in proteins which regulate the platelet cytoskeleton. Double KO of *Twf1* and *Cof1* resulted in severe macrothrombocytopenia and greatly increased megakaryocyte numbers in the bone marrow and spleen. The megakaryocytes demonstrated defective proplatelet formation, impaired spreading and altered assembly of actin nodules. This was associated with aberrant high F-actin accumulation and hyperstable microtubules. This was attributed in part to dysregulation of the actin and MT-binding proteins mDia1 (Becker *et al.*, 2020).

1.2.2.7 Rho GTPase regulation

Rho GTPases are important upstream proteins in the regulation of their formation. Upon activation they bind to effectors such as protein kinases to regulate the microtubule and F-actin cytoskeletons (Aslan *et al.*, 2013).

Rho GTPases can be GDP or GTP-bound. They are inactive when GDP-bound and active when GTP-bound. Rho GTPases are regulated by guanine nucleotide exchange factor (GEFs), GTPase-activating proteins (GAPs) and guanine nucleotide dissociation inhibitors (GDIs) (Ngo *et al.*, 2017).

GEFs activate Rho GTPases by exchanging of GDP for GTP (**Figure 1.8**). Rac1 GEFs include Vav1/3, phosphatidylinositol-3,4,5-trisphosphate dependent Rac

Exchange Factor 1 (PRex1), Rac/CDC42 guanine nucleotide exchange factor 6 (ARHGEF6) and dedicator of cytokinesis (Dock) family members. RhoA GEFs include ARHGEF1 and leukemia-associated Rho guanine-nucleotide exchange factor (LARG) (Aslan, 2019).

Rho GTPases are inhibited by GAPs which accelerate GTP to GDP hydrolysis to inhibit Rho GTPase function. An example of a Rac1 GAP is ARHGEF17 and examples of RHOA GAPs include p190RhoGAP and oligophrenin 1 (OPHN1) (Aslan, 2019).

GDIs are less studied and less numerous with only RhoGDI and Ly-GDI expressed in platelets. They are thought to sequester Rho GTPasess to regulate their activity temporally and spatially (Ngo *et al.*, 2017).

1.2.2.8 Rho signalling in platelets

Rho signalling is important for platelet activation and spreading and is involved in numerous pathways downstream of receptors. Activation of GPVI (**Section 1.1.4.2.1)** results in signals occurring through SFKs, 3-phosphoinositide-dependent protein kinase 1 (PDK1) and RhoG which activate Rac1 GEFs including Vav1/3, PRex1, ARHGEF6 and Dock family members. These push Rac1 into the active, GTP-bound form which along with CDC42 activates downstream effectors such as WASPs, WAVEs, Arp2/3, PAKs, and PAK substrates in cytoskeletal remodeling, lamellipodia formation, filopodia formation, secretion and spreading. Rac1 also signals to PLCγ to increase calcium levels as summarised above (**Section 1.1.4.2**). The increase in intracellular calcium contributes to activation of the calcium channel Oria1 which allows the influx of additional calcium to further activation the platelet. Increases in calcium levels also leads, through calmodulin, to the activation of MLCK and phosphorylation of MLC which contributes to shape change. Calcium also contributes to αIIbβ3 activation which signals to further activate SFK (**Figure 1.9**) (Aslan, 2019).

Activation of platelet PAR and TP (discussed earlier) leads to RhoA-GEFs including ARHGEF1 and LARG which pushes RhoA into a GTP-bound, active state.

This in turns leads to activation of ROCK1 and ROCK2. ROCK2 inhibits myosin light chain phosphatase (MLCP) and subsequent MLC phosphorylation preventing platelet inhibition. Activation of ROCK1 leads to phosphatidylserine (PS) exposure and contributes to platelet aggregation (**Figure 1.9**) (Aslan, 2019).

The pool of Rac1 GTPases will also be influenced by the GAP ARHGEF17 and RHOA by the GAPs p190RhoGAP and oligophrenin1, which will push the respective Rho GTPases into an inactive state (**Figure 1.9**) (Aslan, 2019).
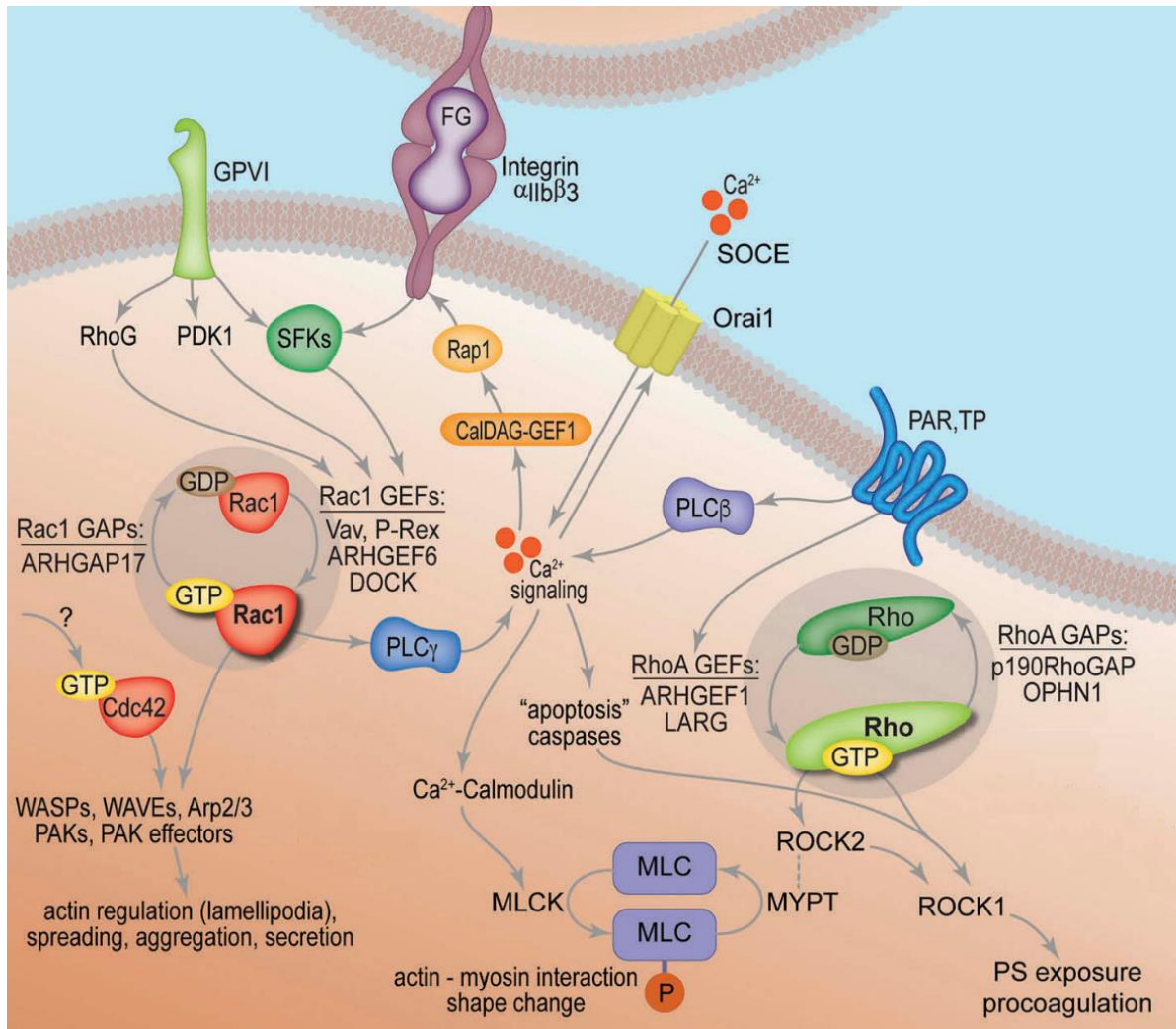
Figure 1.9 – Rho GTPase signalling contributes to platelet activation
GPVI activation leads to activation of RhoG, PDK1 and SFKs which in turn activate Rac1 GEFs. These exchange the GDP for GTP on Rac1 which becomes active. Rac1 and CDC42 signal to downstream proteins including WASP, WAVE, Arp2/3 and PAK which results in lamellipodia formation, spreading, aggregation and granule secretion. Rac1 also activates PLCγ to increase calcium concentration and activate αIIbβ3 through Rap1 and CalDAG-GEFI. Activated αIIbβ3 binds to fibrinogen and fibrin to cross-link platelets and also activates SFKs. The increase in calcium concentration activates the Orai calcium channel which further increases calcium levels by allowing influx. Activation of PAR and TP receptors activates RhoA GEFs that push Rho into an activate state by exchanging GDP for GTP. Active Rho Signals to ROCK1 and 2 which also contribute to PS exposure and coagulation. Activation of PAR and TP receptors also activates PLCβ that increases calcium levels. Through calmodulin, increased calcium levels will activate MLCK that phophorylates MLC that in turn contributes to shape change. Increased cytosolic calcium levels also triggers apoptosis cascades and PS exposure. Adapted from (Aslan, 2019).

1.2.2.9 Regulation of formation of filopodia, lamellipodia and stress fibres

The cytoskeleton can also form specialised structures such as lamellipodia and filopodia during platelet spreading. The regulation of spreading and the formation of these structures is dependent upon actin cytoskeletal reorganisation (Bearer *et al.*, 2002). These structures are formed upon platelet activation and involve the activation of RhoA, Rac1 and CDC42 primarily, but not exclusively which contribute to the formation of stress fibers, lamellipodia, and filopodia, respectively (Aslan *et al.*, 2013). The process of regulation is further complicated by intermediate signalling pathways (Aslan & McCarty, 2013). The signalling pathways include activation of Arp2/3 by WASP, WAVE and PAK (**Figure 1.10**) (Aslan & McCarty, 2013). As explained later in **Section 1.3.7.2**, coronin interacts with Arp2/3 (Uetrecht & Bear, 2006) and PAK1 (Castro-Castro *et al.*, 2011) and therefore may play a role in the regulation of the cytoskeleton through Rho GTPases.
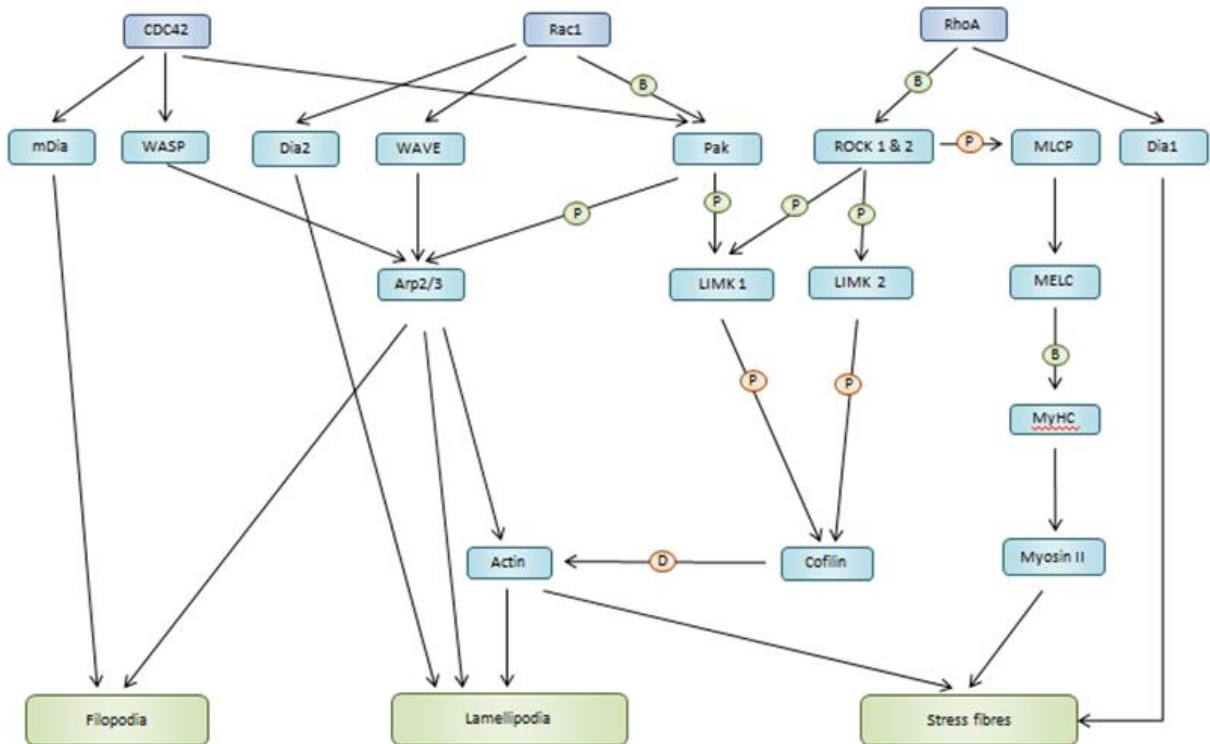
Figure 1.10 - Regulation of formation of filopodia, lamellipodia and stress fibres by Rho GTPases

CDC42 activates WASP which activates Arp2/3 which reorganises the actin cytoskeleton to form filopodia and lamellipodia. CDC42 and Rac1 activate Pak which in turn phosphorylates and activate LIMK1 which phosphorylates and inhibits cofilin, preventing it from depolymerising actin. Rac1 also activates WAVE which in turn activates Arp2/3. RhoA phosphorylates ROCK 1 and 2 which phosphorylates and activates LIMK2 which in turn phosphorylates and inhibits cofilin. ROCK also phosphorylates and inactivates MLCP which in its active form would signal through MELC, MyHC and myosin II to induce formation of stress fibres. All three of the RhoGTPases activate the diaphanous (Dia) proteins which contribute to the formation of filopodia, lamellipodia and stress fibres. Adapted from (Taylor *et al.*, 2011)

1.3 Coronin

Coronin was first identified as a 55KDa protein in *Dictyostelium discoideum*. It was named coronin due to its localisation to crown-like extensions of the dorsal surface of cells (De Hostos *et al.*, 1991). Coronins have since been discovered in all fungi

59

and animals examined with over 700 different coronin proteins found in over 350 different species, however none have been found in true plants (it is present in brown algae) (Eckert *et al.*, 2011) or distant protists (Clemen, 2013). All coronin proteins consists of 3 to 10 WD (tryptophan and aspartic acid) repeat domains which are in either 1 domain for coronins 1-6 or 2 separate domains for coronin 7 (Rybakin & Clemen, 2005). Coronins can bind actin and can modulate a variety of actin mediated cellular processes including cytokinesis, phagocytosis, macropinocytosis and cell locomotion (Uetrecht & Bear, 2006).

1.3.1 Coronin nomenclature and genes

There have been several approaches of nomenclature proposed for coronins (Morgan & Fernandez, 2008). To avoid confusion, this report will exclusively use the nomenclature summarised in **Table 1.1**.

Interestingly almost all of the 7 mammalian coronins are found on different chromosomes in both mice and humans. The only exceptions are coronins 1 and 7 which are both on chromosome 16 in humans. The lengths of the primary isoform of coronins are similar in humans and mice (**Table 1.1**). Most coronin genes can be alternatively spliced into multiple isoforms in humans and the NCBI protein database lists at least 14 coronin proteins in total for humans (Geer *et al.*, 2009).

Table 1.1 – Summary of the nomenclature, synonyms, chromosomal locations and lengths of human and murine coronin proteins

Protein name	Synonyms	Gene name (humans)	Chromosome (humans)	Length (humans) (amino acids)	Gene name (mice)	Chromosome (mice)	Length (mice) (amino acids)
Coronin 1	Coronin 1A, CORO1A, clabp, clipin A, p57, TACO, CRN4	CORO1A	16	461	Coro1a	7	461
Coronin 2	Coronin 1B, p66, CORO1B. coroninse, CRN1	CORO1B	11	489	Coro1b	19	484
Coronin 3	Coronin 1C, CORO1C, HCRNN4, CRN2	CORO1C	12	474	Coro1c	5	474
Coronin 4	Coronin 2A, CORO2A, clipinB, IR10, WDR2, CRN5	CORO2A	9	525	Coro2a	4	524
Coronin 5	Coronin 2B, CORO2B, clipinC, CRN6	CORO2B	15	480	Coro2b	9	480
Coronin 6	ClipinE	CORO6	17	472	Coro6	11	471
Coronin 7	Coronin 7, crn7, POD1, p70	CORO7	16	925	Coro7	16	922

1.3.2 Mammalian coronins

Mammalian coronins can be divided into two superfamilies: long and short coronins. These two superfamilies in mammals can be further divided into three types. Type 1 comprises of the short coronins 1, 2 and 3. Type 2 comprises of the short coronins 4, 5 and 6. Type 3 is comprised of only coronin 7, known as tandem coronin (Eckert *et al.*, 2011). Type 2 coronins are unique to vertebrates and differ relative to type 1 coronins in the last ~200 amino acids of the C terminal and also in the loop between WD repeats 2 and 3. The WD repeat domains form a 7-bladed β-propeller region which is crucial for the structure and function of the protein (Uetrecht & Bear, 2006). Short coronins have 12 highly conserved and highly basic amino acids at the N

terminus which are unique to coronins and can be considered a coronin signature (Oku *et al.*, 2003). They are likely involved in a function unique to coronin (Eckert *et al.*, 2011). In the longer coronins, this signature is reduced to 5 amino acids in front of the core domain (Oku *et al.*, 2003). This N-terminal sequence also contains a phosphorylation site which in rat coronin 1B is at serine 2 (Cai *et al.*, 2005).

Coronin 7, which is relatively structurally dissimilar to the other mammalian coronins. It contains two complete copies of the propeller and extensions segments but lacks the coiled domain. As the coiled domain is required for homo-oligomerisation, a lack of the domains may eliminate the need for homo-oligomerisation. Coronin 7 also contains a C-terminal acidic domain which is homologous to that found in SCAR/WASP proteins (Uetrecht & Bear, 2006). The structures of the seven human coronin proteins are summarised (**Figure 1.11**) (Pieters *et al.*, 2013).
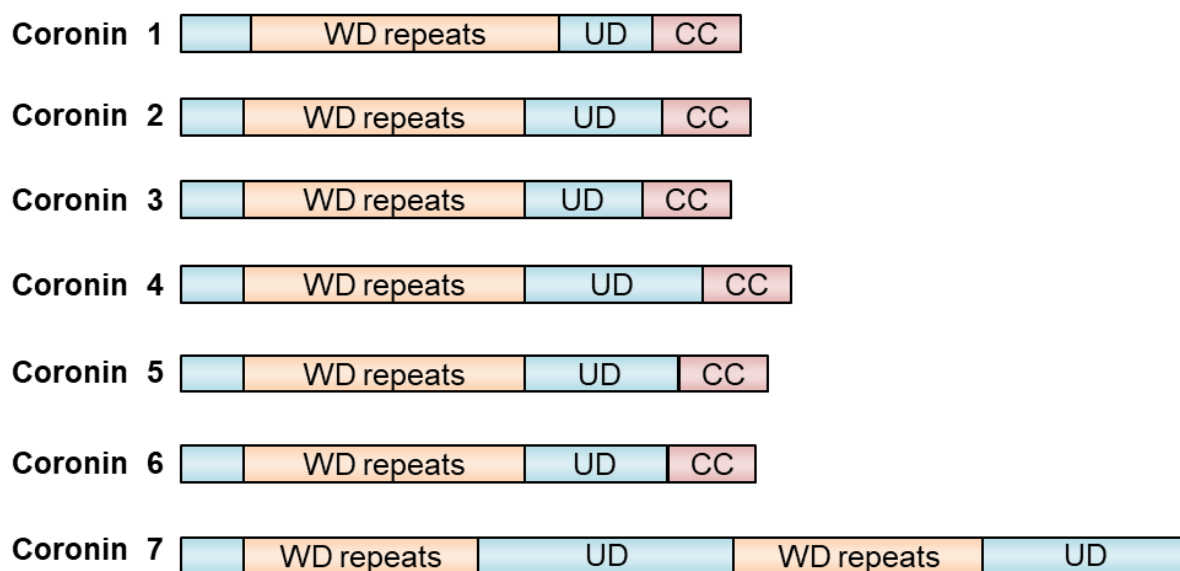
Figure 1.11 – The structure and relative length of 7 human coronin proteins
All 7 coronins have at least one 7-bladed propeller domain which contains 5 canonical and 2 non-canonical WD repeats (orange) and a unique domain (UD) (blue) Coronins 1-6 have a coiled-coil (CC) (red). Redrawn from (Pieters *et al.*, 2013).

1.3.2.1 Mammalian coronins similarity

Since the initial discovery in *Dictyostelium discoideum*, coronins have been discovered in many animals and fungi. Mammalian coronin proteins have 60% similarity and there is 30% similarity of coronins between all organisms. The similarity is highest at the N terminal and the WD repeats. The similarity is lowest at the regions flanking the WD repeats and at the coil at the C-terminus (De Hostos, 1999). The fourth repeat of the third propeller blade represents another region of variability (De Hostos, 1999).

The unique region and C terminal represent the region responsible for cytoskeleton interaction (Gatfield *et al.*, 2005). Multiple regions of coronin 1 have been reported to bind to actin including the regions between amino acids 1-34, 111-204 (Oku *et al.* 2003) and 297-461 (Liu *et al.* 2006). The N terminal and β-propeller represents the region which can bind to the cell membrane with or without the presence of the C terminal domain (Gatfield *et al.*, 2005).

1.3.2.2 Coronin phylogenetics

A phylogenetic tree built from the 420 conserved amino acids of coronin 1-6 demonstrates that coronins are increasingly different from each other in the order they are named (**Figure 1.12**).
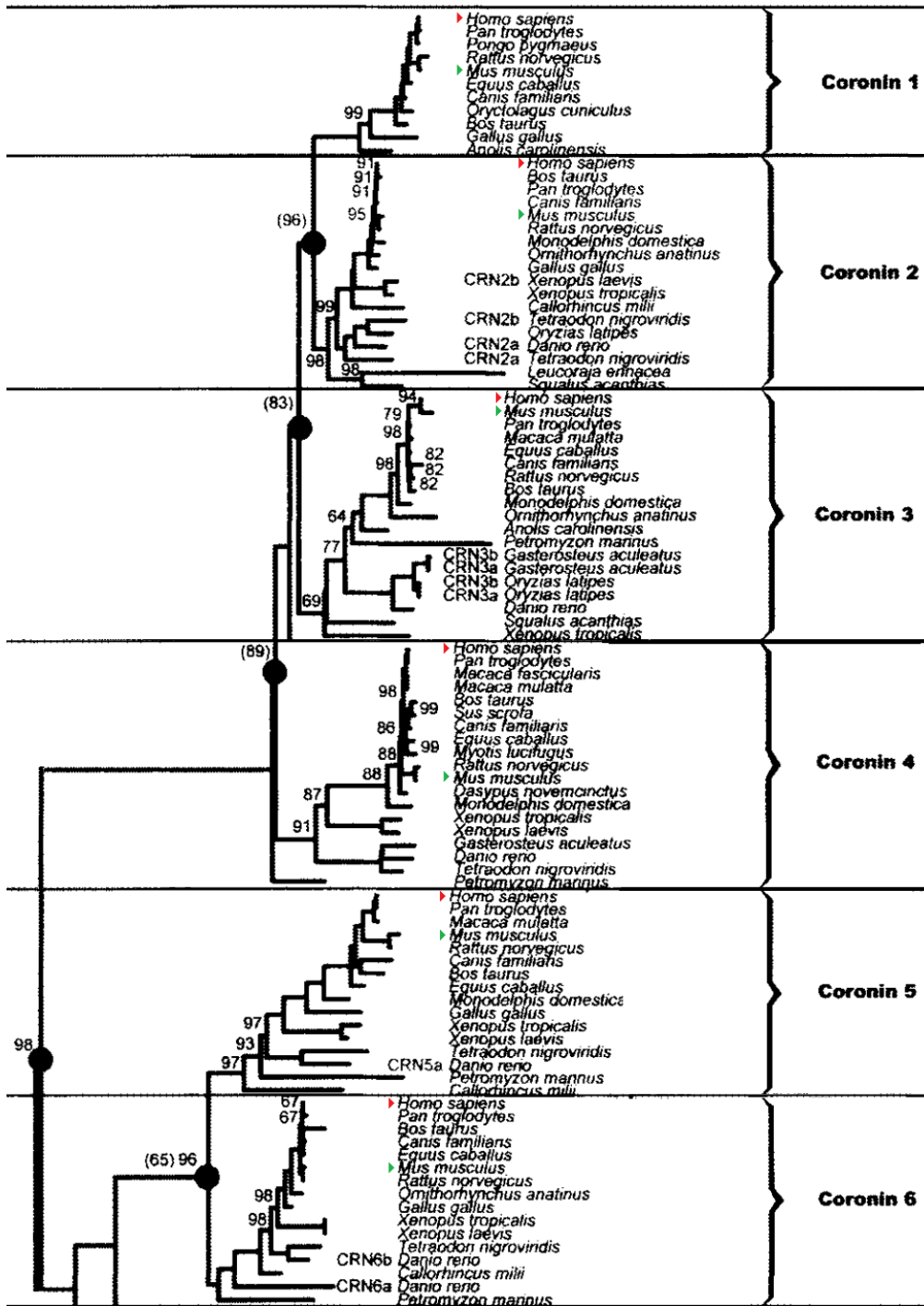
Figure 1.12 – Phylogenetic tree of vertebrate coronins 1-6

The phylogenetic tree was created using 420 amino acids of the conserved N-terminal region which excludes the coiled-coil domain. The tree was built by the neighbour-joining algorithm of MEGA4 using pairwise maximum likelihood distances. 5000 bootstrapped alignments were performed (shown as bootstrap percentages enclosed in brackets). Maximum likelihood values at nodes not in brackets. Red and green arrowheads indicate human and mouse coronins, respectively. Modified from Morgan & Fernandez, 2008.

64

1.3.3 Coronin structure

1.3.3.1 Murine coronin 1 crystal structure

When coronin was first discovered in *Dictyostelium discoideum* it was found to demonstrate a sequence similarity to the β subunits of G proteins (De Hostos *et al.*, 1991). Based on the structure of $G_β$ (Neer & Smith, 1996), the WD repeats were initially predicted to form a 5 bladed 'β-propeller-like structure' although a 7 bladed crystal structure was eventually determined for murine coronin 1 (**Figure 1.13**) (Appleton *et al.*, 2006). The coiled coil of in a single coronin protein is responsible for multimerisation into a homodimer (De Hostos 1999; Oku *et al.* 2005) or homotrimer (Gatfield *et al.*, 2005).

The crystal structure of murine coronin 1, which has 95% identity with human coronin 1, was published in 2006 at 1.75 A˚ resolution (**Figure 1.13**). A eukaryote expression system was utilised using High Five cells (ovarian cells of the cabbage looper, *Trichoplusia ni*), to preserve post translational modification and transfected with a virus to express murine coronin 1 (Appleton *et al.*, 2006). It was found that coronin has seven 'blades' on the 'propeller'. Five blades are due to a canonical WD repeats and this is then followed by two additional non-canonical WD-like repeats forming two additional propeller blades. The two additional blades lack apparent homology with the canonical WD40 repeat motifs and are atypical in both sequence and structure. The C terminal extension is tightly packed against the bottom of the propeller. Amino acids 1-392 of murine coronin 1 are conserved between coronins with 353-367 and 372-387 very highly conserved. It has been hypothesised that amino acids 1-392 may represent a folding region of the propeller with amino acids Tyr364 and Trp379 stabilising it. However, amino acids 392-428 are less conserved and represent a unique region within each coronin. The coiled coil domain, which is required for multimerisation and part of the function was omitted from the structure (**Figure 1.13**) (Appleton *et al.*, 2006).
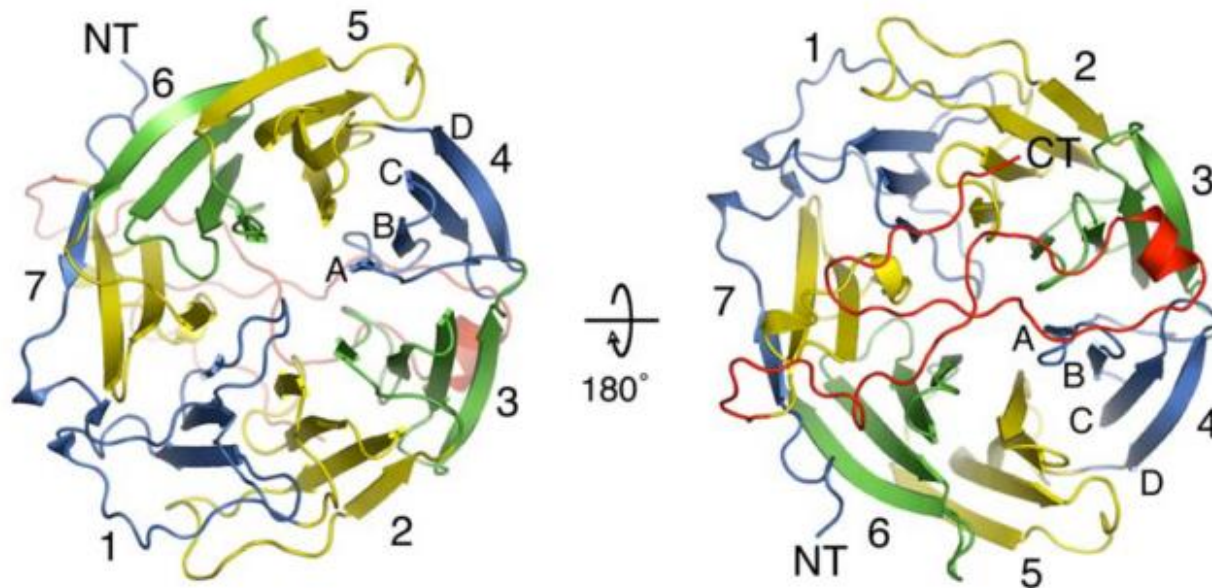
Figure 1.13 – Ribbon diagram of the crystal structure of murine coronin 1A
Viewed from the 'top' (left) and viewed from the 'bottom' (right). Amino acids 8 to 352 contain the seven 'propeller blades' labeled 1 to 7 and are in represented as yellow, green and blue. The C terminal extension is represented in red. Letters A, B, C and D represent the four β sheets of one propeller blade. CT and NT represent the locations of the C or N terminus respectively (Appleton *et al.*, 2006).

1.3.3.2 Coronin multimerisation

The crystal structure of coronin 1 was resolved with coronin lacking the C-terminal coiled-coil domain that contains a leucine zipper (**Figure 1.13**) which is required for some of the function and for multimerisation of coronin. Homodimers/homotrimers would be more difficult to crystallise than monomers (Appleton et al., 2006). The extent of multimerisation of proteins which contain a coiled-coil is very difficult to predict (Kammerer et al., 2005). By utilising bioinformatic tools such as SCORER (Woolfson & Alber, 1995) and MultiCoil (Wolf et al., 1997), coronin 1 was predicted, with a high degree of probability, to form a homodimer through the coiled coil region (Kammerer et al., 2005). There have been predictions that coronin 1 can form either a homodimer (Oku et al., 2005) or a homotrimer (Gatfield et al., 2005; Kammerer et al., 2005).

In the homotrimerisation model, the short 32 amino acid coiled-coil region on the C terminus of coronin 1 is responsible for forming a three stranded parallel 68

coiled-coil structure. At the other end of the protein, the β-propeller interacts with the plasma membrane, linking coronin to the plasma membrane in leukocytes (Gatfield et al., 2005). The state of homo-multimerisation in which coronins bind actin is unclear. The predominant hypothesis is that coronin trimerises. However one theory is that coronin can both dimerise or trimerise to bind actin, although multimerisation has only been observed in the absence of actin. An alternative theory is that two coronin molecules remain as monomers and utilise two separate actin-binding sites to crosslink actin filaments (Clemen, 2013).

1.3.3.3 Expression of coronins in humans and mice

Coronin 1 protein is very highly expressed in leukocytes (Ferrari *et al.*, 1999). Coronin 1 RNA and protein is also highly expressed in all hematopoietic and lymphoidal tissues which contain white blood cells such as the thymus, spleen, tonsils and bone marrow. It is also expressed to a lesser extent in neuronal tissues such as the adrenal gland (Nal *et al.*, 2004). Coronin 2 RNA and protein is highly expressed and coronin 3 to a lesser extent, in most tissues (Cai *et al.*, 2005). Coronin 4 is expressed in the gastrointestinal tract, bladder, lung and male reproductive tissues with lower expression in the epidermis (Uhlén *et al.*, 2015). Coronin 5 is expressed predominantly in the brain with lower expression in most other tissues (Nakamura *et al.*, 1999). Coronin 7 is expressed relatively highly in the thymus, spleen, brain, kidney with very low expression in most other tissues. Coronin 7 is localised to the cytosol and Golgi apparatus (Rybakin *et al.*, 2004). **Table 1.2** presents a brief summary of the expression pattern of coronins in human and murine tissues.

Coronins 1-3 are abundant in human (Burkhart *et al.*, 2012) and mouse platelets (Zeiler, *et al.* 2014) with a very small amount of coronin 7 present (Burkhart *et al.*, 2012; Zeiler *et al.*, 2014). A comprehensive review of proteomic data of the expression patterns of coronins 1-3 in human tissues and of both murine and human coronins 1-7 in platelets is presented in **Section 1.3.10.2**.

67

Table 1.2 - Summary of human coronin expression, synonyms and accession numbers. Adapted and modified from (Rybakin & Clemen, 2005).

Coronin	Accession no.	Human protein expression	References
1	NP_009005	Macrophages, thymus, spleen, bone marrow, lymph nodes, tonsils, peripheral leukocytes, , cerebral cortex, epidermis, lower expression in adrenal gland, platelets	(Ferrari *et al.*, 1999), (Nal *et al.*, 2004), (Uhlén *et al.*, 2015), Platelets : (Thiele *et al.*, 2016), (Burkhart *et al.*, 2012)
2	NP_065174	Gastrointestinal tract, spleen, bone marrow, lung, kidney, bladder, cerebellum, lower expression in most other tissues, platelets	(Cai *et al.*, 2005), (Uhlén *et al.*, 2015) Platelets: (Banfi *et al.*, 2010), (Burkhart *et al.*, 2012), (Ma *et al.*, 2011), (Thiele *et al.*, 2016)
3	NP_055140	All tissues including brain, adrenal & thyroid glands, lung, intestine, kidney, gastrointestinal tract, epidermis, lower expression in other tissues, platelets	(Cai *et al.*, 2005), (Uhlén *et al.*, 2015), Platelets: (Thiele *et al.*, 2016), (Burkhart *et al.*, 2012)
4	NP_438171	Colon, small intestine, stomach, gallbladder, bladder, testis, prostate, lung, lower expression in epidermis	(Uhlén *et al.*, 2015)
5	NP_006082	Brain, lower expression in most other tissues	(Nakamura *et al.*, 1999), (Uhlén *et al.*, 2015)
6	NP_116243	Very specific – heart, gallbladder, prostate, bladder and placenta	(Stelzer *et al.*, 2016)
7	NP_078811	Thymus, spleen, brain, kidney, lower expression in most other tissues subcellular cytosol and Golgi apparatus	(Rybakin *et al.*, 2004), (Uhlén *et al.*, 2015)

1.3.4 Coronin 1 subcellular location in mammalian cells

Coronin 1 is by far the most studied of the 7 human coronins. It is predominantly localised at the filamentous actin rich cell cortex and also is punctuated throughout the cytosol in human mast cells (**Figure 1.14A**) (Föger *et al.*, 2011) and neutrophils (**Figure 1.14B**) (Ming Yan *et al.*, 2007). Coronin 1 is also the 'leading edge' of murine T cells (**Figure 1.14C**) (Shiow *et al.*, 2008). Coronin 1 has been found localised at the plasma membrane and the F-actin rich cortex in J774 murine macrophages, human lymphocytes (Jurkat cells) and human embryonic kidney (HEK). Fractionation determined coronin 1 is membrane and cytosol-associated (**Figure 1.14D**) (Gatfield *et al.*, 2005).
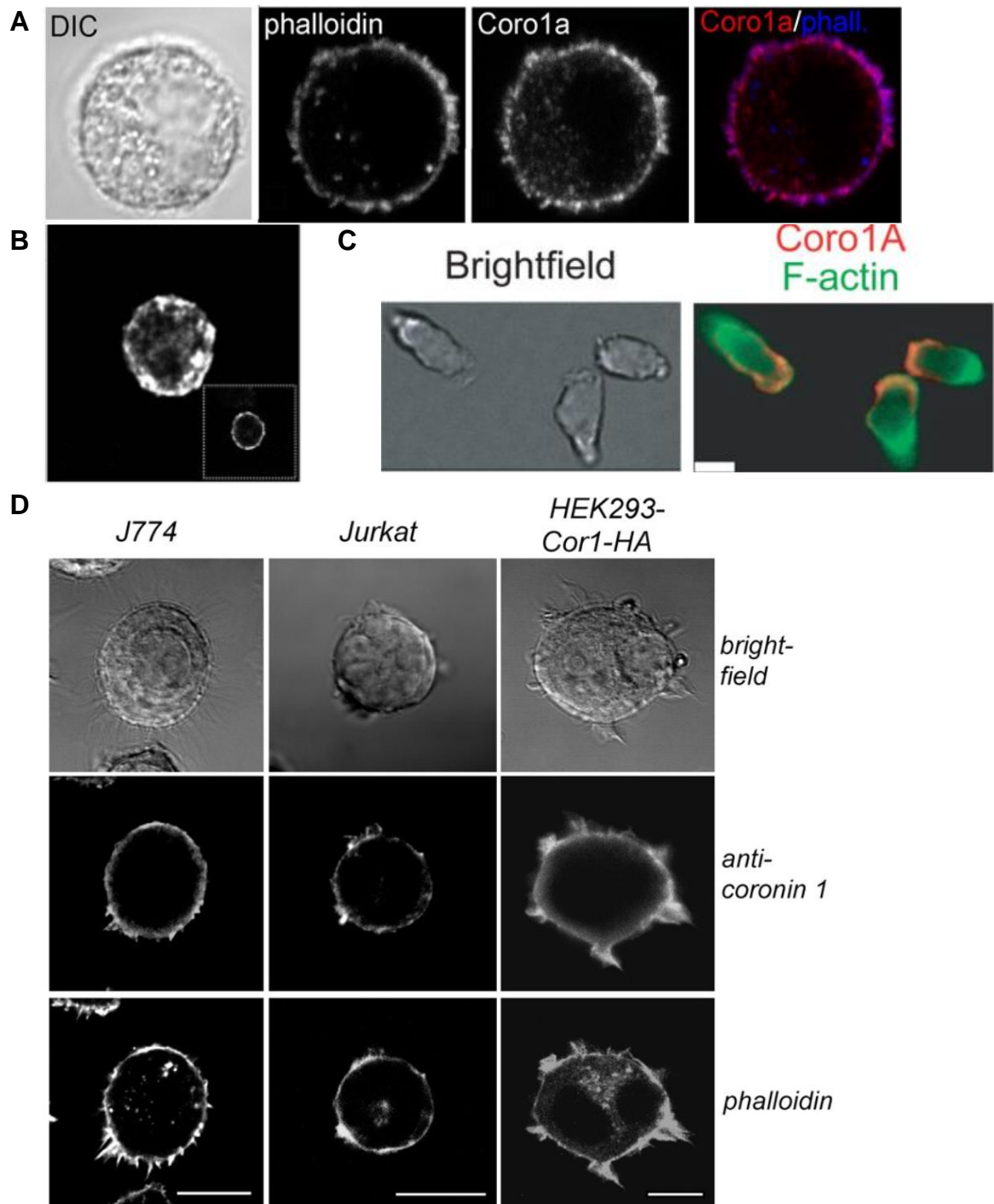
Figure 1.14 – Subcellular localisation of coronin 1
Coronin 1 is localised at the filamentous F-actin rich cell cortex in mast cells. Scale bar = 50 µm (**A**) (Föger *et al.*, 2011). (**B**) Human neutrophils (Ming Yan *et al.*, 2007) Coronin 1 is abundant at the leading edge of murine T cells (**C**) (Shiow *et al.*, 2008). Coronin 1 is located at the F-actin rich cortex in J774 murine macrophages, human lymphocytes (Jurkat cells) and HEK cells (**D**) (Gatfield *et al.*, 2005).

1.3.5 Coronin 2 localisation in mammalian cells

In murine fibroblasts (NIH3T3) and murine brain cell lines (bEnd.3), coronin 2 is mainly expressed in the cytoplasm and is also found at the peripheral regions of extending cells and punctuated throughout the cell cortex (**Figure 1.15A & B**) (Hsu *et al.*, 2013). In Michigan Cancer Foundation-7 (MCF-7) cells coronin 2 is punctuated throughout the cytosol, expressed strongly at the cell cortex and periphery of the nucleus but almost absent from the nucleus itself. Coronin 2 supports RhoA signaling at cell-cell junctions through myosin II. Coronin 2 known down is associated with aberrant cytosolic F-actin and E-cadherin accumulation and a lack of their presence at the cell cortex (**Figure 1.15C**) (Priya *et al.*, 2016)**.**
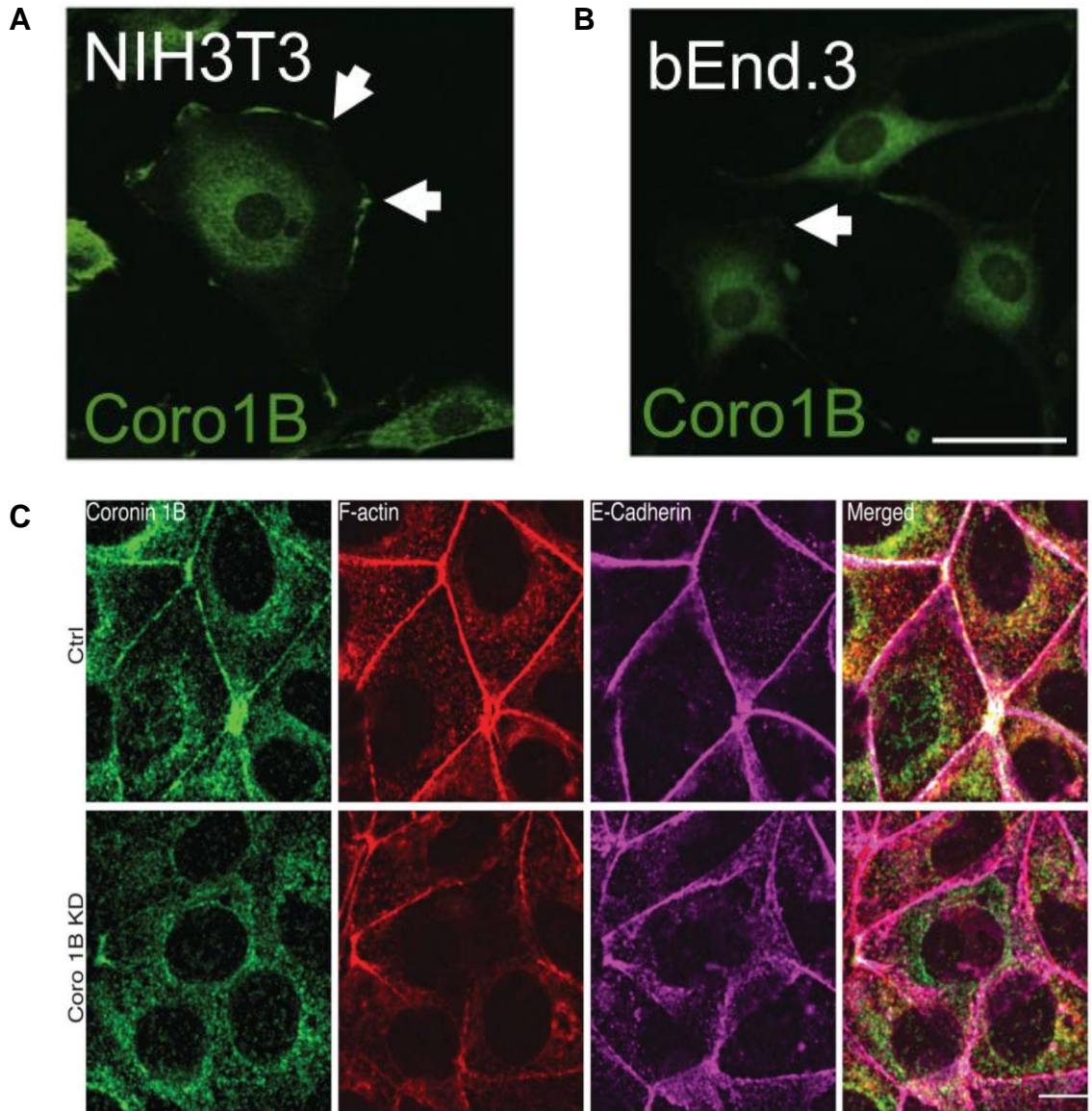
Figure 1.15 - Subcellular localisation of coronin 2 in mammalian cells
(**A**) Murine fibroblasts (NIH3T3). (**B**) Murine brain cell line (bEnd.3). Arrowheads indicated strong coronin 1 staining in crown-like structures (Hsu *et al.*, 2013). (**C**) **MCF-7 control and CORO1B knock down cells stained for coronin 2, F-actin and E-cadherin.** Scale bar = 10 µm (Priya *et al.*, 2016).

1.3.6 Coronin 3 localisation in mammalian cells

In human and murine fibroblasts, coronin 1 is visible at filamentous and punctuated structures in the cytoplasm. It is also enriched around the periphery of the nucleus, the cell cortex and in lamellipodia and filopodia (**Figure 1.16A** & **B**) (Spoerl *et al.*, 2002). Coronin 3 colocalises very strongly with F-actin stress fibres in fibroblasts. Coronin 3 also colocalises in a punctuated manner with tubulin and vimentin along the respective networks (**Figure 1.16C**) (Behrens *et al.*, 2016). Coronin 3 is also found spread diffusely around the cytoplasm of HEK cells and demonstrates strong colocalisation to E-cadherin except at the nucleus (**Figure 1.16D**). Coronin 3 demonstrates colocalisation to F-actin structures including at the cell cortex (**Figure 1.16E**) (Spoerl *et al.*, 2002).
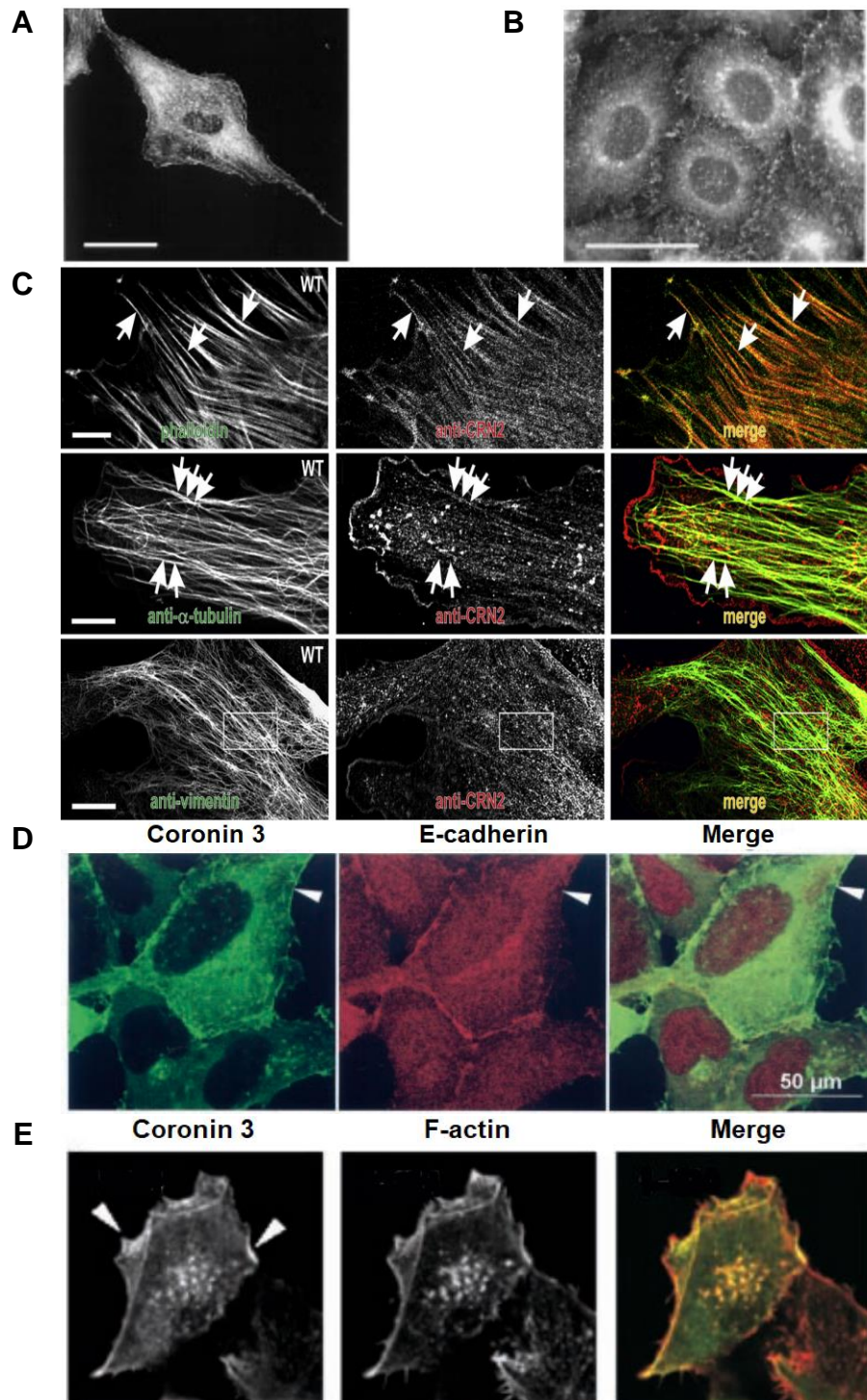
Figure 1.16 – Subcellular localisation of coronin 3 in mammalian cells
Cells stained for coronin 1. (**A**) Human fibroblasts and (**B**) Murine fibroblasts.
Scale bar = 50 µm. (**C**) Murine fibroblasts stained for actin, tubulin, vimentin and
coronin 3. Scale bar = 10 µm. Arrows indicate colocalisation (Behrens *et al.*,
2016). (**D**) HEK cells stained for coronin 3 and E-cadherin. (**E**) HEK cells fixed
and permeabilised with Triton X-100 then stained for coronin 3 and F-actin. Arrow
heads indicate cortical colocalisation with coronin 3 (Spoerl *et al.*, 2002).

73

1.3.7 Coronin regulates the cytoskeleton

1.3.7.1 Interaction of coronin with F-actin

Coronin regulates the actin cytoskeleton through interactions with F-actin, cofilin and the Arp2/3 complex (Gandhi & Goode, 2008). Coronins are involved in modulation of actin and cell cytoskeletal dynamics (Uetrecht & Bear, 2006). As soon as coronins were discovered they were known to be associated with actin. Coronin A from *Dictyostelium discoideum* was first discovered by extraction and purification of actin-myosin complexes and where it co-sediments with F-actin (De Hostos *et al*. 1991; De Hostos *et al*. 1993). Early in coronin research, coronin 1 was found to colocalise with F-actin in phagocytic cups (Maniak *et al*. 1995) and macropinosomes (Fukui *et al*., 1999; Hacker *et al*., 1997). The positively charged region of coronin 1 between amino acids 400-416 is one of the regions responsible for its interaction with the F-actin cytoskeleton (Gatfield *et al*., 2005). Transfection of coronin 1 into a murine macrophage cell line (RAW 264) has been found to cause a rapid and transient association of coronin 1 with phagosomes. It has also been found that coronin 1 is required for an early step of phagosome formation which is consistent with its role as an actin polymerisation regulator (Yan *et al*. 2005). It is accepted that all coronins, except coronin 7, bind to and localise with F actin (Clemen, 2013).

A surface exposed arginine at position 30 (Arg30) of coronin 2 has been found to be responsible for F-actin binding. Coronin 2 has been found to bind to ATP–F-actin with a high affinity and ADP-F-actin with a lower affinity. A point mutation at the Arg30 of coronin 2 results in an inability to bind F-actin and an impaired ability to localise to the leading edge of the cell (Cai, Makhov, *et al*., 2007).

Coronins 2 and 3 are recruited to the actin tail of the *vaccinia* virus. Knock down of either or both of these coronins results in a longer actin tail although this has no effect on the speed of the virus. This is consistent with the role of coronin in actin disassembly and is also an example of redundancy between coronins (Rottner & Stradal, 2015).

1.3.7.2 Coronins interact with the Arp2/3 complex and cofilin

Coronins 1 and 2 have been found to co-localise with the Arp2/3 complex in several cell types (Cai *et al*., 2005). Coronin 1 and 2 bind to the Arp2/3 complex to stabilise its inactive form and inhibit its nucleating activity (Cai, Marshall, *et al*., 2007; Uetrecht & Bear, 2006) in contrast to most other known actin binding proteins of the WASP family which bind to and activate the Arp2/3 complex (Pollitt & Insall, 2009). This suggests that coronins are involved in the modulation of actin processes by means of Arp2/3 downregulation (Welch & Mullins, 2002). However, paradoxically, coronins activate processes which are Arp2/3 dependent such as cellular motility (Clemen, 2013). Studying the effects of coronin on actin is complicated as it functions in synergy with other Arp2/3 regulators to control actin remodeling.

Coronin 2 can simultaneously form a complex with Arp2/3 and Slingshot phosphatase (SSHI), bridging the gap between them. SSHIL is a regulator of actin turnover and actin filament formation which acts on cofilin. SSHIL can dephosphorylate both cofilin and coronin 2. Dephosphorylation of ser3 on cofilin increase its F-actin binding and severing. Dephosphorylation of ser2 on coronin 2 enables its interaction with the Arp2/3 complex (Cai *et al*., 2005; Cai *et al*., 2007). Different cells types have different ratios of Arp2/3 variants and coronin may also be able to distinguish between Arp2/3 variants (Rottner & Stradal, 2015). However it is not yet clear how this may regulate their activity.

A model has been proposed of the role of coronin 1 in modulating the cytoskeleton which is spatially regulated and depends on the location of coronin with regards to ADP and ATP-bound actin. At the front of the actin network, coronin protects new ATP rich filaments from disassembly by cofilin and coronin also recruits Arp2/3 to filament sides, leading to nucleation, branching and network expansion. However at the rear of the networks coronin functions very differently as it cooperates with cofilin to disassemble old ADP-rich actin filaments, recycling actin monomers for polymerisation (**Figure 1.17**) (Gandhi & Goode, 2008).
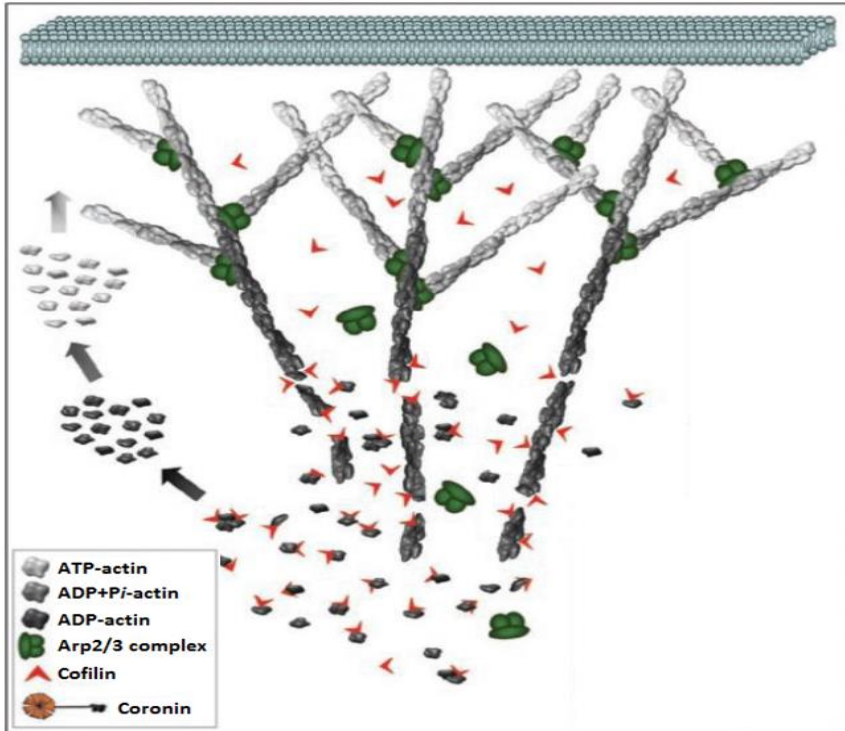
Figure 1.17 - Interaction of coronin with the Arp 2/3 complex and cofilin
Coronin binds to ATP-bound actin at the front of the network, protecting it from severing from cofilin and recruits Arp 2/3 to promote branching. At the rear of the network, coronin binds to ADP-actin and increases actin severing by cofilin to recycle actin monomers for actin polymerisation.
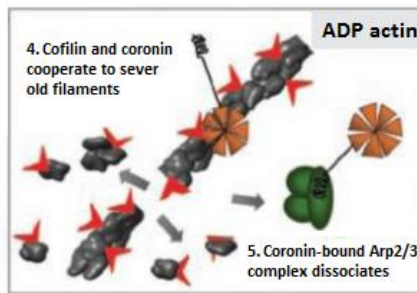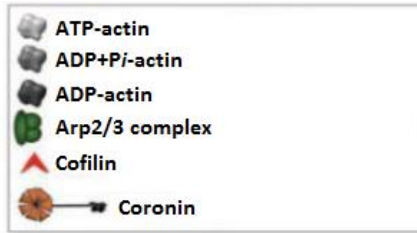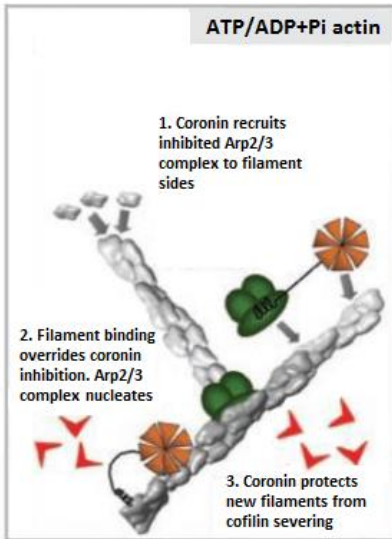
1.3.8 Life without coronin

One way to investigate the roles of a protein is to disrupt or remove the protein. This section briefly summarises disruption studies on coronin in *Dictyostelium* then focuses on coronin 1 disruption studies performed on white blood cells and neurons which are summarised in **Table 1.3**.

The first studies on coronin were performed in *Dictyostelium* discoideum (De Hostos *et al.*, 1993). Since then 3 coronins have been found in *Dictyostelium* – an ortholog of coronin 7, a class 4 coronin (Eckert *et al.*, 2011) and a villidin coronin (Gloss *et al.*, 2003). *Dictyostelium* mutants lacking a coronin ortholog have been found to demonstrate impaired cell motility, phagocytosis and cytokinesis. The cells multiply slowly and also some become multinucleate (De Hostos *et al.*, 1993). Coronin null *Dictyostelium* mutants also demonstrate a significant impairment or complete abolishment of macropinocytosis (Hacker *et al.*, 1997). These impairments can be associated with localised coronin expression which is enriched in the leading edge of cells and in phagocytic cups (De Hostos *et al.*, 1993).

Table 1.3 - Summary of phenotypes arising from coronin 1 mutations

Cell type	Type	Phenotype	Reference
T lymphocytes	Mouse *Coro1a KO*	• Higher basal T lymphocyte F-actin levels. • Lower CCL19-induced F-actin formation. • Defect in SDF1a-mediated Rac1 activation. • Unaffected Erk, Rsk and Akt pathways. • Defect in uropod development and irregular talin clusters at cell cortex. • Dispensable for T cell migration. T cell deficiency.	(Föger *et al.*, 2006)
Macrophages, whole animal,	Mouse *Coro1a* KO	• *Coro1a* is required for the survival of mycobacteria by blocking lysosomal delivery by the calcineurin pathway. • *Coro1a* is dispensable for phagocytosis, motility, and membrane ruffling in macrophages • Peripheral T cell deficiency.	(Jayachandran *et al.*, 2007).

		• No change in macrophage phagocytosis or cell locomotion.	
T cells, B cells, whole animal	Mouse *Coro1a* nonsense mutation	• Lack of development of systemic lupus erythematosus. • Reduced T-dependent humoral responses. • Reduced T cell migration. • T cell deficiency. • No detectable intrinsic B cell defects.	(Haraldsson *et al.*, 2008)
Neutrophils	Mouse *Coro1a* KO	• No neutrophil development abnormalities. • No defects in adherence, membrane dynamics, migration, phagocytosis and oxidative burst.	(Combaluzier & Pieters, 2009)
T cells	Mouse *Coro1a* E26K mutation	• T cell deficiency. • Enhanced Arp2/3 inhibition and mislocalisation away from the leading edge.	(Shiow *et al.*, 2008)
Fibroblasts	Mouse *Coro1a* E26K mutation	• No change in actin cytoskeleton.	(Shiow *et al.*, 2008)
T cells, B cells, NK cells, whole body	Human mutation of coronin 1 gene – 2 bp in gene and deletion of the other	• T cell deficiency. • Severe combined immune deficiency. • Normal B cells and NK cells.	(Shiow *et al.*, 2009)
T cells	Mouse *Coro1a* E26K mutation	• T cell deficiency. • Impaired platelet survival. • Deficient calcium/calcineurin signalling.	(Mueller, *et al.*, 2011)
Mast cells, whole animal	Mouse *Coro1a* KO	• Bone marrow derived mast cells exhibit increased FcεRI-mediated degranulation of secretory lysosomes. • Significantly reduced secretion of cytokines. • Mice displayed enhanced passive cutaneous anaphylaxis	(Föger *et al.*, 2011)
Whole animal	Mouse *Coro1b* KO	• Mice displayed enhanced passive cutaneous anaphylaxis	(Föger *et al.*, 2011)
Mast cells, whole animal	Mouse *Coro1a* KO	• Bone marrow derived mast cells exhibit increased FcεRI-mediated	(Föger *et al.*, 2011)

	Coro1b KO (double KO)	degranulation of secretory lysosomes. • Significantly reduced secretion of cytokines. • Mice displayed enhanced passive cutaneous anaphylaxis	
Dendritic cells	Mouse Coro1a KO	• No change in antigen presentation and processing in dendritic cells.	(Westritschnig et al., 2013)
	Humans V134M mutation in the CORO1A gene	• Immunodeficiency, T cell deficiency and recurrent infections. • EBV-associated B-cell lymphoproliferation at around 1 year old.	(Moshous et al., 2013)
Neural cells	Mouse Coro1a KO	• Defects in cAMP and PKA signalling through Gαs. • Behavioural and cognition defects.	(Jayachandran et al., 2014)
Fibroblasts	Mouse Coro1c KO	• Disrupted actin cytoskeleton • Defects in vimentin network • Disrupted microtubule cytoskeleton • Mitochondria localisation abnormalities	(Behrens et al., 2016)
T cells, whole animal	Mouse Coro1a KO	• Coronin KO leads to a reduction in allograft rejection.	(Jayachandran et al., 2019)

1.3.8.1 Coronin 1 disruption results in T cell deficiency

Coronin 1 ablation is associated with a weakened immune system in both humans and mice (Shiow et al., 2008). In murine Coro1a$^{-/-}$ T lymphocytes, basal actin levels were higher than in Coro1a$^{+/+}$ cells. However chemokine (C-C motif) ligand 19 (CCL19)-induced F-actin formation was lower in Coro1a$^{-/-}$ cells than in the wild type. It was determined that coronin exerts an inhibitory effect on cellular steady-state F-actin formation in an Arp2/3 dependent manner. The cytoskeletal alterations of murine Coro1a$^{-/-}$ T cells also included a selective defect in SDF1a-mediated Rac1 activation; however the Erk, Rsk and Akt pathways were unaffected. In, WT murine T lymphocytes, stimulation with CCL19 results in the development of a polarised structure with unipolar accumulation of talin beneath the cell membrane and opposite to the uropod. Coro1a$^{-/-}$ T lymphocytes are impaired in the ability to develop uropods and demonstrate talin clusters irregularly around the cell cortex.

Coronin 1 also plays an important role in cell motility and chemokine-regulated migration of T lymphocytes to secondary lymphocyte organs. A loss of Coro1a is also associated with a deficiency in T cells which this study attributed to increased apoptosis associated with defects in the mitochondria potential due associated with increased F-actin levels (Föger *et al.*, 2006).

Systemic lupus erythematosus is an autoimmune disease affecting multiple organs, in which the sufferer produces autoantibodies to attack nuclear components of their own cells. In mice, a nonsense lmb3 mutation causes the loss of 3 blades and a loss of the constant region of the propeller region of the coronin 1 gene (*Coro1a*^{Lmb3}). This results in suppression of the autoimmune phenotype of systemic lupus erythematosus and result in an inability of the disease to develop; suggesting coronin 1 is involved in the disease. The mutation is also associated with developmental and functional alterations of T cells and reduced T-dependent humoral responses; however B cells appear to be unaffected. *Coro1a*^{Lmb3} is also associated with T cell deficiency (Haraldsson *et al.*, 2008).

Another study attributed the T cell deficiency of the Cataract Shionogi (CTS) strain of mice to an E26K (Glu to Lys) point mutation which affects the β-propeller domain of coronin 1 (Coro1A^{E26K}). These T cells demonstrated a migration defect which impaired thymic egress and trafficking of the cells through lymph nodes. This resulted in aberrant localisation of coronin 1 away from the leading edge of T cells, which reportedly resulted in an increased association with Arp2/3 complex and increased inhibition, despite that observation that Arp2/3 continued to concentrate at the leading edge. Coro1A^{E26K} T cells demonstrated large irregular protrusions due to a defect in actin cytoskeletal regulation (Shiow *et al.*, 2008).

Another study also found coronin 1 contributes to immune system homeostasis and its ablation lead to a lack of T cell survival (Mueller, *et al.*, 2011). However, this study found no differences in F-actin upon *Coro1a* ablation. The T-cell deficiency caused by coronin 1 ablation has been suggested to be due to defects in prosurvival signals in *Coro1a*$^{-/-}$ mice, rather than from T cell apoptosis due to F-actin turnover defects (Mueller, *et al.*, 2011). Calcineurin Aβ is required for the survival of naive T cells (Manicassamy *et al.*, 2008) and deficient

80

calcium/calcineurin signaling has been proposed as the cause of T cell deficiency upon coronin 1 ablation (Mueller, *et al.*, 2011).

The role of coronin 1 in the calcium/calcineurin pathway was found when it became clear that it is responsible for the survival of mycobacteria in macrophages. In *Coro1a$^{+/+}$* cells, coronin 1 binds to the phagosome and inhibits lysosomal delivery via the calcineurin pathway. In *Coro1a$^{-/-}$* cells the mycobacteria is delivered to the lysosome and destroyed. This study also found coronin 1 does not mediate the actin related processes of phagocytosis, macropinocytosis or cell locomotion in murine macrophages (Jayachandran *et al.*, 2007). Coronin 1 may be dispensable for F-actin dependent processes such as phagocytosis and cell locomotion in macrophages but is involved in calcium/calcineurin signaling which may also be the cause of T cell deficiency upon coronin 1 ablation.

Coronin 1 has been found to be involved in activation of stimulation-induced Ca^{2+}/calcineurin signalling pathway not only in T cells, but also in B cells and macrophages (Westritschnig *et al.*, 2013). As calcium signalling is important in platelets and coronin is present in platelets it is worth investigating this pathway in platelets.

1.3.8.2 Coronin 1 deficiency in humans leads to T cell deficiency and SCID

Coronin 1 is essential for the development of a functional T-cell compartment not only in mice, but also in humans. During the normal development of the murine thymus, mature thymocytes first upregulate sphingosine-1-phosphate receptor 1 (S1P$_1$). SIP$_1$ and its ligand SIP are required for migration of mature thymocytes towards the naïve T cell compartment. In one study, 16 patients with severe combined immunodeficiency (SCID) were analysed. In one patient there was a *de novo* deletion of one coronin allele and an inherited 2 bp mutation in exon 3 of the other allele, resulting in a missense and a premature stop codon resulting in a truncation, effectively resulting in a homozygous coronin deletion. Protein analysis found absence of coronin 1 in the patient. The patient presented atypical mild

severe SCID and was previously hospitalised at age 13 for post-vaccination varicellar infection. Similarly to the coronin 1 knockout mice, the patient also had low levels of T cells but normal levels of both B and natural killer cells ($T^-B^+NK^+$) which is atypical in SCID patients (Shiow *et al.*, 2008, 2009). SCID can be caused by at least 13 different gene mutations and the patients normally have an absence of a thymus (Tasher & Dalal, 2012). Unfortunately Shiow *et al.* (2008) did not perform mutation analysis for the other genes to rule out an effect from multiple genes in the patients.

Another study found 3 human siblings presenting with immunodeficiency, recurrent infections, T cell deficiency and EBV-associated B-cell lymphoproliferation at around 1 year old. These siblings had a V134M mutation in the CORO1A gene, mutating a residue in the β-propeller, completely ablating the proteins expression (Moshous *et al.*, 2013).

Interestingly, coronin 1 ablation also leads to a decrease in the chance of allograft rejection. This has been attributed to increased cAMP concentrations which suppresses allo-specific T cell responses (Jayachandran *et al.*, 2019) and also likely as a direct result of the impairment of the immune system from a reduced number of T cells

1.3.8.3 Coronin 1 mutations in other white blood cells

Coronin 1 mutations affect T cells, but appear redundant in most other WBCs. Coronin 1 is redundant in murine neutrophils and KO cells develop normally and show no defects in adherence, membrane dynamics, migration, phagocytosis and the oxidative burst (Combaluzier & Pieters, 2009).

Antigen processing and presentation by *Coro1a* knockout dendritic cells is normal and functions in the same way as the wild cells (Westritschnig *et al.*, 2013). This suggests redundancy of coronin 1 for this process.

Coronin 1 is involved in the activation of the Ca^{2+}/calcineurin signalling pathway, following cell surface stimulation in not only T cells, but also B cells and macrophages (Westritschnig *et al.*, 2013). As calcium signalling is important in

platelets and coronin is present in platelets it is worth investigating potential defects which could be caused by *Coro1a* ablation.

1.3.8.4 Coronin 1 and 2 double knockout mast cells

Bone marrow derived mast cells from $Coro1a^{-/-}$ mice exhibited increased FcεRI-mediated degranulation of secretory lysosomes. They also demonstrated significantly reduced secretion of cytokines and the mice displayed enhanced passive cutaneous anaphylaxis. They hyperdegranulation phenotype was increased in $Coro1a^{-/-}/Coro1b^{-/-}$ double knockout mice. However $Coro1b^{-/-}$ mice did not display the degranulation defects but did display the enhanced passive cutaneous anaphylaxis phenotype (Föger *et al.*, 2011).

1.3.8.5 Coronin 2 is required for lamellipodia function

In murine fibroblasts, both coronin 2 and cortactin have been reported to be required for normal dynamics of lamellipodial actin. Using kymographs, it was found knockdown of either protein resulted in a decreased the distance of cell travel and the retrograde flow of actin. This is consistent with the function of coronin 2 of interacting with Arp2/3 to contribute to lamellipodia formation and actin dynamics (Cai *et al.*, 2008).

1.3.8.6 Coronin 3 ablation affects F-actin, vimentin and tubulin networks

Coronin 3 is the least studied of the class 1 coronins. It is a substrate of casein kinase II (CK2), which phosphorylates it on the coiled coil C-terminal at Ser463. This results in coronin 3 losing its ability to inhibit actin polymerisation, bundle actin filaments and bind to Arp2/3 (Xavier *et al.*, 2012).

In murine fibroblasts, coronin 3 strongly colcoalises with F-actin and only sporadically colocalises with vimentin and tubulin in a punctuated manner. Despite this, the ablation of coronin 3 not only disrupted the actin cytoskeleton, but also

83

caused major disruption to the vimentin intermediate filaments and microtubule networks (**Figure 1.18**). The KO cells demonstrated shorter, thinner, less bundled and less parallel stress fibres compared to WT (**Figure 1.18A**). In KO cells the vimentin filaments were much less visible, thinner and more tightly packed than the WT (**Figure 1.18B**). The KO cells also demonstrated disorganized, overlapping directions of microtubules, whereas the WT cells tended to have microtubules pointed from the center to the periphery of the cells (**Figure 18C**). The *Coro1c*$^{-/-}$ fibroblasts demonstrated a reduced proliferation rate, impaired cell migration and defects in protrusion formation. In addition, the mitochondria were affects and demonstrated aberrant subcellular localisation and defects in function (Behrens *et al.*, 2016).

WT   **Coronin 3 KO**

A

phalloidin

B

anti-vimentin

C

DAPI
anti-α-tubulin   anti-γ-tubulin
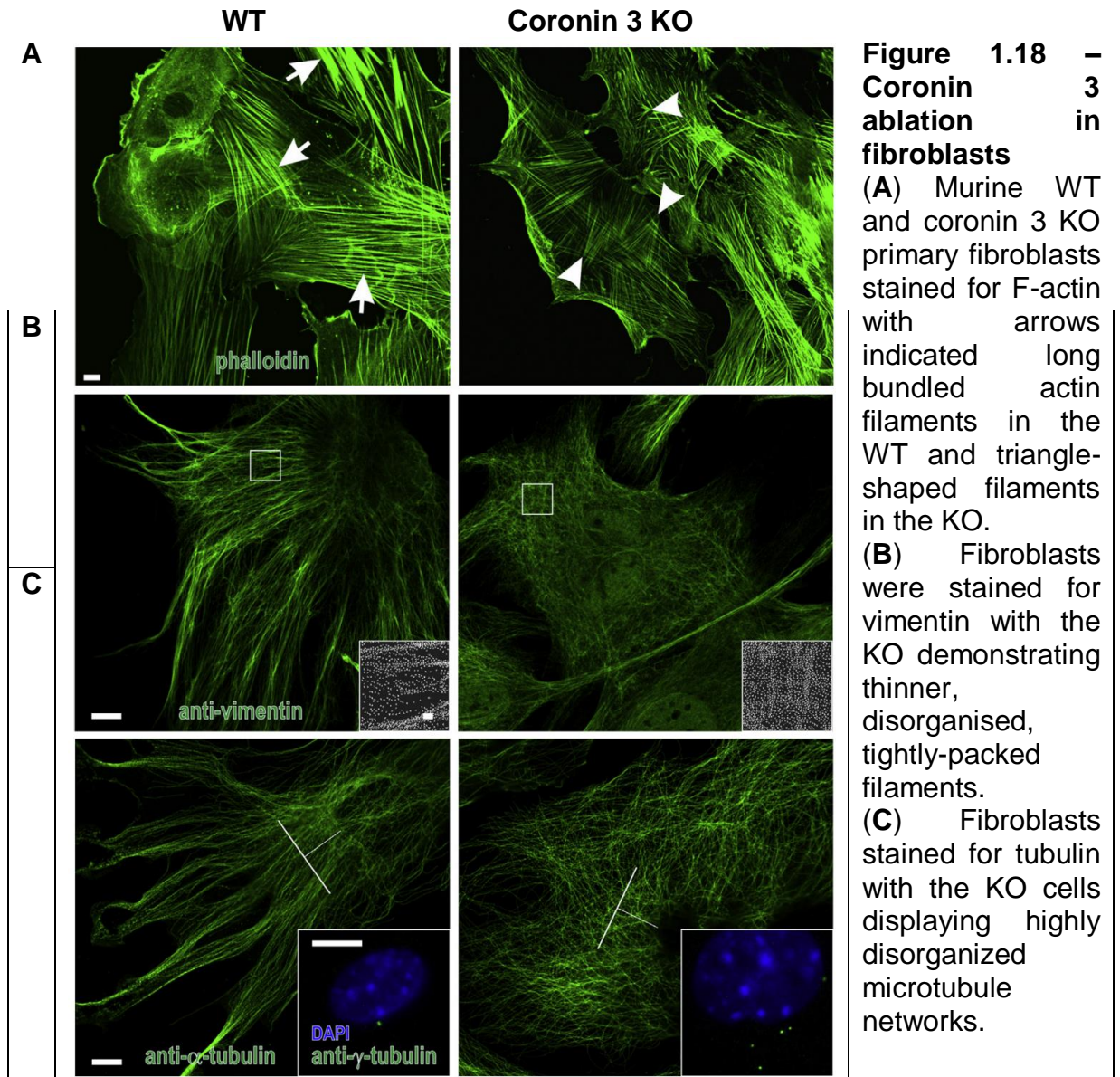
Figure 1.18 – Coronin 3 ablation in fibroblasts
(**A**) Murine WT and coronin 3 KO primary fibroblasts stained for F-actin with arrows indicated long bundled actin filaments in the WT and triangle-shaped filaments in the KO.
(**B**) Fibroblasts were stained for vimentin with the KO demonstrating thinner, disorganised, tightly-packed filaments.
(**C**) Fibroblasts stained for tubulin with the KO cells displaying highly disorganized microtubule networks.

1.3.9 Roles of coronin in signalling

Coronin is involved in a plethora of signalling pathways including Rho (Castro-Castro *et al.*, 2011), PKC (Föger *et al.*, 2011), PKA (Jayachandran *et al.*, 2014), calcium/calcineurin (Mueller *et al.*, 2008) and integrin β2 (Pick *et al.*, 2017). As mentioned in **Section 1.1.4.2**, Rho, PKC, PKA and calcium/calcineurin are important in platelet activation and spreading (van der Meijden & Heemskerk, 2019). Integrin β2 is less studied and appears to be important for platelet lifespan (Piguet

et al., 2001) and binding to intercellular adhesion molecule 1 (ICAM1) bearing cells (Philippeaux *et al.*, 1996). It is also worth noting that coronin 3 has been predicted to be a substrate of the tyrosine protein kinase FYN (Amano *et al.*, 2015) which is involved in GPVI signalling, although this does not appear to have been investigated in detail.

1.3.9.1 Coronin regulates Rho signalling

As mentioned in **Section 1.2.2.9**, Rho GTPases are regulators of platelet cytoskeleton and function with RhoA, CDC42 and Rac1 being particularly important regulators of the actin cytoskeleton (Aslan & McCarty, 2013). Platelet functions including spreading, lamellipodia formation and aggregation require reorganisation of the cytoskeleton (Hall, 1998).

Dictyostelium coronin contains a CDC42 and Rac-interactive binding (CRIB) motif between blades 2 and 3. This enables it to bind Rho GTPases with a preference for GTP loaded Rac. Mutation of the domain abrogates Rac binding and coronin deficient cells demonstrate a defect in myosin II assembly. (Swaminathan *et al.*, 2013)

While mammalian coronins haven't been reported to contain a CRIB domain, they do contribute to Rho signalling through other means. Coronin 1 is a regulator of Rac1 and facilitates Rac1 translocation and activation. Activation of Rac1 during cell signalling includes its translocation from the cytosol to membranes, release from sequestering Rho GDP dissociation inhibitors and GDP/GTP exchange. Coronin 1 and the Rac1 exchange factor ArhGEF7 contribute to a downstream, cytoskeletal-based feedback loop that is required for optimal Rac1 activation. Upon Rac1 mediated actin polymerisation, coronin and ArhGEF7 form a cytosolic complex that translocates to membranes and increases the levels of activated membrane-bound Rac1. This also involves Pak1 and RhoGDIa that form complex with coronin 1, which mediated by ArhGEF7, promotes the Pak1-dependent dissociation of Rac1 from the Rac1/RhoGDIa complex, contributing to Rac1 activation (Castro-Castro *et al.*, 2011).

86

Xenopus coronin, called Xcoronin is localised at the leading edges of lamellipodia during spreading in murine 3T3 fibroblasts. In these cells, truncated Xcoronin resulted in an impairment of spreading and an inability to form Rac induced lamellipodia. However Xenopus coronin is only 63% identical to human coronin (Mishima & Nishida, 1999).

Non-muscle myosin II (NMII) contributes to the generation of contractile forces in eukaryotic non-muscle cells. NMII accumulation and stability at specific subcellular locations, such as cell junctions, contributes to the formation of a zone of Rho signalling. In MCF-7 cells, knock down of coronin 2 results in disrupted non-muscle myosin IIA and IIB localisation away from cell junctions. This resulted in defects in RhoA signaling due to an enhanced recruitment of the RhoA p190B Rho GAP at the cell junctions. This leads to a lack of signalling and NM!!-mediated junction-localisation of downstream ROCK1 which is turns leads to a lack of NMII phosphorylation. This shows that coronin 2 can support RhoA signaling at cell junctions through myosin II (Priya *et al.*, 2016).

Further support for coronins as regulators of Rho signalling come from studies on coronin 3. Knockdown of coronin 3 reduces fibroblast migration which presents as defects in wound healing (Williamson *et al.*, 2014). This has been attributed to coronin 3-mediated Rac1 recycling as coronin retrieves inactive Rac1 from the rear and sides of fibroblasts for redistribution or degradation. Coronin 3 also binds to regulator Of Chromosome Condensation 2 (RCC2) as well as Rac1 and this interaction may enrich GTP-Rac1 at membrane protrusions (Williamson *et al.*, 2015).

1.3.9.2 Coronin signalling through protein kinase C

Coronin 1 and 2 can both be regulated by phosphorylation of Ser2 which can be phosphorylated by PKC. In wild type murine bone marrow-derived mast cells, coronin 1 demonstrates strong localisation to the F-actin rich cell cortex and is found in the detergent-insoluble cytoskeleton pellet. The *Coro1a*-S2A mutant, which cannot be phosphorylated at Ser2, demonstrated the same localisation. In contrast,

the phosphomimetic *Coro1a*-S2D mutant demonstrated no Arp2/3 activity and was found in the Triton soluble fraction and demonstrated reduced cortical staining (Föger *et al.*, 2011). As mentioned previously, PKC is important in platelet shape change (see **Section 1.1.4.2**). Due to the regulation of coronin 1 and 2 by PKC it is possible that coronins may be involved in this pathway.

Coronin 2 function can also be modulated by phosphorylation by PKC (Cai *et al.*, 2005). Disruption studies have been carried out in rat fibroblasts of the phosphorylation site on rat coronin 2 by mutating the Ser2 to an alanine (S2A mutant), which can't be phosphorylated. These mutants demonstrate increased ruffling induced by phorbol 12-myristate 13-acetate (PMA) and also increased speed during single cell tracking assays. The serine at the phosphorylation site of coronin 2 has also been mutated to an aspartic acid to mimic phosphorylated coronin 2, termed S2D mutant. In contrast to the S2A loss of function mutant, the S2D mutant demonstrated attenuated PMA-induced ruffling and slower cell speed (Cai *et al.*, 2005). This suggests phosphorylation of coronin is important in regulating cell motility.

In murine T cells, coronin 1 can recruit PKCθ. The WD40 domains of coronin 1 can bind to the C2-like domain of PKCθ. Overexpression of coronin 1 reduced the recruitment of PKCθ to both the lipid rafts and plasma membrane upon CD3/CD28-activation (Siegmund *et al.*, 2015). In platelets, PKCθ activation occurs downstream of the PAR, GPVI and αIIbβ3 receptors (Cohen *et al.*, 2011). PKCθ$^{-/-}$ mice demonstrated reduced static adhesion and filopodia generation on fibrinogen. They also demonstrated a significant increase GPVI-dependent a-granule secretion but dense granule secretion was at normal levels. Thrombus formation on collagen under a flow rate of 1000^{-s} was also increased (Hall *et al.*, 2008).

1.3.9.3 Coronin signalling through cAMP and PKA

In murine neural cells, coronin 1 has been found to modulate cAMP and PKA signalling (Jayachandran *et al.*, 2014). Upon activation of neuron cell surface receptors, coronin 1 stimulates cAMP production and activation of protein kinase A

(PKA). A behavioral phenotype in coronin 1 knockout mice was recovered by addition of a membrane-permeable analogue of cAMP, providing further evidence for a link between the two signalling proteins (Jayachandran *et al.*, 2014). A study of coronin 1 in neurons found that in addition to having a phosphorylation site on Ser2, it also has phosphorylation sites at Thr418/424 which can be phosphorylated by cyclin-dependent kinase 5 (CDK5). This phosphorylation is responsible for the association of coronin 1 with Gαs and the modulation of cAMP production and the modulation of the PKA pathway (Liu *et al.*, 2016). As mentioned previously (see **Section 1.1.4.1**) cAMP is an important component of platelet inhibitory signalling. Therefore it may be possible that coronin effects platelet signalling through this route.

1.3.9.4 Coronin signalling with calcium

As mentioned previously (**see Section 1.3.8.2**), coronin 1 is essential for the survival of T cells. One of the mechanisms of this is mobilisation of Ca^{2+} from intracellular stores. The loss of coronin 1 results in a profound defect in Ca^{2+} mobilisation. Upon T cell triggering, coronin 1 has been found to interact with PLCγ1 and to be essential for the generation of IP_3 from PIP2. IP_3 is important for mobilisation of Ca^{2+} in T cells (Mueller *et al.*, 2008) and in platelets (Broos *et al.*, 2011).

In T cells, there is evidence that rather than modulating F-actin, coronin 1 is instead responsible for the activation of the Ca^{2+} dependent phosphatase calcineurin upon mycobacterial infection which prevents the lysosomal delivery of the bacteria. In T cells, coronin 1 also balances proapoptotic and antiapoptotic signals through regulation of Ca^{2+} and calcineurin activation in T cell receptor dependent manner (Mueller *et al.*, 2011). As this process is dependent on the T cell receptor it is possible that the process does not occur in platelets.

Interestingly, coronin 7 has been predicted to be a substrate of calcium/calmodulin dependent protein kinase I (Amano *et al.*, 2015). However this doesn't appear to have been investigated in detail.

1.3.9.5 Coronin signalling through integrin β2

As mentioned in **Section 1.1.3.2**, integrin β2 is responsible for part of the interaction between platelets and WBCs. Integrin β2 is present on platelets and modulates caspase activation and platelet lifespan. Knock out of integrin β2 in mice leads to a slight thrombocytopenic phenotype with platelet levels reduced by ~22%. The lifespan of platelets is also significantly reduced in the KO and this is slightly compensated by an increase in thrombocytopoiesis. The KO also demonstrated a lack of platelet localisation in the lung in response to injection of tumour necrosis factor. The KO demonstrated greatly decreased caspase 3 levels, greatly increased pro caspase 3 and greatly increased B-cell lymphoma 3-encoded protein levels (Piguet *et al.*, 2001).

Integrin β2 can bind to CD11a, CD11b or CD11c to form LFA-1 that can bind to ICAM1 on WBCS. Platelets also contain CD11a, CD11b and CD11c and the expression of CD11a and CD11b is correlated with that of integrin β2. The binding of platelets to a RAJI cell line increases with thrombin treatment and decreases with anti-CD11a or anti-integrin β2 antibodies. Numbers of platelets bound to a human lymphoblast-like (RAJI) cell line increased upon thrombin treatment and decreased upon treatment with anti-CD11a, anti- integrin β2 and anti-ICAM1 antibodies. This demonstrates that integrin β2 is responsible for at least part of the interactions between human platelets and human WBCs (Philippeaux *et al.*, 1996). It is currently unclear how this transfers to mice.

1.3.10 Coronin in platelets

Coronins 1, 2, 3 and 7 are present in platelets (Burkhart *et al.*, 2012). Until recently there had been a limited number of studies of coronin in platelets. Most of the studies were proteomic studies which found various coronins to be upregulated or downregulated in certain conditions. This section shall summarise these findings

Both coronin 1 and coronin 3 have been discovered in the membrane fraction of human platelets (Lewandrowski *et al.*, 2009). Coronin likely anchors to the membrane using its membrane binding domain.

The counts of platelet and other blood cells are normal in coronin 1 knockout mice (Föger *et al.*, 2006)

A study examined the proteome of human platelets during and after apheresis. Coronin 3 was found to increase in expression very soon after apheresis and then decrease in expression towards the end of recovery (Thiele *et al.*, 2016). These results are difficult to interpret but may mean that coronin 3 is a marker of young platelets or higher platelet turnover.

Salvianolic acid B is a traditional Chinese medicine isolated from Dashen and used to treat cardiovascular disorders. A study found that upon treatment of patients the expression of coronin 2 was upregulated. The also study claims that the platelets of patients treated with salvianolic acid demonstrated altered cytoskeletal shape (Ma *et al.*, 2011) but does not provide convincing evidence.

Another study which identified a change in coronin upon platelets examined patients with coronary artery disease. Coronin 2 was found to demonstrate lower expression in patients with coronary artery disease than control patients (Banfi *et al.*, 2010).

Reduced levels of coronin were found in porcine platelets after treatment with NO for 8 days, followed by platelet extraction and thrombin treatment, (Peña *et al.*, 2011).

As previously mentioned, thrombospondin is an agonist of platelets (Broos *et al.*, 2011). Coronin has been found to bind to thrombospondin 1 in solid-phase binding assays. However the researchers used a peptide sequence MRGSHHHHHHGS to represent the N-terminal of coronin (Vanguri *et al.*, 2000), however this sequence does not appear to show similarity with coronin proteins. As mentioned previously, thrombospondin is important in the regulation of platelet response. As thrombospondin is in the alpha granules it may not interact with coronin, however if coronin binds to thrombospondin then coronin may modulate platelet activity through thrombospondin.

While this project/thesis was in progress, study by Stocker *et al.* (2018) reported that *Coro1a*^{-/-} platelets had an increase in platelet volume, an increase in cell surface receptors, a decrease in time to occlusion in arterial thrombosis with a decrease in thrombus size, a decrease in the F/G actin ratio in response to collagen-induced activation, a decrease in p-cofilin upon collagen activation. The differences were attributed to less p-cofilin activation. The study also found no change in platelet life span, platelet maturity, proplatelet formation, ATP secretion & GTP-Rac1, dense granule secretion, αIIbβ3 integrin activation. The KO platelets were also reported to spread over a different surface area and have a different shape relative to the WT on only some matrices (Stocker *et al.*, 2018). Some of the data may be inconclusive due to low statistical power and particulars aspects were not investigated in that study.

1.3.10.1 Transcriptomic studies found coronins 1, 2 3 & 7 expressed in platelets

Prior to experimentally investigating coronins in platelets, a review of transcriptomic and proteomic literature was completed. Human platelets were found to have high levels of coronin 3 mRNA, moderate levels of coronin 1 and 2 mRNA, low levels of coronin 7 RNA and extremely low levels of coronin 4, 5 and 6 mRNA. In murine platelets, moderate/high levels of coronin 2 and 3, low levels of coronin 1 and 7 and extremely low levels of coronin 4, 5 and 6 were detected (Figure 1.19) (Rowley *et al.*, 2011). However the protein levels, described next, were found to be different from the mRNA levels.

.
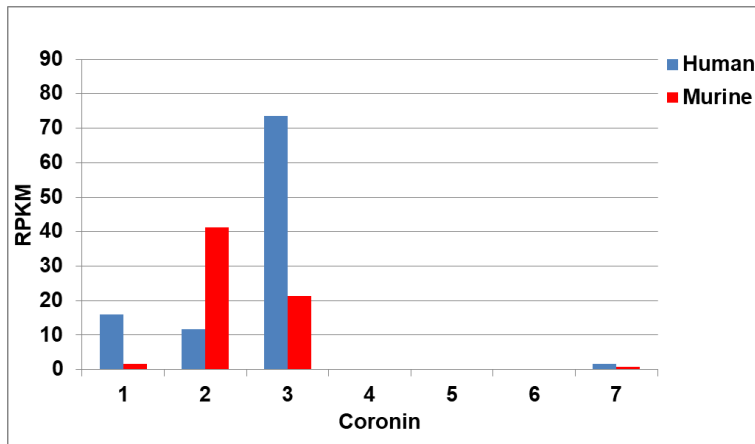
Figure 1.19 - Estimated mRNA levels of coronins 1-7 in human and mouse platelets
RNA seq analysis was used to determine mRNA levels, expressed in reads per kilobase of exon model per million mapped reads (RPKM), of human (blue) and murine (red) coronins. Data collated from (Rowley *et al.*, 2011).

1.3.10.2 Proteomic studies found coronins 1, 2 3 & 7 expressed in platelets

The coronin 1, 2 and 3 proteins have been reported to be abundantly expressed in human platelets (Burkhart *et al.*, 2012). Coronins 1, 2, 3 have been reported to be the 145th, 146th and 491st most abundant proteins in human platelets with an estimated 23,400, 23,300 and 6,900 copies per cell, respectively. If coronins 1-3 were counted as one protein they would be the 67th most abundant protein, making up 0.23% of the total level of proteins. Coronin 7 was at the lower limit of detection by quantitative mass spectrometry, ranking as the 3089th most abundant protein with only 700 copies/cell (500 copies/cell was the lower limit of detection). Coronins 4-6 were not found (Burkhart *et al.*, 2012) (**Figure 1.20A**), reflecting the transcriptomic results (Rowley *et al.*, 2011).

The murine proteins coronins 1-7 displayed similar expression patterns to human coronins with coronin 1 the highest (Zeiler *et al.*, 2014). Despite the high murine mRNA levels (Rowley *et al.*, 2011), coronin 2 protein levels are much lower. Coronin 7 is barely detectable and coronins 4, 5 and 6 absent. The main difference was that coronin 3 levels were considerably lower in murine platelets (Zeiler *et al.*, 2014). The human and murine protein numbers are from different studies, relating their respective controls, therefore they are not displayed on the same graph

(**Figure 1.20B**). A detailed list of transcriptomic and proteomic data, including that from less sensitive studies, can be found in (**Appendix 8.1.3**).
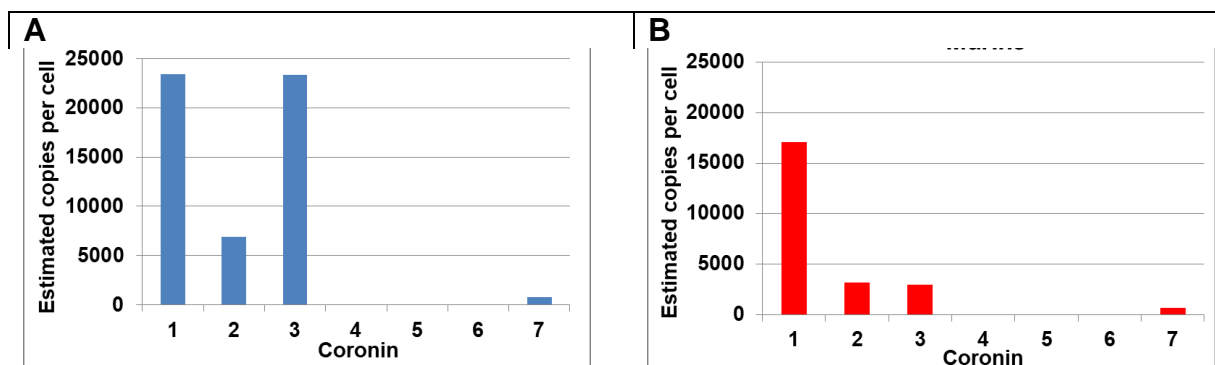
Figure 1.20 - Estimated protein levels of coronins 1-7 in human and mouse platelets
(**A**) Quantitative mass spectrometry was used to measure the protein copy number of coronins 1-7 in human. Produced from supplementary data from (Burkhart *et al.*, 2012) and murine platelets (**B**). Produced from supplementary data from (Zeiler *et al.*, 2014). The protein copy number was from two different sources and is therefore is not compiled into one graph.

1.3.10.3 Proteomic studies found coronins 1, 2 3 & 7 expressed in several tissues and cells including platelets

Coronin 1 mRNA and protein is highly expressed in all hematopoietic and lymphoid tissues which contain white blood cells such as the thymus, spleen, tonsils and bone marrow. It is also expressed to a lesser extent in neuronal tissues such as the adrenal gland (Nal *et al.*, 2004). Coronin 2 mRNA and protein and to a lesser extent coronin 3, is highly expressed in most tissues (Cai *et al.*, 2005). Coronin 4 is expressed in the gastrointestinal tract, bladder, lung and male reproductive tissues with lower expression in the epidermis (Uhlén *et al.*, 2015). Coronin 5 is expressed predominantly in the brain with lower expression in most other tissues (Nakamura *et al.*, 1999). Coronin 7 is expressed relatively highly in the thymus, spleen, brain, kidney with lower expression in most other tissues. Coronin 7 is usually subcellularly localised to the cytosol and Golgi apparatus, rather than spread throughout the

94

whole cell (Rybakin *et al.*, 2004). Coronins 1-3 are expressed almost ubiquitously and their presence is found in many cell types (**Figure**).
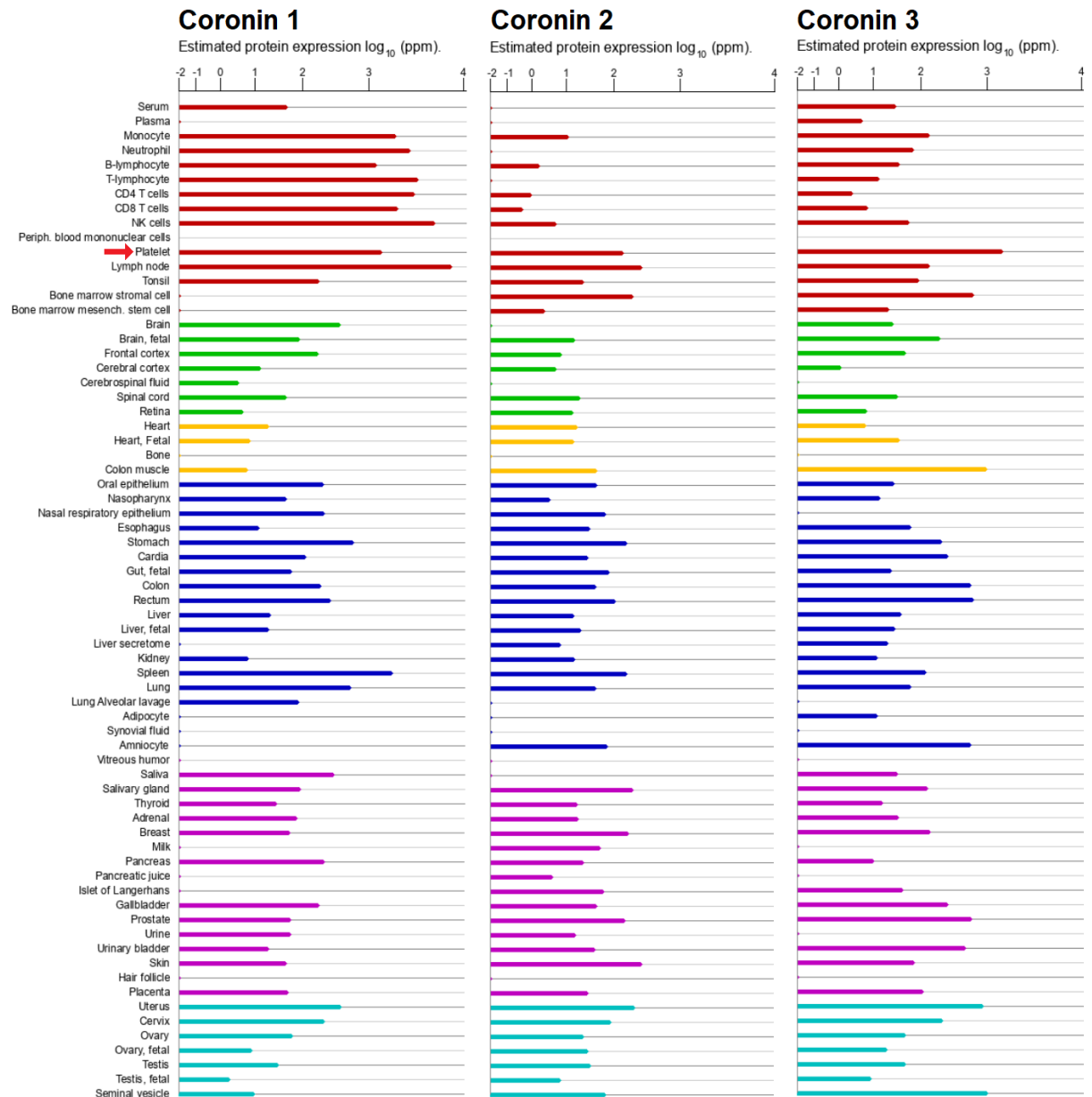
Figure 1.21 – Expression of coronins 1-3 in various tissue and cell types
Coronin 1, 2 and 3 proteins are found in most cell types in various levels. All 3 are highly expressed in platelets (red arrow). Data from Genecards, incorporating ProteomicsDB, MaxQB, and MOPEDGenecards (Stelzer *et al.* 2020).

1.4 Cyclase-associated protein

CAP1 is a highly conserved monomeric actin-binding protein (Ono, 2013). CAP was first discovered in yeast in which it is also called Srv2/CAP (Field *et al.*, 1990). CAP works with cofilin, profilin and ADF to modulate actin turnover. CAP1 enhances nucleotide exchange on actin monomers with ATP and also promotes severing of F-actin in along with cofilin. CAP1 is also capable of homo-oligomerisation and interacting with other proteins which regulates its activity. CAP has roles in cell signalling, development, vesicle trafficking and migration (Ono, 2013).

CAP is evolutionarily conserved and is present in all eukaryotes so far investigated (**Figure 1.22**). Vertebrates have two genes encoding CAP proteins and multiple isoforms are also present in nematodes and green plants, however fungi, protists and many other invertebrates only have 1 CAP gene (Ono, 2013).
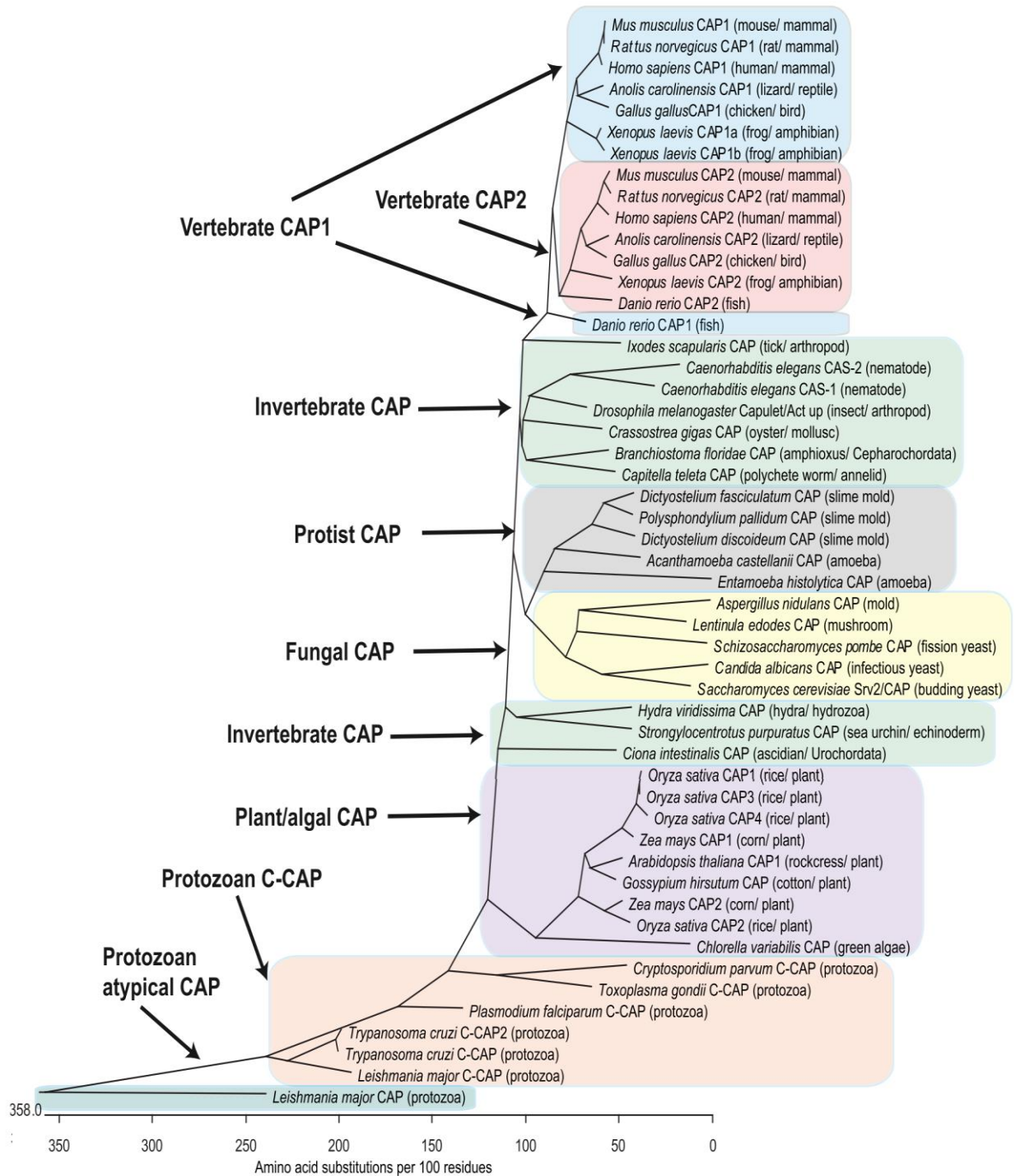
Figure 1.22 - Phylogenetic tree of CAPs in eukaryotes
Amino acid sequences of CAP-related proteins from representative organisms were analysed by Clustal W and classified as shown on the left. Adapted from (Ono, 2013).

97

1.4.1 CAP1 structure

The N-terminal of CAP contains a coiled coil domain which in yeast is required for binding to adenyl cyclase (Ono, 2013). The N-terminal region is required for the formation of hexameric structures in murine CAP1 (Jansen *et al.*, 2014).The helical fold domain of CAP is responsible for binding to ADF/cofilin-G-actin complexes. The central region contains two proline-rich regions (P1 and P2) which flank the WH2 domain. P1 is responsible for profilin recruitment with murine CAP1 (Makkonen *et al.*, 2013) and yeast Srv2/CAP (Bertling *et al.*, 2007). With human CAP1, P1 binds to the SH3 domain of the tyrosine kinase Abl (Freeman *et al.*, 1996; Kotila *et al.*, 2018). P2 binds to abp1 with yeast Srv2/CAP (Freeman *et al.*, 1996). The Wiscott Aldrich syndrome protein homology 2 (WH2) domain is capable of binding both ADP and ATP-G-actin (Kotila *et al.*, 2018). However, the CAPs and retinitis pigmentosa 2 protein (RP2) (CARP) domain is capable of binding only specifically ADP-G-actin. The dimerisation motif (DM) is responsible for the interaction of two CAP1 proteins through the β sheets on the C terminal (Ono, 2013) (**Figure 1.23A**). As the CAP1 C terminal contains a domain for hexamerisation which would make it very hard to crystalise, most approaches use computer models (**Figure 1.23B**) (Ono, 2013) or crystalise a part of the protein (**Figure 1.23C**) (Kotila *et al.*, 2018).

A

Formation of hexamers

Binding to abl and profilin

Binding ADP-actin and nucleotide exchange

Binding ADF/cofilin/G-actin

Binding to SH3 domain proteins

Formation of dimers

Nucleotide exchange, F-actin severing and ADP/ATP G-actin sequestration

B

C
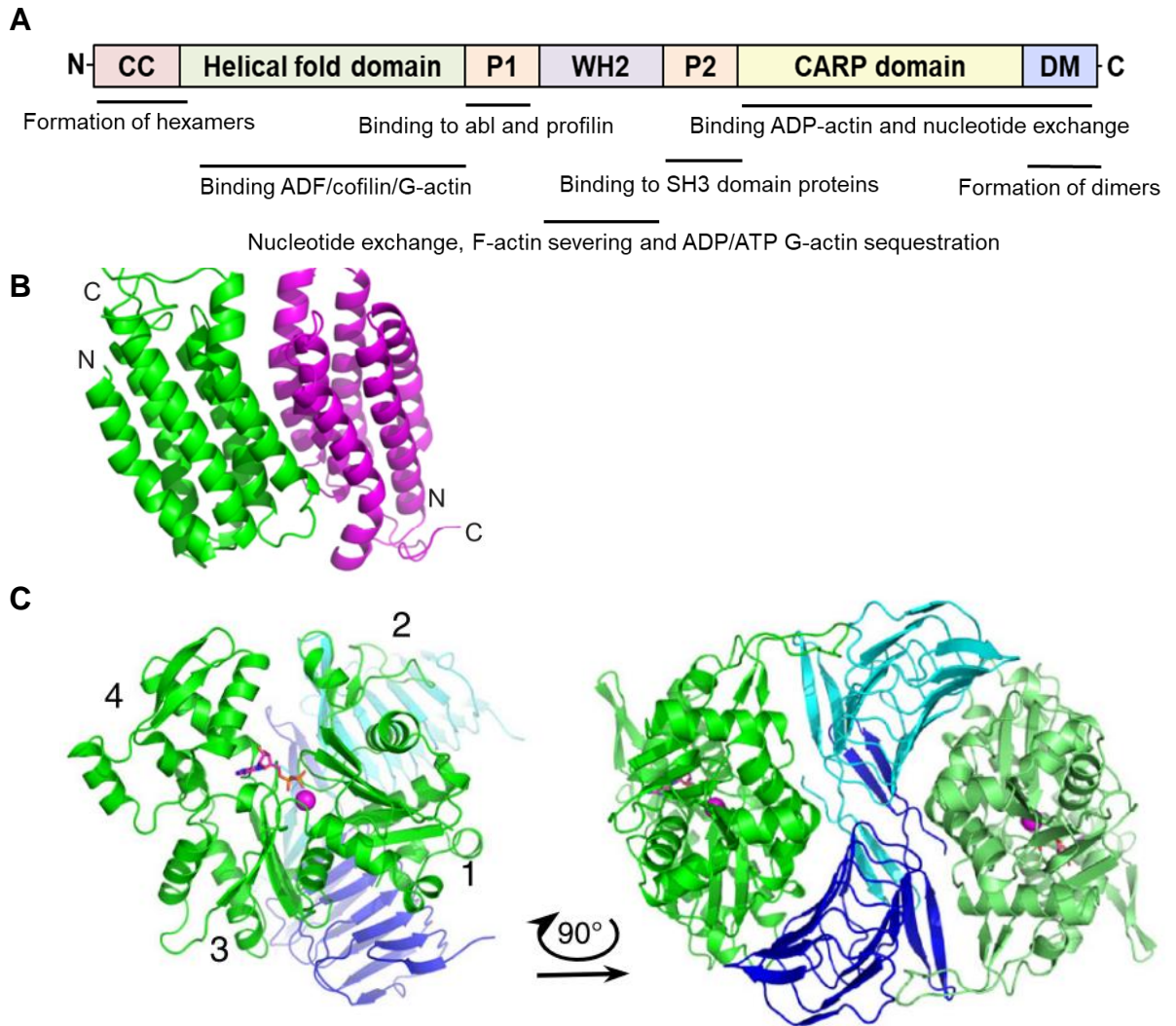
Figure 1.23 - Structure of CAP

(**A**) CAP contains a CC domain, a helical fold domain, 2 proline rich domains (P1 and P2), a cyclase-associated protein and retinitis pigmentosa 2 (CARP) domain and a dimerisation motif (DM). Redrawn from Ono, 2013. (**B**) Two dimerised helical fold domains of CAP1 as predicted from a computer model (Ono, 2013). (**C**) Crystal structure of a dimer of the CARP domain and dimerisation motif (amino acids 317-474) (blue and cyan) section of murine Cap1 bound to two molecules of ADP-actin (green) (Kotila *et al.*, 2018).

1.4.2 CAP expression

There are two genes encoding CAPs in mammals – CAP1 and CAP2. They are 60% identical in their amino acid sequence and exhibit different expression patterns (Ono, 2013). CAP1 is fairly ubiquitously expressed with the exceptions being the bone muscle tissues. CAP2 is expressed in the brain, heart, skeletal muscle, lung, skin

99

and reproductive tissues with extremely low levels in the kidney, bone and WBCs (Stelzer *et al.*, 2016). CAP1 and CAP2 are both present in mouse platelets (Zeiler *et al.*, 2014). However, only CAP1 is present in human platelets and has been identified as the 85th most abundant protein out of over 4000 present (Burkhart *et al.*, 2012).

1.4.3 CAP1 regulates actin turnover

CAP functions with cofilin, profilin and actin depolymerising factor (ADF) to modulate actin turnover (Ono, 2013). As mentioned in **Section 1.2.1.1**, actin filaments experience faster polymerisation at their barbed ATP-actin end and faster depolymerisation at the ADP-actin pointed end. Cofilin can sever filaments with a preference for ADP-actin (Kardos *et al.*, 2009) and profilin is involved with nucleotide exchange (Moriyama & Yahara, 2002).

The N-terminal of CAP1 is responsible for enhancing cofilin-mediated severing and depolymerisation of actin filaments (Moriyama & Yahara, 2002). Oligomerisation of CAP may be required for this process as mutations of yeast coronin at conserved residues of N-terminal abolishes this ability (Chaudhry *et al.*, 2013) and deletion of the dimerisation motif weaken this ability (Zelicof *et al.*, 1996). CAP1 alone can sever F-actin in acidic but not neutral pH at which it requires the presence of ADF/cofilin (Normoyle & Brieher, 2012).

CAP can catalyse the nucleotide exchange of ADP-actin monomers. The C-terminal segment of the CARP domain can 'penetrate' into an actin monomer and induces a conformational change in the 'D-loop' segment of an actin monomer (Kotila *et al.*, 2018). The C-terminal also competitively displaces cofilin which has a strong inhibitory effect on nucleotide exchange. In the presence of cofilin, the WH2 domain is additionally required for nucleotide exchange (**Figure 1.24**) (Jansen *et al.*, 2014).
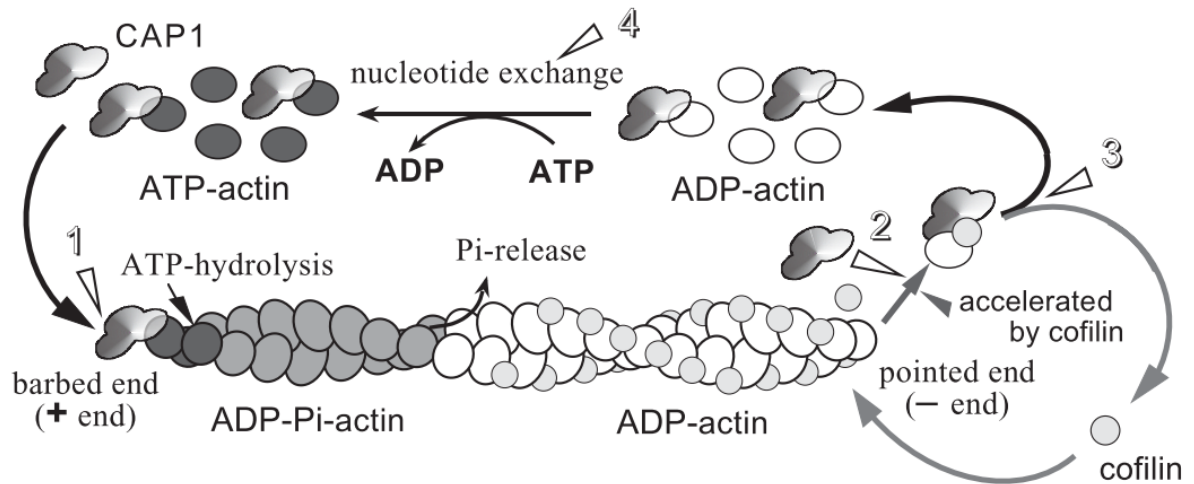
Figure 1.24 – Role of CAP1 in actin turnover
(**1**) CAP1 facilitates the addition of ATP-actin monomers onto the barbed ends of the network. (**2**) CAP1 accelerates ADP-actin depolymerisation and enhances the F-actin severing ability of cofilin. (**3**) CAP1 inhibits the inhibitory effect of cofilin on nucleotide exchange on actin monomers. (**4**) CAP1 accelerates the nucleotide exchange onto actin monomers from ATP. Adapted from (Moriyama & Yahara, 2002).

1.4.4 CAP1 localisation

CAP1 is a predominantly cytosolic protein with a small fraction membrane associated (Lee *et al.*, 2014). In murine fibroblasts, CAP1 demonstrates diffuse cytoplasmic localisation and accumulates at dynamic actin structures including lamellipodia (**Figure 1.25A** & **B**) and areas of ruffling where it co-localises with cofilin (**Figure 1.25B**) (Moriyama & Yahara, 2002) and at actin stress fibres (**Figure 1.25C**) (Freeman & Field, 2000). Even in organisms as distantly related as plants, CAP colocalises with F-actin structures called 'actin foci' and ADF during pollen tube self-incompatibility (**Figure 1.25D**) (Poulter *et al.*, 2010). In yeast, Srv2/CAP colocalises with 'actin patches' which are normally found at the cell cortex (Freeman *et al.*, 1996).

101
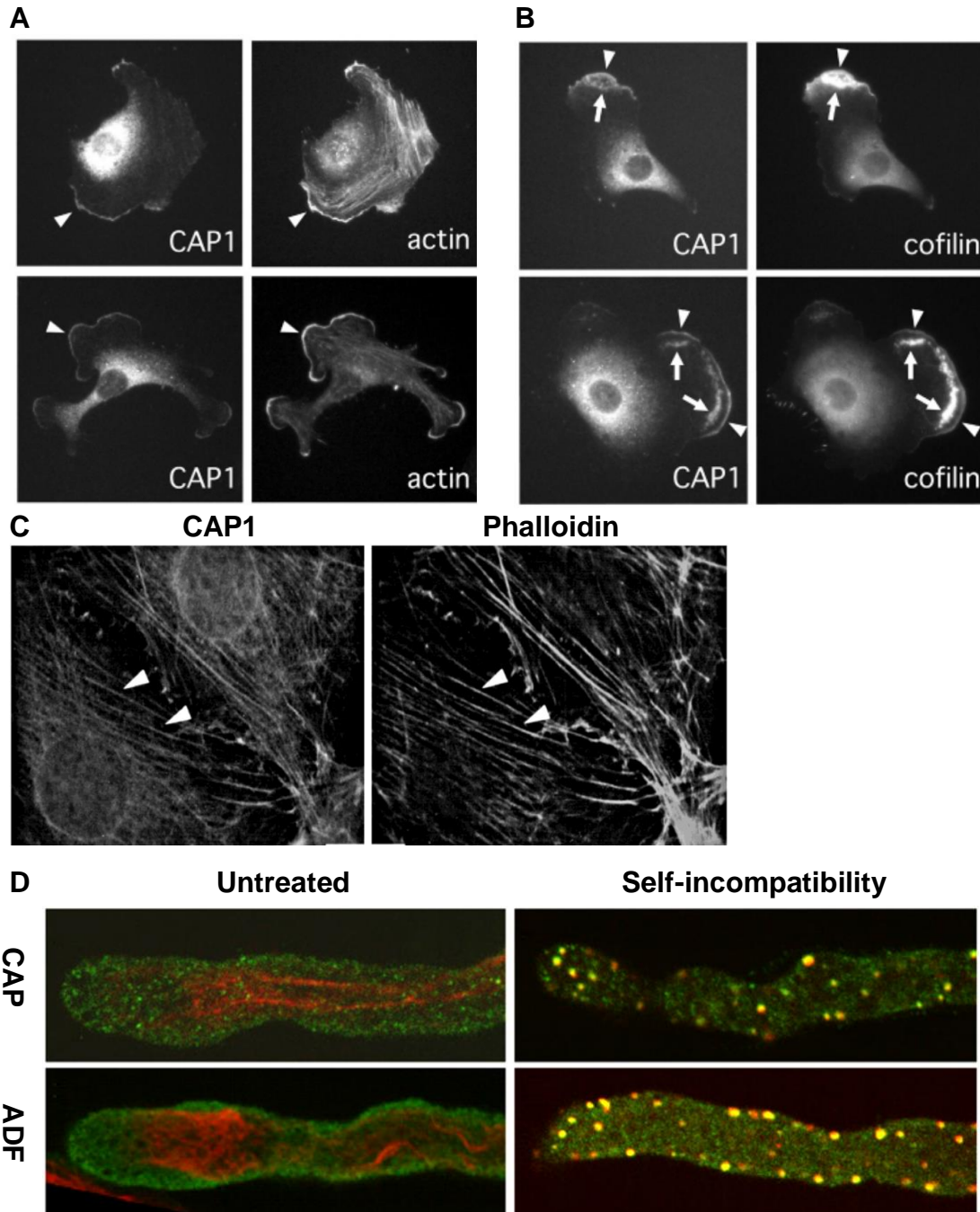
Figure 1.25 – CAP1 localisation in murine fibroblasts
(**A**) Spread murine C3H-2K fibroblasts stained for CAP1 and actin. CAP1 is diffusely in the cortex and also at the lamellipodia where it colocalises with actin (arrowheads). (**B**) Fibroblasts stained for CAP1 and cofiln. Arrowheads indicate colocalisation at the lamellipodia and areas of ruffling Adapted from (Moriyama & Yahara, 2002). (**C**) Murine 3T3 fibroblasts stained for CAP1 and phalloidin. Arrowheads indicate colocalisation at the stress fibres (Freeman & Field, 2000).(**D**) Pollen tubes untreated and 3 hours after the induction of self-incompatibility. Stained for CAP or ADF (red) phalloidin (green) (Poulter *et al.*, 2010).

1.4.5 CAP1 as a potential receptor

CAP1 has been proposed as a receptor for resistin due to the results of a set of experiments by Lee, *et al.* (2014). However CAP1 does not contain a transmembrane domain. Human resistin bound to a mouse Fc chain (called mFc-hResistin) was found to pull down a protein in lysates from a monocytic leukemia cell line. This protein was identified by matrix-assisted laser desorption/ionization time-of-flight to be CAP1. CAP1 was also found to colocalise with mFc-hResistin at the cell cortex/membrane. CAP1 was also found to bind to resistin using IP and Biocore (Lee, *et al.*, 2014).

The researchers then fluorescently labelled resistin and generated CAP1 up or down-regulated monocytic leukemia cells. Flow cytometry was performed on cells which were fixed with 1% PFA which should not have permeabilised the cell to expose binding to intracellular proteins. The levels of resistin were found to be lower on the cell surface on CAP1 down-regulated cells and higher on CAP1 up-regulated cells. This suggests that resistin has an effect on CAP1 exposure. However CAP1 itself does not contain a transmembrane domain but it could be associated with a receptor (Lee, *et al.*, 2014). The precise mechanism remains a mystery.

1.4.6 Life without CAP

Saccharomyces cerevisiae lacking Srv2/CAP demonstrate a lack of activation of membrane AC upon stimulation by RAS2 proteins. The cells were also larger, demonstrated a lack of growth on yeast extract peptone dextrose medium and were sensitive to increased temperature and nitrogen starvation (Field *et al.*, 1990). In yeast the coiled-coil N terminal is responsible for the interaction with AC (Nishida *et al.*, 1998).

CAP knock down *Dictyostelium discoideum* cells displayed altered cell morphology with greater disparity in cell sizes. They demonstrated defects in

cytokinesis, endocytosis and motility. They also underwent delayed development and grew slower than WT controls (Noegel *et al.*, 1999).

CAP is required for a variety of processes including cell morphology, polarity, motility and endocytosis (Ono, 2013). CAP1 KO studies are impractical in mammals as CAP1 is deletion embryonically lethal (Jang *et al.*, 2020), probably due to placental defects (Hummler *et al.*, 2013). Therefore inducible or cell type-specific knock outs or known downs are required.

In murine fibroblasts (NIH3T3), melanoma cells (B16F1), and neuroblastoma cells (Neuro2A), knock down (SiRNA) of CAP1 leads an accumulation of abnormal F-actin structures, larger cells, a lack of polarity and abnormal morphology. Fibroblasts and melanoma cells demonstrated a lack of membrane ruffles and displayed an accumulation of thick and less dynamic stress fibres which can be attributed to an increase in actin the depolymerisation rate. Neuroblastoma cells contained ruffles but they were significantly less polarised (Bertling *et al.*, 2004). CAP1 knock down in fibroblasts resulted in half motility speed due to polarisation defects. Both fibroblasts and melanoma cells subjected to CAP1 knock down demonstrate severely disrupted cofilin localisation, with cofilin spread sporadically throughout the cells in aggregates (Bertling *et al.*, 2004).

CAP1 also appears to be a proapoptotic protein. Upon apoptosis, CAP1 rapidly translocates to the mitochondria independently of caspase activation. CAP1-knockdown cells are resistant to apoptosis inducers and overexpression of CAP1 does not stimulate apoptosis independently but stimulates cofilin-induced apoptosis (C. Wang *et al.*, 2008).

1.4.7 CAP in platelets

The first mammalian CAP was incidentally discovered in porcine platelet lysates (Gieselmann & Mann, 1992). Until recently, the functions of CAP in platelets had not been investigated.

In mice, platelets with gene trapped CAP2 have been reported to be larger, display increased agonist-induced activation of αIIbβIII, increased P-selectin

recruitment and display no spreading defects on fibrinogen. That study concluded that CAP1 may at least partially compensate for the lack of CAP2 in murine platelets (Heck, 2019).

1.4.8 Regulation of CAP1 activity

CAP1 is regulated by a number of factors including phosphorylation by GSK3 (Zhou *et al.*, 2014) and cell division kinase 5 (CDK5) (H. Zhang *et al.*, 2020). In murine embryonic fibroblasts, phosphorylation of serines S307 and S309 of CAP1 regulate cofilin binding, actin binding and therefore actin turnover. CAP1 S307A/S309A non-phosphorylatable mutants display drastically increased binding of CAP1 to cofilin and reduced binding to actin. The phosphomimetic mutant S307D/S309D loses CAP1 ability to bind cofilin but displays greater actin binding. Both mutants demonstrate F-actin accumulation at stress fibres. GSK3 has been found to phosphorylate CAP1 S309, however the additional phosphorylation of S307 appears to be required for functional change. CAP1 is likely regulated by phosphorylation from multiple proteins (Zhou *et al.*, 2014).

It has also been found that CDK5, which is present in platelets (Burkhart *et al.*, 2012), phosphorylates S307 and S309 to regulate its cofilin and actin binding. It has also been discovered that cAMP signalling induces dephosphorylation of CAP1, through PKA and exchange proteins directly activated by cAMP (Epac) (Zhang *et al.*, 2020).

1.5 Aims

Coronin 1 and CAP1 are abundant proteins in platelets. They both interact with other regulators of the cytoskeleton to contribute to actin turnover. They also both have roles at the cell membrane.

1.5.1 Coronin-related aims

- To validate anti-coronin antibodies and determine the presence and abundance of coronin in platelets
- Investigate the association of coronins to the membrane, actin cytoskeleton and lipid rafts
- Characterise the cellular localisation of coronins and interacting proteins
- Investigate any potential compensation of the ablation of coronin 1 by coronin 2 or 3
- To assess any possible defects in inhibitory signals upon coronin 1 ablation
- To analyse basal and stimulated basal and stimulated receptor levels, αIIbβ3 activation and platelet secretion of $Coro1a^{-/-}$ platelets
- To determine the ability of $Coro1a^{+/+}$ and $Coro1a^{-/-}$ platelets to spread on various matrices
- To investigate the role of Coronin 1 ablation on haemostasis

1.5.2 CAP1-related aims

- To characterise the association of CAP1 with interacting proteins
- To analyse the association of CAP1 to the F-actin cytoskeleton
- Characterise the subcellular localisation of CAP1 and colocalisation with F-actin structures
- To investigate the translocation of CAP1 in response to platelet stimulants and inhibitors

2 Chapter 2 – Materials and methods

2.1 Materials

2.1.1 Coronin 1 knockout mice

The generation of C57Bl/6 mice with a homozygous constitutive knockout of the *Coro1A* gene has been described elsewhere (Jayachandran *et al*., 2007). The animals were kept in the animal facility of the University of Hull using standard conditions. All animal work was performed in accordance with UK Home Office regulations, UK Animals (Scientific Procedures) Act of 1986, under the Home Office project license no. PPL 70/8253. For all experiments, age-matched wild-type (WT) littermates or cousins were used as controls

2.1.2 Plasmids

Table 2.1 – List of plasmids

Protein	Species	Source
Coronin 1	Human	kindly provided by Christoph Clemen, University of Bochum, Germany
Coronin 2	Human	kindly provided by Christoph Clemen, University of Bochum, Germany
Coronin 3	Human	kindly provided by Christoph Clemen, University of Bochum, Germany
Coronin 1	Mouse	Amplified using Q5 high fidelity polymerase (New England Biolabs, Hitchin, UK) and cloned into the EcoRI/KpnI sites of pCMV-myc
Coronin 2	Mouse	N-terminal myc fusion proteins purchased from Sino Biological (Beijing, China)
Coronin 3	Mouse	N-terminal myc fusion proteins purchased from Sino Biological (Beijing, China)

2.1.3 Antibodies for Western blot and Immunofluorescence

Table 2.2 - List of antibodies for Western blot and Immunofluorescence

Antibody	Host	Source	Catalogue no.	WB	IF
β-actin-HRP	Mouse	Abcam	ab20272	10,000	N/A
β3-integrin	Rabbit (polyclonal)	Santa Cruz	SC-14009	1:1,000	N/A
Arp C2	Rabbit (polyclonal)	Merck Millipore	07/227	1:1,000	1:100
Arp C2	Rabbit	Merck Millipore (upstate)	07/272	1:1,000	N/A
CAP1	Rabbit	Abcam	ab133655	1:5,000	1:150
CAP1	Rabbit	Abcam	ab155079	1:5,000	1:150
CD36	Rabbit (polyclonal)	Santa Cruz	sc-9154)	1:1000	1:100
Cofilin	Rabbit (monoclonal)	Cell Signalling	#5175	1:1000	
Coronin 1	Mouse (monoclonal)	Abcam	ab56820	1:1,000	1:100
Coronin 1	Rabbit (polyclonal)	Abcam	ab72212	1:1,000	1:100
Coronin 2	Rabbit (polyclonal)	Abcam	a99407	1:1000	1:100
Coronin 3 hybridoma SN	Mouse	kindly provided by Christoph Clemen, University of Bochum, Germany (K6-444 hybridoma SN)	NA	Used neat	
Coronin 7 hybridoma SN	Mouse	kindly provided by Christoph Clemen, University of Bochum, Germany (K37-142-1 hybridoma SN)		Used neat	
Gαs	Rabbit (polyclonal)	Santa Cruz	SC-823	1:300 in 2% milk	1:50
GAPDH	Mouse (monoclonal)	Merck Millipore	CB1001	1:6,000 in 2% milk	N/A
Gelsolin	Mouse (monoclonal)	Abcam	ab11081	1:1000	N/A
Phospo-	Mouse	Cell signalling	#3671	1:1000	N/A

108

MLC (Ser19)	(monoclonal)				
Phospo-VASP (Ser157)	Rabbit (polyclonal)	Cell signalling	#3111	1:1000	N/A
Syk	Mouse (monoclonal)	Santa Cruz	sc-1240	1:1000	

2.1.4 Antibodies for flow cytometry

Table 2.3 – List of antibodies for flow cytometry

Antibody	Host	Source	Catalogue no.	Fluorophore
Anti- αIIbβ3 (GPIIb/IIIa, CD41/CD61) (JON/A)	Rat anti-mouse (IgG2b)	Emfret	M023-2	PE
Anti-CD41 (integrin α2b)	Rat anti-mouse IgG1	BD Bioscience	553848	FITC
Anti-CD42b (GP1bα)	Rat anti-mouse (IgG2b)	Emfret	M040-1	FITC
Anti-CD49 (GPIa) (integrin α2)	Rat anti-mouse (IgG2b)	Emfret	M071-1	FITC
Anti-integrin β2	Rat anti-mouse (IgG2a)	BD	101407	PE
Anti-CD63	Rat anti-mouse (IgG2a)	Biolegend	143908	APC/Cy7
Anti-GPVI	Rat anti-mouse (IgG2a)	Emfret	M011-1	FITC
Anti-P-selectin	Rat anti-mouse IgG1	BD Bioscience	553744	FITC

2.1.5 Antibodies for Immunoprecipitation

Table 2.4 – List of antibodies for Immunoprecipitation

Antibody	Host	Source	Catalogue no.
Coronin 1	Mouse (monoclonal)	Abcam	ab56820
Coronin 1	Rabbit (polyclonal)	Abcam	ab72212
Coronin 2	Rabbit (polyclonal)	Abcam	a99407

2.1.6 Secondary antibodies for Western blot and Immunostaining

Table 2.5 – List of secondary antibodies for Western blot and Immunostaining

Antibody	Host	Source	Dilution
Anti-mouse HRP	Goat	Merck	1:10,000
Anti-rabbit HRP	Goat	Merck	1:10,000
Anti-mouse Licor 800	Goat	Li-cor Bioscience	1:15,000
Anti-rabbit Licor 800	Goat	Li-cor Bioscience	1:15,000
Anti-mouse Licor 680	Goat	Li-cor Bioscience	1:15,000
Anti-rabbit Licor 680	Goat	Li-cor Bioscience	1:15,000
Anti-mouse Alexa 568	Goat	Molecular Probes, Thermo Fisher Scientific	1:10,000
Anti-rabbit Alexa 568	Goat	Molecular Probes, Thermo Fisher Scientific	1:10,000
Anti-mouse Alexa 488	Goat	Molecular Probes, Thermo Fisher Scientific	1:10,000
Anti-rabbit Alexa 488	Goat	Molecular Probes, Thermo Fisher Scientific	1:10,000
Anti-rabbit (light chain specific)	Mouse	Jackson Immunoresearch	1:10,000

2.1.7 Stains

Table 2.6 – List of stains

Stain	Source	Catalog no	Dilution
Cytopainter blue	Abcam	ab112124	1:300
Far red phalloidin (Alexa Fluor 680-conjugated phalloidin)	Thermo Fisher Scientific	A22286	1:40
FITC Phalloidin	Sigma	P5282	1:2000 from 100 µg/ml stock
Fluo-3	Sigma		
TRITC Phalloidin	Sigma	P1951	1:2000 from 100 µg/ml stock

2.1.8 Agonists/inhibitors

Table 2.7 – List of agonists/inhibitors

Agonist	Source
ADP	Merck
Collagen (Kollagenreagens Horm)	Takeda
CRP	Cambridge University
Gly-Phe-Hyp-Gly-Glu-Arg (GFOGER)	Cambridge University
Human fibrinogen	Enzyme Research
Latrunculin B	Enzo Life Sciences
PGI2	Cayman Chemical
Thrombin	Sigma
U46619	Enzo Life Sciences

2.2 Methods

2.2.1 Preparation of samples for genotyping

Biopsies (ear punches) were incubated in 100 µl of ear buffer at 37°C at 350 RPM for 18 hours. The samples were boiled at 95°C for 10 minutes then moved to ice. 400 µl of RNAse A buffer was added and the samples were incubated at 21°C for 20 minutes. The samples were either genotyped immediately or frozen at -20°C for later use.

Ear buffer: 100 mM Tris pH 8.5, 5 mM EDTA, 0.2% SDS, 200 mM NaCl & 200 µg/ml proteinase K.
TE RNAse A buffer: 100 mM Tris, 10 mM EDTA & 0.14 mg/ml RNAse A

2.2.2 Genotyping of coronin 1 KO mice

1.5 µl of DNA was added to 19 µl of a mixture containing 0.25 mM dNTPs, 0.17 µl OneTaq polymerase (New England Biolabs, USA), 1x OneTaq buffer, 1x GC

enhancer, 0.5 µM forward and reverse primers in sterile MiliQ water. WT results in a band at 392 and KO results in a band at 478 bp.

Settings:

1x 98°C for 3 minutes

35 x (95°C for 1 minute then 56°C for 45 seconds then 72°C for 50 seconds)

1x 72°C for 5 minutes

1x 4°C (pause)

Samples were resolved on 1.7% agarose gel in 1x TAE buffer with 1:50,000 ethidium bromide.

Forward primer: 5'-CTGTTGTAGGGGCTGATGGT-3'

WT Reverse primer: 3' CAAGTGGTTTGTGAGACGCG-5'

KO Reverse primer 5'-CTTCATGTGGTCGGGGTAG-3'

2.2.3 Generation of coronin proteins

HEK 293T cells were cultivated at 37°C in a humidified incubator supplied with 5% CO_2. The cells were grown in Dulbecco's modified Eagle's medium (4.5 g/l glucose) (Merck) enriched with 10% fetal bovine serum (FBS) (Biochrom AG, Berlin, Germany), 2 mM glutamine (Merck), 1 mM sodium pyruvate (Merck), 100 U/ml penicillin, and 100 µg/ml streptomycin (PAA Laboratories GmbH, Pasching, Austria). Cells were split and $1x10^5$ cells were added to each well of a 6-well plate to achieve 50-80% confluence after 24 h. Cells were transiently transfected with plasmids (table 2.1) using Lipofectamine 2000 (Invitrogen, ThermoFisher Scientific) as follows (calculated for one well of a 6-well plate): 1 µg of DNA and 5 µl of Lipofectamine were separately mixed with 100 µl of pre-warmed DME medium without FBS and after 5 minutes, mixed together and incubated for 30 min at room temperature. Medium was removed from the well and replaced with 400 µl of medium without serum, to which Lipofectamine-DNA complexes were then added. After 4 h at 37°C, 800 µl of medium with 20% serum were added. Cells were collected 24 h post-

112

transfection. Transfected cells were lysed with 50 mM Tris–HCl, pH 8.0, 150 mM NaCl, 1% Triton X-100 and protease inhibitors for 30 min. Cell debris was removed by centrifugation at 10,000 ×g at 4 °C for 10 min. The lysate was resolved by SDS-PAGE and blotted onto PVDF.

2.2.4 Preparation of washed platelets using the pH method

Whole blood was collected into acid-citrate dextrose (ACD) buffer at 1:5 ratio (e.g. 4 ml ACD and 16 ml blood) and gently mixed. This was centrifuged at 190 xg at 21°C for 15 minutes. The platelet rich plasma (PRP) supernatant was transferred into a clean conical tube and the pH was adjusted to 6.4 by adding 20 µl of 0.3 M citric acid per ml of PRP (6 mM citric acid). This solution was centrifuged at 800 xg at 21°C for 12 minutes then the pellet was resuspended in 5 ml of platelet wash buffer. This was again centrifuged at 800 xg at 21°C for 12 minutes and the pellet resuspended in modified Tyrode's buffer

Platelet wash buffer: 0.036 M citric acid, 0.01 M EDTA, 0.005 M glucose, 0.005 M KCl, 0.09M NaCl in Milli-Q adjusted to pH 6.5
Acid-citrate dextrose buffer: 113.8 mM D-Glucose, 29.9 mM Tri-Na citrate, 72.6 mM NaCl, 2.9 mM citric acid in Milli-Q adjusted to pH 6.4, stored at 4°C and 0.22 µm filtered before use.
Modified Tyrode's buffer (MTB): 150 mM NaCl, 5 mM HEPES, 0.55 mM NaH_2PO_4, 7 mM NaHCO3, 2.7 mM KCl, 0.5 mM $MgCl_2$, 5.6 mM D-glucose (added fresh) in Milli-Q water, stored at 4°C and 0.22 µm filtered before use.

2.2.5 Preparation of murine PRP and platelets

Murine blood was collected into 100 µl of ACD for most studies or in 100 µl of 109 mM trisodium citrate (pH 7.4) for flow cytometric studies and added to a tube containing 500 µl MTB. This was centrifuged at 100 xg for 5 minutes, the PRP was removed and 500 µl MTB was added to the blood. The blood was once again

centrifuged at 100 xg and the PRP was removed. The PRP was centrifuged at 800 xg for 6 minutes, the supernatant removed and the platelet pellet resuspended in MTB

2.2.6 Subcellular fractionation

Subcellular fractionation was performed to separate the platelet cytosol from the membrane. Washed platelets at 1×10^9/ml were incubated with 10 µM indomethacin 2 U/ml apyrase and 1 mM EGTA for 20 minutes at 37°C. Latrunculin B (LatB) was added to some samples at 20-30 µM for 20 min at 37°C to inhibit actin polymerisation prior to lysis. Platelets were then left at basal condition or treated with 0.1 U/ml thrombin, 50 µg/ml collagen or 100 nM PGI_2 for 1 minute at 37°C then mixed with an equal volume of fractionation buffer and immediately subjected to 5 freeze-thaw cycles in liquid nitrogen. Intact platelets were removed by centrifugation at 1,000xg for 5 minutes at 4°C and fractionation was done by centrifugation at 100,000xg for 60 minutes at 4°C. The supernatants were normalised by volume and analysed by 10% SDS-PAGE Western blot.

Fractionation buffer: 320 mM sucrose, 4 mM HEPES, 0.5 mM Na3VO4, pH 7.4. 2x phosphatase, protease inhibitor cocktail and 0.001M PMSF were added before use.

2.2.7 Triton X-100 insoluble pellet fractionation

Washed platelet suspensions at 1×10^9/ml in modified Tyrode's bbuffer were treated with 0.1 U/ml thrombin, 50 µg/ml collagen, or left untreated at 37 °C and then lysed in an equal volume of Triton X-100 lysis buffer. Lysates were centrifuged at 15,600 × g for 20 minutes at 4°C to separate the detergent soluble fraction from the detergent insoluble pellet. The supernatant was collected and the pellet was washed once with Triton X-100 lysis buffe. The pellet was suspended in 50 µl 2x Laemmli buffer by pipetting to obtain the 'low speed' pellet fraction. A fraction of the

114

supernatant was collected and mixed with 5x Laemmli buffer to obtain the 'low speed' supernatant fraction.

The remainder of the supernatant was then centrifuged at 100,000 xg for 1 hour at 4°C, the supernatant was then collected and mixed with 5 x Laemmli buffer to obtain the 'high speed' supernatant. The pellet was washed with Triton X-100 lysis buffer then suspended in 2x Laemmli buffer by pipetting to obtain the 'high speed' fractiion. Once the pellets were mixed with Laemmli buffer, they were heated at 95°C for 5 minutes and then frozen at -20°C. The fractions were normalised by volume, resolved on 10% SDS-PAGE and analysed by Western blot

Triton X-100 lysis buffer: 2% Triton X-100, 100 mM Tris-HCl (pH 7.4), 10 mM EGTA, 0.001M PMSF and 2x protein inhibitor cocktail.

2.2.8 Spreading and immunostaining

5 or 12 mm coverslips were coated by the addition of 30 µl or 200 µl of matrix, respectively, overnight at 4-8°C. Matrix included 100 µg/ml fibrinogen or 100 µg/ml collagen (or other matrix as specified in the figure legend). The liquid was removed and the coverslips were incubated with 0.5% fatty acid free BSA in PBS (which had been previously heat denatured at 95°C for 5 minutes) for 1 hour at 21°C. The BSA was removed and the coverslip was washed 3 times with PBS. Platelets at 1×10^7 were either treated with 0.1 U/ml thrombin or left untreated, then 100 µl was added to 12 mm coverslips for 45 minutes (unless otherwise specified in the corresponding figure legend) at 37°C in a moist chamber. In some studies, agonists or inhibitors were added to platelets as indicated in the respective figure legends. The liquid was removed and the platelets were fixed with 4% PFA in PBS for 10 minutes at 21°C. The samples were then permeabilised with 0.3% Triton X-100 in PBS for 5 minutes at 21°C. The liquid was removed and the samples were washed 3 times with PBS. Immunostaining was performed by adding primary antibody diluted in PBG to the coverslip for 1 hour at 21°C then washing 3 times with PBS. Diluted fluorescently labeled secondary antibodies (Alexa 488 or Alexa 568) were added to the coverslip

for 1 hour at 21°C. TRITC, FITC, Far red (660) or cytopainter blue phalloidin, was diluted and added to the coverslip for at least 30 minutes at 21°C. The coverslips were washed 3 times with PBG and once with PBS and then mounted using gelvatol or Prolong diamond antifade mountant (Thermo Fisher) onto glass slides. The coverslips were imaged using a Zeiss ApoTome.2 equipped with an AxioCam 506 and a Zeiss Plan-Apochromat 100x/1.4 objective. Images were processed with Zeiss Zen software. Cells were manually counted on FIJI and thresholding was performed using the "Li" method where appropriate and including holes.

1x PBS: 137 nM NaCl, 10 nM Na_2HPO_4, 2.7 nM KCl, 1.8 nM KH_2PO_4 in Mili-Q water, pH7.4

PBG: 1x PBS, 0.5% BSA, 0.05% fish gelatin

Gelvatol: 2.4 g PVA, 6 ml glycerol, 6 ml dH_2O, 2.5% DABCO

2.2.9 Platelet aggregation

Platelet aggregation was performed using a Chronolog aggregometer (Chronolog Instrument 490 + 4). 800 µl of MTB was added to a Chronolog cuvette and in the PPP compartment. Platelets were incubated at 37°C then 250 µl of platelet suspensions at 2 x 10^8/ml (for murine studies) or 3 x 10^8 (for human studies) were added to cuvettes containing a magnetic stir bar. The samples were stirred at 1000 RPM at 37°C and the graph was baselined at 0. Agonists such as 0.01-0.1 U/ml thrombin, 1-10 µg/ml CRP-XL, 1-20 µg/ml collagen, 10 µM ADP or 0.3 – 10 µM U46619 were added after 30 seconds of channel activation and the response for recorded for at least 7 minutes.

2.2.10 SDS-PAGE / Western blot

Proteins were denatured by boiling for 5 minutes in Laemmli buffer and resolved on 10-12% resolving gel with 4% stacking by sodium dodecyl sulphate polyacrylamide gel electrophoresis (SDS-PAGE) at 70-130 V (Biorad, Powerpac basic). Gels were

116

then blotted onto polyvinylidene difluoride (PVDF) membrane (GE Healthcare) using either semidry blot (Biorad, Trans-Blot, turbo) at 25 V (limit) & 1.3 A (constant) for 12 minutes or wet blot using Towbin's buffer at 100 V for 1 hour on ice. The membrane was blocked with 5% milk in TBST or 5% BSA in TBST, washed with TBST then incubated at 4-8°C for ~18 hours with diluted relevant primary antibody with gentle rocking then washed three times with TBST for 10 minutes with gentle rocking. The membranes were incubated with a secondary antibody for 1 hour at 21°C with gentle rocking. Membranes were then visualised with a LI-COR Odyssey CLx Imaging System and quantified with Image studio software V 5.2 (LI-COR) for the vast majority of antibodies. For some antibodies. 3 ml of ECL A and B were mixed, the membrane added for 3 minutes and then pressed against X-ray film in a dark room. The film was then developed and fixed, scanned and quantified by densitometry with Image J.

10% Acrylamide resolving gel: 4 ml of buffer 1 (1.5 M Tris and 0.4% SDS, pH 8.8) 5.3 ml of 30% acrylamide/bis acrylamide, 6.48 ml dH20, 0.07 ml of 10% APS, 0.03 ml of TEMED

6% Acrylamide stacking gel: 1 ml 30% acrylamide/bis acrylamide, 1.4 ml 0.5 Tris-HCl pH 6.8, 0.04 10% SDS, 2.53 dH$_2$0, 0.045 ml 10 % APS & 0.015 ml TEMED.

TBST: 0.15 M NaCl$_2$, 0.01 M Tris pH 7.6 and 0.1% Tween-20.

TBST-SDS: 0.15 M NaCl$_2$, 0.01 M Tris pH 7.6, 0.2% Tween-20 and 0.01% SDS.

Running buffer: 0.025 M Tris-Hcl pH 8.3, 0.1% SDS, 0.19 M glycine

Towbin's buffer: 20% methanol, 25 mM Tris & 192 mM glycine

ECL: ECL A - 10 ml 1 M Tris pH 8.5, 88.6 ml dH$_2$O, 0.996 ml 250 mM luminol in DMSO & 90 mM p-coumaric acid in DMSO. ECL B – 10 ml 1 M Tris pH 8.5, 90 ml dH$_2$O 65 µl H$_2$O$_2$. ECL A and B were mixed in equal ratios before addition to any membrane.

2x Laemmli buffer: 4% SDS, 20% glycerol, 0.004% bromophenol blue, 100 mM Tris pH 6.8 & 4% β-mercaptoethanol

2.2.11 Immunoprecipitation

Platelets at 1×10^9/ml were lysed 1:1 with lysis buffer for 30 minutes on ice. 200-500 µg/ml of protein lysate was incubated at 4-8°C at 6 rpm for 18 hours with 1 µg of specific or control antibody. Protein G Sepharose beads were pre-equilibrated to lysis buffer by first adding 20 µl to 200 µl PBS then centrifuged at 3000 xg at 4°C for 2 minutes then resuspending in PBS. This was repeated twice with 200 µl lysis buffer. The lysate-antibody mixture was added to the beads and incubated at 4-8°C 6 rpm for 1 hour. The sample was centrifuged at 3000 xg at 4°C for 2 minutes and resuspended in lysis buffer; this was repeated two more times with TBS-T. The pellet was then resuspended in 2x Laemmmli buffer and analysed by SDS-PAGE Western blot.

Lysis buffer: 20 mM HEPES, 30 mM NaCl, 0.3 mM EDTA, 2% n-dodecyl β-D-maltoside, 0.5 mM DTT, 0.2 mM PMSF and 2x protease inhibitor cocktail)

2.2.12 Production of tissue lysates

Tissue lysates were performed by homogenising tissue with a 7 ml Dounce homogeniser in 2 ml of tissue lysis buffer. The liquid was centrifuged at 10,000 xg for 20 minutes at 4°C. The supernatant was removed and measured by BCA protein assay and the samples were frozen at -20 or -80°C.

Tissue lysis buffer: 50 mM Tris-HCl pH 7.5, 1% Triton X-100, 1 mM DTT, 1 mM PMSF and 1x protease inhibitor cocktail.

2.2.13 Protein determination

Protein concentrations were measured by the BCA protein assay. Fresh BSA standards were produced at 0, 25, 50, 125, 250, 500, 750, 100, 1500 and 2000

118

µg/ml in modified Tyrode's buffer. Working reagent was made by mixing BCA A and BCA B 50:1 (e.g. 1 µl BCA A and 49 µl BCA B). 175 µl of working reagent was added to each well of a 96 well plate then 25 µl of standard or sample was added to each well in triplicate. The plate was incubated at 37°C for 30 minutes then the absorbance was measured at 562 nm. The blank was subtracted from the average absorbance from the triplicates of each standard and test. A 4 parameter logistic curve was produced in Graphpad and the sample concentration was measured against it to obtain the concentration which was only used if the % recovery of the standard curve was between 80-120%.

2.2.14 Haemostasis measurements

Mice were weighed and anesthetised with 2 µl of working anesthetic/analgesia per g of body weight. The tail was cut off at 2 mm from the tip and immediately immersed in 37°C PBS. Bleeding time was monitored until it stopped for one minute for a period of up to 10 minutes.

Working anesthetic/analgesia: 1 part MTB, 1 part 100 mg/ml Anesketin (anesthetic) and 2 parts 1 mg/ml Dormitan (analgesic)

2.2.15 Flow cytometer setup and calibration

To set up the LSRFortessa flow cytometer, the machine was first cleaned with BD FACSclean, BD FACSRinse fluid then Mili-Q water for 5 minutes. To set up a baseline, one drop of setup and tracking (CS&T) beads was added to 250 µl of FACS flow in a FACS tube, mixed thoroughly and a baseline was set up. Prior to each experiment, the machine was cleaned and CS&T was passed utilising CS&T beads. The machine was cleaned with FACSclean, FACSRinse and Mili-Q for 10 minutes before shut down.

2.2.16 Flow cytometric analysis of platelet surface receptors

5 µl of PRP containing platelets at 3 x 10^8/ml, 40 µl of MTB and 5 µl of FITC-GPVI or FITC-CD41 or FITC-CD42b or FITC-CD49b was added to a FACS tube. 0.1 U/ml thrombin was used for stimulated samples with a final reaction volume of consistently 50 µl and samples were mixed thoroughly. This was incubated at 37°C for 20 minutes then 450 µl of MTB was added. The samples were immediately read in an LSRFortessa flow cytometer using FACSDiva (BD) with 444 V FSC, 290 V SSC, 474 V FITC, 526 V PE & 5000 FSC threshold. The platelets were gated and a bisector gate was added at 2.5% of the negative control to measure the percentage of platelets positive for a particular receptor. Values were expressed as median fluorescent intensity.

2.2.17 Flow cytometric analysis of αIIbβ3 activation and secretion

5 µl of PRP at 3 x 10^8/ml, 40 µl of MTB and 5 µl of PE-JONA, FITC-P-selectin, and APC-cy7-APC was added to a FACS tube which measure active integrin αIIbβ3, alpha granule secretion and dense granule secretion, respectively. 10 µM of Gly-Pro-Arg-Pro-NH2 peptide (Sigma) was used and agonists including thrombin, CRP, ADP and U46619 were used to stimulate platelets. The final reaction volume of consistently 50 µl and samples were mixed thoroughly. This was incubated at 37°C for 20 minutes then 450 µl of 1x BD fix/lyse buffer was added to fix the platelets. The samples were immediately read in an LSRFortessa flow cytometer with 440 V FSC, 297 V SSC, 480 V FITC, 534 V PE, 562 V APC-cy7 & 2500 FSC threshold. The platelets were gated and a bisector gate was added at 2.5% of the basal control to measure the percentage of platelets positive for a particular receptor. Compensation was performed from single antibody control reactions using FlowJo V10. Values were expressed as median fluorescent intensity.

2.2.18 Flow cytometric analysis of platelet size

5 µl of platelets at 5 x 10^8/ml and 495 µl of MTB were added to a FACS tube. The samples were immediately read in an LSRFortessa flow cytometer, the platelets were gated and 444 V FSC 290 V SSC & 1000 FSC threshold was used. The FSC-H and FSC-A were recorded

2.2.19 cAMP ELISA

180 µl of murine platelets at 2 x 10^8/ml were pre-warmed at 37°C then treated with either 100 nM or 3 mM PGI_2 for 3 minutes or left untreated (final volume was consistently 200 µl). Phosphodiesterase inhibitors were not used, Samples were lysed with 22 µl of lysis buffer and frozen at -20°C and then a non-acetylated cAMP enzyme9-linked immunoassay (Amersham cAMP Biotrak System, GE Healthcare, RPM 2251) was performed using the manufacturer's instructions Amersham cAMP Biotrak Enzyme immunoassay (EIA) System (GE Healthcare, RPM 2251)..

2.2.20 Determination of pVASP/pMLC levels

80 µl of murine platelets at 1 x 10^9/ml were pre-warmed at 37°C then treated with either 100 nM PGI_2 for minutes, 5 nM PGI_2 for minutes or 100 nM PGI_2 for minutes followed by 0.1 U/ml thrombin for 3 minutes at 37°C or left untreated (final volume was consistently 100 µl). The reaction was stopped by the addition of 25 µl of 5x Laemmli buffer, samples were boiled at 95°C for 5 minutes and subjected to SDS-PAGE/Western blot on 12% acrylamide gels.

2.2.21 Apoptosis

Apoptosis was induced in platelets by three methods:
a) Incubating 1 x 10^9/ml platelets at 37°C with 6 RPM rotation for 28 hours.

121

b) Incubating 1 x 10^9/ml platelets with 1, 2 or 5 U/ml thrombin for 15 minutes at 37°C.

c) Incubating 1 x 10^9/ml platelets with 10 µm A23187 for 15 minutes at 37°C.

5x Laemmli buffer was then added to the samples which were boiled for 5 minutes at 95°C then subjected to SDS-PAGE/WB.

2.2.22 Statistical analysis

Data are presented as average ± standard error (SE) (unless standard deviation (SD) is indicated in the figure legend). Normality was tested using Shapiro-Wilk's test and statistics were performed using appropriate non-parametric (Mann Whitney-U, Wilcoxon or Kruskal-Wallis) or parametric tests (paired t-test, unpaired t-test or ANOVA) in Graph Pad Prism V 6. P values < 0.05 were considered significant. * = p ≤ 0.05, ** = p ≤ 0.01, *** = p ≤ 0.001 unless otherwise specified in the respective figure legend.

3. Chapter 3 – Characterisation and localisation of coronins in platelets

3.1 Aims

- Investigate the presence and abundance of different coronin proteins in human and mouse platelets
- Validate the specificity of anti-coronin 1, 2, 3 and 7 antibodies
- Investigate the association of coronins to the membrane, F-actin cytoskeleton and lipid rafts using biochemical approaches including subcellular fractionation and insoluble pellet fractionation
- Characterise the cellular localisation of coronins and putative interacting proteins using immunocytochemical approaches

3.2 Results

3.2.1 Characterisation of anti-coronin antibodies on human proteins

Coronins 1, 2 and 3 have a similar structure (McArdle & Hofmann, 2013). Antibodies specific to these coronins were used extensively throughout the project. Therefore their specificity was tested thoroughly. Plasmids encoding Myc-tagged human coronins 1, 2 and 3 were transfected into HEK cells, the proteins were expressed and the lysates were probed first for the Myc tag (**Figure 3.2.1A**), then for coronin 1 (**Figure 3.2.1B & Figure 3.2.1C**), coronin 2 (**Figure 3.2.1D**) and coronin 3 (**Figure 3.2.1E**). All three coronins probed positive for Myc in the coronin samples and negative in the untransfected control demonstrating that the transfection and expression was successful, The extra band above coronin 1 detected with the anti-Myc antibody could be due to coronin 1 with post translational modification or unspecific staining of a non-coronin protein (**Figure 3.2.1A**).

Probing for coronin 1 (ab72212) resulted in a strong band slightly above the 55 KDa marker in the coronin 1 lane. Coronin 1 is 56 KDa and the Myc-tag is 9 KDa so this will be approximately the correct size for the fusion protein. The untransfected control resulted in an extremely faint band corresponding to endogenous to coronin 1 in HEK cells (**Figure 3.2.1B**). Coronin 1 (ab56820) resulted in very similar results but without the endogenous band, probably due to lower exposure (**Figure 3.2.1C**).

Coronin 2 probing picked up a strong band for coronin 2 in the coronin 2 lane between the 55 and 72 KDa markers. There are also faint bands for smaller, non-tagged, endogenous coronin in the other lanes (**Figure 3.2.1D**).

Probing with the coronin 3 hybridoma supernatant (K6-444) identified up a strong band for coronin 3 slightly above the 55 KDa marker. Faint bands for smaller, non-tagged, endogenous coronin 3 are visible in the other lanes (**Figure 3.2.1E**). In summary, these results demonstrate that the antibodies which were tested reacted specifically to each coronin.
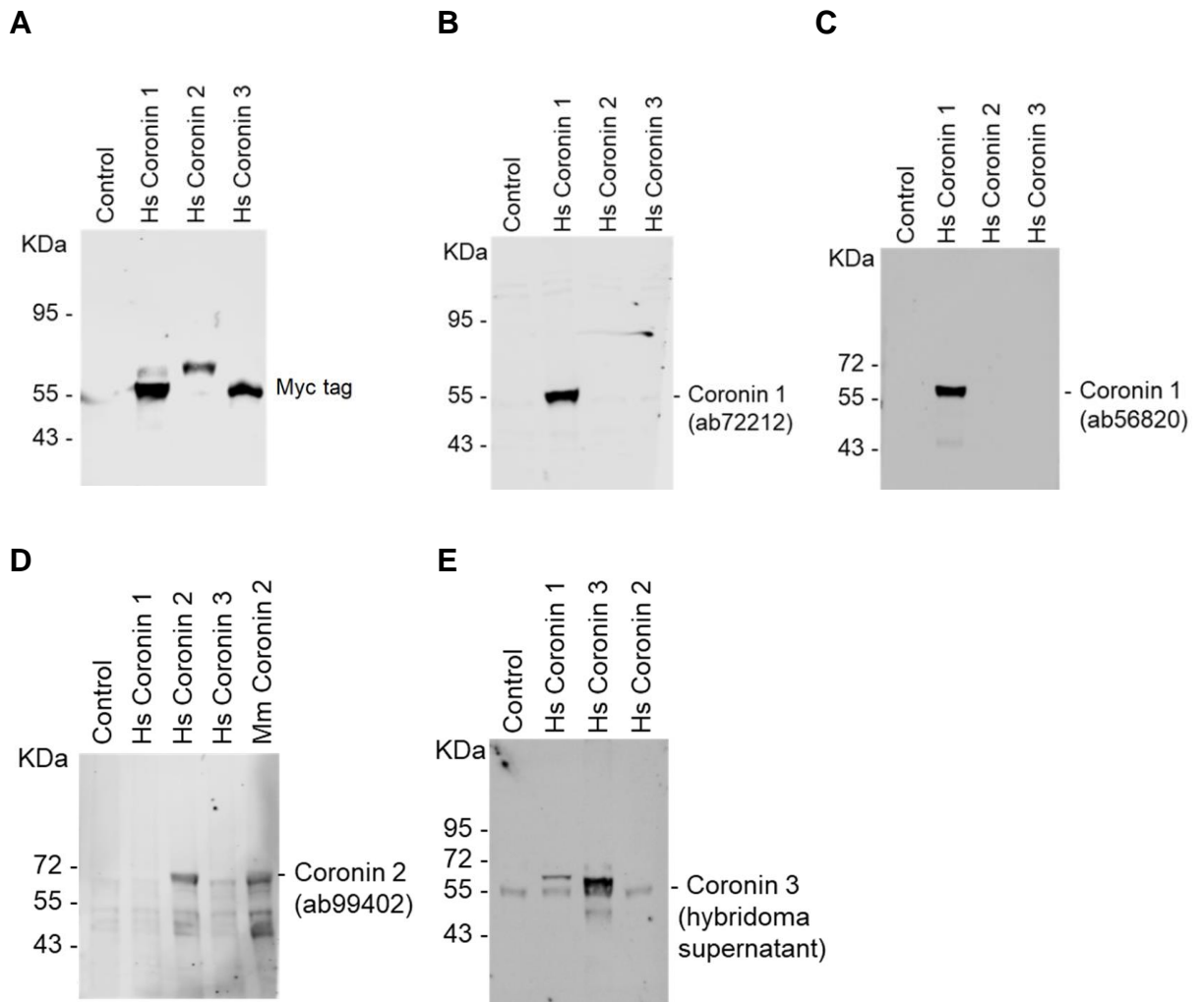
Figure 3.2.1 - Characterisation of anti-coronin antibodies (human)
Plasmids containing human coronins 1, 2 or 3 were transfected into HEK cells and
Myc-tagged proteins were expressed except in the untransfected control. ~20 μg of
lysate from each sample were subjected to SDS-PAGE, blotted onto PVDF and
probed with antibodies for Myc (**A**), coronin 1 (ab72212) (**B**), coronin 1 (ab56820)
(**C**), coronin 3 (ab99402) (**D**) and coronin 3 (K6-444) followed by incubation with
anti-rabbit 680 nm or anti-mouse 800 nm secondary Licor antibodies. Membranes
were imaged using a Licor with Image Studio (V 5.2). Hs = human,

3.2.2 Characterisation of anti-coronin antibodies on mouse platelets

Similarly to the human coronins above, antibodies were tested against murine coronin proteins. Plasmids encoding murine coronins 1-3 fused to a Myc tag were expressed in HEK cells and the HEK lysates probed by Western blot. The Myc tag demonstrated the presence of the tagged protein slightly above the 55 KDa marker, with the absence of the tag in the untransfected (negative) control (**Figure 3.2.2A).** Likewise, coronin 1 was detected using the relevant coronin 1 antibodies on transfected cell lysates (**Figure 3.2.2B & C**). Endogenous coronin 1 should be present in the untransfected lanes and lanes transfected with plasmids for coronins 2 and 3 but the bands are probably under the detection limit of the exposure used.

A relatively strong band for coronin 2 was detected using the relevant antibodies on transfected cell lysates with expected weaker bands demonstrating the presence of endogenous coronin in untransfected samples and samples transfected with coronins 1 or 3 (**Figure 3.2.2D & E**).

Likewise, a relatively strong band for coronin 3 was detected using the anti-coronin 3 hybridoma supernatant on transfected cell lysates with weaker bands demonstrating the presence of endogenous coronin 3 in untransfected samples and samples transfected with coronins 1 or 2 (**Figure 3.2.2F**).

Both of the coronin 1 antibodies seem to perform similarly, although at the time of writing, the Abcam (ab56820) antibody is discontinued (**Figure 3.2.2B & C**). The anti-coronin 2 Abcam (ab99402) antibody seems to produce a more intense band and perform better than the Bethyl Laboratories (A301-317A) anti-coronin 2 antibody (**Figure 3.2.2D & E**), which was considered inadequate for reliable quantification in future experiments with platelets.
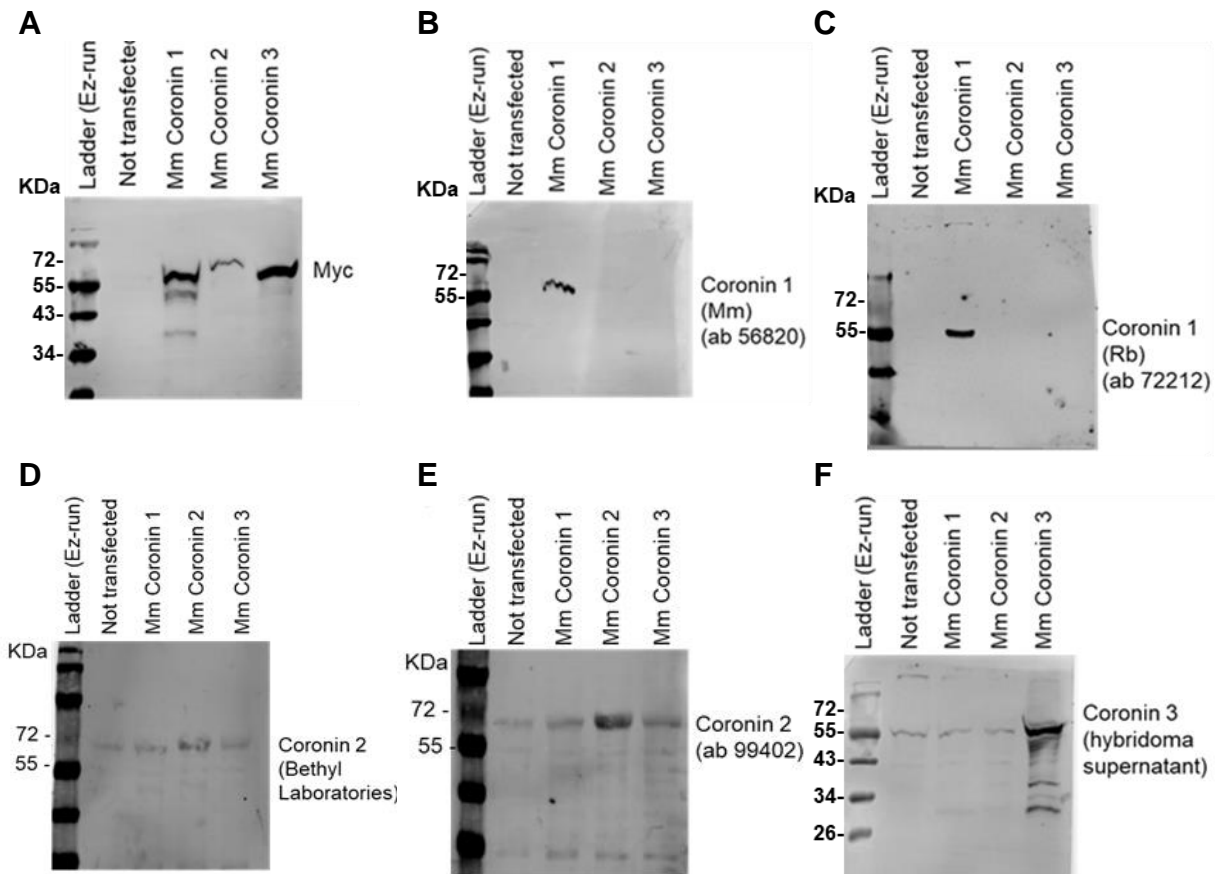
Figure 3.2.2 - Characterisation of anti-coronin antibodies (mouse)
HEK cells were untransfected or transfected with plasmids containing Myc-tagged murine coronin 1, 2 or 3. ~20 µg of lysate from each sample was subjected to SDS-PAGE, blotted onto PVDF, incubated with antibodies for Myc (**A**), coronin 1 (ab56820) (**B**), coronin 1 (ab72212) (**C**), coronin 2 (A301-317A) (**D**), coronin 2 (ab99402) (**E**), or coronin 3 (K6-444) (**F**), then incubated with anti-rabbit 680 nm or anti-mouse 800 nm secondary Licor antibodies. Membranes were imaged using a Licor with Image Studio (V 5.2). Mm = mouse, Rb = rabbit.

3.2.3 Coronins 1, 2, 3 and 7 are expressed in human and murine platelets

The review of transcriptomic (**Figure 1.19**) and proteomic literature revealed coronin 1, 2, 3 are abundant and coronin 7 is present at low levels, in human (Burkhart *et al.*, 2012) and mouse platelets (Zeiler *et al.*, 2014) (**Figure 1.20**). Western blots were performed to confirm their presence in human and murine platelets. Coronin 1 and 3 were present in appropriate control tissues and cells. Strong bands were observed for coronin 1, 2 and 3 in both mouse and human platelets. Coronin 7 was present in the brain control tissue and present in both human and mouse platelets albeit as an extremely faint in human platelets (**Figure 3.2.3A**) which was greatly enhanced to become obvious (**Figure 3.2.3B**). GAPDH was used as a loading control (**Figure 3.2.3A**). Coronin 2 was not probed in control tissues and cells as this antibody was acquired at a later date after the relevant lysates were no longer available These results confirm the proteomic results that coronins 1-3 are abundant and coronin 7 present, in both human and murine platelets.

As reported in **Section 1.3.10,** there have been no reports of the presence of coronin 6 mRNA in human or coronin 5 mRNA mouse platelets. However, human coronin 4 and 5 and murine coronin 4 and 6 mRNA have been found at extremely low levels (Rowley *et al.*, 2011), which were far below the sensitivity of most experiments reported (**Appendix 8.1.3**).

As reported in **Section 1.3.10**, even in the most sensitive experiments, there have been no reports of coronins 4-6 proteins present in human platelets (Burkhart *et al.*, 2012) or murine platelets (Zeiler *et al.*, 2014)**.** Coronins 4-6 are outside the scope of the project and no suitable antibodies were available so the lysates were not probed for them.
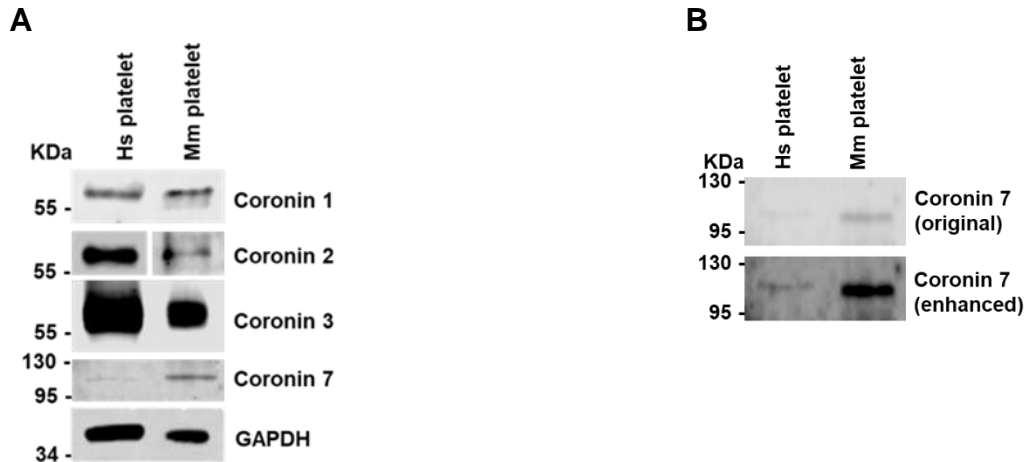
Figure 3.2.3 – Expression of coronins in platelets, tissues and cell line lysates
(**A**) Human and murine platelets at 1 x 10^9 were lysed 1:1 with 1% triton in PBS.
Tissues (brain, heart and spleen) were lysed 1:1 in RIPA buffer, homogenised with
a 2 ml Dounce homogeniser on ice, subjected to centrifugation at 2000 xg for 10
minutes at 4°C and the supernatant was collected. Samples were diluted in PBS
and a BCA protein assay was used to measure protein concentration. 20 µg of
protein for coronin 1, 2, 3, 7 and GAPDH, was subjected to SDS-PAGE then blotted
onto PVDF membrane which was incubated with antibodies for the indicated
proteins followed by anti-rabbit 680 or anti-mouse 800 secondary Licor antibodies.
Membranes were imaged utilising Licor with Image Studio (V 5.2). GAPDH was
used as a loading control. (**B**) Coronin 7 was greatly enhanced with ImageJ by
setting the minimum and maximum intensity values at 178 and 225 respectively,
equivalent to linearly decreasing the brightness and increasing the contrast. GAPDH
= Glyceraldehyde 3-phosphate dehydrogenase; HEK = Human embryonic kidney;
HT29 = Human colorectal cell line.

3.2.4 Coronin 1 and 3 associate with the Triton X-100 insoluble pellet in human platelets

Coronins 1, 2 (Cai, Makhov, *et al.*, 2007) and 3 (Chan *et al.*, 2012) are known to
bind to F-actin and regulate the actin cytoskeleton (Gandhi & Goode, 2008). As F-
actin is insoluble in Triton X-100, platelets in basal or activated states at various
time points can be lysed, fractionated and subjected to SDS-PAGE/WB the extent of
association of proteins (in this case coronins) with F-actin (Asyee *et al.*, 1987; Fox
et al., 1993; Tardieux *et al.*, 1998).

   It has previously been reported from insoluble pellet fractionations that
coronin 1 associates with F-actin in the supernatant and the pellet in low speed (LS)

(15,600 xg) insoluble fractionation and latrunculin treatment reduces the amount of coronin 1 in the pellet. This suggests the ability of coronin 1 to associate with the LS pellet, where cross-linked F-actin filaments are, is dependent F-actin polymerisation. Coronin 1 associates with only the pellet and not the supernatant in high speed (HS) (100,000 xg) insoluble pellet fractionation where small F-actin filaments or lipid rafts reside, and this is unchanged by latrunculin treatment, demonstrating this is independent of F-actin polymerisation. Profilin was reported in the supernatant as expected by a monomeric binding protein. CD36 was reported in all fractions, indicating the presence of membrane components, possibly from lipid rafts (Riley *et al.*, 2019).

First, aggregation by stimulation was performed to confirm the agonist dose which would result in a strong platelet response (**Appendix 8.1.2**). Coronin 1 and 3 were both found to associate with F-actin in human platelets. The levels of coronin 1 and 3 bound to F-actin increased concurrently with the levels of F-actin which increased over time due to actin polymerisation, induced by thrombin stimulation (**Figure 3.2.5A**). 0.1 U/ml thrombin was used as it is a high dose which also causes aggregation of over 80% after 5 minutes of stimulation (**Appendix 8.1.2A**). The F-actin was significantly higher than basal at 15 seconds and continued to increase until 45 seconds at which stage it plateaued. Coronin 1 and 3 both increased, becoming statistically significantly higher than the basal at 45 seconds at which stage coronin 1 plateaued but coronin 3 continued to increase until 180 seconds (**Figure 3.2.5A**).

Upon stimulation with 50 µg/ml collagen, which causes ~90% aggregation within 5 minutes (**Appendix 8.1.2B**), the levels of coronin 1 and coronin 3 again increased as the F-actin also increased due to their association. The increase was slower with the peak F-actin increase significant at 45 as opposed to 15 seconds with thrombin, and peaking at around 60 seconds as opposed to 45 seconds with thrombin (**Figure 3.2.5B**). The levels of coronin 1 and 3 bound to F-actin also increased slower with coronin 3, becoming significantly higher than the basal at 45 and 15 seconds, respectively The coronin 3 increase appeared faster in the collagen treated samples compared to the thrombin treated samples (**Figure**

3.2.4B), but this could be due to the considerable variation from this particular experiment rather than due to an agonist-specific phenomenon. This demonstrates that coronin 1 and 3 associate with F-actin in platelets and that their associate is closely linked to the amount of F-actin present.

A similar result to coronins 1 and 3 was observed with coronin 2, however the inter-experimental variation was high and the protein bands appeared degraded so the quantification was less reliable (**Appendix 8.1.1**).

A

B
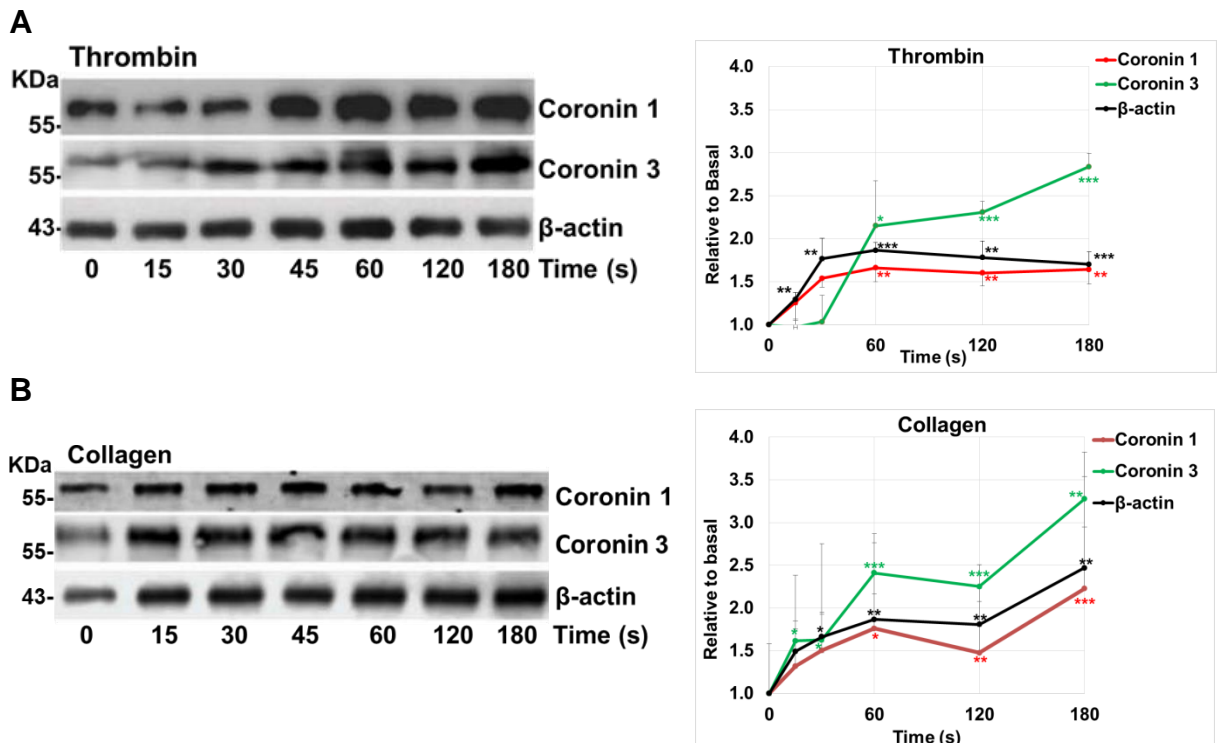
Figure 3.2.4 – Coronin 1 and 3 associate with the Triton X-100 insoluble pellet in human platelets
(**A**) 1 x 10^9 µl of washed human platelets were stimulated with 0.1 U/ml thrombin or 50 µg/ml collagen then lysed at 0, 15, 30, 45, 60, 120 or 180 seconds in Triton X-100 lysis buffer. The Triton insoluble pellets were prepared by centrifugation at 15,600 × g for 15 minutes at 4°C then subjected to SDS-PAGE/WB and probed using the indicated antibodies. (**B**) Densitometry values are mean ± SEM for 3–7 experiments *p < .05, **p< .01, ***p < .001 relative to basal. Unpaired t-test. (The data for coronin 1 upon thrombin treatment was in collaboration with Jawad Khalil).

131

3.2.5 Coronin 1 associates with the Triton X-100 insoluble pellet in murine platelets

After proof of principle utilising human platelets, the Triton X-100 insoluble pellet, was also performed with WT murine platelets. As with human platelets (Riley *et al.*, 2019), a proportion of coronin 1 was found in the LS pellet, with most of the coronin in the supernatant fraction. Upon HS fractionation coronin 1 was found in the pellet but not in the supernatant, indicating association with F-actin (**Figure 3.2.5A**)

A similar response to human platelets was also observed with β-actin and coronin 1 upon treatment with 0.1 U/ml thrombin or 25 µg/ml collagen when compared to human platelets (**Figure 3.2.5B**). Murine platelets were also subjected to Triton X-100 insoluble pellet after latrunculin treatment. Due to resource restrictions this was performed once and the raw densitometry values were plotted as the results with latrunculin, compared to without latrunculin, was considered binary. The treatment resulted in extremely small levels of detectable coronin 1 and β-actin in the pellet (**Figure 3.2.5C**). This provided further evidence that coronin 1 is associated with F-actin in platelets.
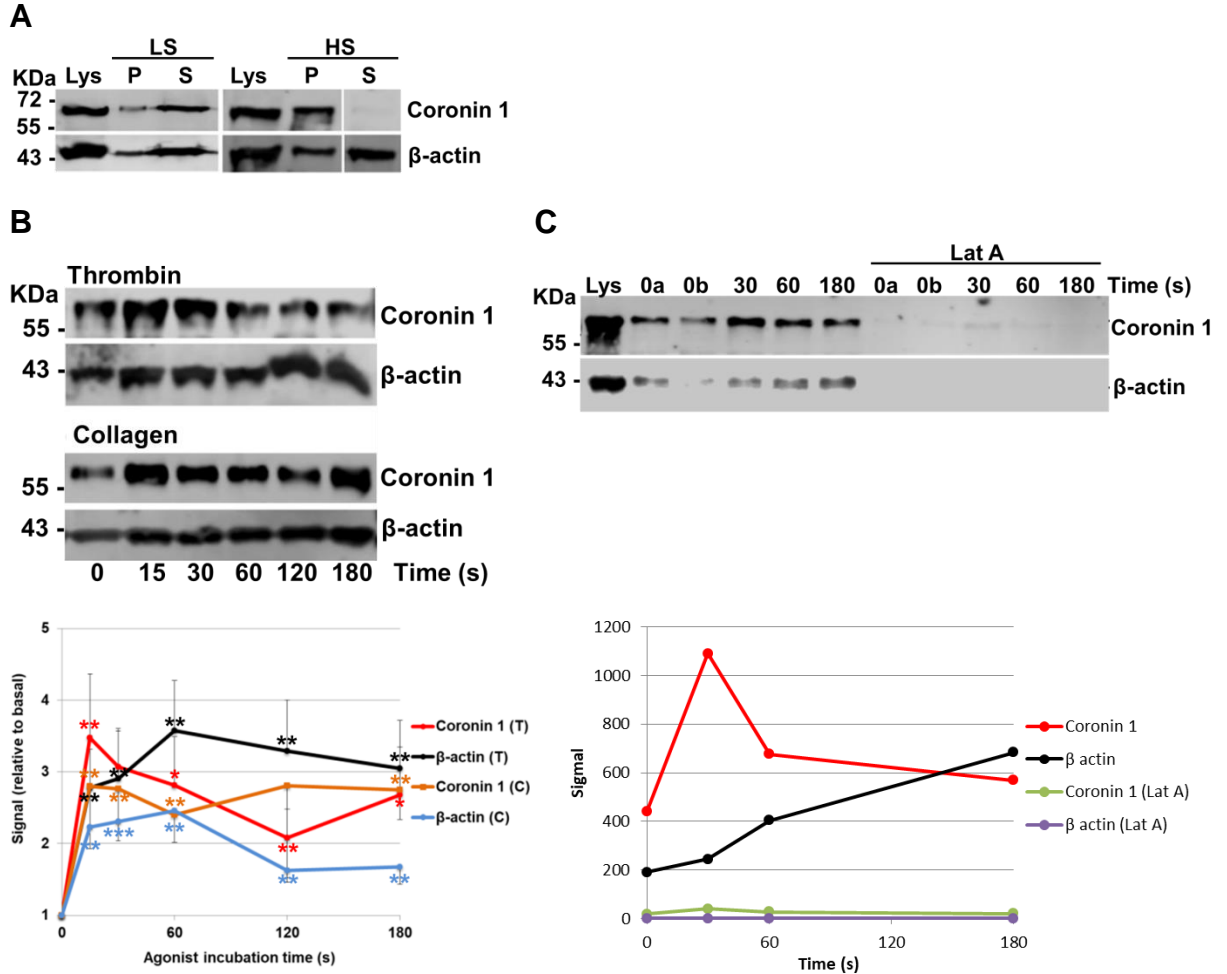
Figure 3.2.5– Coronin 1 associates with triton X-100 insoluble pellet in murine platelets

Similarly to **Figure 3.2.4**, murine platelets were subjected to Triton X-100 insoluble pellet fractionation (**A**). Murine platelets were stimulated with 0.1 U/ml thrombin or 25 µg/ml collagen then lysed at 0, 15, 30, 60, 120 or 180 seconds in 1% Triton X-100 lysis buffer. The Triton insoluble pellets were prepared by centrifugation at 15,600 × g for 15 at 4°C, subjected to SDS-WB and probed using the indicated antibodies. Densitometry values are mean relative to basal ± SEM for 5–7 experiments Unpaired t-test (**B**). Murine platelets were subjected to incubation with 20 µM latrunculin A at 37°C for 30 minutes prior to stimulation with 0.1 U/ml thrombin and then subsequent fractionation and SDS-PAGE/WB. Raw densitometry values are displayed. n = 1 as the analysis was considered binary. The average values of 2 basals per condition were plotted (**C**). Lat = latrunculin; T = thrombin; C = collagen; Lys = lysate; HS = High speed; LS = Low speed.

3.2.6 Human coronin 1 and 3 are cytosol and membrane associated but do not translocate to or from the platelet membrane

Approximately one-third of coronin 1 is membrane associated in platelets (Riley *et al.*, 2019). It has been suggested that coronin 1 can translocate to or from the membrane upon stimulation by isoproterenol in Mel JuSo (melanoma) cells (Jayachandran *et al.*, 2014). To investigate whether exposure to various platelet agonists and inhibitors would affect coronin membrane-association or translocation, human platelets were treated in suspension with either 0.1 U/ ml thrombin, 50 µg/ml collagen, or 100 nM PGI$_2$ (**Figure 3.2.6A** & **B**), or thrombin followed by PGI$_2$ or PGI$_2$ followed by thrombin treatment (**Figure 3.2.6D**). The platelets were then subjected to lysis, then membrane/cytosol fractionation followed by SDS-PAGE/WB and then were probed for coronin 1 (**Figure 3.2.6C**) and coronin 3 (**Figure 3.2.6B**). Membranes were analysed and the coronin was measured relative to β3 integrin. No significant changes in the proportion of coronin 1 in the membrane were observed upon any of the treatments. This suggests that coronin 1 or 3 do not translocate between the membrane and cytosol in platelets upon stimulation or inhibition.
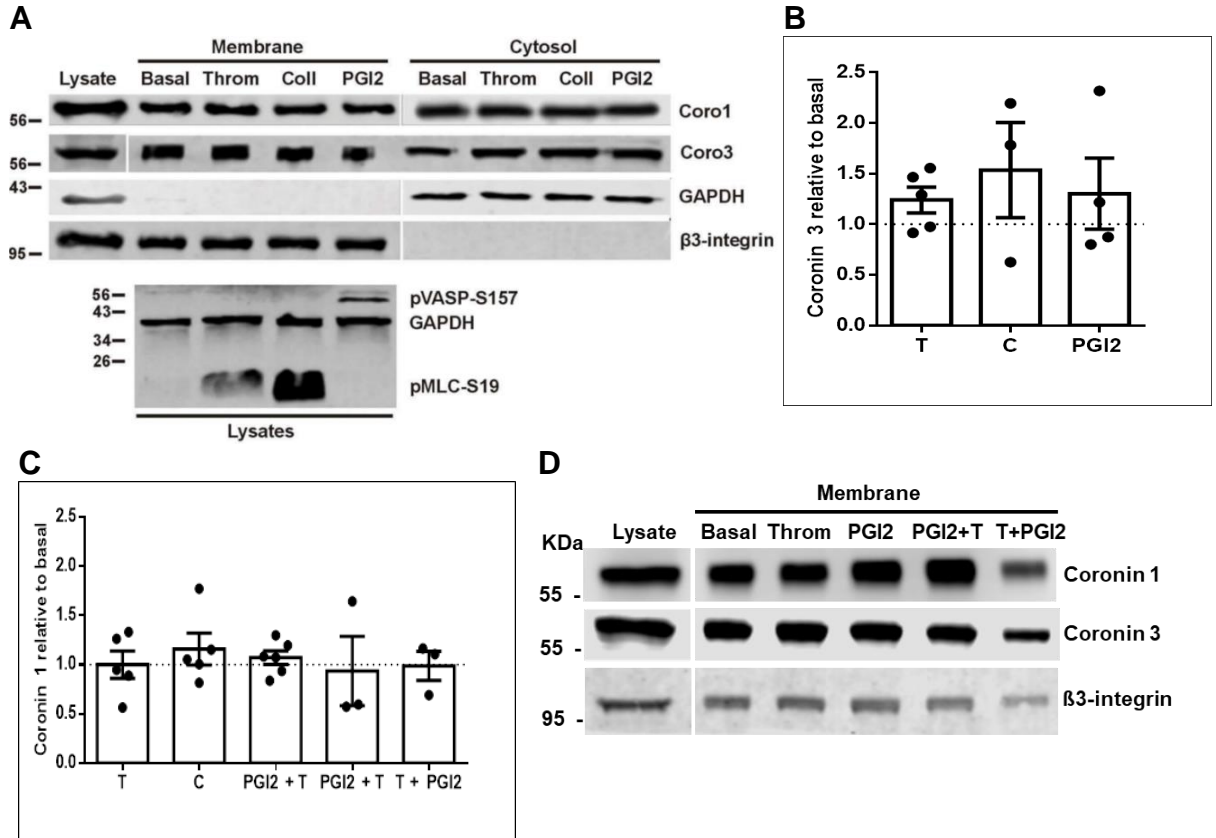
Figure 3.2.6 – Membrane/cytosol fractionation of human platelets

200 µl of washed human platelets at 1×10^9/ml were treated with 1 mM EGTA, 10 nM indomethacin and 2 U/ml apyrase for 20 minutes at 37°C to prevent aggregation. They were then treated with either 0.1 U/ml thrombin, 50 µg/ml collagen or 100 nM PGI$_2$ for 1 min (**A**), or 0.1 U/ml thrombin for 1 min followed by 100 nM PGI$_2$ for 1 min, or 100 nM PGI$_2$ followed by 0.1 U/ml thrombin for 1 min (**D**) at 37°C prior to lysis and subcellular fractionation to separate the membrane and cytosol. Fractions were normalised by volume and subjected to SDS-PAGE/WB then probed for coronin 1 and 3. β3 Integrin and GAPDH were used as membrane and cytosolic markers, respectively. The phosphoproteins pMLC-S19 and pVASP-S157 were used as markers of thrombin/collagen stimulation or PGI$_2$-induced inhibition, respectively (**A & D**). Membrane-associated coronin 3 (**B**) and 1 (**C**) were quantified by densitometry, normalised to β3 integrin and expressed relative to the respective coronin in the basal membrane fraction. Data is mean ± SEM of 3–6 experiments. No significant differences were found relative to basal for any coronin (Kruskal-Wallis tests). T = thrombin, C = collagen.

3.2.7 Coronins 1 and 2 both form complexes with ARPC2 and Gαs

Coronin 1 (Appleton *et al.*, 2006; Humphries *et al.*, 2002; Ojeda *et al.*, 2015) and 2 (Cai, Marshall, *et al.*, 2007) have been reported to bind to F-actin and the Arp2/3 complex to regulate its activity. Gαs binds with coronin 1 in neurons as demonstrated by IP and surface plasmon resonance (SPR) (Jayachandran *et al.*, 2014). Gαs is also important for platelet inhibition signalling by PGI2 through IP (Broos *et al.*, 2011). Immunoprecipitation (IP) provides some evidence that proteins may bind together or associate in a complex. An IP using an anti-coronin 1 antibody was performed in human platelets and strong bands were apparent for coronin 1, ARPC2 and Gαs which are almost absent in the unspecific IgG negative control. This provides some evidence there may be specific binding of ARPC2 and Gαs to coronin 1. The presence of heavy chain bands originate from the secondary antibody binding to the denatured antibody on the membrane, and prove that the pellet containing the beads was not entirely washed away. The wash SN bands provide further evidence that proteins are binding to the anti-coronin antibody rather than to the unspecific IgG as the bands for coronin 1, Gαs and ARPC2 are fainter on the IP compared to the control (**Figure 3.2.7A**). This gives evidence that coronin 1 may bind or form a complex specifically with Gαs and ARPC2 in platelets.

Coronin 2 behaved similarly to coronin 1. Strong bands were found in the coronin 2 IP for coronin 2, ARPC2 and Gαs with almost no signal in the unspecific IgG, indicating specificity. The specific binding can be further demonstrated as the amount of protein in the Wash SN in lower in the specific IP than the unspecific IgG, again indicating specificity (**Figure 3.2.7B**). This not only provides evidence that coronin 2 may bind or form a complex with Gαs and ARPC2, but also suggests possible redundancy between coronin 1 and 2 in platelets.

Coronins 2 and 3 were found to co-IP together (**Figure 3.2.7B**). This association has previously been reported with reciprocal IPs (Abella *et al.*, 2016). This may provide evidence of the possibility of redundancy between the coronins.
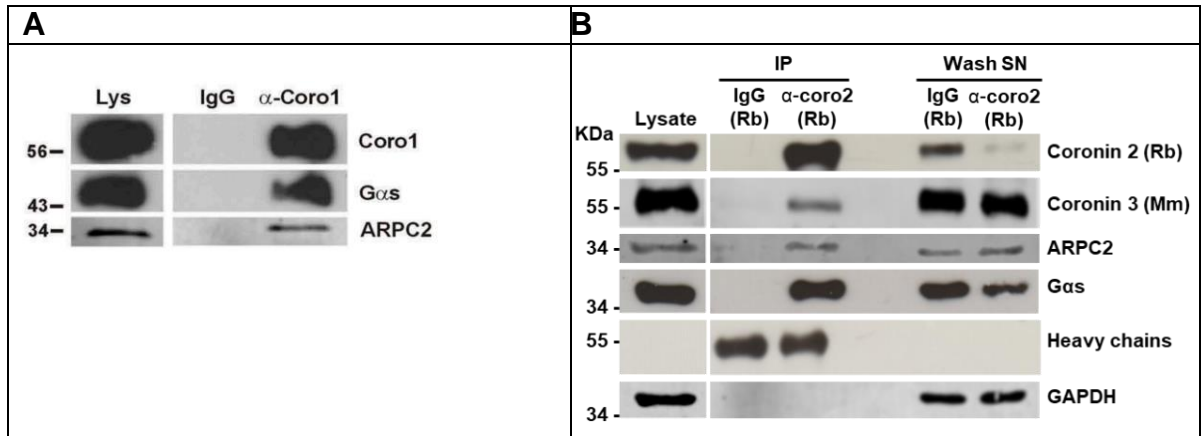
Figure 3.2.7 - Immunoprecipitation of coronins
420 µl of human platelets suspensions at 1 x 10^9/ml (~500 µg) were lysed 1:1 with lysis buffer, for 30 minutes on ice, incubated overnight with an 0.5 µg of indicated unspecific or an indicated specific antibody at 4°C with rotation at 6 RPM, incubated with pre-equilibrated beads for 1 hour at 4°C with 6 RPM rotation, then boiled for 5 minutes at 95°C in WB denaturing/loading buffer and subjected to SDS-PAGE/WB. Membranes were probed with anti-coronin 1 or anti-coronin 2 antibodies overnight followed by a light chain specific HRP-conjugated secondary antibody for 1 hour at RT then developed with film. Then the membranes were incubated wth the other indicated primary antibodies overnight at 4°C, followed by anti-rabbit or anti-mouse HRP or anti-rabbit (800 nm) or anti-mouse (680 nm) (Licor) secondary antibodies for 1 hour at RT. IPs were performed with an anti-coronin 1 antibody (**A**) and an anti-coronin 2 antibody (**B**). Mm = mouse; Rb = rabbit and refers to the species from which the antibody used to probe originated.

3.2.8 Coronin 1 localises at actin nodules

To ascertain coronin 1 function in relation to F-actin in platelets, it is important to examine where in the platelet it localises in various conditions. As an F-actin binding protein, coronin 1 regulates it's turnover (Gandhi & Goode, 2008) and plays roles in both the membrane and the cytosol (Pick *et al.*, 2017). Coronin 1 and F-actin were stained in human platelets to investigate colocalisation. Coronin 1 appeared diffused around the cell, with stronger staining around the cortex of platelets in their basal state which were centrifuged onto poly-L-lysine (**Figure 3.2.8A**). On fibrinogen, coronin 1 appeared punctuated throughout the platelets with greater staining in the cell cortex. There appeared be a small increase in the punctuated coronin 1 staining along F-actin stress fibres. The coronin 1 staining along actin stress fibres was faint

137

on platelets spread on fibrinogen (**Figure 3.2.8B**) and very pronounced on collagen (**Figure 3.2.8C**).

Actin nodules are regions of very dense F-actin and phosphorylated proteins (Poulter *et al.*, 2015). There was very strong staining for coronin 1 at actin nodules on cells which were not fully spread on fibrinogen (**Figure 3.2.8D**) and also on cells which were treated with PGI_2, which encourages the development of actin nodules.

Vinculin (Mitsios *et al.*, 2010; Poulter *et al.*, 2015) and CAP1 (Joshi *et al.*, 2018) have both previously been identified as markers of actin nodules. Coronin 1 colocalises with F-actin and vinculin at the actin nodules, Coronin 1 also partially colocalises with F-actin at other areas including the cortex and throughout the cytoplasm (**Figure 3.2.8D**, **F** & **G**). Similar localisation was found with coronin 1 and CAP1 (**Figure 3.2.8E**). Taken together this is further evidence that coronin 1 binds F-actin and may have roles in actin remodelling in platelets at the cortex and actin nodules.
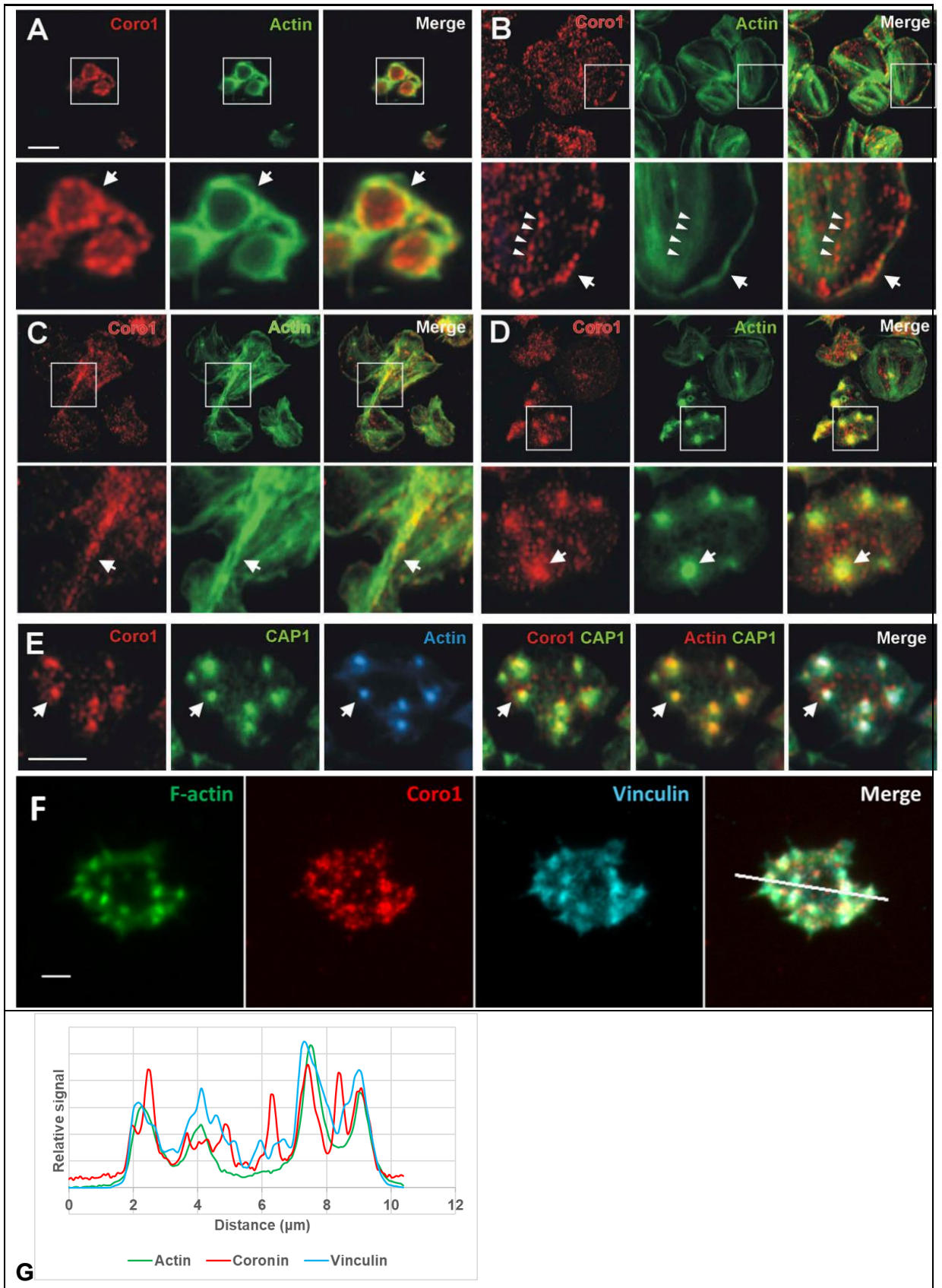
Figure 3.2.8 - Subcellular localisation of Coronin 1
Human platelets were fixed in suspension and centrifuged onto poly-L-lysine (**A**), or spread on 100 µg/ml fibrinogen (**B & D-F**) or 100 µg/ml collagen coated coverslips (**C**), fixed and stained for indicated proteins. (**E & F**) Platelets were treated with 100 nM PGI$_2$ at 37°C for 5 minutes prior to fixation to increase the proportion of cells displaying actin nodules. Images were acquired with a fluorescence microscope with an apotome and deconvolved with Zen software. Magnified regions are indicated with a square. Arrows point at regions of interest: cell cortex (**A & B**), actin filaments (**C**) or actin nodules (**D & E**). Colocalisation plot of coronin 1, F-actin and vinculin produced using FIJI (ImageJ) (**G**). Arrowheads indicate coronin 1 at stress fibres (**B**). Scale bars = 5 µm. Scale bars on **A** applies to **B**, **C** and **D** non-magnified rows only. Scale bar on **F** = 2 µm.

3.2.9 Coronins 2 and 3 colocalise with F-actin nodules

The insoluble pellet experiment demonstrated that coronins 1 and 3 associate with F-actin. To investigate the distribution and F-actin association of coronins 1, 2 and 3, co-immunostaining experiments were performed similarly to that of the previous section. Coronins 2 and 3 were found to have a similar distribution pattern as with coronin 1 above. Coronins 2 (**Figure 3.2.9A**) and 3 (**Figure 3.2.9D**) demonstrated diffused staining on platelets centrifuged onto poly-L-lysine with stronger staining at the cortex. Coronins 2 (**Figure 3.2.9B**) and 3 (**Figure 3.2.9E**) were found to be punctuated through the cell, when spread on fibrinogen, with stronger staining localised with actin at the actin ring around the cell cortex. Like coronin 1, coronins 2 (**Figure 3.2.9C**) and 3 (**Figure 3.2.9F**) also displayed strong staining at the actin nodules when partially spread on fibrinogen (**Figure 3.2.9B, C & E**). This indicates that coronin 1-3 all appear to localise with F-actin in a similar manner and possibly are redundant and all involved in F-actin turnover.
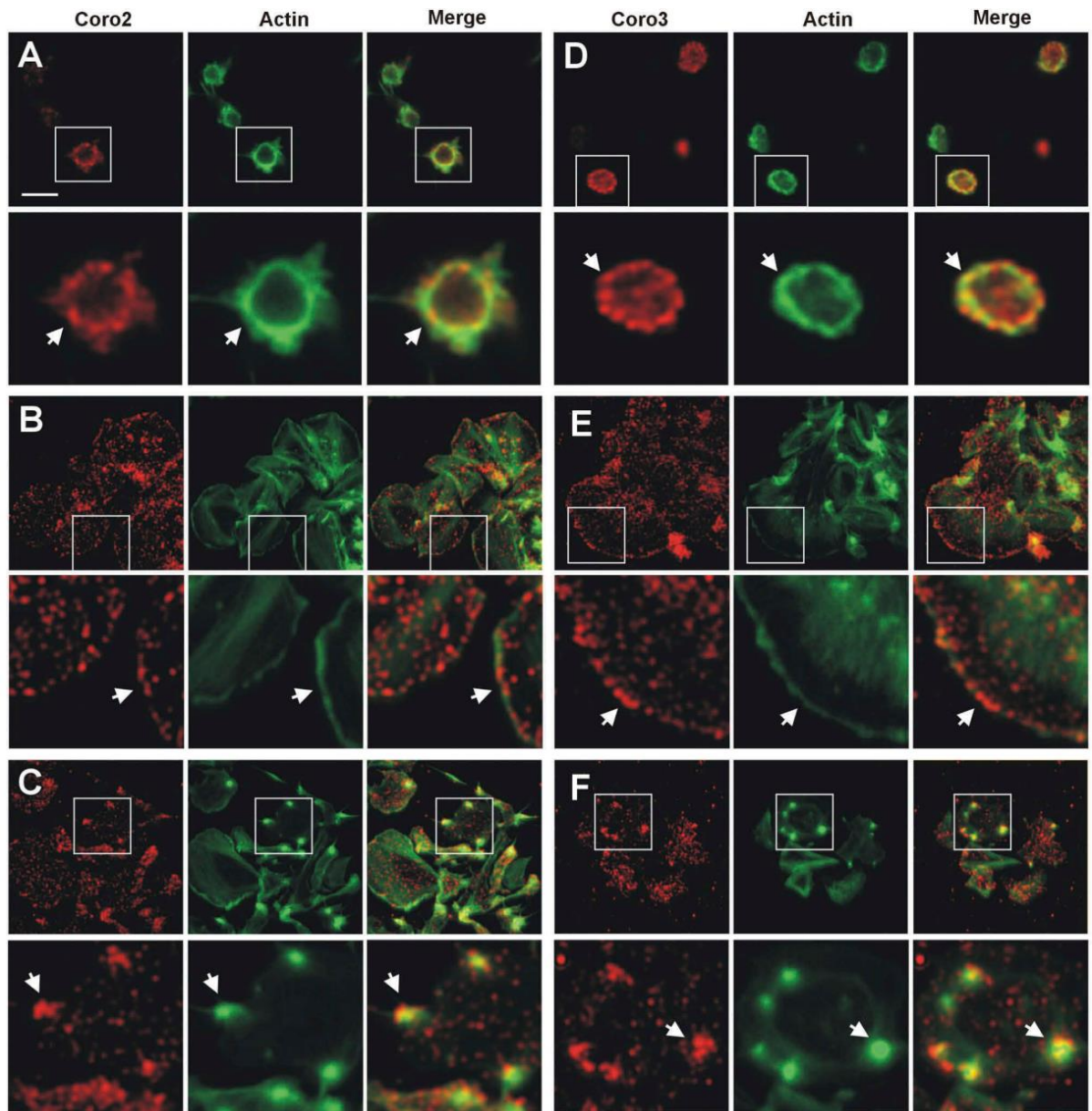
Figure 3.2.9 - Subcellular localisation of coronin 2 and 3
Human platelets were fixed in suspension with PFA then centrifuged onto poly-L-lysine (**A, D**), or were allowed to spread on 100 µg/ml fibrinogen coated coverslips (**B, C, E, F**). Cells were stained for the indicated proteins. Magnified regions are indicated with a square. Arrows point to cell cortex (**A, B, D, E**) or actin nodules (**C, F**). Scale bar = 5 µm.

141

3.2.10 Coronin 1 localisation is dependent on F-actin

Coronin 1 localisation could be influenced by several factors several factors. To investigate if coronin 1 localisation depends on F-actin polymerisation or microtubule assembly/disassembly, they were disrupted with latrunculin or nocodazole, which bind to monomeric G-actin or β-tubulin respectively.

Similarly to the previous section, coronin 1 was found at the cell cortex in basal platelets which were centrifuged onto poly-L-lysine in the untreated control (**Figure 3.2.10A**). Upon latrunculin A treatment, the F-actin staining was greatly reduced as expected, demonstrating the treatment was successful. Coronin 1 appeared more diffuse than in the basal, indicating latrunculin had an effect and that the distribution of coronin 1 is dependent on F-actin turnover (**Figure 3.2.B**). In contrast, nocodazole treatment had no effect on coronin 1 distribution, while displaying dispersed tubulin staining demonstrating microtubule successfully disrupted microtubule formation (**Figure 3.2.C**). This indicates the distribution of coronin 1 is specific to F-actin turnover, not tubulin.
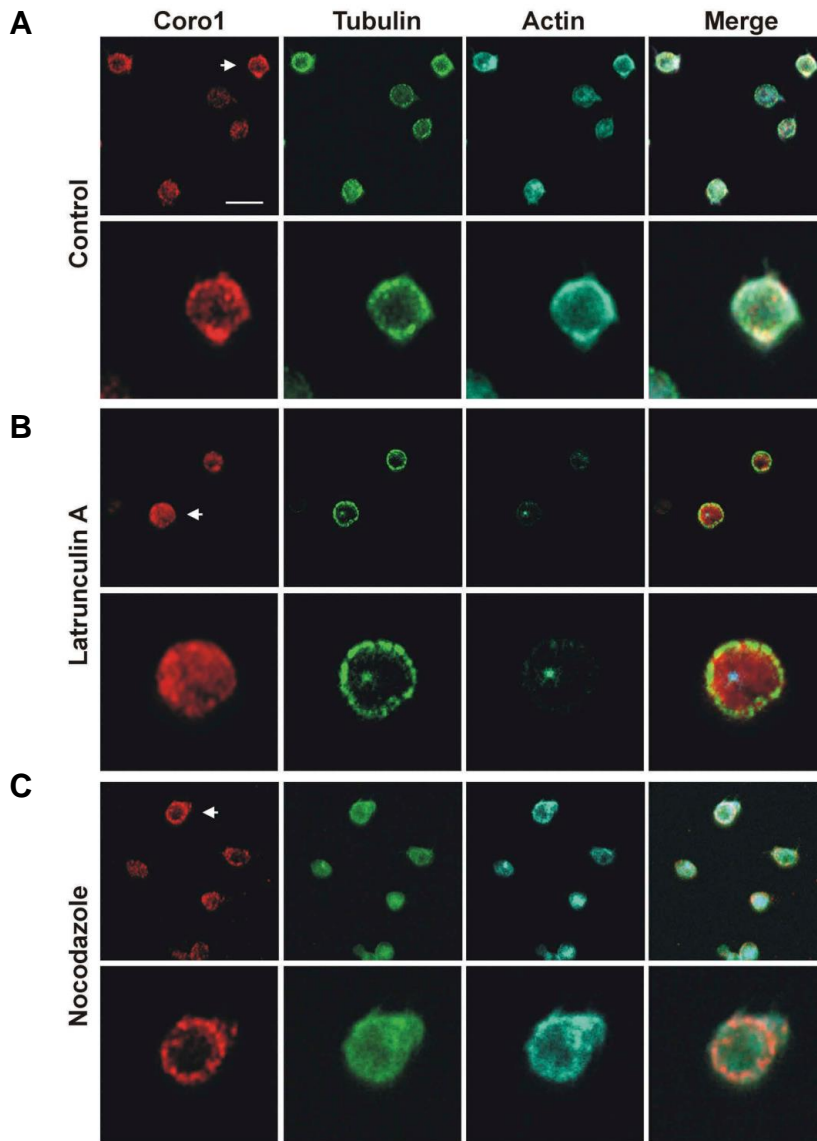
Figure 3.2.10 - Coronin 1 localisation is dependent on F-actin

Human platelets were either stimulated with 3 µM latrunculin A for 20 minutes, 10 µM nocodazole for 20 minutes or left in their basal state. Platelets were then centrifuged onto poly-L-lysine coverslips, fixed, permeabilised, then stained for the indicated proteins. Arrows indicate cell enlarged in next row. Scale bar = 5 µm. (Performed in collaboration with Francisco Rivero) (Riley *et al.*, 2019).

143

3.2.11 Coronins 1-3 partially localise together

Individual immunostainings demonstrated that coronins 1 (**Figure 3.2.8**), 2 and 3 localise to F-actin structures including the platelet cortex and actin nodules when spread on fibrinogen (**Figure 3.2.9**). To confirm coronins 1-3 and F-actin colocalise together, several stainings were undertook. Due to technical limitations, a maximum of 3 simultaneous stainings could be performed. Coronin 1, 2 and F-actin (**Figure 3.2.11A**); coronin 1, 3 and F-actin (**Figure 3.2.11B**); coronin 2, 3 and F-actin (**Figure 3.2.11C**) were stained in platelets which were spread on 100 µg/ml fibrinogen. In addition to coronins 1-3 localising at F-actin nodules, they also appear to localise together at the cell cortex and actin nodules (**Figure 3.2.11**). As coronins 1, 2 and 3 colocalise at actin nodules, they may have a similar function in that region. However coronins 1, 2 and 3 also appear to only partially colocalise at other areas, punctuated throughout the cell, indicating a lack of redundancy (**Figure 3.2.11**). Taken together with the similar IP and fractionation results, this indicates a strong possibility of overlap of the roles of the coronins, but also a potential for unique roles..
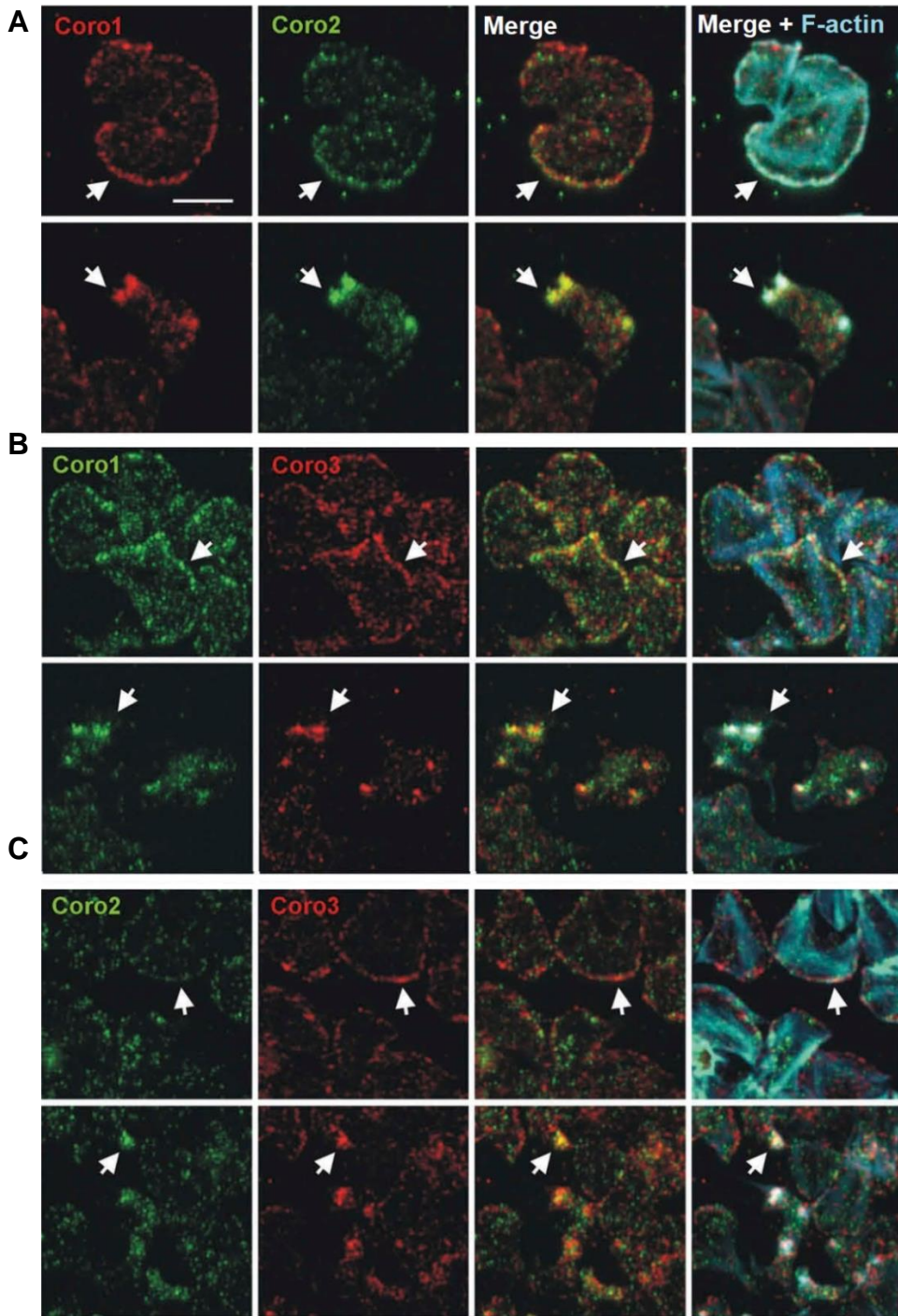
Figure 3.2.11 - Coronins 1-3 localise together

Platelets were spread on 100 µg/ml fibrinogen and stained for coronin 1, 2 and F-actin (**A**); coronin 1, 3 and F-actin (**B**); coronin 2, 3 and F-actin (**C**). Arrows indicate regions of interest: cell cortex (upper panels), actin nodules (lower panels). Scale bar = 5 µm.

145

3.2.12 Coronin 1 colocalises with putative binding partners ARPC2 and Gαs

Coronin 1 is known to bind F-actin and interact with the actin cytoskeleton regulators ARPC2 of the Arp2/3 complex and cofilin to regulate actin turnover at the leading edge of the cell (Gandhi & Goode, 2008). Coronin 1 is known to play roles in both the membrane and the cytosol. It is also known to bind to membrane components including Gαs (Jayachandran *et al.*, 2014). Co-Immunostainings were performed on human platelets with coronin 1 and the putative binding partners of coronin 1 - Gαs and ARPC2 to examine if they colocalise. Coronin 1 appeared to colocalise with Gαs (**Figure 3.2.12A**) and ARPC2 very strongly at the cell cortex/membrane and sporadically throughout the cell (**Figure 3.2.12B-C**). This demonstrates that coronin 1 localises partially in the areas of Gαs and ARPC2 and they may interact.
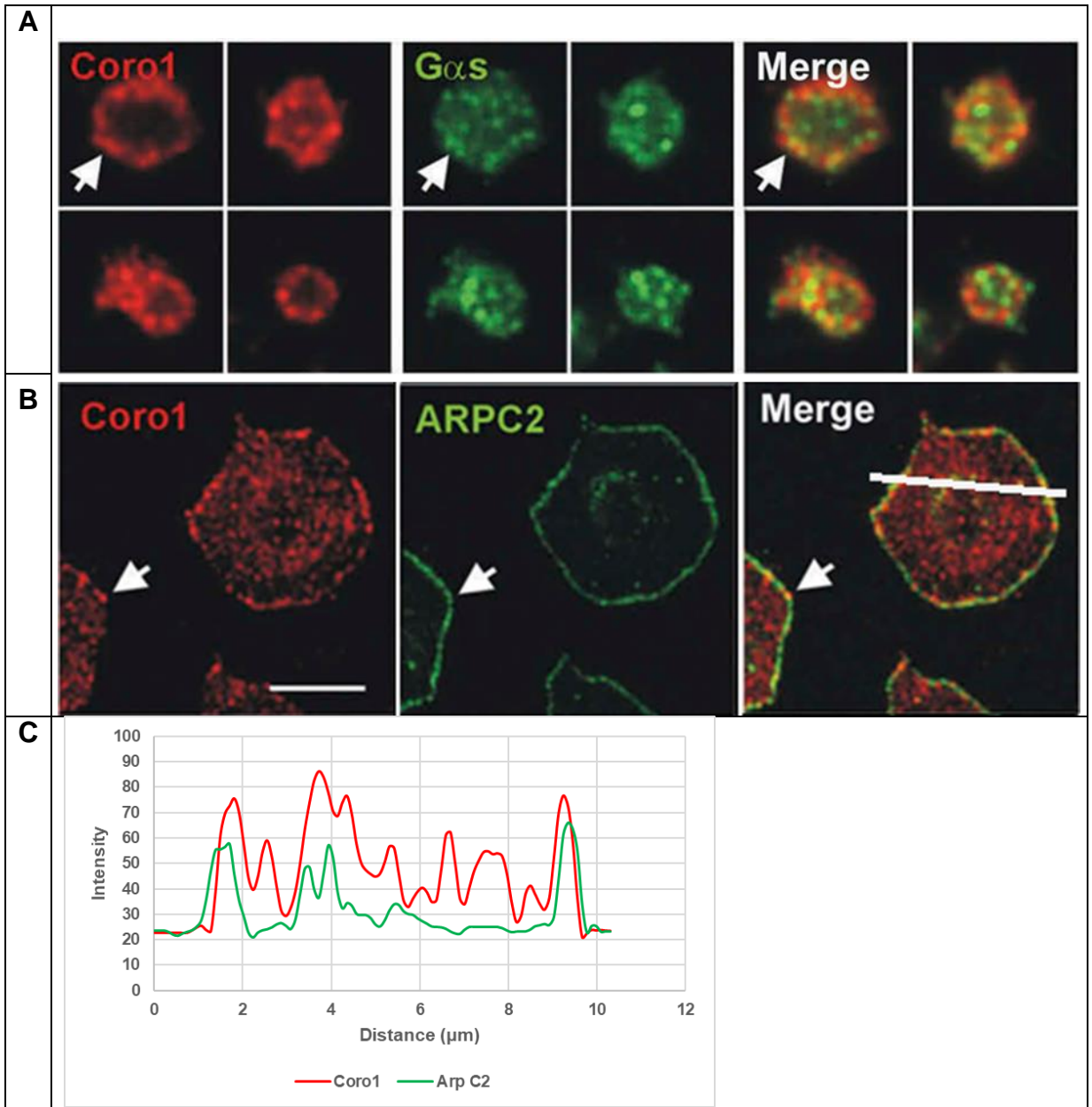
Figure 3.2.12 – Coronin 1 colocalises with Gαs and ARPC2
Human platelets were fixed in suspension with PFA and centrifuged onto poly-L-lysine coated coverslips then stained for Gαs (**A**). Platelets were spread on 100 µg/ml fibrinogen coated coverslips then stained for ARPC2 (**B**). Arrows point at regions of apparent colocalisation at the cell cortex. Scale bar is 5 µm. Colocalisation of coronin 1 and ArpC2 (**C**), produced using FIJI ImageJ.

147

3.2.13 Murine coronin 1, 2 and 3 localise with F-actin in platelets

It is important to investigate if similar colocalisation patterns are found with proteins in murine platelets as well as human, because ultimately the protein would need to be removed, likely in murine platelets, to study its function further. Murine platelets spread less than human platelets on fibrinogen and so are often treated with 0.1 U/ml thrombin to increase spreading (Thomas et al., 2016). WT murine platelets were treated with 0.1 U/ml thrombin, spread on 100 ug/ml fibrinogen and stained for coronin 1, 2, 3 and F-actin to assess colocalisation (**Figure 3.2.13**). Similarly to **Figure 3.2.8B** and **Figure 3.2.11**, coronins 1, 2 and 3 in murine platelets also localise to F-actin structures, punctuated around the cortex of spread platelets and also where the granulomere is expected. Very limited localisation of coronins and F-actin was found at stress fibres. Coronins 1, 2 and 3 demonstrate similar localisation patterns to each other (**Figure 3.2.13**) and also to human platelets (**Figure 3.2.8B & Figure 3.2.11).** As they colocalise to the same regions in humans and mice, they may perform similar roles in both species and potentially may also be redundant and compensate each other.
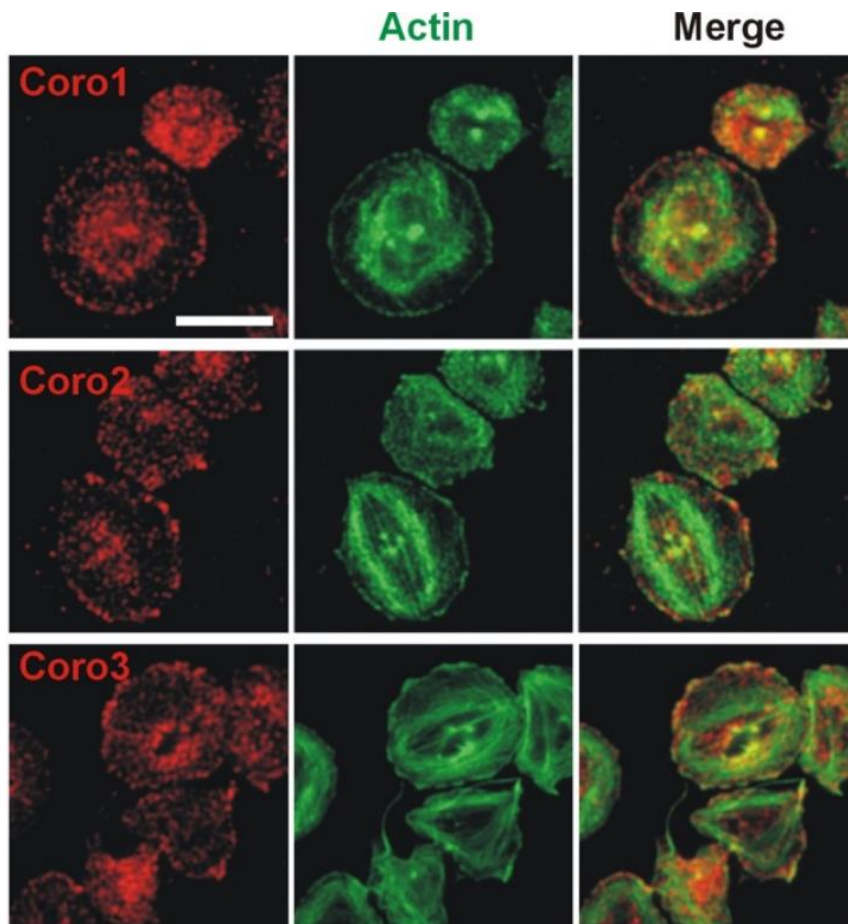
Figure 3.2.13 - Murine coronin 1, 2 and 3 localise with F-actin in platelets
Murine platelets were stimulated with 0.1 U/ml thrombin, spread on 100 µg/ml fibrinogen-coated coverslips, fixed with PFA then stained for the indicated proteins. Images were acquired with a fluorescence microscope equipped with a structured illumination attachment (Apotome) and deconvolved (Zen). Scale bar = 5 µm.

3.2.14 Murine coronin 1 is membrane and cytosol associated

Previous work has demonstrated that approximately one third of coronin 1 is in the membrane of human platelets under basal conditions. Upon latrunculin treatment, which depolymerised all detectable membrane F-actin into G-actin, the majority of the coronin 1 which was in the membrane prior to latrunculin treatment remains in the membrane with the reduction not statistically significant (Riley *et al.*, 2019). This demonstrates that in human platelets a proportion of the membrane-associated coronin 1 may not be F-actin associated.

149

This research was repeated in murine platelets, albeit with a lower power due to resource availability. Murine platelets, like human platelets, contain a proportion of coronin 1 in the membrane. Conversely to human platelets, treatment with latrunculin depolymerised most, but not all F-actin in the membrane. Another difference was that after latrunculin treatment, there was extremely little coronin 1 in the membrane (**Figure 3.2.14**). This suggests that coronin 1 plays a role in the membrane but the association of coronin with membrane F-actin greatly differs, therefore the role of membrane-associated coronin 1 may differ between species.

A
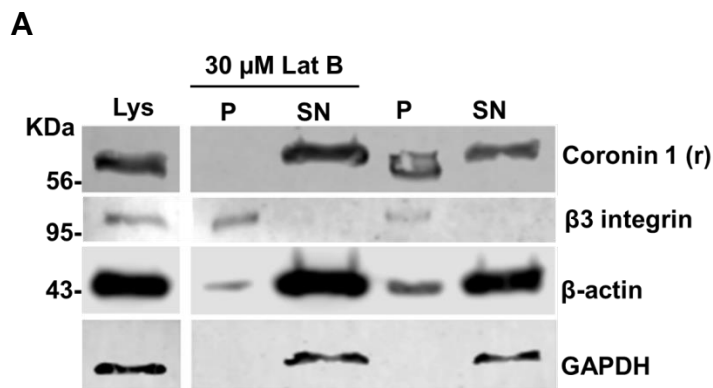
Figure 3.2.14 - Membrane/cytosol fractionation of murine platelets after latrunculin treatment
Platelets at 5 x 10^8/ml were either treated with 30 µM latrunculin B for 20 minutes or left untreated. The platelets were then lysed, subjected to membrane/cytosol fractionation, then to SDS-PAGE/WB and probed for the indicated proteins.. β3-integrin and GAPDH were used as membrane and cytosol markers, respectively. SN = supernatant. Lat B = latrunculin B. Two independent experiments were performed due to sample availability, therefore no statistics could be performed.

3.3 Discussion

Proteomic studies found that coronins 1-3 are abundant in human and mouse platelets, whereas only an extremely small amount of coronin 7 is present (**Figure**) (Burkhart *et al.*, 2012; Zeiler *et al.*, 2014). This mostly reflects transcriptomic data of the mRNA levels, with the exception of murine *Coro1a*, (**Figure 1.20B**), of which transcriptomic studies found low mRNA levels (**Figure 1.20**) (Rowley *et al.*, 2011) but the protein is abundant (**Figure 1.20B**) (Zeiler *et al.*, 2014). However, the levels

150

of mRNA in a platelet can be very misleading and often there is not a correlation between the levels of mRNA and the protein copy number (Zeiler *et al.*, 2014). This is due to factors including mRNA turnover, and microRNAs (Huntzinger & Izaurralde, 2011). In platelets there is not a strong correlation between mRNA levels and protein levels for most genes and proteins.

This is the first study to show the presence of coronins 1-3 and 7 in human and mouse platelets by Western blot. Coronins 1-3 are abundant in human and mouse platelets, whereas only an extremely small amount of coronin 7 is present (**Figure 3.2.3**). This reflects proteomic reports on human (**Figure 1.21A**) (Burkhart *et al.*, 2012) and murine coronins (**Figure 1.21B**). Both species demonstrated similar amounts of coronin 1 (**Figure 3.2.3**), as expected by proteomic studies (**Figure 1.21A** & **B**). Coronin 2 levels appeared slightly lower in murine platelets than human (**Figure 3.2.3**) despite proteomic studies predicting they would be similar (**Figure 1.21A** & **B**). This could be due to higher affinity of the antibody for human coronin 2 than murine, as it was raised against a fragment of human coronin 2. Coronin 3 levels appeared higher in murine platelets compared to humans (**Figure 3.2.3**), as predicted by proteomic studies (**Figure 1.21A** & **B**). Very faint bands for coronin 7 were found in both species (**Figure 3.2.3**) which confirms the very low levels found in proteomic studies (**Figure 1.21A** & **B**).

Coronin 7 is found at the Golgi apparatus and has been hypothesised to play roles in protein trafficking and not bind actin (Clemen, 2013) and therefore may be left over from the megakaryocyte with no functional role in mature platelets. However, recent studies have suggested coronin 7 may regulate actin turnover in concert with Cdc42 and N-WASP and its ablation leads to increased F-actin levels and a disrupted Golgi network (Bhattacharya *et al.*, 2016). Coronin 7 levels in platelets are probably too low to be an important F-actin regulator. Attempts were made to blot for coronins 4 and 5 but many unspecific bands and background artefacts appeared, therefore the antibodies were deemed unreliable (data not shown). A suitable coronin 6 antibody could not be acquired. Taken together, the presence of coronins 1-3 and 7 can be confirmed in a manner reflective of the proteomic reports.

Coronins 1, 2 and 3 have similar structures, (McArdle & Hofmann, 2013) as detailed in **Section 1.3.2**. Coronin 1 and 3 are both the same size on a Western blot at around 56 KDa, with coronin 2 a bit bigger. To investigate each coronin separately, antibodies need to be specific to each coronin. Antibodies against proteins from coronin 1, 2 and 3 were tested and the antibodies appeared specific (**Figure 3.2.1 & 3.2.2**). Therefore coronins 1-3 can be specifically investigated.

3.3.1 Coronin 1, 2 and 3 associate with F-actin and may regulate actin turnover

Coronins 1 (Liu *et al.*, 2006), 2 (Cai *et al.*, 2007) and 3 (Rosentreter *et al.*, 2007) have long been known to bind F-actin in various cell types, but have only recently been investigated in platelets. The ability of coronins 1, 2 and 3 to associate with the Triton X-100 insoluble pellet has not previously been reported. The fractionation revealed that coronins 1, 2 and 3 are F-actin associated in both human (**Figure 3.2.4**) and murine platelets. Latrunculin treatment resulted in a lack of association of coronin 1 to the F-actin pellets in murine (**Figure 3.2.5**) and human platelets (Riley *et al.*, 2019). Murine platelets were subjected to Triton X-100 insoluble pellet fractionation with a view to achieving higher power and then ultimately performing the fractionation with $Coro1a^{-/-}$ platelets, but this was not possible due to the high number of platelets required and resource limitations.

Detailed immunocytochemistry studies of coronins 1, 2, 3 with their putative binding partner, F-actin, have not previously been reported. Detailed immunostainings revealed that under basal conditions, in platelets centrifuged onto poly-L-lysine, coronin 1, 2 and 3 distribution appears mostly dispersed with stronger staining at the cortex. When spread on fibrinogen, the distribution is punctuated throughout the cell (**Figure 3.2.11**) with denser accumulation at F-actin nodules (**Figure 3.2.8** & **Figure 3.2.9**), the cell cortex (**Figure 3.2.11**) and where the granulomere is expected (**Figure 3.2.13**). Coronins 1, 2 and 3 also colocalise together in platelets (**Figure 3.2.11** & **Figure 3.2.13**). ARPC2 of the Arp2/3 complex

is also very apparent at the cortex of spread platelets where it may interact with coronin to regulate actin branching.

Novel IPs on platelet lysates also revealed that coronins 1 and 2 associate with ARPC2. Coronin 3 was picked up in an IP for coronin 2 (**Figure 3.2.7**) which has been reported in HeLa cells (Abella *et al.*, 2016), however this may be because they both bind ARPC2, rather than binding each other. An IP for coronin 3 was attempted but the unspecific IgG control was not clean and optimisation of this IP was not pursued due to time constraints and competing priorities. The Triton X-100 insoluble pell*et al*so found an association between coronins 1-3 and F-actin which increased over time due to stimulation with an agonist (**Figure 3.2.4**). The F-actin polymerisation inhibitor, but not a tubulin inhibitor, prevented coronin 1 accumulation in the cell cortex. Taken together, this supports the role of coronins as F-actin binding proteins and regulations of the F-actin cytoskeleton in platelets.

Cofilin has been reported to be mostly present in the supernatant of the insoluble platelet pellet fractionation with some present in the pellet. The levels present in the pellet are greatly reduced upon latrunculin treatment (Riley *et al.*, 2019). This is consistent with its role as an F-actin and monomeric actin binding protein. Cofilin is known to function in concert with coronin to sever F-actin filaments at the rear of the F-actin network to contribute to actin treadmilling (Gandhi & Goode, 2008). As cofilin is also found at the cell cortex in platelets, (Falet *et al.*, 2005) and displays a similar subcellular staining pattern to coronin 1, 2 and 3 (**Figure 3.2.8** & **Figure 3.2.9**), it is likely that they would colocalise, especially in stimulated platelets. Unfortunately detailed analysis of colocalisation of coronin and cofilin was not possible due to time limitations.

Both coronin 1 (Humphries *et al.*, 2002) and coronin 2 (Cai, Marshall, *et al.*, 2007) have been reported to interact with the Arp2/3 complex and cofilin to regulate actin turnover (Gandhi & Goode, 2008). As coronins 1-3 colocalise in platelets and have similar roles, this suggests a potential for functional overlap and thus redundancy within the three coronins.

The amount of immunostainings simultaneously performed on platelets was initially limited and was optimised through experiments until three stainings could be

performed simultaneously. Unfortunately 4 could not be performed to visualise coronins 1, 2, 3 and F-actin on the same platelet. Future steps to demonstrate association and colocalisation of coronins 1, 2 and 3 to their putative binding partners ARPC2, Gαs, and cofilin may include using surface plasmon resonance, staining 5+ proteins simultaneously, utilising proximity ligation assay or super resolution microscopy.

3.3.2 Coronin 1 remains membrane associated independently of F-actin association and platelet stimulation

Previous studies have shown that in J774 macrophages 20% of coronin 1 is membrane bound (Gatfield *et al.*, 2005) and in HEK 293 cells a proportion of coronin 3 is membrane associated (Spoerl *et al.*, 2002). Membrane/cytosol fractionation of human platelets revealed that coronin 1 is mostly present in the cytosol but approximately one third is membrane-bound (Riley *et al.*, 2019). No translocation to or from the membrane, upon stimulation, could be detected by Western blot for either coronin 1 or 3 (**Figure 3.2.6**). Membrane/cytosol fractionation of coronin 2 was not pursued due to poor antibody performance and degradation of coronin 2. It has previously been reported that latrunculin treatment of human platelets resulted in a small proportion of coronin 1 remaining membrane-bound (Riley *et al.*, 2019). This suggests potential roles for coronin in the platelet membrane in a manner not associated to F-actin.

Coronin 1 is known to bind membrane-bound components including Gαs (Jayachandran *et al.*, 2014) and β2 integrin (Pick *et al.*, 2017), which are both present in platelets (Burkhart *et al.*, 2012; Piguet *et al.*, 2001). Gαs is a subunit of heterotrimeric G proteins involved in the cAMP/PKA (Jayachandran *et al.*, 2014) and PGI$_2$ signalling pathways (Rivera *et al.*, 2009). Integrin β2 binds with CD11a to form an ICAM1 receptor (Pick *et al.*, 2017), which may facilitate platelet-WBC interactions. Upon platelet stimulation with agonists or inhibitors and subsequent membrane/cytosol fractionation, coronin 1 remains partially membrane associated, suggesting roles at the membrane. Coronin 1 associates with Gαs in IPs (**Figure**

3.2.7), although a suitable β2 antibody for WB was not available to analyse that association. Future work should investigate the interactions between coronins and Gαs or β2.

There are several factors which may facilitate coronin 1 to remain in the membrane including its ability to bind Gαs (Jayachandran *et al*., 2014), β2 (Piguet *et al*., 2001) or phosphatidylinositol 4,5-biphosplate (PIP$_2$) (Tsujita *et al*., 2010). Taken together with the IP result, which demonstrated binding of coronin 1 to Gαs, there are potential roles for coronin 1 at the platelet membrane. The next chapter will explore some of these potential roles, among others including platelet responses and activation, utilising *Coro1a*$^{-/-}$ platelets.

3.3.3 Coronin 1 is associated with functional membrane proteins

Coronins 1-3 localise at actin nodules and the cell cortex (**Figure 3.2.8, Figure 3.2.9** & **Figure 3.2.11**) as well as with each other (**Figure 3.2.11**). They also colocalise with the markers of actin nodules – CAP1 and vinculin (**Figure 3.2.8F**), of which the latter is interestingly dispensable for platelet function (Mitsios *et al*., 2010). Coronins 1 and 2 also co-IP with ARPC2 and Gαs (**Figure 3.2.7**) and coronin 1 appears to colocalise with ARPC2 and Gαs. Therefore it is possible that coronins 2 and 3 also likely colocalise in with ARPC2 and Gαs. It is also possible that there is some redundancy in the coronins with regards to their interactions not only with F-actin and ARPC2, but also Gαs. This report strengthens the view of complex functional overlap and redundancy among coronins in platelets which is an aspect to consider in future functional studies.

It has previously been found that coronin 1 binds the G protein subtype Gαs in neurons to stimulate cAMP/PKA signalling. The ablation of coronin 1 is associated with a reduction in cAMP signalling leading to neurological and behavioural defects in mice (Jayachandran *et al*., 2014). As Gαs and cAMP signalling is involved in the PGI$_2$ signalling pathway to inhibit platelets (Raslan & Naseem, 2014), it was hypothesised that ablation of coronin 1 may lead to a reduction in this pathway and

a reduction in the ability of PGI$_2$ to inhibit platelets. This was investigated in the next chapter with *Coro1a$^{-/-}$* platelets.

To summarise, Coronins 1, 2, 3 are abundant and coronin 7 present in human and mouse platelets. They associate with the F-actin insoluble pellet and their levels increase over time with platelet agonist stimulation. They colocalise together at F-actin rich structures including the cortex and actin nodules. Coronin 1 and 2 IP with ARPC2 and they likely play roles in F-actin turnover in platelets which would be consistent with their roles in other cells. Coronins 1, 2 and 3 are also present in the membrane fractions but do not translocate in response to stimulation and their association is in a manner independent of actin turnover. Coronins 1 and 2 associate with Gαs and may associate with other membrane components and may play roles in their signalling. Some of these aspects will be investigated in the next chapter with *Coro1a$^{-/-}$* platelets.

4 Chapter 4 – The effects of coronin 1 ablation on murine platelets

4.1 Aims

- By utilising $Coro1a^{-/-}$ platelets from KO mice, to gain insight into the roles of coronin 1 in platelet function,
- To assess potential compensation of the lack of coronin 1 by coronin 2 or 3
- Investigate any possible defects in inhibitory signals (pVASP and cAMP)
- To determine basal and stimulated receptor levels
- Analyse αIIbβ3 activation and platelet secretion
- Investigate the ability of $Coro1a^{+/+}$ and $Coro1a^{-/-}$ platelets to spread on various matrices

4.2 Results

4.2.1 Genotyping of $Coro1a^{+/+}$ and $Coro1a^{-/-}$

To analyse the function of a protein, one method is to remove the protein. $Coro1a^{-/-}$ platelets were obtained from $Coro1a^{-/-}$ mice. Our lab received 10 $Coro1a^{-/-}$ mice on a C57BL/6 from our collaborator Jean Pieters, which had a deletion of $Coro1a$ caused by an insertion mutation into exon 2 of the gene (Jayachandran *et al.*, 2007). These mice were bred with $Coro1a^{+/+}$ mice to produce $Coro1a^{+/-}$ mice which were then bred and their offspring were genotyped. A 333 bp band indicated a WT, a band just under the 500 bp marker indicated a KO mouse and a heterozygous mouse was identified by the presence of both bands (**Figure 4.2.1**).
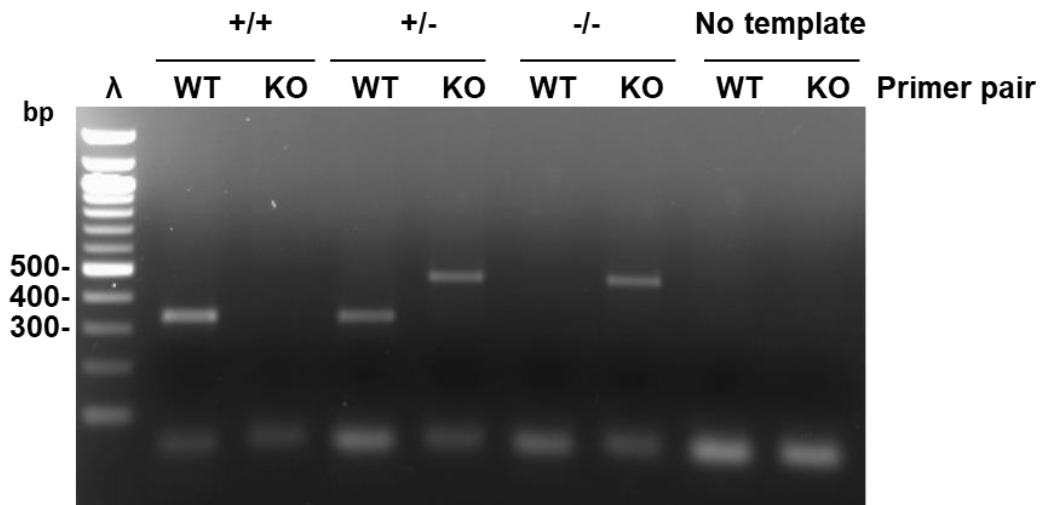
Figure 4.2.1 - Genotyping of coronin 1 mutant colony
A single band of 300-400 bp, ~500 bp or both bands indicated a *Coro1a*^+/+^, *Coro1a*^+/+^, or *Coro1a*^+/+^, mouse, respectively. The first row of labelling indicates the genotype of the template DNA and the second row indicates the type of reaction (WT or KO primer pair). bp = base pair. λ = Quick Load Purple 100 bp DNA ladder.

4.2.2 Knock out of coronin 1 in platelets

Platelet lysates from *Coro1a*^+/+^ and *Coro1a*^-/-^ mice were probed for coronin 1 protein, the absence of which confirmed the protein was successfully knocked out. The heterozygous mice had approximately half the coronin 1 of the WT mice which was a statistically significant change (p = 0.0079) (**Figure 4.2.2A** & **B**). WT, KO and heterozygous murine platelets were also probed for coronin 3 to test for any compensation of coronin 3 due to deletion of coronin 1 (**A**). The KO and heterozygous mice had no significant change in levels of coronin 3 relative to the WT demonstrating a lack of protein compensation by coronin 3 (**A** & **C**). Attempts were made to blot for coronin 2 proteins to evaluate any compensation by that protein but the signal was too weak and impractical for accurate quantification.

A

B

C
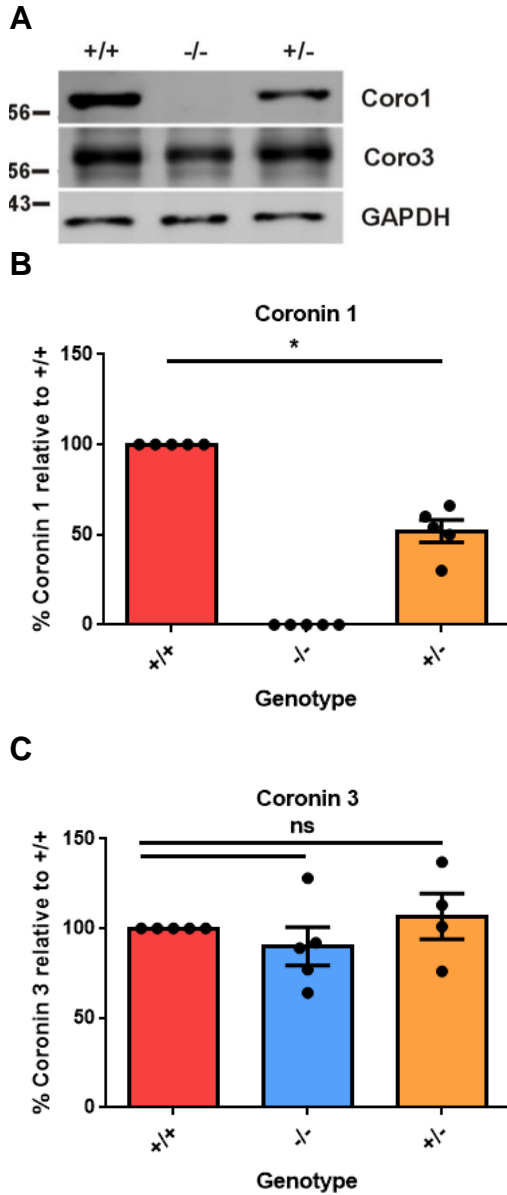
Figure 4.2.2 – Successful KO of coronin 1 in platelets

A) *Coro1a*$^{+/+}$, *Coro1a*$^{-/-}$ and *Coro1a*$^{+/-}$ murine platelet lysates were subjected to SDS-PAGE Western blot and probed for coronin 1 and 3. GAPDH was used as a loading control. **B**) The levels of coronin 1 were quantified. The KO demonstrated a total absence of coronin 1 and the heterozygous samples demonstrated a significantly different level of coronin 1 relative to the WT n = 5. **C**) The levels of coronin 3 were quantified (n = 4). No statistically significant difference was found in coronin 3 protein levels between the three genotypes (Mann-Whitney U). * = $p < 0.05$. GAPDH = Glyceraldehyde 3-phosphate dehydrogenase. Data is mean signal relative to WT platelets ± SEM.

4.2.3 Coronin 1 ablation does not affect GPVI, CD41, CD42b and CD49b receptor levels

Platelets contain several receptors, the levels of which can be altered by ablation of specific proteins (H Falet, 2017). These receptors include the collagen receptor GPVI, integrin αIIb (CD41) which makes αIIbβ3 for fibrinogen binding, GP1b (CD42b) which makes GP1b/IX/V for von Willebrand factor binding, and integrin α2 (CD49b) makes makes α2β1 for collagen binding (Rivera *et al.*, 2009). Murine *Coro1a*$^{+/+}$ and *Coro1a*$^{-/-}$ platelets were analysed for the cell surface expression of the receptors GPVI, CD41, CD42b and CD49b under basal (n = 7) and stimulated conditions (n = 14) using flow cytometry. Thrombin-induced stimulation resulted in a significant increase of surface GPVI, CD41 and CD49b levels, and a significant decrease in CD42b levels for both *Coro1a*$^{+/+}$ and *Coro1a*$^{-/-}$ platelets. The amount of experiments was higher for basal because after the initial basal data was collected, the effect of stimulation was investigated as an additional aspect and these experiments required a basal control.

No statistically significant difference was observed in the basal or stimulated levels between the *Coro1a*$^{-/-}$ or *Coro1a*$^{+/+}$ platelets (although the *Coro1a*$^{-/-}$ platelet basal levels were marginally higher) indicating *Coro1a* is dispensible for this trait (**Figure 4.2.3**).
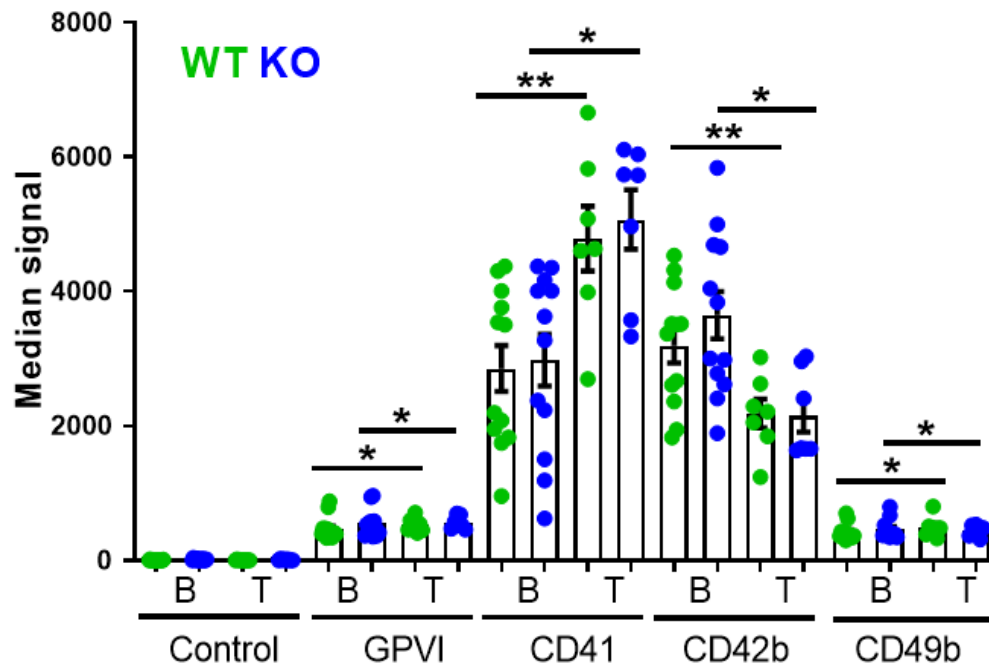
Figure 4.2.3 - Flow cytometric analysis of cell surface receptors under basal and stimulated conditions
Murine platelets were incubated with FITC conjugated antibodies specific to GPVI, CD41, CD42b or CD49b for 20 minutes at 37°C in either basal (B) or stimulated with 0.1 U/ml thrombin (T) conditions then analysed with flow cytometry. Unpaired t-tests or Mann-Whitney tests were used for parametric or non-parametric data, respectively, for WT to KO comparisons. Paired or t-test or Wilcoxon matched pairs tests were used for parametric or non-parametric data, respectively, for basal to stimulated comparisons. N = 7 – 14. Data is median fluorescence intensity ± SEM of n = 7-14.* = p < 0.05; ** = p < 0.01 p; *** = < 0.001.

4.2.4 Integrin β2 translocation is impaired in Coro1a$^{-/-}$ platelets

Integrin β2 (CD18) combines with CD11a to form LFA-1 (CD11a/CD18) and with CD11b to form Mac-1 (CD11b/CD18). Coronin 1 has been identified as a regulator of β2 by interacting with its cytoplasmic tail (Pick *et al.*, 2017). Platelets express increased integrin β2 levels on their surface upon thrombin-induced activation (Philippeaux *et al.*, 1996). By utilising flow cytometry, the cell surface levels of integrin β2 examined and found to be similar at basal levels in *Coro1a$^{-/-}$* and

161

Coro1a$^{+/+}$ murine platelets. However the integrin β2 levels increased in the WT (paired t-test, p = 0.0010) but not the KO (paired t-test, p = 0.0630) upon stimulation and the difference between the stimulated WT and KO was significant (unpaired t-test, p = 0.0039) indicating a defect in integrin β2 translocation (**Figure 4.2.4A)** and an obvious difference in the signal intensity count (**Figure 4.2.4B & C**). WT platelets which were treated with thrombin then centrifuged onto poly-L-lysine coated coverslips also demonstrate an increase in the translocation of β2 integrin to the cell surface that is impaired in *Coro1a*$^{-/-}$ platelets (**Figure 4.2.D**). This demonstrates β2 translocation in platelets is dependent upon coronin 1.
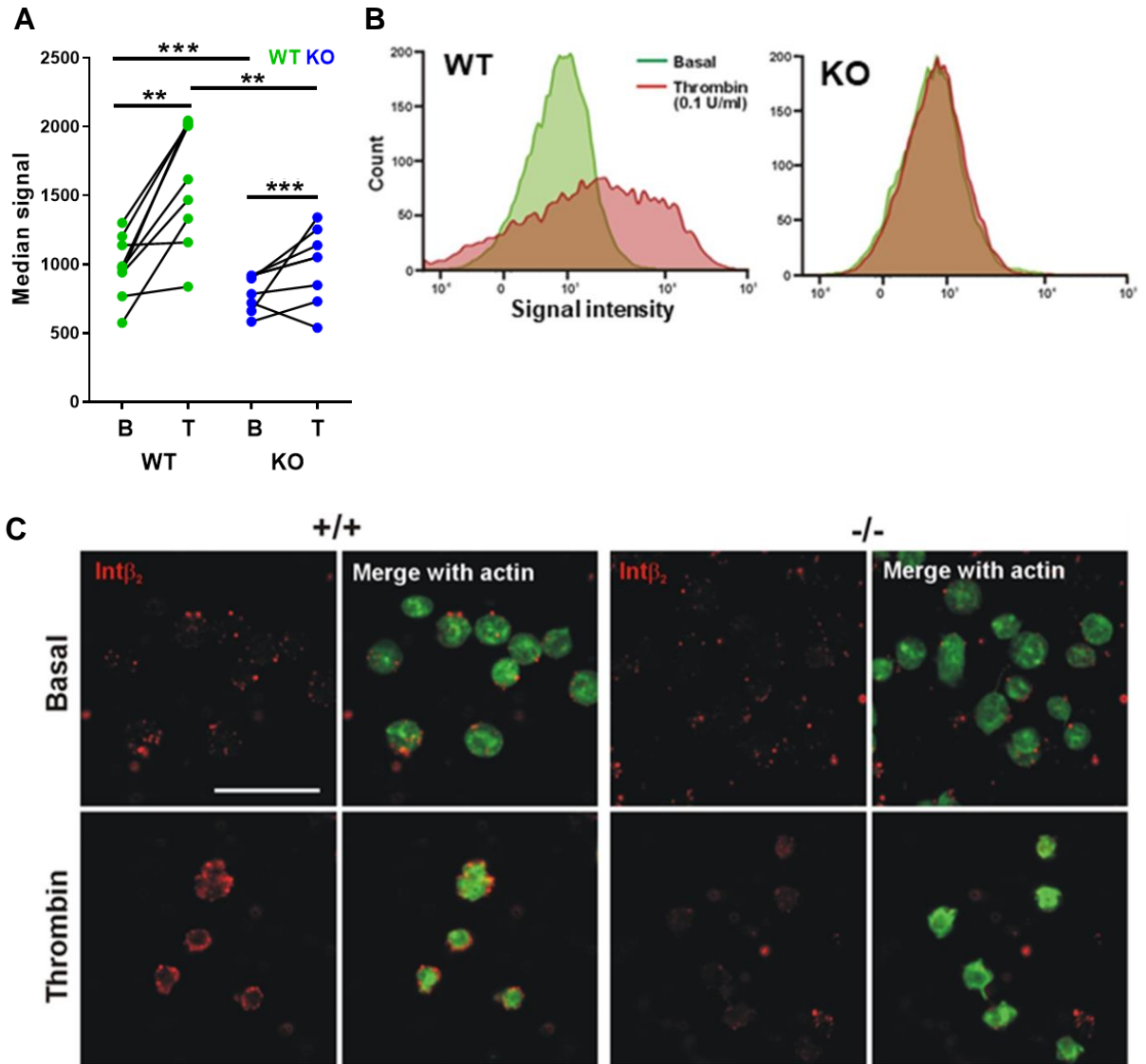
Figure 4.2.4 – Thrombin induced Integrin β2 translocation is impaired in *Coro1a*^{-/-} platelets

Murine platelets were treated with PE-conjugated antibodies specific to integrin β2 for 20 minutes at 37°C in basal or stimulated with 0.1 U/ml thrombin conditions then analysed by flow cytometry (**A**). The difference in intensity by count for a representative samples. Data is median fluorescence intensity ± SEM of n = 8-9. B = basal; T = thrombin stimulated. Unpaired t-tests were used for WT to KO comparisons. Paired or t-test were used for basal to stimulated comparisons. * = p < 0.05; ** = p < 0.005; *** = p < 0.001 (**B**). Murine platelets were stimulated in suspension with 0.1 U/ml thrombin, fixed with 4% PFA and centrifuged onto poly-L-lysine coated coverslips. Permeabilisation was omitted and platelets were stained for β2 then Alexa568-coupled secondary antibody (red) with FITC-phalloidin for filamentous actin (green). Images were acquired with a fluorescence microscope equipped with an Apotome and deconvolved with Zen. Scale bar = 10 μm (**C**).

163

4.2.5 *Coro1a^{+/+}* and *Coro1a^{-/-}* platelets have similar size

Coro1a^{-/-} mice have previously been reported to exhibit unaffected hematological parameters, including platelet counts, indicating that hematopoiesis is not affected.by the loss of coronin 1 (Foger *et al.*, 2006). A difference in platelet size may lead to differences in other parameters such as receptor expression and spreading area. The platelet size of *Coro1a^{+/+}* and *Coro1a^{-/-}* platelets was measured indirectly using mean forward scatter area (FSC-A) in flow cytometry which represents the of the height of the signal detected by PMT voltage of laser passing directly through the cells, multiplied by the mean time the cell took to flow through the laser beam. No statistically significant difference was found (unpaired t-test, $p = 0.7372$) (**Figure 4.2.5**).
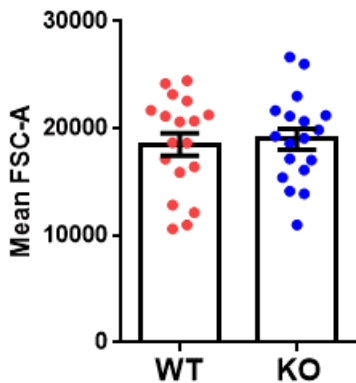
Figure 4.2.5 - Flow cytometric analysis of platelet size
Coro1a^{+/+} and *Coro1a^{-/-}* platelets were analysed by flow cytometry in their unfixed state from PRP. An unpaired t-test was used to compare. Data is mean fluorescence intensity from FSC-A ± SEM for n = 18.

4.2.6 Flow cytometric analysis of platelet activation

Integrin αIIbβ3 plays a central role in platelet function and when activated it has a high affinity for binding of platelets to fibrinogen and von Willebrand factor (Huang *et al.*, 2019). The activation state of *Coro1a*$^{+/+}$ and *Coro1a*$^{-/-}$ platelets were examined in basal conditions and upon stimulation by various agonists by utilising flow cytometry with JON/A which is the antibody specific for the activated form of integrin αIIbβ3 (GPIIb/IIIa). The platelets responded to thrombin and CRP in a dose dependent manner. The thromboxane analog, U46619, and ADP provoked weak activation on their own but when used together acted in synergy to produce a strong response. There was no difference between the *Coro1a*$^{+/+}$ and *Coro1a*$^{-/-}$ platelets for any of the conditions used (**Figure 4.2.6A**). This demonstrates that *Coro1a* is dispensable for αIIbβ3 activation.

Alpha-granule secretion and dense-granule secretion occur upon platelet activation (Golebiewska & Poole, 2015) and can be measured using antibodies specific to P-selectin expression (**Figure 4.2.B**) and CD63 (**Figure 4.2.C**), respectively. The platelets responded to the agonists in a dose dependent manner. ADP and U46619 had weak abilities to activate or induce secretion in platelets, however together they resulted in a synergistic effect. *Coro1a*$^{+/+}$ and *Coro1a*$^{-/-}$ platelets responded similarly and no statically significant difference was found between them for any agonists tested (**Figure 4.2.**). This demonstrates that *Coro1a* is dispensable for platel*et al*pha and dense granule secretion
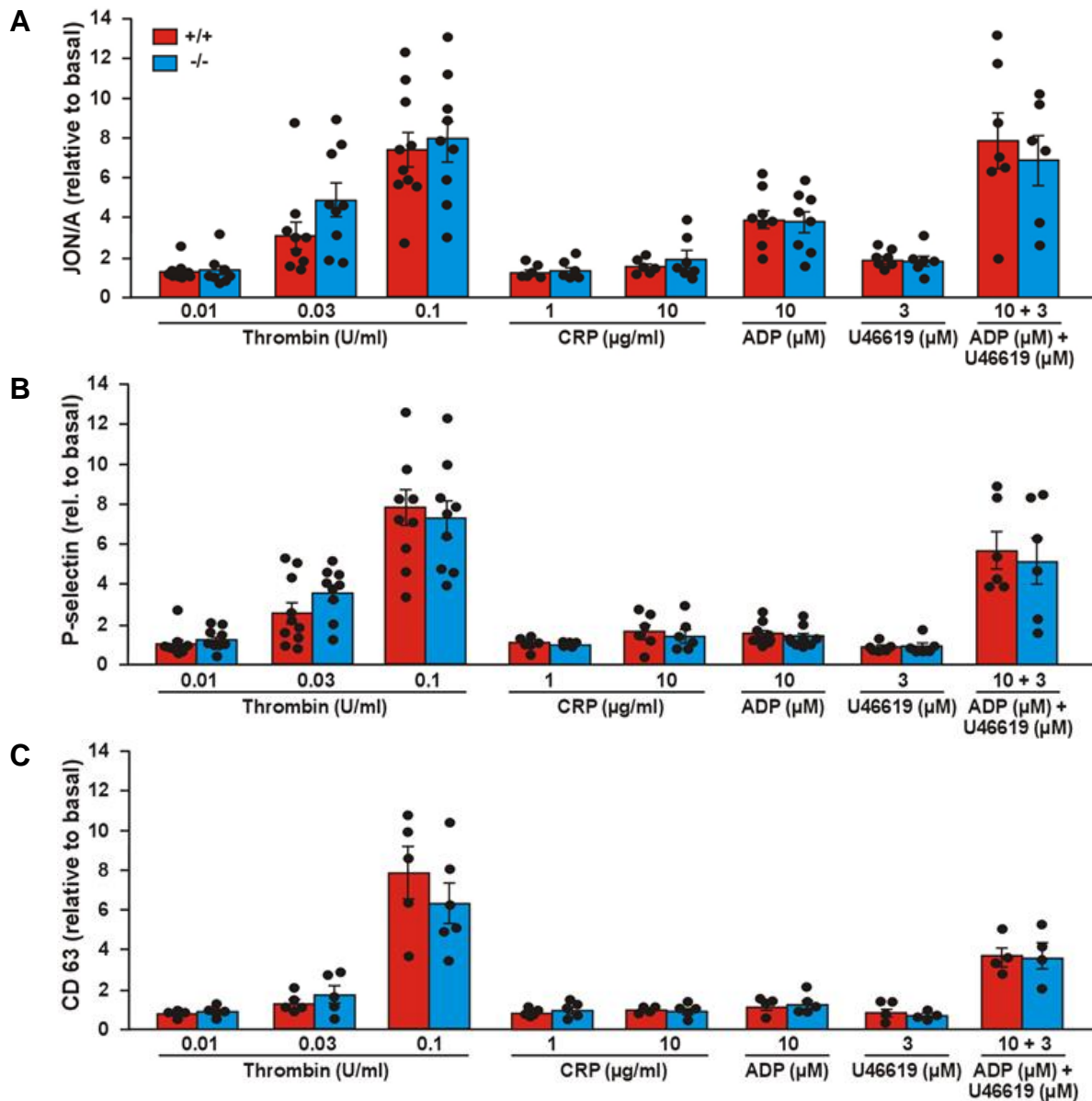
Figure 4.2.6 - αIIbβ3 activation, dense granule secretion and alpha granule secretion of *Coro1a^-/-* platelets

Coro1a^+/+ and *Coro1a^-/-* platelets were either untreated or treated with 0.1, 0.03, 0.01 U/ml thrombin, or 10 or 1 µg/ml CRP. or 10 µM ADP, or 3 µM U46619 (synthetic thromboxane analog), or 10 µM ADP with 10 µM U46619 and incubated with the corresponding antibody for 20 minutes at 37°C. Platelets were then fixed in 1x BD fix/lyse buffer and data immediately acquired with a BD Fortessa. Single antibody compensation was performed with FlowJo. Normality was tested using a Shapiro-Wilk test with a p value over 0.05 considered parametric. Unpaired t-tests or Mann-Whitney tests were used to compare. Data represents the median fluorescence intensity ± SEM for JONA (αIIbβ3) n = 6-12; P-selectin n = 6-12; CD63 n = 4-6.

4.2.7 Effect of *Coro1a* ablation on platelet aggregation

Light transmission aggregometry is used to assess the ability of platelets to aggregometry which during haemostasis would stop bleeding (Petricevic *et al.*, 2013). Subtle defects in aggregation induced by low collagen doses were previously found in $Coro1a^{-/-}$ platelets by utilising impedance-based aggregometry on whole blood (Stocker *et al.*, 2018). Washed murine $Coro1a^{+/+}$ and $Coro1a^{-/-}$ platelets were subjected to light transmission aggregometry utilising 4 doses of thrombin, 4 doses of collagen and 3 doses of CRP. The percentage of aggregation and slope were measured and the platelets responded in dose-dependent manner. The $Coro1a^{+/+}$ and $Coro1a^{-/-}$ platelets responded similarly to most agonists. Compared to WT, the $Coro1a^{-/-}$ platelets demonstrated a small but statistically significant higher aggregation percentage (unpaired t-test $p = 0.0420$) and slope (unpaired t-test $p = 0.0137$) with only a high dose (0.1 U/ml) of thrombin (**Figure 4.2.7A**). No difference between the $Coro1a^{+/+}$ and $Coro1a^{-/-}$ platelets was found in response to the lower doses of thrombin (**Figure 4.2.A**) or any of the doses of collagen (**Figure 4.2.B**) or CRP (**Figure 4.2.C**).

A

B

C

168
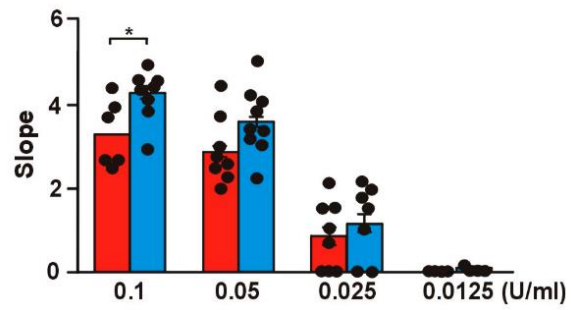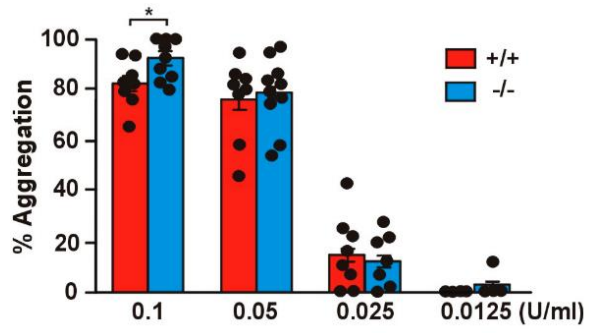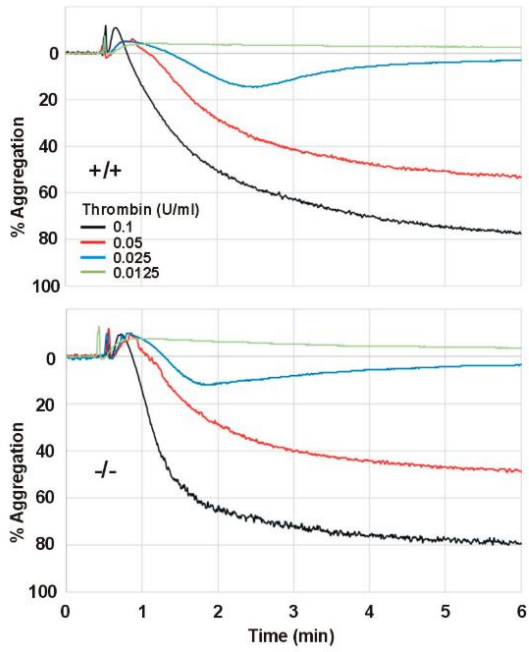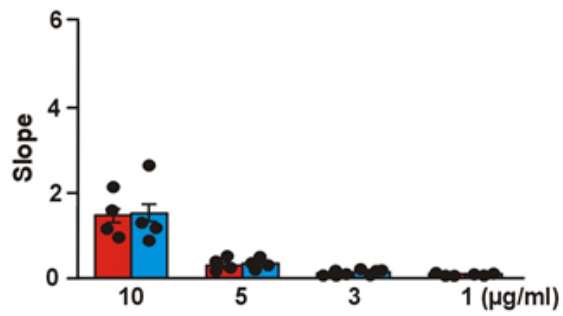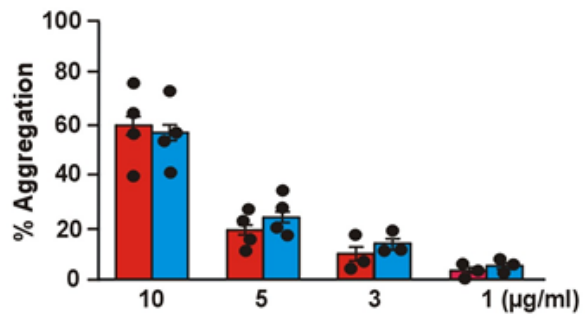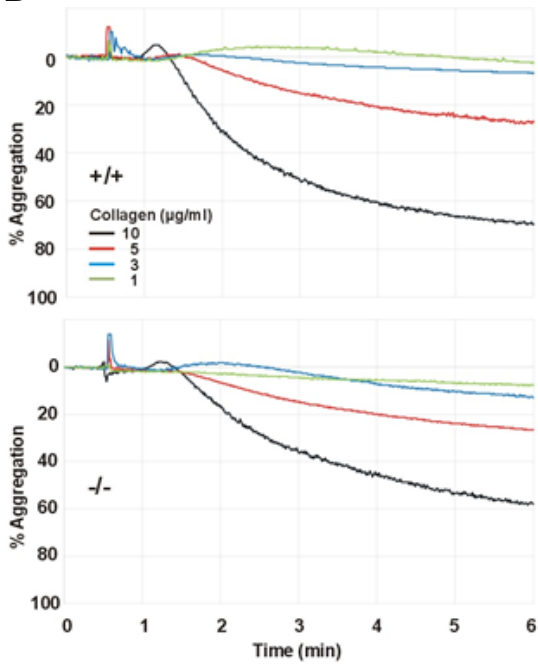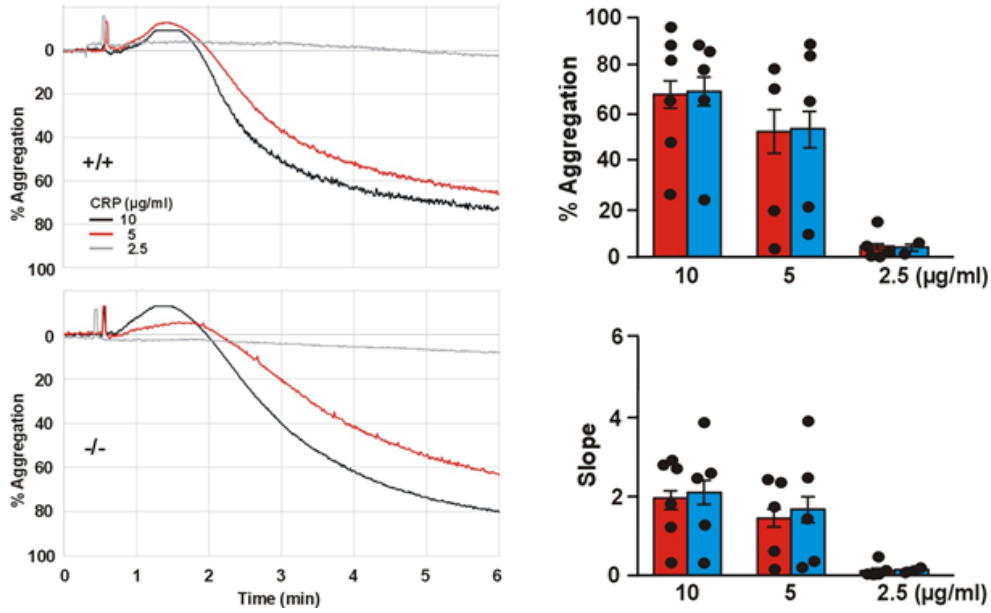
Figure 4.2.7 – Aggregation response of *Coro1a*$^{+/+}$ and *Coro1a*$^{-/-}$ platelets

Coro1a$^{+/+}$ and *Coro1a*$^{-/-}$ platelets at 2×10^8 were subjected to aggregation at 1000 RPM at 37°C in a Chrono-log aggregometer (Chronolog Instrument 490 + 4). On the left are representative aggregation traces and the bar graphs on the right show mean percentage of maximum aggregation within 5 minutes and also aggregation slope ($\Delta Y/\Delta X$). Agonists used were 0.1, 0.05, 0.025 or 0.0125 U/ml thrombin (**A**), 10, 5, 3 or 1 µg/ml collagen (**B**) or 10, 5 or 2.5 µg/ml CRP (**C**). Unpaired t-tests or Mann-Whitney tests, as appropriate, were used to compare genotypes. Data is mean ± SEM for n = 4 -10.

4.2.8 Coronin 1 is dispensable for haemostasis

Upon vessel wall injury, bleeding is prevented by the formation of a platelet plug which involves aggregation of platelets (Lisman *et al.*, 2005). To investigate the effects of *Coro1a* ablation on haemostasis *in vivo*, bleeding time measurements were performed. The bleeding time of coronin 1 WT and KO mice was assessed. No significant difference was found between the coronin 1 WT, KO or heterozygous animals (Kruskal-Wallis, p = 0.3860) (**Figure 4.2.8**). 2 heterozygous and 2 WT mice re-bled after initial cessation. This suggests that *Coro1a* is dispensable for haemostasis.
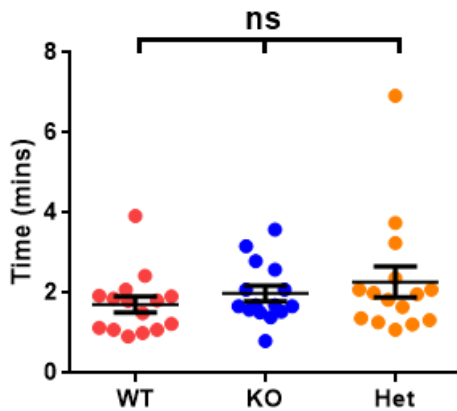
Figure 4.2.8 - The effects of Coronin 1 ablation on haemostasis.
Coro1a$^{+/+}$, *Coro1a*$^{-/-}$ and *Coro1a*$^{+/-}$ mice were analysed for haemostasis using a tail bleeding assay. 2 mm of tail was removed the tail immersed in 37°C PBS then the time until the cessation of blood flow was measured. A Kruskal-Wallis test was used to assess significance. Data is mean time (minutes) ± SEM for n = 15.

4.2.9 Coronin 1 ablation does not affect spreading on various matrixes

Functional actin cytoskeleton remodeling is critical for platelet for adhesion and spreading on matrix proteins. The effect of *Coro1a* ablation on platelet adhesion and spreading on surfaces coated with 100 µg/ml fibrinogen, 100 µg/ml collagen, 30, 10 and 3 µg/ml GFOGER and 3 µg/ml CRP was investigated by fluorescence microscopy. Murine platelets spread on fibrinogen displayed filopods, actin nodules and few stress fibers. Platelets on collagen mostly displayed stress fibers with no apparent actin nodules and some filopods. There were no morphological shape differences between *Coro1a$^{+/+}$* and *Coro1a$^{-/-}$* platelets for any matrices used (**Figure 4.2.9A**). This provides evidence that *Coro1a* is dispensable for platelet spreading.

GFOGER and CRP were used for the collagen receptors α$_2$β$_1$ and GPVI, respectively, because initial studies demonstrated a difference in surface area on collagen between the genotypes However, scrutiny with a larger power found no statistically significant differences in adhesion (**Figure 4.2.9B**) or cell surface area between the *Coro1a$^{+/+}$* and *Coro1a$^{-/-}$* platelets for any matrix used (**Figure 4.2.C**). This again provides evidence that *Coro1a* is dispensable for platelet spreading.

Platelets spread on GFOGER and CRP demonstrated approximately half of the adhesion as those on collagen. Platelets demonstrated dose dependent adhesion and surface area when spread on GFOGER although the difference was small (**Figure 4.2.B** & **C**). The surface area of platelets on CRP was larger than any other matrix used (**Figure 4.2.C**).

171
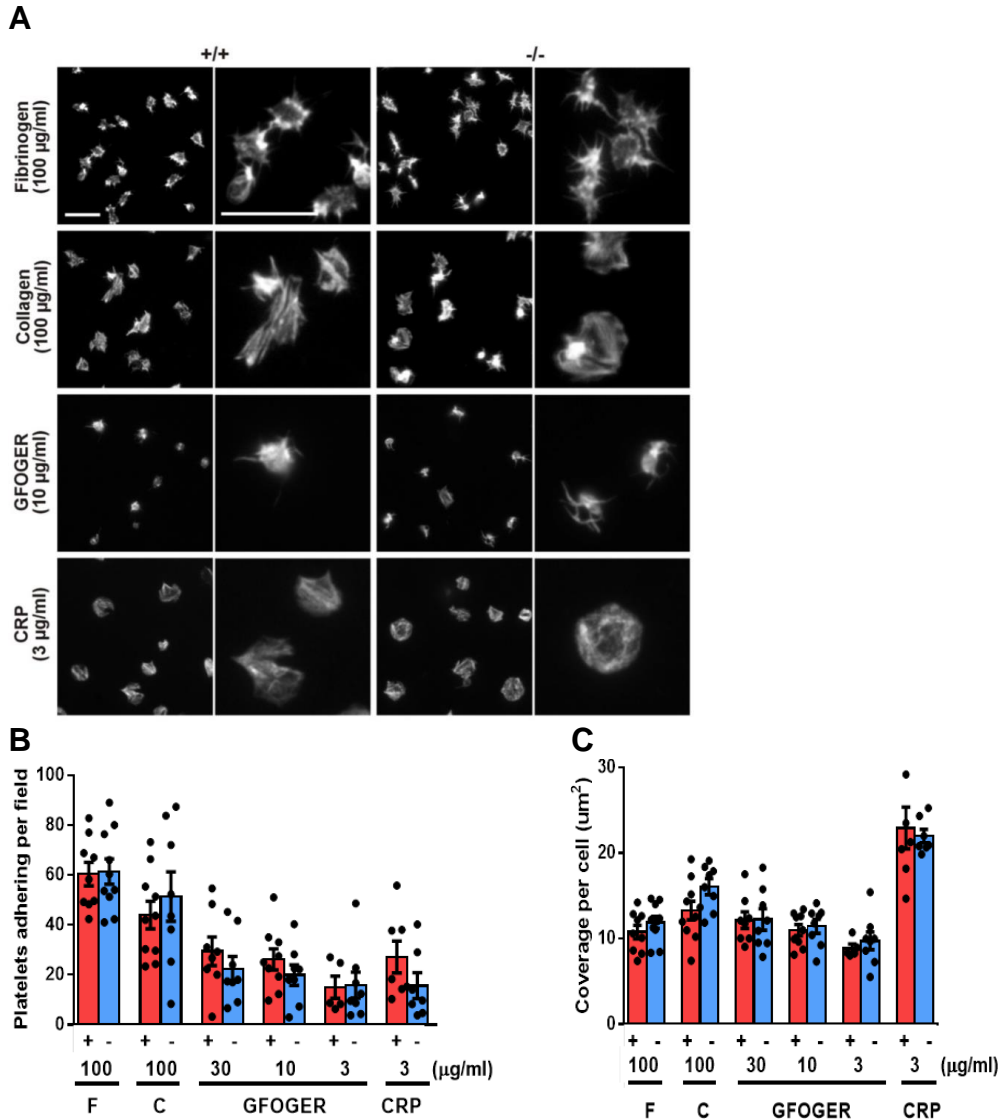
Figure 4.2.9 - Coronin 1 i*s* dispensable for platelet spreading

Coro1a$^{+/+}$ and *Coro1a*$^{-/-}$ platelets were spread on 100 µg/ml fibrinogen, 100 µg/ml collagen, 30, 10 and 3 µg/ml GFOGER and 3 µg/ml CRP for 45 minutes at 37°C, fixed with 4% PFA in PBS, permeabilised and stained with 0.05 µg/ml TRITC-phalloidin in PBS for 30 minutes at RT, mounted and imaged with a fluorescence microscope equipped with an apotome then deconvolved. Two magnifications are shown and scale bar is 10 µm (**A**). The mean of five 12,500 µm^2 fields were measured for each data point. 250-1000 platelets were measured for each condition. Surface area was measured by thresholding using the 'Li' method on ImageJ and dividing by the number of platelets for every image (**B**). Adherence was counted manually (**C**). Data is mean ± SEM. F n = 10; C n = 10; 30 µg/ml GFOGER n = 8; 10 µg/ml GFOGER = 8; 5 µg/ml GFOGER = 5; CRP n = 7. F = fibrinogen; C = collagen; CRP = collagen related peptide. All data except adhesion for low concentration GFOGER was parametric. No significant differences were found using unpaired t-tests or Mann-Whitney U as appropriate.

4.2.10 Coronin 1 is dispensable for thrombin-induced Arp2/3 translocation

Coronin 1 is known to interact with the Arp2/3 complex to regulate F-actin turnover (Gandhi & Goode, 2008). Upon stimulation, the Arp2/3 complex moves to the edge of platelets (Bearer *et al.*, 2002; Zhi Li *et al.*, 2002). The aim of this experiment was to investigate if the translocation is dependent on coronin 1. *Coro1a*$^{+/+}$ and *Coro1a*$^{-/-}$ platelets were stained for phalloidin and the Arp C2 subunit of the Arp2/3 complex in basal and thrombin stimulated conditions to investigate if the translocation of Arp2/3 is altered in the *Coro1a*$^{-/-}$ platelets. Arp C2 was granulated throughout the cell in basal conditions and accumulations were present at the edges in stimulated conditions in the WT platelets as expected. This was also the case for the KO platelets (**Figure 4.2.12A**) and quantification of Arp C2 distribution in platelets revealed no statistically significant difference between the *Coro1a*$^{+/+}$ and *Coro1a*$^{-/-}$ platelets (**Figure 4.2.12B**). It appears coronin 1 is dispensable for Arp2/3 translocation to the cell cortex in platelets upon stimulation
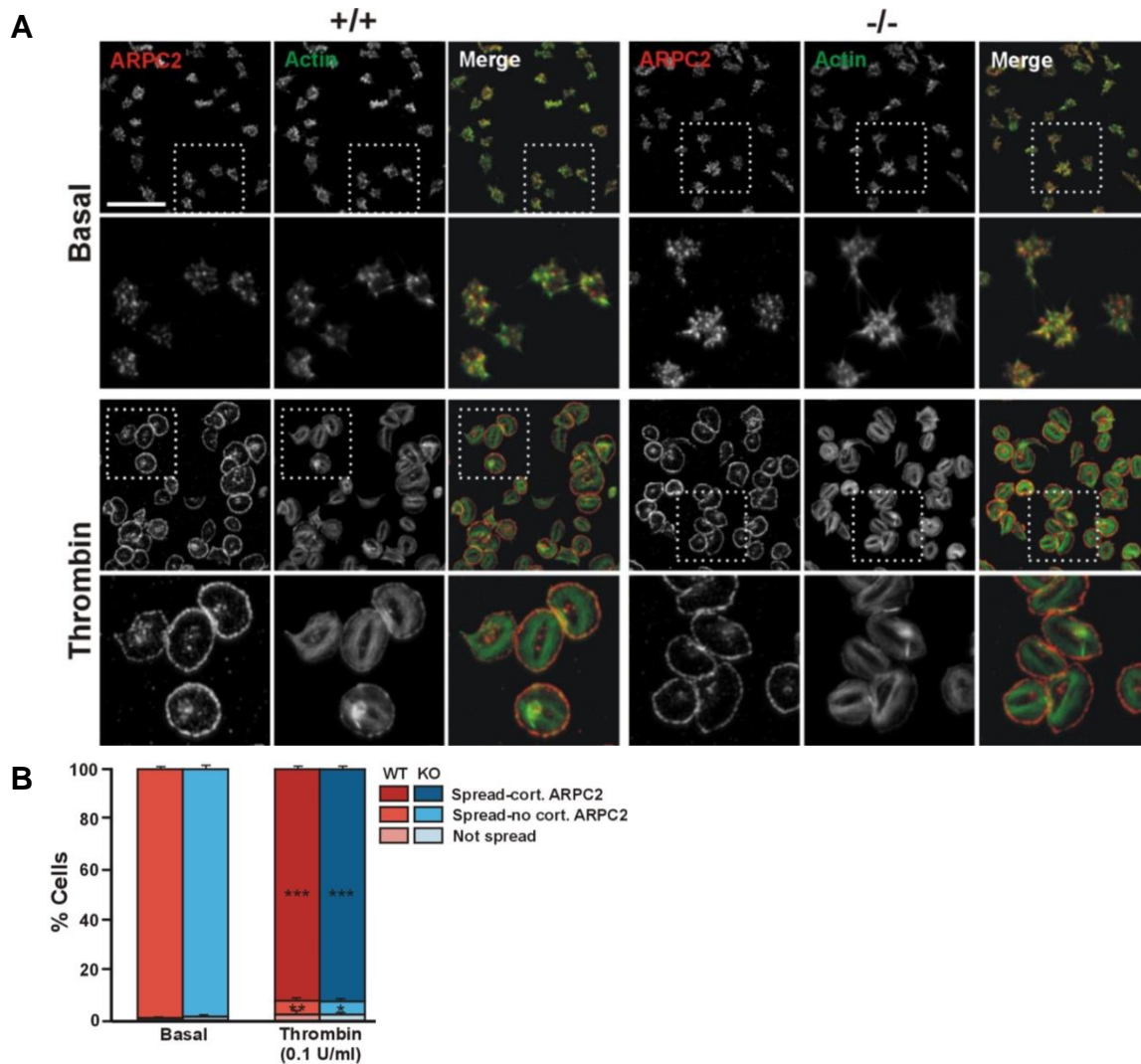
Figure 4.2.10 - Coronin 1 is dispensable for Arp2/3 translocation
Washed *Coro1a*^{+/+} and *Coro1a*^{-/-} murine platelets were spread upon 100 µg/ml fibrinogen in basal or 0.1 U/ml thrombin treated conditions for 45 minutes at 37°C. The platelets were fixed with 4% PFA, permeabilised with 0.3% Triton X-100 in PBS, stained with an anti-ARPC2 antibody followed by an Alexa568 secondary antibody (red) and counterstained with FITC-phalloidin for F-actin (green). Images were acquired with a fluorescence microscope equipped with an apotome and deconvolved in Zen software. Representative images at two magnifications are shown. Boxes mark the enlarged regions. Scale bar = 25 µm (**A**). Platelets were manually assigned to one of three groups - spread with cortical Arp C2, spread without obvious cortical Arp C2 or not spread. 5 fields of 36,670 µm^2 from 4 independent experiments were analysed for each condition. The data is percentage of platelets from each group and represented as mean ± SEM. * $p<0.05$, ** $p<0.01$, *** $p<0.001$ relative to the corresponding basal condition. No significant differences were found between WT and KO platelets for any condition (Mann-Whitney U) (**B**).

174

4.2.11 Coronin 1 may be dispensable for cAMP signalling

PGI_2 inhibits platelets by stimulating the prostacyclin receptor, which signals through Gαs, increasing cAMP levels and leading to PKA mediated phosphorylation of VASP and ultimately platelet inhibition (Nagy & Smolenski, 2018). It has previously been reported that coronin 1 binds to Gαs in neurons (Jayachandran *et al.*, 2014) and associates with Gαs in IPs of platelet lysate (**Section 3**). The focus of this experiment was to investigate if the ablation of coronin 1 would affect cAMP levels. Murine platelets were either untreated or treated with 100 or 5 nM PGI_2 for 5 minutes at 37°C then immediately lysed. By utilising Western blots, pVASP-S157 was measured as a marker of cAMP activity and platelet inhibition in response to PGI_2. 100 nM PGI_2 demonstrated the highest inhibition, with 5 nM showing much less inhibition and both treatments displaying more inhibition than the basal (**Figure 4.2.11A**). The *Coro1a*$^{-/-}$ platelets demonstrated lower pVASP levels inresponse to PGI_2 than the *Coro1a*$^{+/+}$ platelets, but the experiments had high variability and the difference was not statistically significant for basal (Mann-Whitney U, p = 0.4359), 5 nM PGI_2 (unpaired t-test, p = 0.7959), 100 nM PGI_2 (Mann-Whitney U, p = 0.5787) or PGI_2 + thrombin (Mann-Whitney U, p = 0.5414) **Figure 4.2.B**).

By utilising flow cytometry, murine platelets were analysed for the markers αIIbβ3, P-selectin and CD63. Murine *Coro1a*$^{+/+}$ and *Coro1a*$^{-/-}$ platelets were either left untreated, treated with 0.1 U/ml thrombin, 100 nM PGI_2 or 100 nM PGI_2 with 0.1 U/ml thrombin for 20 minutes at 37°C then immediately fixed and analysed by flow cytometry. Relative to basal, the thrombin treated platelets demonstrated an increase in all 3 parameters which was much greater than the PGI_2 or PGI_2 + thrombin treated samples. The response to platelets to PGI_2 was not significantly different to the PGI_2 + thrombin samples. No statistically significant difference was found between the *Coro1a*$^{+/+}$ and *Coro1a*$^{-/-}$ platelets (**Figure 4.2.C**).

Finally, a determination of cAMP levels was performed for murine *Coro1a*$^{+/+}$ and *Coro1a*$^{-/-}$ platelets under basal, low and high PGI_2 stimulated conditions. There was little increase in cAMP levels upon stimulation. There was no statistically significant difference in the cAMP levels between the two genotypes under any

175

conditions. However it should be noted that a phosphodiesterase inhibitor was not used in this experiment (**Figure 4.2.D**). Taken together, this indicates that *Coro1a*may be dispensable for cAMP levels and possibly PGI$_2$ signalling.

A

B

C

D
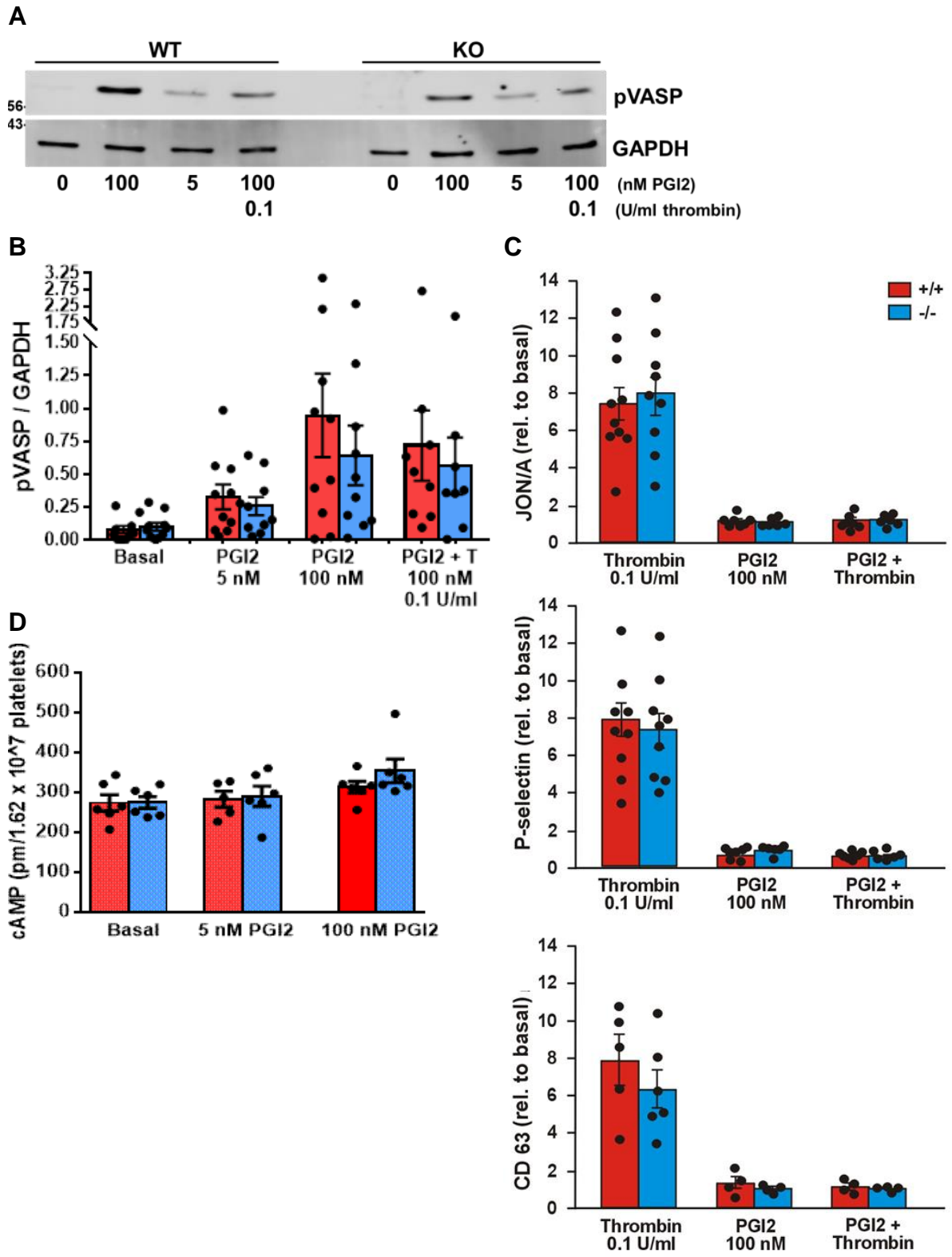
Figure 4.2.11 – Effect of coronin 1 ablation on the cAMP pathway
Washed murine platelets were treated with 5 nM PGI or 100 nM PGI_2, for 5 minutes at 37^oC. Another sample was treated for 5 minutes with 100 nM PGI_2 + 0.1 U/ml thrombin for 2 additional minutes. Control samples were left untreated at 37^{oC}. The samples were lysed, subjected to SDS/PAGE Western blot, blotted for pVASP-Ser157, GAPDH and the signal normalised to GAPDH. The data is represented as mean ± SEM for n = 10. No statistically significant differences were found between $Coro1a^{+/+}$ and $^{-/-}$ platelets (**A**). αIIbβ3 **i**ntegrin activation, P-selectin exposure and CD63 exposure was measured under basal, thrombin stimulated, PGI_2 stimulated and PGI_2 + thrombin stimulated conditions. Murine platelets in PRP were treated with 100 nM PGI_2 for 5 min prior to stimulation with 0.1 U/ml thrombin with relevant antibodies, fixed with 1x BD fix/lyse buffer and subsequently analysed by flow cytometry. The mean of the median fluorescence intensities are expressed relative to basal platelets. The data represents mean ± SEM independent experiments. αIIbβ3 n = 9; P-selectin n = 9; CD63 n = 4-6 (**B**). Washed murine platelets were treated 5 or 100 nM PGI_2 for 5 at 37^oC, lysed and subjected to a cAMP ELISA. A phosphodiesterase inhibitor was not used. No difference was found between the $Coro1a^{+/+}$ and $^{-/-}$ platelets. n = 6. Data is mean ± SEM (**C**). Platelets were treated with 5 or 100 nM PGI_2 for 3 minutes at 37^oC, lysed and the cAMP levels were obtained by ELISA. The values are p moles of cAMP per 1.62 x 10^7 platelets (**D**).

4.3 Discussion

The availability of animal models has significantly contributed to elucidate the roles in platelet function of cytoskeleton proteins, which usually cannot be targeted pharmacologically (H Falet, 2017). In this chapter a functional characterisation of *Coro1a*, an abundant class I coronin, in a KO mouse model is presented. The salient phenotype of $Coro1a^{-/-}$ platelets is the impaired translocation of integrin β2 to the cell surface upon thrombin stimulation, in the absence of any alteration in a range of morphological and functional tests. The study broadly confirms a recent report by Stocker *et al*. (2018) and explores aspects not covered there. However, we did not observe some of the mild defects reported by Stocker *et al*. (2018), specifically: increased relative platelet size, increased adhesion receptor expression, decreased platelet spreading area upon stimulation with thrombin or collagen, and decreased velocity of aggregation in response to low-dose collagen (Stocker *et al.*, 2018). These divergent outcomes could be tracked back to methodological differences, size of experimental populations, and statistical analysis.

178

Regarding methodical differences, for example, Stocker *et al.* (2018) used an impedance-based method on whole blood to study aggregometry, whereas we used light transmission aggregometry on washed platelets. Impedance-based aggregometry on whole blood captures responses that depend on interactions with leukocytes and red blood cells and is, therefore, closer to the physiological situation, however, it is considered insensitive to low levels of platelet activation. Light transmission aggregometry by contrast, requires more manipulations but takes platelets at face value, without the influence of variations in hematocrit and cellular content (Jarvis, 2004). The different methods might have influenced platelet reactivity, causing opposite outcomes, although the differences between WT and KO were always small.

The present study found no difference in relative platelet size as measured by FSC and in the basal and stimulated levels of GPVI, CD41, CD42b and CD49b in *Coro1a*$^{-/-}$ KO platelets. The findings that platelet FSC, as well as the basal levels of receptors CD41 and CD42 were not statistically significantly different in *Coro1a*$^{-/-}$ platelets was in contrast to a study by Stocker *et al.*, (2018), which found greater FSC values and higher CD41 and CD42 levels in *Coro1a*$^{-/-}$ platelets. The difference can be traced to experimental repeats. The current study performed 18 and 14 experimental repeats of FSC and basal receptor levels, respectively. This is in contrast to 6 experimental results from the Stocker *et al.*, (2018) study and should provide a more reliable result. The difference in platelet spreading results is due to both a larger number of experimental repeats and more robust statistical analysis, as explained later.

4.3.1 Integrin β2 translocation is impaired in *Coro1a*$^{-/-}$ platelets

While the basal levels and thrombin-induced translocation of GPVI. CD41, CD42b and CD49b were unaffected in *Coro1a*$^{-/-}$ KO platelets, there was impaired translocation of integrin β2, suggesting that coronin 1 is specifically implicated in the regulation of this integrin in platelets. Integrin β2, a component of lymphocyte

179

function-associated antigen 1 (LFA-1) when associated with integrin αL, is one of the 6 integrins expressed in mouse platelets and the fourth most abundant (Zeiler *et al.*, 2014). β2 integrin is important for polymorphonuclear neutrophil adhesion to the endothelium and subsequent events, like extravasation (Fagerholm *et al.*, 2019). *Coro1a* is critical for these processes because it interacts with the cytoplasmic tail of integrin β2 and regulates the accumulation of activated integrin in focal zones of adherent cells (Pick *et al.*, 2017). In platelets, LFA-1 has not been extensively investigated. Platelets from mice deficient in integrin β2 are characterised by a shorter lifespan, reduced adhesion to the endothelium in response to tumor necrosis factor (TNF), and caspase activation (Piguet *et al.*, 2001). Stocker *et al.* (2018) reported a normal lifespan of *Coro1a*$^{-/-}$ platelets, suggesting that this coronin is not the only protein responsible for the regulation of integrin β2. Similarly, no defective adhesion and spreading on an ICAM-1 surrogate matrix has also been reported (Riley *et al.*, 2020), suggesting that *Coro1a*$^{-/-}$ platelets retain sufficient binding capacity through LFA-1 and/or other mechanisms. In line with this observation unaffected accumulation of neutrophils within arterial thrombi in *Coro1a*$^{-/-}$ platelets have been reported (Stocker *et al.*, 2018). However, the role of integrin β2 in platelet–leukocyte interaction is difficult to dissect due to concurrent and more prevalent mechanisms mediating those interactions (Cerletti *et al.*, 2010) and to the fact that the interactions mediated by LFA-1 and ICAM family molecules are reciprocal: both are present simultaneously in platelets and leukocytes. A rigorous attempt at exploring this aspect would require the generation of a platelet-specific *Coro1a* knockout model combined with platelet-specific deletion of ICAM-2, the adhesion molecule isoform present in the platelet membrane (Zeiler *et al.*, 2014). Attempts were made to explore platelet-WBC binding and to block specific mediators of their interactions including P-selectin, but this was not optimised due to time constraints as well as poor antibody and inhibitor responses (**Appendix, 8.1.5**).

4.3.2 Coronin 1 is dispensable for platelet spreading and adhesion

Rho signalling is involved in platelet lamellipodia formation (Gao *et al.*, 2009). In *Dictyostelium discoideum* coronin 1 can act similarly to a Rho protein GDP dissociation inhibitor that binds GDP-bound Rho GTPases and prevents them from becoming available for activation of their downstream targets such as PAK. (Swaminathan *et al.*, 2013). PAK is involved in actin dynamics as it phosphorylates and activates LIMK1 which phosphorylates and inhibits cofilin, preventing it from depolymerising actin (Joseph E Aslan *et al.*, 2013).

RhoA and Rac1 are particularly important and act as regulators of the actin cytoskeleton (J E Aslan & McCarty, 2013). *Rac1*^{-/-} platelets are characterised by defects in lamellipodia formation (McCarty *et al.*, 2005). Coronin contains a CRIB motif between blades 2 and 3 which enables coronin to bind Rho GTPases with a preference for GTP loaded Rac (Swaminathan *et al.*, 2014). Coronin is also a regulator of Rac1 which facilitates Rac1 translocation and activation (Castro-Castro *et al.*, 2011). As platelet spreading requires actin turnover and coronin influences signalling pathways involved in actin dynamics, the spreading ability of *Coro1a*^{-/-} platelets was examined.

Coronin 1 was found to be dispensable for the adhesion and spreading area of on fibrinogen, collagen, CRP and 3 doses of GFOGER. This is in contract to a study by Stocker, *et al.*, (2018) that claimed to find statistically significant defects in spreading with *Coro1a* platelets on fibrinogen. The difference between the findings of the two studies can be explained by population size and statistics. The experimental repeats for fibrinogen in this study was 10 which provides a robust and more reliable representation of platelet behaviour than the 3 experimental repeats in the Stocker *et al* (2018) study. Stocker *et al* (2018) stated the use of non-parametric statistical tests on sample sizes too small to test for normality - in this case 3. Therefore they claimed to find statistical significance with a Mann-Whitney U test which is mathematically impossible with three experimental repeats.

4.3.3 Coronin 1 is dispensable for αIIbβ3 activation and platelet secretion

Coronin 1 is known to regulate the activity of the calcium/calcineurin pathway in T cells, B cells and macrophages (Westritschnig *et al.*, 2013) and regulates the survival of T cells (Mueller *et al.*, 2008). Coronin 1 is also known to regulate sympathetic final target innervation via coronin-1-dependent calcium release via PLCγ1 signaling which releases PI3K-dependent suppression of GSK3β (Suo *et al.*, 2015). Calcineurin is activated by calmodulin (Rumi-Masantea *et al.*, 2012) which is associated with the platelet receptors GP1b-V-IX and GPVI where it may play roles in receptor expression (Gardiner *et al.*, 2005). Calcium is also important for the activation of receptors including αIIbβ3 as well as granule release (van der Meijden & Heemskerk, 2019). Therefore the ability of *Coro1a*$^{-/-}$ platelets to undergo αIIbβ3 activation and secretion of alpha and dense granules was analysed in response to an array of agonists and it appeared that coronin 1 was dispensable. Several attempts were made to optimise a method to investigate calcium levels in platelets during a time course with agonist-induction but were not pursued due to time limitations (**Appendix 8.1.6**).

4.3.4 Coronin 1 may be dispensable for the cAMP signaling pathway

Coronin 1 has *a* role in modulating the cAMP signaling pathway in excitatory neurons, where deficiency of the protein resulted in the loss of excitatory synapses and a range of neurobehavioral disabilities. *Coro1a* interacts with Gαs in a stimulus-dependent manner, leading to increased cAMP production (Jayachandran *et al.*, 2014). The association of Coronin 1 with Gαs is regulated by cyclin-dependent kinase 5 (CDK5)-mediated phosphorylation of Coronin 1 on two particular threonine residues (X. Liu *et al.*, 2016). Furthermore, *Coro1a* regulates cAMP signaling in T cells (Jayachandran *et al.*, 2019) whereas the homolog in *Dictyostelium discoideum* regulates cAMP-dependent initiation of multicellular aggregation (Vinet *et al.*, 2014) and the homolog in the fungus *Magnaporthe oryzae* interacts with a Gαs subunit to regulate cAMP production and pathogenicity (X. Li *et al.*, 2019). In platelets, Gαs

activation and subsequent cAMP production are coupled to binding of PGI$_2$ to its G protein-coupled receptor.

Although *Coro1a* is able to co-IP with Gαs in platelets (**Section 3.2.7**), absence of Coronin 1 does not appear to be detrimental to the production of cAMP, as demonstrated by the ability of *Coro1a$^{-/-}$* platelets to function indifferently to *Coro1a$^{+/+}$* platelets with regards to PGI$_2$-induced VASP phosphorylation, PGI$_2$-induced inhibition of thrombin stimulation, and PGI$_2$-induced cAMP levels.However some of these experiments suffered from technical limitations and variability (**Section 4.2.11**). Platelets contain phosphodiesterase 2A, 3A and 5A (Burkhart, *et al.*, 2012; Rondina & Weyrich 2012). Phosphodiesterase inhibitors such as cilostazol, milrinone or anagrelide prevent hydrolysis of cAMP by PDE3, Inhibitors such as dipyridamole and sildenafil prevent cGMP hydrolysis by PDE5 (Rondina & Weyrich 2012). Future experiments could perform the cAMP ELISA in the presence of such inhibitors The *Coro1a$^{-/-}$* platelets had less than 70% of the p-VASP levels relative to the *Coro1a$^{+/+}$* after treatment with PGI$_2$. (**Section 4.2.11**), The lack of statistical significance may be due to high data variation and a lack of repeats that may be worth investigating further.

The role of Coronin 1 in cAMP regulation is, however, complex. In T cells, ablation of Coronin 1 results in reduced production of cAMP, however, cAMP levels are increased due to a compensatory decrease in phosphodiesterase 4 (PDE4) levels (Jayachandran *et al.*, 2019). Further research would be needed to clarify whether Coronin 1 regulates the cAMP pathway in platelets and, if so, through which molecular mechanisms. PDE4 is absent (Rondina *et al.*, 2016) but CDK5 is present both in human and mouse platelets (Burkhart *et al.*, 2012; Zeiler *et al.*, 2014), although the role of the latter in platelets has not been addressed so far. Coronin 2 and Coronin 3 associate with Gαs in IPs (**Chapter 3**), suggesting that these two class I coronins may compensate for the absence of Coronin 1 in regulation of the cAMP pathway.

4.3.5 Coronin 1 is dispensable for Arp2/3 translocation

Arp2/3 has previously been reported to function in concert with coronin 1 and cofilin to regulate actin turnover (Gandhi & Goode, 2008). Coronin 2 has previously been reported bind to Arp C2 of the Arp2/3 complex and phosphorylate it and regulate cell motility (Cai *et al.*, 2005). Indeed, coronins 1, 2 and 3 were all found to associate with ARPC2 in IPs and also accumulate at the cell cortex of spread platelets. Functional compensation by other class I coronins might also explain the retained ability of the Arp2/3 complex to accumulate at the cell cortex in response to thrombin where it presumably enables the formation of lamellipodia and consequently spreading.

4.3.6 Summary

To summarise, it appears class I coronins display a large extent of functional overlap in platelets. This would explain the absence of a strong phenotype in most platelet functional assays while aspects like integrin β2 translocation reported by us and the formation of F-actin and cofilin dephosphorylation in response to agonists reported by others (Stocker *et al.*, 2018) are specifically or more strongly dependent on Coronin 1 function. This is not uncommon among components of the actin cytoskeleton, examples include vinculin (Mitsios *et al.*, 2010), cortactin and HS1 (Thomas *et al.*, 2017) and Rif (Goggs *et al.*, 2013). Thus, disruption of the Arp2/3 complex regulators cortactin and its homolog HS1 does not cause any noticeable alteration in platelet function, indicating that their roles might be fulfilled by other proteins (Thomas *et al.*, 2017). Similarly, disruption of the formin mDia results in no major platelet phenotype, pointing at functional compensation by other formins present in platelets (Zuidscherwoude *et al.*, 2019). Future studies toward the elucidation of coronin function in platelets will, therefore, require the generation of mouse models lacking two or three class I coronins in order to arrive at a complete picture of the shared and unique roles of these proteins.

5. Chapter 5 – The membrane-associated fraction of cyclase associate protein 1 translocates to the platelet cytosol upon stimulation

5.1 Introduction

5.1.1 Aims

- To characterise the association of CAP1 with interacting proteins.
- To analyse the association of CAP1 to the F-actin cytoskeleton.
- Characterise the subcellular localisation of CAP1 and colocalisation with F-actin.
- To investigate the translocation of CAP1 in response to platelet stimulants and inhibitors.

.

5.2 Results

5.2.1 Subcellular distribution and of CAP1 in platelets

CAP1 was predicted to be present from proteomic studies in platelets (Burkhart *et al.*, 2012) and also in several other cell types which were utilised as positive controls in a Western blot, including melanoma cells, HT29 colon cells, HEK cells, human umbilical vein endothelial cells (HUVEC) and COS7 fibroblast-like monkey kidney cells. can be visualised as a strong band at around 56 KDa in human platelets (**Figure 5.2.1A**). A full blot of CAP1 is available elsewhere (Joshi, 2017),

CAP1 is predominantly a cytosolic protein but a small proportion of CAP1 has been detected in the membrane by membrane/cytosol subcellular fractionation of human acute monocytic leukemia cells (THP-1) (Lee *et al.*, 2014). The subcellular localisation of CAP1 in basal human platelets was investigated using membrane/cytosolic subcellular fractionation. Approximately 77% of CAP1 was

found in the cytosol with the remaining 23% in the membrane fraction. CD36 and Syk were used as membrane and cytosol markers respectively (**Figure 5.2.1B**).

As CAP1 is both membrane and cytosol associated and also binds actin, we investigated whether the membrane bound CAP1 is dependent on the presence of actin. 20 µM latrunculin was utilised to bind to G-actin, pushing actin turnover into a depolymerised state. A small amount of β-actin was found in the membrane in the untreated platelets, but was completely absent from the membrane of the latrunculin-treated platelets, indicating the F-actin was depolymerised successfully. The levels of CAP1 in the membrane in the untreated (~22%) and latrunculin treated (~23%) samples remained similar (Mann-Whitney U). CD36 and Syk were used as markers of the membrane and resting platelet cytosol, respectively (Joshi *et al.*, 2018) (**Figure 5.2.1B**). This indicates the association of CAP1 to the membrane fraction is independent of its ability to bind actin.
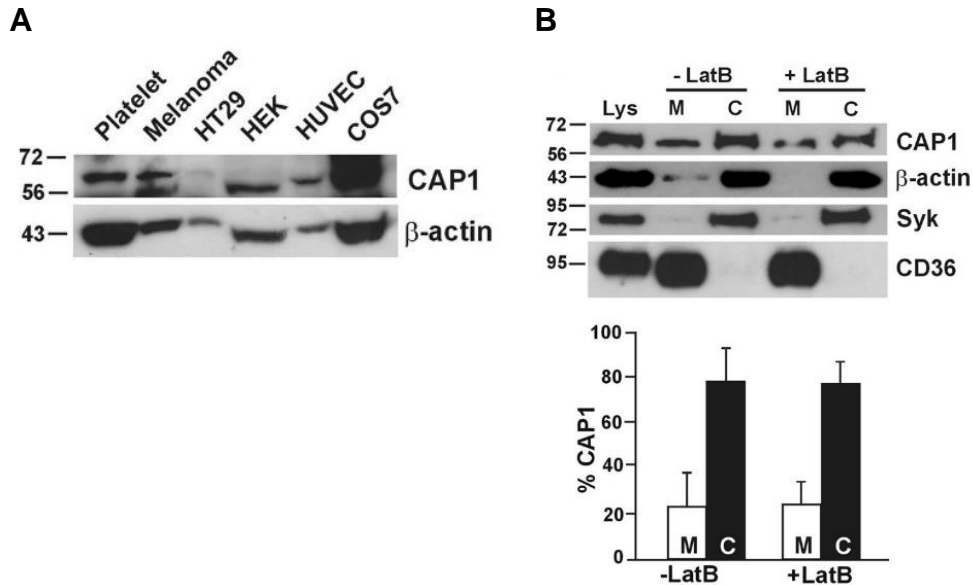
Figure 5.2.1 - Subcellular distribution of CAP1 in platelets
(**A**) 30 µg of human platelet or cell lysates (total protein) were resolved by SDS-PAGE/WB and probed for CAP1 and β-actin as a loading control. Melanoma, HT29 human colorectal cells, HEK cells, HUVEC cells and COS7 cells were used as controls (**B**) Platelets at 1×10^9/ml were mixed 1:1 with fractionation buffer, lysed by freeze-thaw in liquid nitrogen and centrifuged at 100,000 ×g for 1 hour to separate membrane (M) and cytosolic (C) fractions. The fractions were normalised by volume and resolved by SDS-PAGE/WB and probed for indicated proteins. CD36 & Syk were used as membrane or cytosolic markers respectively. 20 µM latrunculin B (LatB) for 20 minutes was used to depolymerise F-actin prior to lysis. CAP1 distribution was quantified by densitometry and expressed as percentages relative to the total (M + C) CAP1 in the lysate. Data is mean ± SD of n = 3. Mann-Whitney U tests were performed to test for differences between latrunculin treated and untreated samples. No statistically significant differences were identified. Performed in collaboration with Pooja Joshi (Joshi *et al.*, 2018).

5.2.2 CAP1 does not associate with large F-actin filaments

The Triton X-100 insoluble fractionation can be utilised to analyse the association of proteins to the detergent insoluble F-actin cytoskeleton (Fox *et al.*, 1993; Jung & Moroi, 1988; Tardieux *et al.*, 1998) as explained in **Section 3.2.5**. To investigate the behaviour of CAP1, resting platelets were subjected to Triton X-100 insoluble fractionation at LS and HS. At LS (15,600 ×g), CAP1 was present in the soluble fraction only and not detectable in the insoluble fraction

187

where cross-linked actin filaments and their associated proteins are present. However, at HS (100,000 xg), the majority of CAP1 was in the soluble fraction, but ~17% of CAP1 was present in the insoluble pellet (**Figure 5.2.2A & B**). This could indicate association to either the membrane components or possibly some association with F-actin.

Upon treatment with latrunculin, CAP1 remained absent in the LS insoluble fraction and comparable levels remained in the LS soluble fraction. However the levels of CAP1 in the HS insoluble fraction slightly increased, but this was not statistically significant (Mann-Whitney U) (**Figure 5.2.A & B)** (Joshi *et al.*, 2018). This indicates that the CAP1 in the HS insoluble is not F-actin associated. Syk was used as a marker of the cytosol of resting platelets.

CAP1 functions with both cofilin and profilin to regulate actin turnover (Makkonen *et al.*, 2013), so any possible association of these proteins with F-actin was investigated. Profilin was recovered in the soluble fractions at both LS and HS which is consistent with its role as monomeric actin binding protein. Cofilin, which interacts with both F-actin and G-actin, was observed in both the HS and LS insoluble fractions. F-actin depolymerisation caused cofilin to be absent from the LS insoluble fraction as expected due to the absence of large cross linked F-actin filaments. Cofilin demonstrated similar patterns to CAP1 in the HS insoluble fraction (**Figure 5.2.A**). Cofilin and profilin behaved as expected by their ability to bind F-actin and G-actin, or only G-actin, respectively.

CD36 was used as a marker of the membrane and also of the detergent insoluble lipid rafts. The HS fraction appeared to contained lipid, as indicated by the presence of CD36. This indicates that CAP1 and cofilin in the HS insoluble fraction could be associated to the soluble membranes or the membrane proteins in the lipid rafts (**Figure 5.2.A**).
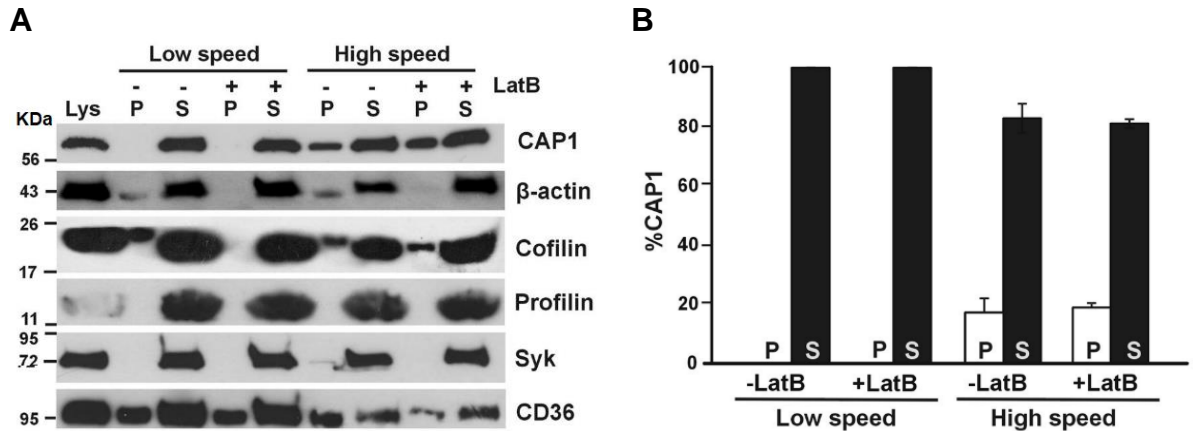
Figure 5.2.2 - CAP1 does not associate with F-actin filaments but is present in lipid rafts

(**A**) Platelets were lysed in 1% Triton X-100 and lysates centrifuged at low speed (15,600 × g) for 20 min then high speed (100,000 ×g) for 1 hour. Supernatant (S) and pellet (P) were normalised by volume and resolved by SDS-PAGE/WB, and probed for the indicated proteins. Syk was used as a cytosol marker and CD36 was used as a marker of the membrane and lipid rafts (**B**) CAP1 concentration in pellet and supernatant were quantified by densitometry and expressed as a percentage of total (P + S). Data represent mean ± SD of n = 3. HT29 = human colorectal cancer cell line, HEK = human embryonic kidney 293 cell line; HUVEC = human umbilical vein endothelial cell; COS7 = fibroblast-like tissue from monkey kidney tissue. Data is mean ± SD of n = 3. Mann-Whitney U tests. Performed in collaboration with Pooja Joshi (Joshi *et al.*, 2018).

5.2.3 CAP1 localises to the cortex and actin nodules

The localisation of CAP1 in platelets has not yet been investigated. In fibroblasts, CAP1 localises diffusely at the cytosol and also accumulates at actin structures such as membrane ruffles (Nancy L. Freeman & Field, 2000) and lamellipodia in fibroblasts where it co-localises with cofilin (Moriyama & Yahara, 2002). The distribution of CAP1 in spread platelets was investigated in resting platelets and in platelets spread on fibrinogen.

Platelets centrifuged onto poly-L-lysine displayed a discoid shape and the majority of them demonstrated CAP1 localisation at predominantly cortical areas, displaying colocalisation with F-actin. However, a proportion of CAP1 was also diffusely spread in the cytoplasm (**Figure 5.2.3A**).

189

Platelets spread on fibrinogen covered a larger surface area than resting platelets on poly-L-lysine. In most fibrinogen-spread platelets, a proportion of CAP1 was distributed diffusely through the cytoplasm, but it also accumulated with rich F-actin areas not only broadly around the cell cortex, but also in the central areas of platelets where the granulomere is expected (**Figure 5.2.3B**), in filopodia (**Figure 5.2.3C**) and actin nodules (**Figure 5.2.3D**).

Actin nodules are areas of platelets which are rich in F-actin. Both F-actin and vinculin staining can be utilised as markers of actin nodules (Poulter *et al.*, 2015). CAP1 was found to strongly accumulate at the actin nodules together with F-actin and vinculin (**Figure 5.2.3E**). CAP1 appears to have very minimal localisation to the same areas as actin stress fibres in platelets (**Figure 5.2.3**). This supports the notion of CAP1 as a G-actin binding protein in platelets which contributes to actin turnover.
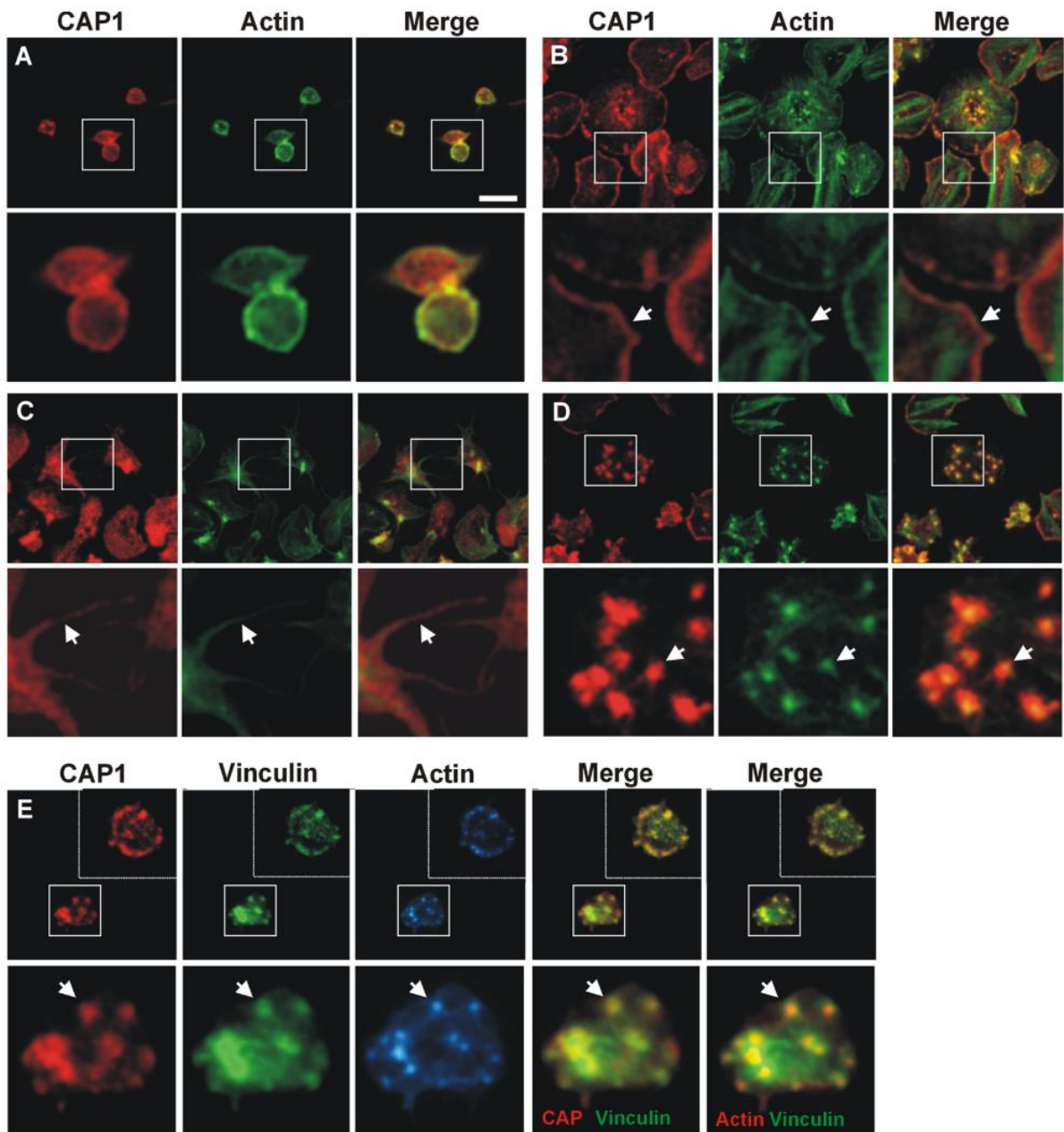
Figure 5.2.3 – CAP1 localises to the cortex and actin nodules
Platelets were fixed in suspension with 4% PFA and centrifuged on poly-L-lysine coated coverslips, permeabilised and stained for the indicated proteins (**A**), or spread on 100 µg/ml fibrinogen coated coverslips for 45 minutes, fixed with PFA, permeabilised and stained (**B–E**). Platelets were treated with 100 nM PGI_2 for 5 minutes prior to fixation in order to increase the proportion of cells displaying actin nodules (**E**). Optical sections were acquired with a fluorescence microscope equipped with a structured illumination attachment. Sections were 230 nm apart. Maximum intensity projection images after deconvolution (Zen) is shown. Enlarged regions are indicated with squares. Arrows point at regions of interest: cell cortex (**B**), filopodia (**C**) and actin nodules (**D,E**). Scale bar = 5 µm.

191

5.2.4 CAP1 translocates from the platelet cortex upon thrombin stimulation

Proteins can translocate between locations of platelets during platelet activation. For example, thrombin-stimulation induces translocation of PKC-α, β and ζ to the membrane (Baldassare *et al.*, 1992), Src to the cytoskeleton (Horvath *et al.*, 1992) and Bid, Bax and Bak to the mitochondria (Lopez *et al.*, 2008). Thrombin is a potent platelet activator which, in humans, acts on receptors including PAR1 and PAR4 (Coughlin, 2000). Translocation of CAP1 in response to thrombin was analysed. Platelets were spread on fibrinogen then either left untreated or treated with 0.1 U/ml thrombin for up to 3 minutes. Platelets were then fixed at various time points, stained for F-actin and CAP1 and the cells with either predominantly cortical or predominantly cytoplasmic CAP1 were counted (**Figure 5.2.4A**).

In platelets spread on fibrinogen with no thrombin treatment, CAP1 displays a predominantly cortical accumulation in ~70% of cells. Within 30 seconds of thrombin treatment, only ~43% of platelets demonstrate predominantly cortical CAP1 staining which was similar to the amount which demonstrated predominantly cytosolic CAP1 accumulation (~46%). By 3 minutes of thrombin stimulation, the majority of CAP1 has reverted to the cell cortex (~60%). A proportion of the cells demonstrated no clear cortical or cytosol accumulation (**Figure 5.2.4B**). This demonstrates CAP1 appears to rapidly translocate from the cell cortex to the cytoplasm in a significant proportion of cells upon thrombin stimulation.
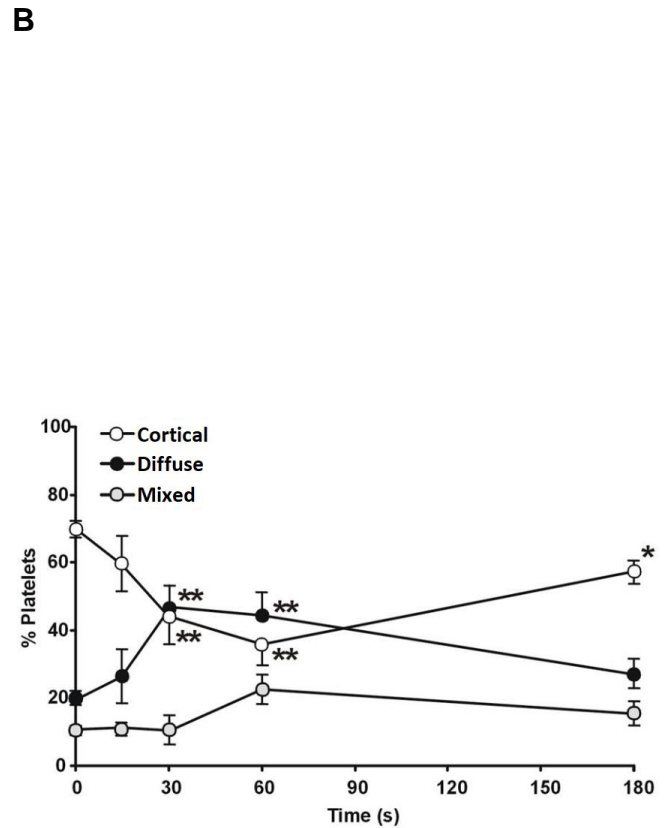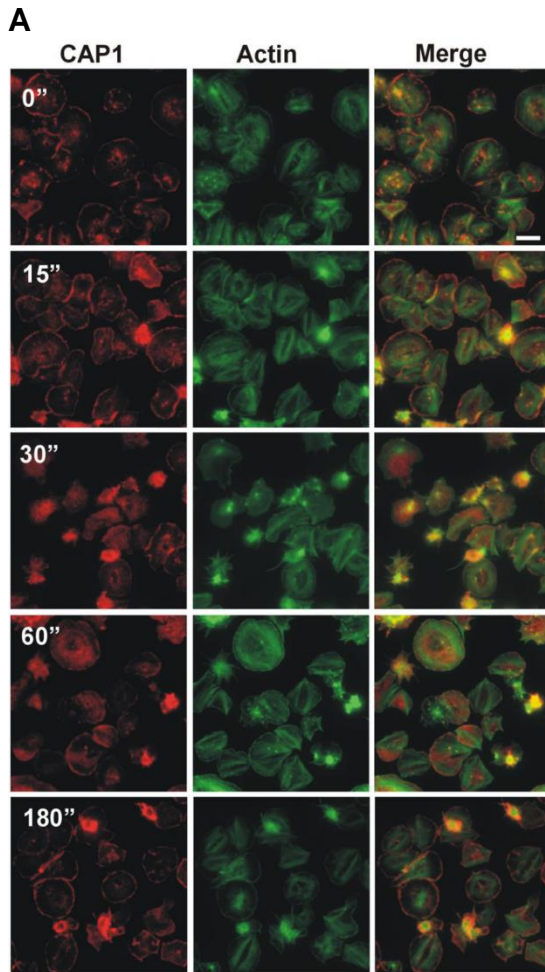
Figure 5.2.4 - CAP1 relocalises to the platelet cortex upon thrombin stimulation
(**A**) Platelets were spread on fibrinogen-coated coverslips, stimulated with 0.1 U/ml thrombin as indicated, fixed with PFA then immunostained for the indicated proteins. Images were acquired with a fluorescence microscope equipped with a structured illumination attachment. Scale bar 5 = µm. (**B**) The proportions of cells with predominantly cortical or diffuse distribution of CAP1 were calculated from 4-5 independent experiments, each performed with duplicate coverslips. At least 1000 cells per time point for each experiment were scored. Unclear/mixed = cells not sufficiently spread to score. Data = mean $\pm$ SEM of 4-5 independent experiments. *p $\leqslant$ 0.05, **p $\leqslant$ 0.01, relative to 0 s, (Mann-Whitney test).

5.2.5 CAP1 translocates away from the membrane upon thrombin stimulation

The previous section described the presence of CAP1 at the platelet cortex and that stimulation with thrombin caused CAP1 to translocate, temporarily, away from the cortex, towards the cytosol before partially returning to the cortex (**Figure 5.2.4**). To investigate if the cortical CAP1 is associated with the membrane and to investigate any changes caused by stimulation, the behaviour of CAP1 was analysed biochemically. Platelets were subjected to a thrombin-stimulation time-course for up to 3 minutes then subcellular fractionation was performed to separate the cell membrane and cytosol (**Figure 5.2.5**). The levels of CAP1 in the membrane rapidly decreased until at 30 seconds less than half of the original amount of CAP1 was present. This persisted at least until the end of the time course of 3 minutes. The proportion of β-actin in the membrane appeared unchanged (**Figure 5.2.A**); indicating that CAP1 translocation does not depend on membrane associated actin. This indicates that the fraction of CAP1 which rapidly translocates from the cell cortex upon stimulation is membrane associated.

Next, experiments were performed to investigate if the effects on CAP1 by thrombin are also caused by other platelet stimulants including resistin and collagen. CAP1 has been proposed as a receptor for, or associated with a receptor for resistin (Lee *et al*., 2014). Collagen is a platelet agonist which signals to the α2β1 and GPVI receptors (Clemetson & Clemetson, 2001). To investigate the subcellular distribution CAP1 changes upon stimulation with resistin and collagen, membrane/cytosol subcellular fractionation was performed on platelets which were previously treated by 10 μg/mL collagen for 3 minutes or 200 ng/mL resistin for 15 minutes. Similarly to thrombin, both collagen and resistin caused a decrease in the amount of CAP1 associated to the membrane of the platelets (**Figure 5.2.B**). This indicates this translocation phenomenon is not specific to thrombin and can occur from a broader range of platelet stimulants.

A

B
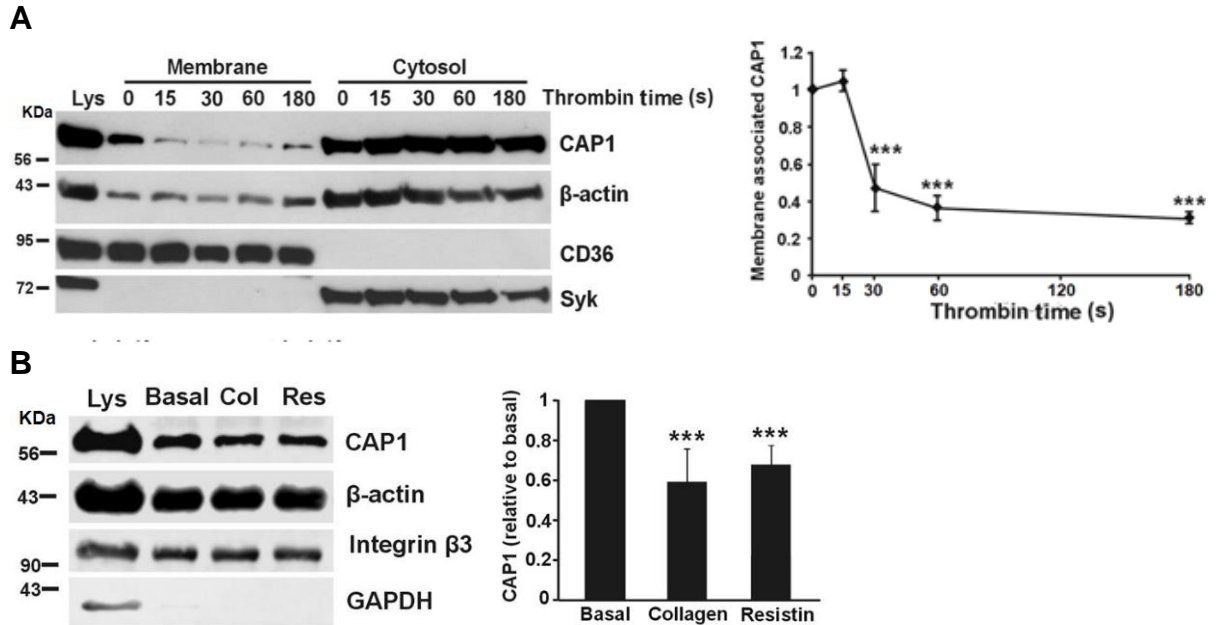
Figure 5.2.5 - CAP1 translocates away from the membrane upon stimulation
(**A**) Platelets (1 × 10^9/ml) were treated 1 mM EGTA for 20 minutes at 37°C to prevent aggregation prior to stimulation with 0.1 U/ml thrombin for the indicated times. Platelets were added 1:1 with fractionation buffer and lysed by 5 freeze/thaw cycles using liquid nitrogen then samples were subjected to membrane/cytosol subcellular fractionation. Fractions were normalised by volume and subjected to SDS-PAGE/WB then probed with antibodies for the indicated proteins. CD36 and Syk were used as membrane and cytosol markers, respectively. Membrane-associated CAP1 was quantified by densitometry, normalised to CD36 and expressed relative to CAP1 in the 0 s membrane fraction. Data represents mean ± SEM of four independent experiments. (**B**) The experiment was performed as in **A** using 10 μg/mL collagen for 3 minutes or 200 ng/mL resistin for 15 minutes. Only the membrane fractions were analysed. Integrin β3 was used as membrane marker and for normalisation. GAPDH was utilised as a marker of the platelet cytosol. Data represent mean ± SEM of 4 to 6 independent experiments. For all panels *p $\leqslant$ 0.05, **p $\leqslant$ 0.01, ***p $\leqslant$ 0.001 relative to 0 s or basal. Mann-Whitney test was used for non-parametric data and t-tests were used for parametric data. Performed in collaboration with Pooja Joshi (Joshi *et al.*, 2018).

5.2.6 CAP1 translocation is independent of F-actin

Similarly to **Figure 5.2.2** which identified CAP1 in the HS insoluble fraction but not in the LS insoluble fraction, the Triton X-100 insoluble pellet fractionation can also be used on platelets to assess the association over a simulation time course (Fox *et al.*, 1993; Jung & Moroi, 1988). The association of CAP1 to the F-actin in the insoluble fraction was measured in platelets which were previously subjected to a time course of thrombin stimulation. The amount of actin in both the LS and HS insoluble fractions rapidly increased, reaching the maximum upon 30 (~1.7x basal) and 60 second (~1.2x basal), respectively. The increase in actin was lower in the HS insoluble fraction and did not reach statistical significance, whereas the LS insoluble fraction reached significance at 30s and 180s but not at 60 and 120s (**Figure 5.2.6A**).

As the amount of F-actin rapidly increased over the first 30, the levels of CAP1 rapidly decreased. This was statistically significant for CAP1 within 15 seconds and the significance increased until 45 seconds, after which the levels of CAP1 troughed (**Figure 5.2.A**). As there was no correlation in the levels of CAP1 and actin in the HS or LS insoluble fractions, it appears CAP1 is not associated with F-actin in platelets.

Next, to demonstrate that CAP1 re-distribution is due to the action of thrombin and not caused by secondary mediators, platelets were pre-treated with 10 µM indomethacin (which inhibits thromboxane A_2 synthesis via COX-1 inhibition) and 1 U/ml apyrase (which degrades ADP and ATP). Platelets were then treated with 0.1 or 0.5 U/ml thrombin and subjected to Triton X-100 fractionation. There was a striking dose dependent re-distribution of CAP1 away from the HS insoluble fraction in upon thrombin stimulation. 0.1 U/ml thrombin resulted in 60-70% of CAP1 remaining in the HS pellet, whereas 0.5 U/ml thrombin resulted in 20-35% of CAP1 remaining. The treatment of platelets with indomethacin and apyrase did not result in a statistically significant difference in CAP1 levels in the HS insoluble fraction when compared to platelets without indomethacin and apyrase treatment (**Figure 5.2.B**). Taken together with the previous data which demonstrated no change in

196

CAP1 in the insoluble fraction upon latrunculin treatment (**Figure 5.2.1B** & **Figure 5.2.2**) this demonstrates that the redistribution of CAP1 away from the HS insoluble fraction upon thrombin stimulation is thrombin dose dependent, is not associated to F-actin and is not mediated by secondary mediators.

A

B
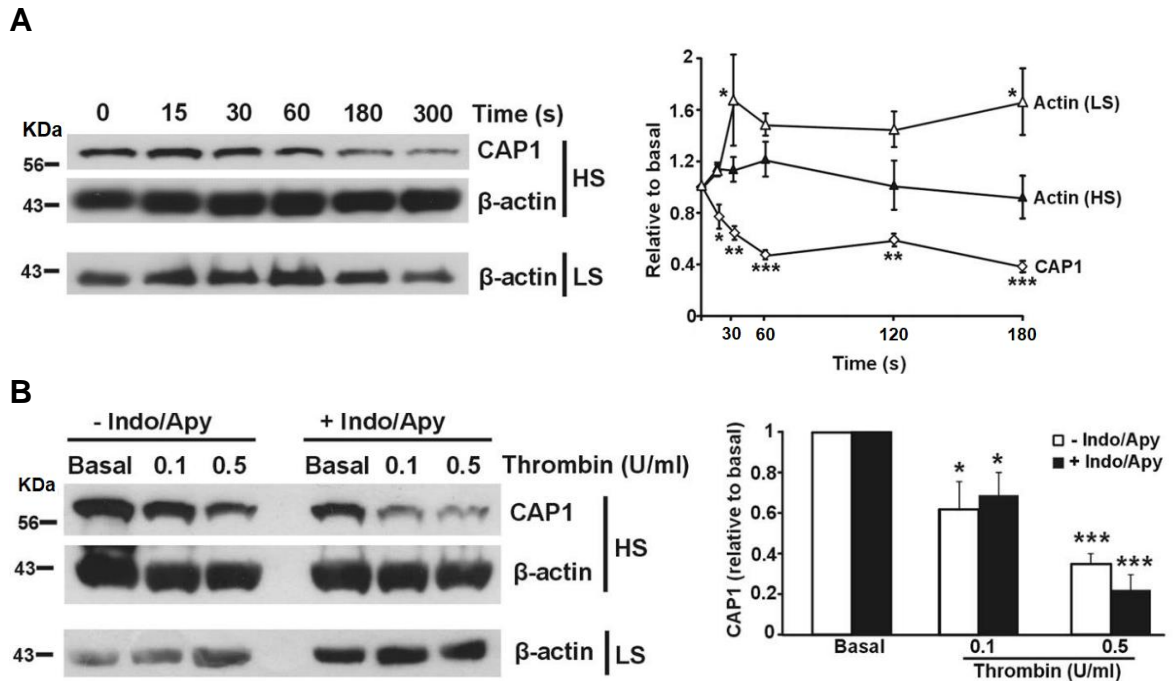
Figure 5.2.6 - CAP1 translocation is independent of F-actin
Platelets were treated with 0.1 U/ml thrombin for the indicated times, lysed, then subjected to Triton X-100 insoluble pellet at LS (15,600 xg) and HS (100,000 xg) centrifugation. Samples were subjected to SDS-PAGE/WB and probed for CAP1 and β-actin. CAP1 and β-actin were quantified by densitometry, normalised to β-actin and expressed relative to the basal pellet fraction. Data represents mean ± SEM of four independent experiments. (**B**) Platelets were untreated or incubated for 20 minutes at 37°C with 10 µM indomethacin and 1 U/ml apyrase, then treated with thrombin for 1 minute as indicated at 37°C. Triton X-100 insoluble pellet was performed as in **A**. Data represents mean ± SEM of three independent experiments. * = $p \leqslant 0.05$, ** = $p \leqslant 0.01$, *** = $p \leqslant 0.001$ relative to 0 s or basal. Mann-Whitney test was used for non-parametric data and t-tests were used for parametric data. Performed in collaboration with Pooja Joshi (Joshi *et al.*, 2018).

197

5.2.7 Thrombin-induced CAP1 relocalisation is inhibited by PGI$_2$, GSNO and GSK3 inhibition

The project next aimed to investigate the effects of PGI$_2$ and the nitric oxide donor S-nitrosoglutathione (GSNO), on thrombin-induced CAP1 relocalisation. Circulating platelets *in vivo* are maintained in an inactive state and aggregation is prevented by endogenous inhibitors, released from healthy, intact endothelial cells. These include PGI$_2$ and NO, which increase levels of cAMP and cGMP, that in turn signal to PKA and PKG, respectively, inhibiting platelet activation (Nagy & Smolenski, 2018). The aim of this experiment was to investigate if increased cyclic nucleotide levels can inhibit the thrombin-induced translocation of CAP1. Platelets were spread on 100 µg/ml fibrinogen then treated with 100 nM PGI$_2$ for 5 minutes, or 10 µM of GSNO for 20 minutes at 37°C prior to stimulation with 0.1 U/ml thrombin for 30 seconds before being fixed. Both PGI$_2$ and GSNO caused a reduction in stress fibres and an increase in actin nodules, with PGI$_2$ causing the stronger effect of the two (**Figure 5.2.7A**). CAP1 remained predominantly cortical (~70%) in the controls without thrombin and also in the cells treated with PGI$_2$ or GSNO followed by thrombin. Similarly to what was previously described, platelets treated with thrombin, demonstrated a reduction in the number of platelets displaying cortical CAP1 from ~70% to ~56% and an increase in the number of cells with CAP1 diffused in the cytosol from 21% to ~39% (**Figure 5.2.7B**). This demonstrates that PGI$_2$ and GSNO can inhibit the thrombin-induced redistribution of CAP1 from the cortex to the cytosol.

198
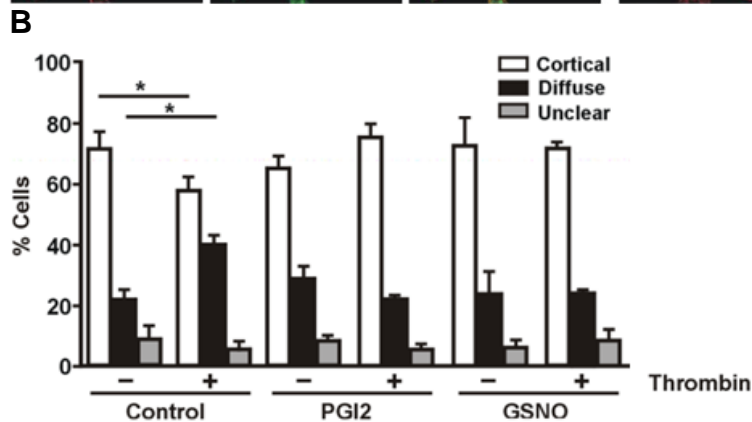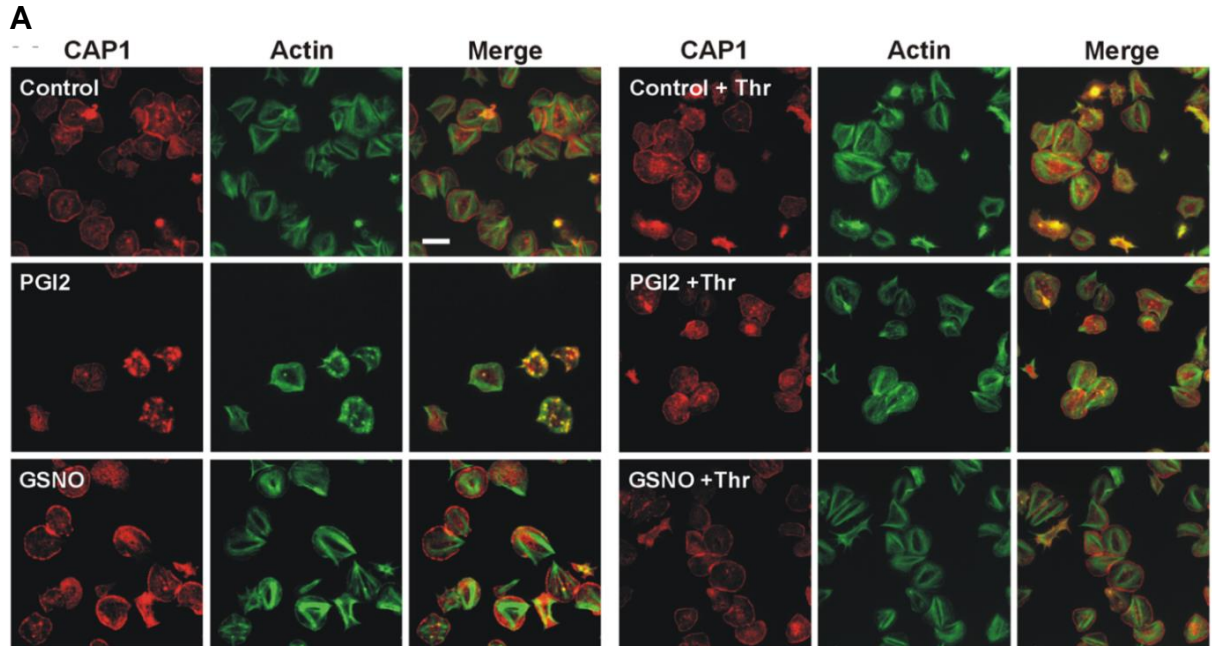
Figure 5.2.7 - Thrombin-induced CAP1 relocalisation is inhibited by PGI₂ & GSNO

(**A**) Platelets were spread on fibrinogen-coated coverslips then treated with 100 nM PGI₂ for 5 minutes or 10 µM GSNO for 20 minutes prior to stimulation with 0.1 U/ml thrombin for 30 seconds at 37°C. Platelets were fixed with PFA and stained for the indicated proteins. Images were acquired with a fluorescence microscope with a structured illumination attachment. Scale bar = 5 µm. (**B**) Quantification of CAP1 distribution before (−) and after (+) thrombin stimulation. The proportions of cells with predominantly cortical or diffuse CAP1 distribution in images were calculated from 2 -5 independent experiments performed on duplicate coverslips. More than 1000 cells per condition in each experiment were scored. Unclear refers to cells that were not sufficiently enough spread to make a judgment. Data are average $\pm$ SEM. *$p \leqslant 0.05$ relative to the respective population not stimulated with thrombin. (Mann-Whitney U test).

199

5.2.8 Thrombin-induced CAP1 relocalisation is inhibited by GSK3 inhibition

In pancreatic cells, the subcellular localisation and the association of CAP1 with cofilin and actin has been reported to be regulated by a phosphorylation-dependent cycle mediated by GSK3. Inhibition of GSK by CHIR99021 prevents CAP1 enrichment at the cell cortex (Zhou *et al.*, 2014). Thrombin has also been reported to phosphorylate and inhibit GSK3 activity (Moore *et al.*, 2013). To investigate if GSK3 activity affects CAP1 localisation in platelets, the number of platelets displaying a majority of either cortical or cytosolic CAP1 were counted after treatment with the GSK3 inhibitor CHIR99021, or CHIR99021 + thrombin. No difference was observed in the CAP1 localisation before and after CHIR99021 treatment, suggesting that translocation of CAP1 is not caused by GSK inhibition. However, no differences were found between CHIR99021 and CHIR99021 + thrombin treatments, suggesting that CHIR99021 did appear to stop the relocalisation of CAP1 from cortical to cytosol states (**Figure 5.2.8A** & **B**). This may indicate that GSK3 activity has little effect on CAP1 localisation in platelets but is required for relocalisation upon thrombin stimulation.

A time course was performed to ensure that any potential effects of CHIR99023 on CAP1 localisation were not missed. Platelets were spread on fibrinogen for 45 minutes at 37°C then treated with 2 µM of CSK3 inhibitor CHIR99023 for 1-10 minutes before being fixed by PFA. The number of cells displaying cortical or diffuse CAP1 were counted with the majority of cells (~70%) displaying cortical CAP1. No difference was found in CAP1 localisation over the time course with the GSK inhibitor (**Figure 5.2.C** & **D**). This demonstrates that GSK3 activity may be not essential for CAP1 localisation on platelets spread on a weak agonist - fibrinogen.
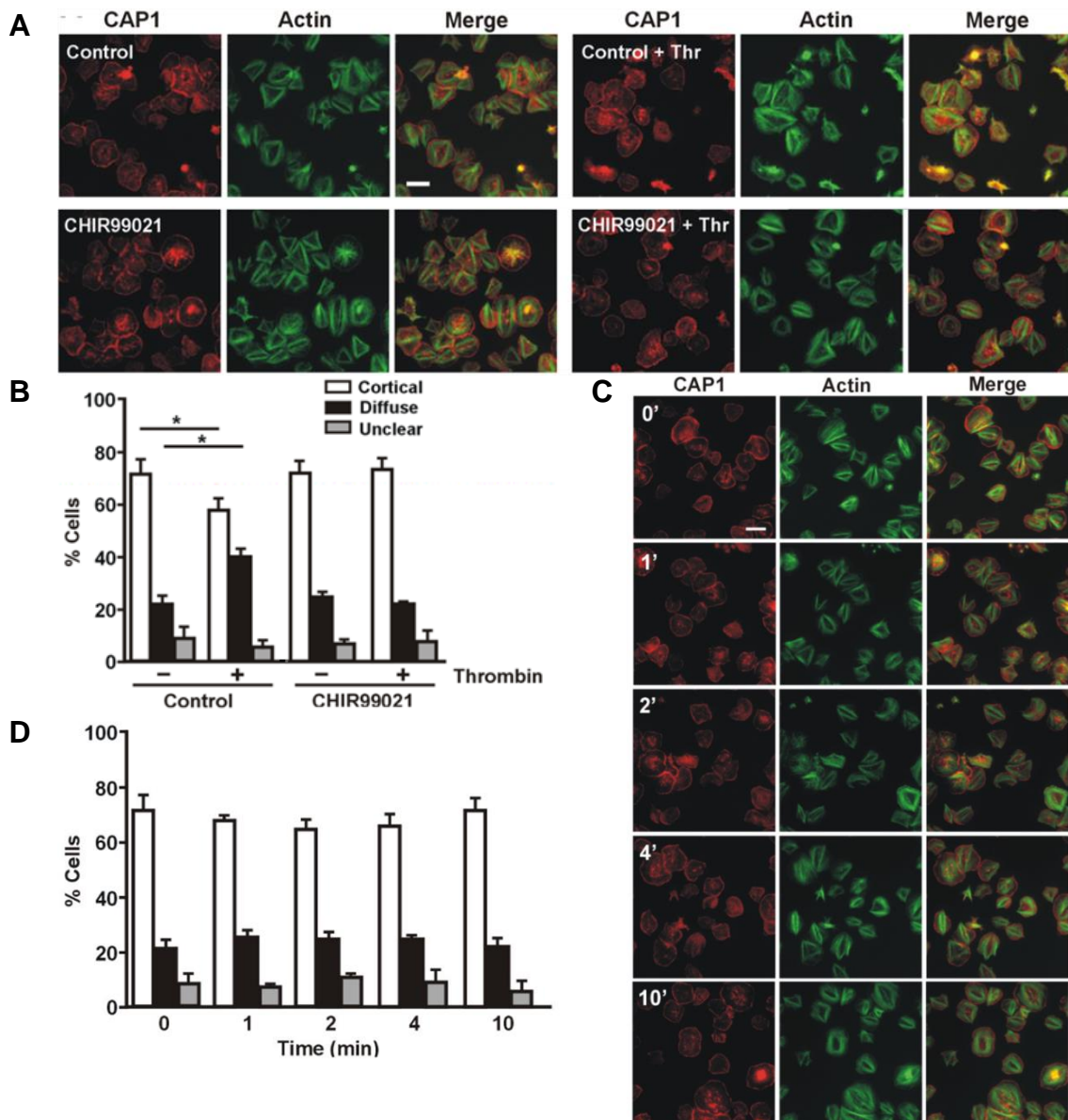
Figure 5.2.8 - Thrombin-induced CAP1 relocalisation is inhibited CHIR99023
Platelets were spread on fibrinogen-coated coverslips then treated with 2 μM CHIR99021 for 10 minutes (**A**) or the indicated times (**C**) minutes prior to stimulation with 0.1 U/ml thrombin for 30 seconds at 37°C. Platelets were fixed with PFA and stained for the indicated proteins. Images were acquired with a fluorescence microscope with a structured illumination attachment. Scale bar = 5 μm. (**B** & **D**) Quantification of CAP1 distribution before (−) and after (+) thrombin stimulation. The proportions of cells with predominantly cortical or diffuse CAP1 distribution in images were calculated from 2-5 independent experiments performed on duplicate coverslips. More than 1000 cells per condition in each experiment were scored. The experiment was performed simultaneously to that of 5.2.7 and therefore share the control Unclear refers to cells that were not sufficiently enough spread to classify. Data is mean ± SEM. *p ⩽ 0.05 relative to the respective population not stimulated with thrombin. (Mann-Whitney test).

201

5.3 Discussion

This study is the first to verify CAP1 to be abundant in human platelets by Western blot (**Figure 5.2.1A**). With an estimated 41,700 copies per platelet, it is the 85th most abundant protein out of over 4000 proteins in platelets (Burkhart *et al.*, 2012). The presence of both CAP1 (Burkhart *et al.*, 2012) and CAP2 proteins (Zeiler *et al.*, 2014) has been reported in murine platelets, whereas CAP2 protein (Burkhart *et al.*, 2012) and mRNA (Rowley *et al.*, 2011) is absent from human platelets.

5.3.1 CAP1 is membrane and cytosol associated independently of actin

CAP1 has previously been reported to be in the membrane of platelets in proteomic studies (Lewandrowski *et al.*, 2009; Moebiust *et al.*, 2005). This supports the findings of this study which is the first to find CAP1 as predominantly a cytosolic protein with approximately 20-25% of it associated with the platelet membrane fraction. The amount of CAP1 in the membrane is unaffected by latrunculin treatment (**Figure 5.2.1B**), indicating its association to the membrane is not dependent on any association to F-actin.

CAP1 is known to sequester monomeric G-actin (Ono, 2013). This study as the first to find that, as expected, CAP1 was not found in the LS detergent insoluble fraction (**Figure 5.2.1**) where cross-linked F-actin filaments would pellet, suggesting CAP1 does not bind to those large cross-linked F-actin filaments.

CAP1 has been previously reported to associate with membrane lipid rafts from mouse brains (Noegel *et al.*, 1999). This may explain why CAP1 was found in the HS insoluble fraction where smaller F-actin filaments and detergent insoluble membrane-containing structures pellet, as confirmed by the presence of CD36. Most of the CAP1 was found as expected in the supernatant where G-actin and very smaller F-actin filaments are found. This occurred both with and without latrunculin treatment (**Figure 5.2.2**), suggesting the association of CAP1 to these fractions is not F-actin dependent.

202

In previous reports utilising the Triton X-100 insoluble fractionation, the levels of actin in the LS fraction was significantly higher than the basal at 30 seconds and remained so until 3 minutes (**Section 3.2.5**) (Riley *et al.*, 2019). However, in this instance the LS and HS fractions demonstrated maximal actin levels at 30 seconds (~1.7x basal) and 60 second (~1.2x basal), respectively. The HS insoluble fraction actin did not reach statistical significance, whereas the LS insoluble fraction reached significance at 30s and 180s but not at 60 and 120s (**Figure 5.2.6A**).This may be a limitation of the power of the experiment, the standard error and the statistics used. It is reasonable to suggest the increase in actin in the LS insoluble fraction may persist through the remainder of the time course after 30 seconds.

5.3.2 Subcellular localisation of CAP1

CAP1 is known to contribute to actin turnover by interacting with proteins including Ras-responsive adenylyl cyclase and cofilin (Moriyama & Yahara, 2002). This explains why, despite not being associated with F-actin in the detergent insoluble LS pellet, CAP1 does colocalise with F-actin at the cell cortex on unstimulated cells centrifuged onto poly-L-lysine (**Figure 5.2.3A**). This colocalisation is even more obvious on platelets spread on fibrinogen where CAP1 is observed not only at the cortex but also at the filopods and actin nodules with actin nodules markers (**Figure 5.2.B-E** & **Figure 5.2.3**). Actin nodules have been described as podosome-like structures with a core of densely phosphorylated proteins, devoid of integrins and rich in proteins including talin and vinculin (Poulter *et al.*, 2015), although the latter is redundant for platelet function (Mitsios *et al.*, 2010). The role of CAP1 in these structures is likely related to actin turnover. Interestingly, in HeLa cells, CAP1 co-IPs with both focal adhesion kinase (FAK) and talin and appears to interact directly with talin (Zhang *et al.*, 2013). Accumulations of CAP1 at actin structures in platelets may be recruited by an interaction with either talin, G-actin or cofilin. CAP1 may contribute to the actin turnover of these highly dynamic structures through its actin filament depolymerising and monomer regeneration activities.

203

CAP appears to be extremely evolutionarily conserved, with similar subcellular colocalisation patterns found between CAP1 and actin in a variety of species as diverse as yeast (Ono, 2013) and poppies (Poulter *et al.*, 2010). Yeast CAP enhances recharging actin monomers with ATP antagonistically to ADF/cofilin and promotes actin filaments severing by ADF/cofilin (Ono, 2013). CAP1 localises to actin patches in yeast (Lila & Drubin, 1997) and to the leading edge of cultured mammalian cells (Bertling *et al.*, 2004; Moriyama & Yahara, 2002). The pollen tube actin foci in *Papaver rhoeas* are an equivalent to actin nodules as they are areas of dense F-actin staining. CAP also colocalises with F-actin in these structures during the self-incompatibility response (Poulter *et al.*, 2010). This indicates a potentially important and conserved role of CAP in actin structures.

Colocalisation of CAP1 and F-actin has been reported in various mammalian cells with various F-actin structures. For example in mouse C3H-2K fibroblasts CAP, actin and cofilin colocalise together at lamellipodia (Moriyama & Yahara, 2002); and in murine B16F1 melanoma cells CAP1 displays strong localisation with monomeric actin in both the cytoplasm and the cortex (Makkonen *et al.*, 2013).

Despite being found at both actin nodules and the cell cortex, CAP1 was only extremely rarely found at stress fibres (**Figure 5.2.**), which supports its function as a protein which binds to monomeric actin, profilin and cofilin, but not F-actin. The very few instances in which CAP1 was found to be present in stress fibres was probably due to transient binding with cofilin, profilin or talin.

In platelets, cofilin has been found to localise at the cortex (Hervé Falet *et al.*, 2005). As CAP1 is known to bind to cofilin in mammalian cells (Moriyama & Yahara, 2002) and also localises at the cortex (**Figure 5.2.3**, **Figure 5.2.4**, **Figure 5.2.7** & **Figure 5.2.8**), future studies should examine colocalisation of CAP1 with cofilin and profilin and confirm interactions in platelets by techniques such as SPR or proximity ligation assay (PLA).

5.3.3 CAP1 relocalises away from the cortex upon thrombin stimulation

This study was the first to discover that a significant proportion of platelets demonstrate translocation of CAP1 from the membrane or cortex to the cytosol in response to the agonist thrombin in both Triton insoluble fractionation (**Figure 5.2.5A**) and immunostaining experiments (**Figure 5.2.7**). This was also found by subcellular fractionation experiments utilising the agonist collagen (**Figure 5.2.5B**). This shows the translocation may involve a common signalling step downstream of the respective receptors for thrombin and collagen. The pellet fraction in subcellular fractionation contains the membrane and probably also the insoluble lipid raft membrane components (**Figure 5.2.2**). The colocalisation stainings could show either the cortex or the membrane or both as normal light microscopy would not usually have the power to distinguish between them in platelets. PGI_2 and GSNO prevented the thrombin-induced translocation of CAP1 away from the cortex (**Figure 5.2.7A**) although this could be due to an overall effect on the cell shape from inhibition of platelet activation, rather than a specific effect on CAP1 as treated platelets were not fully spread, displayed some actin nodules and often did not have a clear cortex.

In murine embryonic fibroblasts, phosphorylation of serines S307 and S309 of CAP1 regulate cofilin binding, actin binding and therefore actin turnover. CAP1 S307A/S309A non-phosphorylatable mutants display drastically increased binding of CAP1 to cofilin and reduced binding to actin. The phosphomimetic mutant S307D/S309D loses CAP1 ability to bind cofilin but displays greater actin binding. Both mutants demonstrate F-actin accumulation at stress fibres. GSK3 has been found to phosphorylate CAP1 S309, however phosphorylation of S307 appears to required for functional change (Zhou *et al.*, 2014).

To investigate if the phosphorylation state of CAP1 effects its translocation, platelets were spread and treated with the GSK3 inhibitor CHIR99021 to prevent S309 phosphorylation. This was not sufficient to induce CAP1 translocation (**Figure 5.2.8C** & **D**). There are several explanations including actin turnover, platelet activation and protein phosphorylation. The lack of translocation may be because

both S307 and S309 phosphorylation are required for functional change (Zhou *et al.*, 2014) and so CAP1 phosphorylation specific antibodies would be required to investigate this further. It has been hypothesised that both S307 and S309 may be phosphorylated by several proteins, further complicating the interaction (Zhou *et al.*, 2014). The translocation may be from other pathways common to platelet activation, as thrombin also affects several receptors and induces platelet activation (van der Meijden & Heemskerk, 2019), whereas as CHIR99021 is believed to be specific, although a proteomic study upon CHIR99021 treatment has not been undertaken. As inhibition of GSK3 is not sufficient for CAP1 translocation, other pathways are likely required for CAP1 translocation and CAP1 cortical enrichment is not seen S307A and S3909A non-phosphorylable mutants (Zhou *et al.*, 2014). Analysis of the phosphorylation state of CAP1 with phosphorylation specific antibodies in platelets before and after either inhibition of GSK3 with CHIR99023, or stimulation with thrombin should provide some clarification.

The lack of translocation of CAP1 upon CHIR99021 treatment may indicate that GSK3 activity has little effect on CAP1 localisation. However, CHIR99021 did prevent thrombin-induced translocation of CAP1 (**Figure 5.2.8A** & **B**). Thrombin reduces activity of GSK3 in platelets (Moore *et al.*, 2013) and therefore similar effects on CAP1 translocation with CHIR99021 and thrombin treatments may be predicted. However, there are several explanations including platelet activation and protein phosphorylation as mentioned above or actin turnover. Lack of S309 phosphorylation may push actin turnover into a different state, with increases in CAP1-cofilin binding and actin severing activity juxtapositioned with retained ADP-ATP nucleotide exchange capability. It would be worth investigating if CHIR99021 inhibits collagen induced CAP1 translocation to determine if this is thrombin specific or activation specific.

It is worth noting that very recently, it has been found that cell division kinase 5 (CDK5) phosphorylates S307 and S309 to regulate its cofilin and actin binding. It has also been discovered that cAMP signalling induces dephosphorylation of CAP1, through PKA and exchange proteins directly activated by cAMP (Epac) (Zhang *et al.*, 2020). CDK5 is present in platelets (Burkhart *et al.*, 2012) and this is a signalling

pathway which should be further investigated with regards to CAP1 function and phosphorylation.

An increasing body of literature is investigating the interaction of resistin and CAP1 (Avtanski *et al.*, 2019; Jang *et al.*, 2020). Platelets were treated with resistin which also caused translocation of CAP1 to the cytosol, from the membrane (**Figure 5.2.5B**) demonstrating the translocation is not unique to thrombin or collagen. As explained above, several possibilities for the effects of resistin on CAP1 can be ruled out. This could further be investigated by assessing the binding of CAP1 to putative binding partners, exploring the phosphorylation status of CAP1 upon stimulation and GSK3 inhibition.

During apoptosis, CAP1 has been reported to rapidly translocate to the mitochondria independently of caspase activation (C. Wang *et al.*, 2008). Attempts were made to stain for CAP1 in spread platelets undergoing apoptosis but this was not pursued due to unsatisfactory apoptosis controls (**Appendix 8.1.4)** and staining.

In human monocytes, resistin has been reported to bind to CAP1 and upregulate protein kinase A (PKA) activity, cyclic AMP (cAMP) concentration, and NF-κB-related transcription of inflammatory cytokines. As CAP1 does not contain a transmembrane domain, it is likely that rather than directly binding resistin, it binds to a receptor that is associated with resistin(Lee *et al.*, 2014). PKA and cAMP levels are important for platelet inhibition (Broos *et al.*, 2011) and the relationship of them to CAP1 in platelets has not yet been investigated. The receptors for resistin have been proposed to be CAP1 (Lee *et al.*, 2014) and Toll-like receptor 4 (Zhang *et al.*, 2019). Platelet specific TLR4$^{-/-}$ mice are characterised by significant protection from hypoxia-induced pulmonary hypertension and decreased platelet activation in response to lipopolysaccharide but not to collagen (Bauer *et al.*, 2014). Unfortunately this study was released (Bauer *et al.*, 2014) before TLR4 was found to act as a resistin receptor (Zhang *et al.*, 2019) so this parameter was not analysed Binding studies would reveal more information relating to the receptors CAP1 could bind to

Resistin has been reported to cause increased LDL production in the liver and also increased LDL-uptake by macrophages, leading to foam cell formation.

207

Resistin-mediated chronic inflammation can lead to atherosclerosis, obesity and coronary artery disease and is associated with increased CAP1 (Munjas *et al.*, 2017). Increased CAP1 levels are associated with rheumatoid arthritis (Sato *et al.*, 2017). CAP1 has recently been reported as a binding partner of proprotein convertase subtilisin/kexin type-9 (PCSK9) and is required for the degradation of LDL receptors by PCSK9 (Jang *et al.*, 2020).

AC3, 5 and 6 are present in platelets at very low levels with only unquantifiable traces of AC3 and AC5 detected in the membrane and only an estimated ~2,500 copies per platelet of AC 6 (Burkhart *et al.*, 2012). It has been reported that CAP1 co-IPs with AC1, 3, 4 and 7 in pancreatic cancer cells. Upon stimulation with forskolin, which increases cAMP levels through AC activation, CAP1 forms a complex with AC3 and G-actin which enhances cAMP levels, inhibits cell motility, inhibits filopodia formation and inhibits cell invasion (Quinn *et al.*, 2017). Attempts were made to blot for AC6 in platelet lysates but this was not continued due to poor antibody performance, low protein levels and time constraints. Blots for the less abundant AC 3 and 5 were not attempted. Attempts were also made to investigate CAP1 translocation and platelet morphology upon forskolin treatment, but these attempts also were not continued due to time constraints. It could reasonably be hypothesised that a fraction of CAP1 may be associated to ACs at the platelet membrane, contributing to their inhibitory effects. Stimulation with agonists like thrombin and collagen would disrupt that interaction, shifting the balance towards platelet activation. Future studies could investigate the interaction between CAP1 and AC3, AC5 and AC6 in platelets.

5.3.4 CAP2 and potential functional redundancy

CAP2 is much less studied than CAP1 although both are known to bind actin and contribute to F-actin disassembly (Peche *et al.*, 2013). CAP1 demonstrates a relatively broad expression pattern whereas CAP2 is predominantly limited to areas including the brain, heart, skeletal muscle, skin and WBCs. Although only 62% identity and 76% similarity is found between with murine CAP1 and CAP2, both

CAPs bind actin and contribute to disassembly of F-actin (Peche *et al.*, 2007). In mice CAP2 ablation leads to cardiomyopathy and disarrayed sarcomeres with development of fibrosis (Peche *et al.*, 2013).

Both CAP1 and CAP2 present in murine platelets (Zeiler *et al.*, 2014), whereas only CAP1 is present in human platelets (Burkhart *et al.*, 2012) with no detectable CAP2 protein (Burkhart *et al.*, 2012) or mRNA (Rowley *et al.*, 2011). Therefore CAP1 may compensate for CAP2 ablation in murine platelets in a manner which may not occur in human platelets if CAP1 was conditionally knocked out.

Approximately on third of gene KOs are embryonically lethal (Mohun *et al.*, 2013). Constitutive KO of CAP1 is embryonically lethal (Jang *et al.*, 2020), possibly due to decreased vascularisation and reduced cell maturation in the placenta (Hummler et al., 2013a). A *Cap1*$^{-/-}$ would have to be platelet specific to be viable or at least to avoid any off-target effects. As humans express only CAP1 in platelets (Burkhart *et al.*, 2012), whereas mice have both *Cap1* and *Cap2* expressed (Zeiler *et al.*, 2014), platelets from a species with only CAP1 present would be preferable to murine platelets for functional studies.

In mice, platelets with gene trapped CAP2 have been reported to be larger, display increased agonist-induced activation of αIIbβIII, increased P-selectin recruitment and display no spreading defects on fibrinogen. That study concluded that CAP1 may at least partially compensate for the lack of CAP2 in murine platelets These studies appeared to have some CAP2 still remaining in blots which may or may not have been inactive and the results were derived from only a few experimental repeats (Heck, 2019). A platelet specific double KO would also yield valuable information about the functional roles of CAP1 and 2 in platelets.

5.3.5 Summary

In summary, CAP1 is an abundant cytoskeleton regulator in platelets. It may play roles in the platelet membrane and lipid rafts and likely is involved in actin turnover with cofilin and G-actin at the cell cortex and actin nodules during platelet spreading. In the majority of platelets, CAP1 translocates from the membrane and cortex, to the

cytosol in response to thrombin, collagen and resistin, placing it at a crossroad of the signalling pathways that control platelet activation. Further analysis of these roles in platelets could involve the utilisation of a platelet-specific CAP1 KO model. Although as both proteins are present in murine but only CAP1 Is present in human platelets, it is possible that $Cap1^{-/-}$ platelets may not reflect the absence of CAP1 in human platelets. Therefore a species more closely reflecting the expression pattern of CAP1 and 2 in platelets may be more relevant.

6 Chapter 6 – General discussion

Heart disease is a major cause of death with abnormal platelet levels (Fawzy *et al.*, 2019), size or activity identified as major risk factors (Ranjith *et al.*, 2016). Studies of the function and interactions of proteins in platelets increase our understanding of how platelets function. Until recently there had been a limited number of studies of coronin in platelets. Most of the previous research on coronin in human platelets has been proteomic studies which detected altered coronin levels after various treatments. For example, higher coronin 3 levels were detected in platelets very soon after apheresis (Thiele *et al.*, 2016), higher coronin 2 levels upon salvianolic acid B treatment (Ma *et al.*, 2011) and lower coronin 2 levels in patients with coronary artery disease (Banfi *et al.*, 2010).

For the first time, this found that coronin 1, 2 and 3 localise to actin nodules and the actin-rich cell cortex. Coronin 1 was dispensable for most platelet functions. A novel finding was that coronin 1 was required for integrin β2 translocation. CAP1 also colocalised with actin nodules and this study was the first to find it to translocate away from the cortex/membrane upon stimulation.

6.1 Coronin and CAP in the platelet cytoskeleton

The current project found that coronin 1 colocalises with F-actin structures such as actin nodules and at the actin-rich cortex in platelets. Colocalisation of coronin with actin rich structures such as the cortex, leading edge or lamellipodia have been reported in various cell types (Föger *et al.*, 2011; Yan *et al.*, 2007; Shiow *et al.*, 2008; Gatfield *et al.*, 2005). Coronins 1, 2 and 3 are also associated with the Arp2/3 complex which is involved in actin turnover (Xavier *et al.*, 2012). This would suggest that coronin 1 plays a role in regulating the actin cytoskeleton in platelets. However, *Coro1A*^{-/-} platelets have been reported to have normal F/G-actin levels in unstimulated conditions (Stocker *et al.*, 2018). The present study found that coronin 1 is dispensable for some processes which are dependent upon rearrangement of the cytoskeleton including spreading (see **Section 4.2.9**) and aggregation (see

211

Section 4.2.7). It appears that coronin 1-mediated regulation of the actin cytoskeleton in platelets is instead compensated for by other proteins of the coronin family.

This is not surprising as coronin 1 has also been found from KO, knock down or disruption studies to be dispensable for actin cytoskeleton dynamics in several cells including murine neutrophils (Combaluzier & Pieters, 2009), macrophages (Jayachandran *et al.*, 2007), B cells, NK cells (Shiow *et al.*, 2009), dendritic cells (Westritschnig *et al.*, 2013), fibroblasts (Shiow *et al.*, 2008, supplementary material) and dendritic cells (Westritschnig *et al.*, 2013). In contrast, the relatively limited number of studies on other class 1 coronins found involvement in cytoskeletal dynamics. For example, in murine fibroblasts, knockdown of coronin 2 results in lamellipodia and motility defects (Cai *et al.*, 2008). Also, in murine fibroblasts, coronin 3 knock out results in actin cytoskeletal defects, and severe vimentin network and microtubule cytoskeleton defects (see **Section 1.3.8.6**) despite coronin localising more strongly with actin than with vimentin or tubulin (**Figure 1.16**). Although the platelets of *Coro1C*$^{-/-}$ mice have not been studied in detail, no obvious bleeding defects have been reported (Behrens *et al.*, 2016). It is possible therefore, that coronin 3 may be the predominant coronin contributing to regulation of platelet cytoskeleton dynamics. Coronin 1 KO murine mast cells exhibit defects in lysosome and cytokine secretion with the additional ablation of coronin 2 contributing to the phenotype which was not in a single coronin 2 KO (Föger *et al.*, 2011). This demonstrates that coronins must compensate for each other at least in some cell types

As coronin 1 colocalises with coronins 2 and 3 in platelets it is very likely they are the proteins compensating for coronin 1. Or, instead it may also be the case that the requirement for coronin-mediated regulation of the actin cytoskeleton is dispensable for platelets. Single KOs of coronin 2 and 3, along with double and triple KOs would be needed to further investigate the contribution of coronins in regulating the platelet cytoskeleton. A triple KO may be embryonically lethal therefore a platelet specific approach under the influence of the platelet-factor 4 (PF4) promoter may be required.

The ability of class 1 coronins to interact with Arp2/3 to regulate the actin turnover is mediated by phosphorylation. For example, coronin 1 and 2 can be phosphorylated at Ser2 by PKC which regulates their subcellular localisation and inhibits their interaction with Arp2/3. Coronin 3 is phosphorylated by CK2 at Ser463 on the coiled-coil C-terminal. This results in coronin 3 losing its ability to inhibit actin polymerisation, bundle actin filaments and bind to Arp2/3 (Xavier *et al.*, 2012).

This study found CAP1 also colocalised with actin nodules. CAP1 has also been reported to localised to areas of rich F-actin staining in a very diverse range of cells including the 'actin foci' in pollen tubes undergoing self-incompatibility (Poulter *et al.*, 2010), at lamellipodia and stress fibres in murine fibroblasts (Freeman & Field, 2000) and at 'actin patches' at the cortex in yeast (Freeman *et al.*, 1996). This is in accordance with the role of CAP1 as a regulator of the actin cytoskeleton. CAP1 binds to cofilin, ADF, profilin and actin to contribute to actin cytoskeleton dynamics (see **Section 1.4**) (Ono, 2013) and is likely performing this role in platelets.

Like coronins, CAP1 Is regulated by phosphorylation and It has been hypothesised there are likely multiple proteins which phosphorylate CAP1 (Zhou *et al.*, 2014). CDK5 phosphorylates CAP1 at both S307 and S309 to regulate its cofilin and actin binding (Zhang *et al.*, 2020); CDK5 is present in platelets (Burkhart *et al.*, 2012). CAP1 is also phosphorylated by GSK3, although only at S309, but S307 is additionally required for functional change (Zhou *et al.*, 2014). The complete repertoire of proteins that regulate CAP1 activity is still to be determined. Coronin is phosphorylated by CDK5 also, but this appears to affect its ability to regulate PKA/cAMP through Gαs rather than affecting its ability to contribute to actin dynamics directly (Liu *et al.*, 2016). Interestingly, both coronin (Gandhi & Goode, 2008) and CAP1 proteins bind to cofilin to regulate actin dynamics (Ono, 2013). Their individual interactions with cofilin may even affect the pool of available cofilin in different subcellular locations.

Phosphorylation may have implications for actin-related functions performed by coronin and CAP1 in platelets. Unfortunately, phospho-specific antibodies for both proteins were not available to investigate their activation status in the current project. However this is an important avenue for future investigation.

213

6.2 Coronin 1 and CAP in platelet signalling

Coronin 1 was found to be dispensable for the majority of platelet functions including spreading, aggregation, platelet size, secretion, integrin activation, PGI_2-induced cAMP levels, basal receptor levels and most receptor translocation. Although it is worth noting that in the vast majority of experiments the $Coro1A^{-/-}$ platelets displayed marginally higher values in those parameters, however, the only statistically significant difference was that in $Coro1A^{-/-}$ platelets, thrombin-induced translocation of integrin β2 to the membrane was defective. Integrin β2 KO murine platelets demonstrate reduced lifespan (Piguet *et al.*, 2001), however the lifespan of $Coro1A^{-/-}$ platelets has been reported to be normal (Stocker *et al.*, 2018), indicating that *Coro1A* ablation is not sufficient to affect platelet lifespan.

Platelet-neutrophil complexes are required for the recruitment of neutrophils to inflamed tissue. Coronin 1 may be involved in the binding of LFA1 on platelets to ICAM1 on WBCs. However, as detailed in **Section 1.1.3.2,** there are several proteins responsible for the majority of platelet-WBC interactions including P-selectin, CD11b/CD18, E-selectin, ICAM-1, ICAM-2 and PSGL-1 (Page & Pitchford, 2013). Therefore the effect of LFA-1 on the interactions is likely minimal. Furthermore, the amount of neutrophils in thrombi from $Coro1A^{-/-}$ mice has been reported to not be significantly different from the WT (Stocker *et al.*, 2018). Therefore it is unlikely that the effect of coronin 1 on integrin β2 has a significant impact on platelet-WBC interactions. Coronin 1 is the only coronin reported to interact with integrin β2 (Pick *et al.*, 2017). While coronin 2 and 3 could potentially be involved in aspects of platelet function, it is likely that the interaction with integrin β2 is unique to coronin 1. As integrin β2 is involved in platelet-WBC interacitons (see Section 1.1.3.2), investigating if coronin is indirectly involved in 'priming' white blood cells is an avenue for future investigation.

It has also been discovered that cAMP signalling induces dephosphorylation of CAP1, through PKA and exchange protein directly activated by cAMP (Epac) (Zhang *et al.*, 2020). Coronin 1 is also involved in cAMP signalling. It can modulate

cAMP and PKA signalling through Gαs (Jayachandran *et al.*, 2014). This requires phosphorylation of coronin by CDK5 (Liu *et al.*, 2016). This suggests potential roles for coronin and CAP 1 in the platelet inhibitory pathway should be further investigated.

In *Dictyostelium discoideum*, coronin has been reported to inhibit Rac1 (Swaminathan *et al.*, 2013) which is an important regulator of platelet spreading (McCarty *et al.*, 2005), however the GTP-Rac1:Rac1 ratio in *Coro1A*$^{-/-}$ platelets have been reported to be normal (Stocker *et al.*, 2018). The ability of coronin to interact with Rac1 may not extend to mammalian coronin 1 or there is compensation from other class 1 coronins.

It is also worth noting that coronin 3 has been predicted to be a substrate of the tyrosine protein kinase FYN (Amano *et al.*, 2015) which is involved in platelet agonist signalling through the GPVI (Gibbins, 2004) and CLEC-2 (Boulaftali *et al.*, 2014) receptors. This is another avenue of future investigation of the role of other coronin in platelet activation through GPVI or CLEC-2.

This study demonstrated that a significant proportion of platelets undergo translocation of CAP1 from the membranes/cortex in response to thrombin, collagen or resistin. This translocation induced by thrombin can be prevented by PGI$_2$, GSNO and CHIR99021. The translocation of CAP1 was not only induced by thrombin or collagen but also by resistin which demonstrated that the translocation may not be due to general platelet activation. The translocation of CAP1 was inhibited not only by the inhibitors PGI$_2$ and the NO donor GSNO, but also by the GSK3 inhibitor CHIR99021. This demonstrates the inhibition of translocation may not be simply due to platelet inhibition. Furthermore, thrombin is also an inhibitor of GSK3 which further complicates the interactions.

It is possible that phosphorylation of CAP1 may be involved in its translocation. In murine embryonic fibroblasts, phosphorylation of both S307 and S309 of CAP1 is required for it to regulate cofilin binding, actin binding and therefore actin turnover. However, GSK3 only phosphorylates CAP1 S309, but S307 is additionally required for functional change. It has also been hypothesised there are likely multiple proteins which phosphorylate CAP1 (Zhou *et al.*, 2014). CDK5

phosphorylates both Ser307 and 309 (H. Zhang *et al.*, 2020) and may contribute to the ability of CAP1 to translocate.

The prevention of translocation of CAP1 in response PGI$_2$ and NO could be due to a different pathway than in response to CHIR99021. This is because upon PGI$_2$ and NO treatment platelets are less spread and have a less clear cortex and less cortical actin which may affect CAP1 localisation. Likewise the translocation of CAP1 in response to thrombin and collagen could be due to the platelet shape and actin distribution which demonstrates a round shape with more cortical actin upon platelet activation.

The reason for CHIR99021 inhibiting CAP1 translocation is unclear. CHIR99021 is believed to be a specific GSK3 inhibitor, thereby preventing CAP1 S307 phosphorylation, but S309 is additionally required to alter CAP1 function (Zhou *et al.*, 2014). CHIR99021 treatment may have other affects besides GSK3 in including modulation of the TGFβ, Notch and MAPK signalling pathways (Wu *et al.*, 2013). Analysis of whether CHIR99021 functions as a general weak platelet inhibitor may provide clarification.

Thrombin is an inhibitor of GSK3 and induces CAP1 translocation, but inhibition of GSK3 by CHIR99021 is not sufficient for CAP1 translocation. This indicates other pathways are likely required for CAP1 translocation rather than through GSK3 inhibition. The effects of agonists and inhibitors on CAP1 translocation and platelet activation, as well as the steps which are unknown are summarised in **Figure 6.1**. Analysis of the phosphorylation state of CAP1 with phosphorylation specific antibodies in platelets before and after either inhibition of GSK3 with CHIR99023, or stimulation with thrombin or collagen should yield insights into the process of translocation.

216
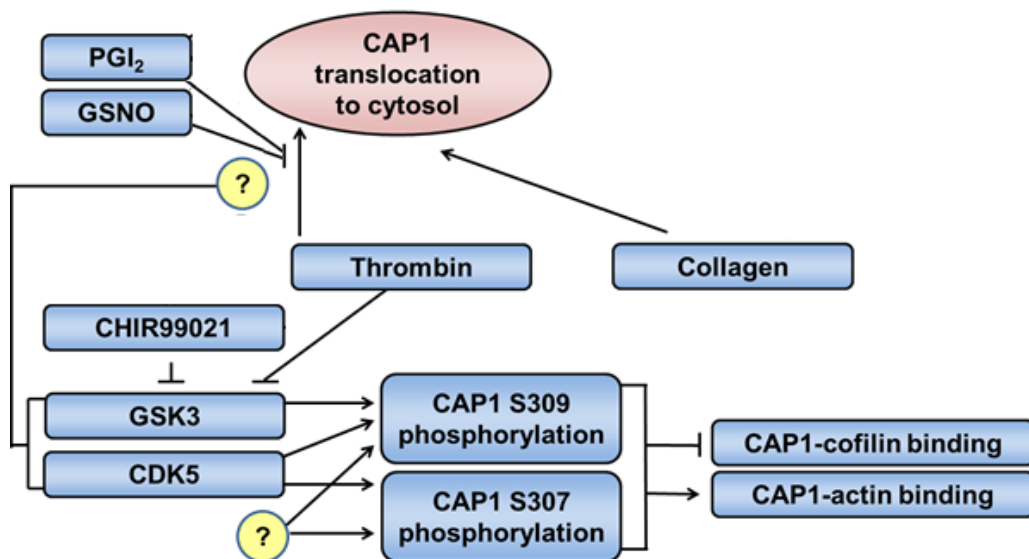
Figure 6.1 – Proposed model of CAP1 translocation
Thrombin and collagen bothlead to CAP1 translocation to the cytosol which can be inhibited by PGI_2 and GSNO. CAP1 is phosphorylated at S309 by GSK3 which can in turn be inhibited by treatment with CHIR99021, which can also prevent CAP1 translocation in response to thrombin. Unknown kinase(s) may phosphorylate S309. Phosphorylation of both S307 and S309 lead to inhibition of CAP1-cofilin binding and increases in CAP1-actin binding. Questions marks refer to unknown parts of the protein interactions.

The reason for the translocation or lack of translocation could also be due to actin turnover. Lack of S307 and S309 phosphorylation of CAP1 may push actin turnover into a different state, with increases in CAP1-cofilin binding and actin severing activity juxtaposed with retained ADP-ATP nucleotide exchange capability. It would be worth investigating if CHIR99021 inhibits collagen or resistin-induced CAP1 translocation to determine if this is agonist specific.

Another possibility for CAP1 translocation could be due to CAP1 association with the mitochondria. In HeLa cells and murine fibroblasts, CAP1 rapidly translocates to the outer mitochondria membrane during early apoptosis and provides a link between the actin cytoskeleton and the mitochondria (C. Wang *et al.*, 2008). Staining of the mitochondria was attempted but was difficult due to the small platelet and mitochondria size, but this is still an important avenue for future studies

It has been reported that the loss of CAP2 results in several cardiovascular and platelet defects (Heck, 2019) (see **Section 1.4.6**). CAP2 has only been

217

reported in murine platelets (Zeiler, *et al.* 2014) and not human platelets (Burkhart, *et al.* 2014). CAP1 KO studies should provide further valuable information about the contribution of CAP1 to the cardiovascular system and platelet function. Such a KO would have to be PF4-specific as CAP1 KO is embryonically lethal (Hummler et al., 2013b). A double knockout of both CAP genes in mice would also provide valuable information

Another possibility rather than using knockout animals may be to target the proteins using technology such as proteolysis-targeting chimera (PROTAC) (Khan, *et al.*, 2019). Platelets produced from megakaryocyte cell lines *in vitro* do not currently reflect platelets very accurately, but as this technology is refined, knocking out proteins with techniques including clustered regularly interspaced short palindromic repeats (CRISPR) and producing platelets in cell lines may be a possibility (Norbnop, *et al.*, 2020). Cardiovascular-related illnesses are a leading cause of deaths, particularly in Western countries with aberrant platelet activity contributing to this (Renga & Scavizzi, 2017). There are around 4,000 proteins present in platelets (Burkhart et al., 2012) and investigating their function in detail is important for understanding platelets and ultimately producing targeted therapies. This thesis characterised coronin 1, 2 3 and CAP1 in detail to contribute to the understanding of their role in platelet function.

7. References

Abella, J. V. G., Galloni, C., Pernier, J., Barry, D. J., Kjær, S., Carlier, M. F., & Way, M. (2016). Isoform diversity in the Arp2/3 complex determines actin filament dynamics. *Nature Cell Biology*. **18**. 76–86

Aburima, A., Walladbegi, K., Wake, J. D., & Naseem, K. M. (2017). cGMP signaling inhibits platelet shape change through regulation of the RhoA-Rho Kinase-MLC phosphatase signaling pathway. *Journal of Thrombosis and Haemostasis*. **15.** 1668–1678.

Amano, M., Hamaguchi, T., Shohag, M. H., Kozawa, K., Kato, K., Zhang, X., Yura, Y., Matsuura, Y., Kataoka, C., Nishioka, T., & Kaibuchi, K. (2015). Kinase-interacting substrate screening is a novel method to identify kinase substrates. *Journal of Cell Biology*. **209.** 895–912.

Appleton, B. A., Wu, P., & Wiesmann, C. (2006). The crystal structure of murine coronin-1: A regulator of actin cytoskeletal dynamics in lymphocytes. *Structure*. **14**. 87–96.

Arandjelovic, S., Wickramarachchi, D., Hemmers, S., Leming, S. S., Kono, D. H., & Mowen, K. a. (2010). Mast cell function is not altered by Coronin-1A deficiency. *Journal of Leukocyte Biology*. **88**. 737–745.

Aslan, J. E., Itakura, A., Gertz, Jacqueline, M., & McCarty, Owen, J. T. (2012). Platelets and Megakaryocytes. In *Platelet shape change and spreading. Platelets and megakaryocytes.* **3.** 91–100.

Aslan, J E, & McCarty, O. J. T. (2013). Rho GTPases in platelet function. *Journal of Thrombosis and Haemostasis*. **11**. 35–46.

Aslan, Joseph E. (2019). Platelet Rho GTPase regulation in physiology and disease. *Platelets*. **30.** 17–22.

Aslan, J. E, Baker, S. M., Loren, C. P., Haley, K. M., Itakura, A., Pang, J., Greenberg, D. L. Larry, D. L. Manser, E., Chernoff, J., & McCarty, O. J. T. (2013). The PAK system links Rho GTPase signaling to thrombin-mediated platelet activation. *American Journal of Physiology. Cell Physiology*. **305**. 519-28.

Asyee, G. M., Sturk, A., & Muszbek, L. (1987). Association of Vinculin to the Platelet Cytoskeleton during Thrombin-Induced Aggregation. *Experimental Cell Research*. **168**. 358–364.

Avtanski, D., Chen, K., & Poretsky, L. (2019). Resistin and adenylyl cyclase-associated protein 1 (CAP1) regulate the expression of genes related to insulin resistance in BNL CL.2 mouse liver cells. *Data in Brief*. **25**. 104112.

Balcer, H. I., Goodman, A. L., Rodal, A. A., Smith, E., Kugler, J., Heuser, J. E., & Goode, B. L. (2003). Coordinated Regulation of Actin Filament Turnover by a High-Molecular- Weight Srv2/CAP Complex, Cofilin, Profilin, and Aip1. *Current Biology*. **13**. 2159–2169.

Baldassare, J. J., Henderson, P. A., Burns, D., Loomis, C., & Fisher, G. J. (1992). Translocation of protein kinase C isozymes in thrombin-stimulated human platelets: Correlation with 1,2-diacylglycerol levels. *Journal of Biological Chemistry*. **267**. 15585–15590.

Banfi, C., Brioschi, M., Marenzi, G., De Metrio, M., Camera, M., Mussoni, L., & Tremoli, E. (2010). Proteome of platelets in patients with coronary artery disease. *Experimental Hematology*. **38**. 341–350.

Bauer, E. M., Chanthaphavong, R. S., Sodhi, C. P., Hackam, D. J., Billiar, T., & Bauer, P. M. (2014). Genetic Deletion of TLR4 on Platelets Attenuates Experimental Pulmonary Hypertension. *Circulation Research*. **114**. 1–6.

Bearer, E. L., Prakash, J. M., & Li, Z. (2002). Actin dynamics in platelets. *International Review of Cytology*. **217**. 137–182.

Becker, I. C., Scheller, I., Wackerbarth, L. M., Beck, S., Heib, T., Aurbach, K., Manukjan, G., Gross, C., Spindler, M., Nagy, Z., Witke, W., Lappalainen, P., Bender, M., Schulze, H., Pleines, I., & Nieswandt, B. (2020). Actin/microtubule crosstalk during platelet biogenesis in mice is critically regulated by Twinfilin1 and Cofilin1. *Blood Advances*. **4**. 2124–2134.

Behrens, J., Solga, R., Ziemann, A., Rastetter, R. H., Berwanger, C., Herrmann, H., Noegel, A. A., & Clemen, C. S. (2016). Coronin 1C-free primary mouse fibroblasts exhibit robust rearrangements in the orientation of actin filaments, microtubules and intermediate filaments. *European Journal of Cell Biology*. **95**.

220

1–13.

Bellenchi, G. C., Gurniak, C. B., Perlas, E., Middei, S., Ammassari-Teule, M., & Witke, W. (2007). N-cofilin is associated with neuronal migration disorders and cell cycle control in the cerebral cortex. *Genes and Development*. **95**. 2347–

Bender, M., Eckly, A., Hartwig, J. H., Elvers, M., Pleines, I., Gupta, S., Krohne, G., Jeanclos, E., Gohla, A., Gurniak, C., Gachet, C., Witke, W., & Nieswandt, B. (2010). ADF / n-cofilin – dependent actin turnover determines platelet formation and sizing. *Platelets and Thrombopoiesis*. **116**. 1767–1775.

Bender, M., Stritt, S., Nurden, P., Van Eeuwijk, J. M. M., Zieger, B., Kentouche, K., Schulze, H., Morbach, H., Stegner, D., Heinze, K., Dütting, S., Gupta, S., Witke, W., Falet, H., Fischer, A., Hartwig, J. H., & Nieswandt, B. (2014). Megakaryocyte-specific Profilin1-deficiency alters microtubule stability and causes a Wiskott-Aldrich syndrome-like platelet defect. *Nature Communications*, **5**. 4746.

Bennett, J. S. (2005). Structure and function of the platelet integrin αIIbβ3. *Journal of Clinical Investigation*. **115**. 3363–3369.

Berger, M., Riley, D. R. J., Lutz, J., Khalil, J . S., Aburima, A., Naseem, K. M. & RIvero, F. (2019). Alterations in platel*et al*pha-granule secretion and adhesion on collagen under flow in mice lacking the atypical Rho GTPase RhoBTB3. *Cells*. **8**. 149.

Berlanga, O., Tulasne, D., Bori, T., Snell, D. C., Miura, Y., Jung, S., Moroi, M., Frampton, J., & Watson, S. P. (2002). The Fc receptor γ-chain is necessary and sufficient to initiate signalling through glycoprotein VI in transfected cells by the snake C-type lectin, convulxin. *European Journal of Biochemistry*. **269**. 2951–2960.

Bernardi, B., Guidetti, G. F., Campus, F., Crittenden, J. R., Graybiel, A. M., Balduini, C., & Torti, M. (2006). The small GTPase Rap1b regulates the cross talk between platelet integrin α2β1 and integrin αIIbβ3. *Blood*. **107**. 2728–2735.

Bertling, E., Hotulainen, P., Mattila, P. K., Matilainen, T., Salminen, M., & Lappalainen, E. (2004). Cyclase-associated Protein 1 (CAP1) Promotes Cofilin-induced Actin Dynamics in Mammalian Nonmuscle Cells. *Molecular Biology of*

the Cell. **15**. 5318–5328.

Bertling, E., Quintero-Monzon, O., Mattila, P. K., Goode, B. L., & Lappalaines, P. (2007). Mechanism and biological role of profilin-Srv2/CAP interaction. *Journal of Cell Science.* **120**. 1225–1234.

Bhattacharya, K., Swaminathan, K., Peche, V. S., Clemen, C. S., Knyphausen, P., Lammers, M., Noegel, A. A., & Rastetter, R. H. (2016). Novel Coronin7 interactions with Cdc42 and N-WASP regulate actin organization and Golgi morphology. *Scientific Reports.* **6**. 25411.

Bluteau, D., Lordier, L., Di Stefano, A., Chang, Y., Raslova, H., Debili, N., & Vainchenker, W. (2009). Regulation of megakaryocyte maturation and platelet formation. *Journal of Thrombosis and Haemostasis.* **7**. 227–234.

Boulaftali, Y., Hess, P. R., Kahn, M. L., & Bergmeier, W. (2014). Platelet ITAM Signaling and Vascular Integrity. *Circulation Research.* **114**. 1174–1184.

Boyanova, D., Nilla, S., Birschmann, I., Dandekar, T., & Dittrich, M. (2011). PlateletWeb: a systems biological analysis of signaling networks in human platelets. *Blood,.* **119**. 22–35.

Broos, K., Feys, H. B., De Meyer, S. F., Vanhoorelbeke, K., & Deckmyn, H. (2011). Platelets at work in primary hemostasis. *Blood Reviews.* **25**. 155-167

Bruehl, R. E., Springer, T. A., & Bainton, D. F. (1996). Quantitation of L-selectin distribution on human leukocyte microvilli by immunogold labeling and electron microscopy. *Journal of Histochemistry and Cytochemistry.* **44**. 835–844.

Bryckaert, M., Rosa, J. P., Denis, C. V., & Lenting, P. J. (2015). Of von Willebrand factor and platelets. *Cellular and Molecular Life Sciences.* **72**. 307–326.

Burkhart, J. M., Gambaryan, S., Watson, S. P., Jurk, K., Walter, U., Sickmann, A., Heemskerk, J. W. M., & Zahedi, R. P. (2014). What can proteomics tell us about platelets? *Circulation Research.* **114**. 1204–1219.

Burkhart, J. M., Vaudel, M., Gambaryan, S., Radau, S., Walter, U., Martens, L., Sickmann, A., & Zahedi, P. (2012). The first comprehensive and quantitative analysis of human platelet protein composition allows the comparative analysis of structural and functional pathways. *E-Blood.* **120**. 73–82.

Butt, E., Abel, K., Krieger, M., Palm, D., Hoppe, V., Hoppe, J., & Walter, U. (1994).

cAMP- and cGMP-dependent protein kinase phosphorylation sites of the focal adhesion vasodilator-stimulated phosphoprotein (VASP) in vitro and in intact human platelets. *Journal of Biological Chemistry*. **269**. 14509–14517.

Butt, E., Immler, D., Meyer, H. E., Kotlyarov, A., Laaß, K., & Gaestel, M. (2001). Heat shock protein 27 is a substrate of cGMP-dependent protein kinase in intact human platelets. Phosphorylation-induced actin polymerization caused by HSP27 mutants. *Journal of Biological Chemistry*. **276.** 7108–7113.

Bye, A. P., Unsworth, A. J., & Gibbins, J. M. (2016). Platelet signaling: A complex interplay between inhibitory and activatory networks. *Journal of Thrombosis and Haemostasis*. **14**. 918–930.

Cai, L., Holoweckyj, N., Schaller, M. D., & Bear, J. E. (2005). Phosphorylation of coronin 1B by protein kinase C regulates interaction with Arp2/3 and cell motility. *Journal of Biological Chemistry*. **280**. 31913–31923.

Cai, L., Makhov, A. M., & Bear, J. E. (2007). F-actin binding is essential for coronin 1B function in vivo. *Journal of Cell Science*. **120**. 1779–1790.

Cai, L., Makhov, A. M., Schafer, D. A., & Bear, J. E. (2008). Coronin 1B antagonizes cortactin and remodels Arp2/3-containing actin branches in lamellipodia. *Cell*. **134**. 828–842.

Cai, L., Marshall, T. W., Uetrecht, A. C., Schafer, D. A., & Bear, J. E. (2007). Coronin 1B Coordinates Arp2/3 Complex and Cofilin Activities at the Leading Edge. *Cell*. **128**. 915–929

Castro-Castro, A., Ojeda, V., Barreira, M., Sauzeau, V., Navarro-Lérida, I., Muriel, O., Couceiro, J. R., Pimentel-Muíños, F. X., Del Pozo, M. A., & Bustelo, X. R. (2011). Coronin 1A promotes a cytoskeletal-based feedback loop that facilitates Rac1 translocation and activation. *The EMBO Journal*. **30**. 3913–3927..

Cerletti, C., de Gaetano, G., & Lorenzet, R. (2010). Platelet-leukocyte interactions: Multiple links between inflammation, blood coagulation and vascular risk. *Mediterranean Journal of Hematology and Infectious Diseases*. **2**.

Chan, K. T., Roadcap, D. W., Holoweckyj, N., & Bear, J. E. (2012). Coronin 1C harbours a second actin-binding site that confers co-operative binding to F-actin. *The Biochemical Journal*. **444**. 89–96.

Chaudhry, F., Breitsprecher, D., Little, K., Sharov, G., Sokolova, O., & Goode, B. L. (2013). Srv2/cyclase-associated protein forms hexameric shurikens that directly catalyze actin filament severing by cofilin. *Molecular Biology of the Cell*. **24**. 31–41.

Cheng, Y., Austin, S. C., Rocca, B., Koller, B. H., Coffman, T. M., Grosser, T., Lawson, J. A., & FitzGerald, G. A. (2002). Role of prostacyclin in the cardiovascular response to thromboxane A2. *Science*. **296**. 539–541.

Chrzanowska-Wodnicka, M., Smyth, S. S., Schoenwaelder, S. M., Fischer, T. H., & White, G. C. (2005). Rap1b is required for normal platelet function and hemostasis in mice. *Journal of Clinical Investigation*. **115**. 680–687.

Ciferri, S., Emiliani, C., Guglielmini, G., Orlacchio, A., Nenci, G. G., & Gresele, P. (2000). Platelets release their lysosomal content in vivo in humans upon activation. *Thrombosis and Haemostasis*. **83**. 157–164.

Clemen, C. S. (2013). The coronin family of proteins. *Journal of Chemical Information and Modeling* **53**.

Clemetson, K. J., & Clemetson, J. M. (2001). Platelet collagen receptors. *Thrombosis and Haemostasis*. **86**. 189–197

Cohen, S., Braiman, A., Shubinsky, G., & Isakov, N. (2011). Protein kinase C-theta in platelet activation. *FEBS Letters*. **585**. 3208–3215.

Combaluzier, B., & Pieters, J. (2009). Chemotaxis and phagocytosis in neutrophils is independent of coronin 1. The Journal of Immunology. **182**. 2745–2752.

Cook, A. L. M., & Haynes, J. M. (2007). Phosphorylation of the PKG substrate, vasodilator-stimulated phosphoprotein (VASP), in human cultured prostatic stromal cells. *Nitric Oxide*. **16**. 10–17.

Coughlin, S. R. (2000). Thrombin signalling and protease-activated receptors. *Nature*. **407**. 258–264.

Crittenden, J. R., Bergmeier, W., Zhang, Y., Piffath, C. L., Liang, Y., Wagner, D. D., Housman, D. E., & Graybiel, A. M. (2004). CalDAG-GEFI integrates signaling for platelet aggregation and thrombus formation. **10**. 1139.

Dang, I., Gorelik, R., Sousa-Blin, C., Derivery, E., Guérin, C., Linkner, J., Nemethova, M., Dumortier, J. G., Giger, F. A., Chipysheva, T. A., Ermilova, V.

D., Vacher, S., Campanacci, V., Herrada, I., Planson, A. G., Fetics, S., Henriot, V., David, V., Oguievetskaia, K., … Gautreau, A. (2013). Inhibitory signalling to the Arp2/3 complex steers cell migration. *Nature*. **503**. 281–284.

de Fougerolles, A. R., Stacker, S. A., Schwarting, R., & Springer, T. A. (1991). Characterization of ICAM-2 and evidence for a third counter-receptor for LFA1. *Journal of Experimental Medicine*. **174**. 253–267.

De Hostos, E. L. (1999). The coronin family of actin-associated proteins. *Trends in Cell Biology*. **9**. 345–350.

De Hostos, E. L., Bradtke, B., Lottspeich, F., Guggenheim, R., & Gerisch, G. (1991). Coronin, an actin binding protein of Dictyostelium discoideum localized to cell surface projections, has sequence similarities to G protein beta subunits. *The EMBO Journal*. **10**. 4097–4104.

De Hostos, E. L., Rehfueß, C., Bradtke, B., Waddell, D. R., Albrecht, R., Murphy, J., & Gerisch, G. (1993). Dictyostelium mutants lacking the cytoskeletal protein coronin are defective in cytokinesis and cell motility. *Journal of Cell Biology*. **120**. 163–173.

De Meyer, S. F., Deckmyn, H., & Vanhoo, K. (2009). von Willebrand factor to the rescue. *Blood, The Journal of the American Society of Hematology*. **113**. 5049–5057.

Diacovo, T. G., DeFougerolles, A. R., Bainton, D. F., & Springer, T. A. (1994). A functional integrin ligand on the surface of platelets: Intercellular adhesion molecule-2. *Journal of Clinical Investigation*. **94**. 1243–1251.

Eckert, C., Hammesfahr, B., & Kollmar, M. (2011). A holistic phylogeny of the coronin gene family reveals an ancient origin of the tandem-coronin, defines a new subfamily, and predicts protein function. *BMC Evolutionary Biology*. **11**. 268.

Edwards, M., Zwolak, A., Schafer, D. A., Sept, D., Dominguez, R., & Cooper, J. A. (2014). Capping protein regulators fine-tune actin assembly dynamics. *Nature Reviews Molecular Cell Biology*. **15**. 677–689.

Eliautou, S., Mangin, P. H., Walter, U., Gachet, C., Eliautou, S., Mangin, P. H., Walter, U., Gachet, C., & Normal, F. L. (2010). Normal filopodia extension in

VASP-deficient platelets upon activation by adhesive matrices or soluble agonists. *Thrombosis and haemostasis*. **102**. 792-794

Enjyoji, K., Sévigny, J., Lin, Y., Frenette, P. S., Christie, P. D., Am Esch, J. S., Imai, M., Edelberg, J. M., Rayburn, H., Lech, M., & Beeler, D. L. (1999). Targeted disruption of cd39/ATP diphosphohydrolase results in disordered hemostasis and thromboregulation. *Nature Medicine*. **5**. 1010–1017.

Escolar, G., & White, J., G. (1991). The platelet open canalicular system: a final common pathway. *Blood Cells*. **17**. 467–485.

Evangelista, V., Pamuklar, Z., Piccoli, A., Manarini, S., Dell'Elba, G., Pecce, R., Martelli, N., Federico, L., Rojas, M., Berton, G., Lowell, C. A., Totani, L., & Smyth, S. S. (2007). Src family kinases mediate neutrophil adhesion to adherent platelets. *Blood*. **109**. 2461–2469.

Fagerholm, S. C., Guenther, C., Asens, M. L., Savinko, T., & Uotila, L. M. (2019). Beta2-Integins and interacting proteins in leukocyte trafficking, immune supression, and immunodeficiency disease. *Frontiers in Immunology*. **10.** 1–10.

Falet, Herve´. (2017). Anatomy of the Platelet Cytoskeleton. In *Platelets in Thrombotic and Non-Thrombotic Disorders*.

Falet, Hervé, Chang, G., Brohard-Bohn, B., Rendu, F., & Hartwig, J. H. (2005). Integrin αIIbβ3 signals lead cofilin to accelerate platelet actin dynamics. *American Journal of Physiology - Cell Physiology*. **289**. 819–825.

Fawzy, A., Anderson, J. A., Cowans, N. J., Crim, C., Wise, R., Yates, J. C., & Hansel, N. N. (2019). Association of platelet count with all-cause mortality and risk of cardiovascular and respiratory morbidity in stable COPD. *Respiratory Research*. **20**. 1–10.

Ferrari, G., Langen, H., Naito, M., & Pieters, J. (1999). A coat protein on phagosomes involved in the intracellular survival of mycobacteria. *Cell*. **97**. 435–447.

Field, J., Vojtek, A., Ballester, R., Bolger, G., Colicelli, J., Ferguson, K., Gerst, J., Kataoka, T., Michaeli, T., Powers, S., Riggs, M., Rodgers, L., Wieland, I., Wheland, B., & Wigler, M. (1990). Cloning and characterization of CAP, the S. cerevisiae gene encoding the 70 kd adenylyl cyclase-associated protein. *Cell*.

61. 319–327.

Fischer, R. S., & Fowler, V. M. (2015). Thematic minireview series: The state of the cytoskeleton in 2015. *Journal of Biological Chemistry*. **290**. 17133–17136.

Flaumenhaft, R., & Sharda, A. (2019). Platelet secretion. In *Platelets* (4th ed., Vol. 2). Elsevier Inc.

Fletcher, D. A., & Mullins, R. D. (2010). Cell mechanics and the cytoskeleton. *Nature*. **463**. 485–492.

Föger, N., Jenckel, A., Orinska, Z., Lee, K.-H., Chan, A. C., & Bulfone-Paus, S. (2011). Differential regulation of mast cell degranulation versus cytokine secretion by the actin regulatory proteins Coronin1a and Coronin1b. *The Journal of Experimental Medicine*. **208**. 1777–1787.

Foger, N., Rangell, L., Danilenko, D. M., & Chan, A. C. (2006). Requirement for Coronin 1 in T Lymphocyte Trafficking and Cellular Homeostasis - supplemental data. *Science*. **313**. 839–842.

Fox, J. E. B., Lipfert, L., Clark, E. A., Reynolds, C. C., Austin, C. D., & Brugge, J. S. (1993). On the role of the platelet membrane skeleton in mediating signal transduction. *Journal of Biological Chemistry*. **268**. 25973–25984.

Freeman, N L, Lila, T., Mintzer, K. A., Chen, Z., Pahk, A. J., Ren, R., Drubin, D. G., & Field, J. (1996). A conserved proline-rich region of the Saccharomyces cerevisiae cyclase-associated protein binds SH3 domains and modulates cytoskeletal localization. *Molecular and Cellular Biology*. **16**. 548–556.

Freeman, Nancy L., & Field, J. (2000). Mammalian homolog of the yeast cyclase associated protein, CAP/Srv2p, regulates actin filament assembly. *Cell Motility and the Cytoskeleton*. **45**. 106–120.

French, S. L., Paramitha, A. C., Moon, M. J., Dickins, R. A., & Hamilton, J. R. (2016). Humanizing the protease-activated receptor (PAR) expression profile in mouse platelets by knocking Par1 into the Par3 locus reveals Par1 expression is not tolerated in mouse platelets. *PLoS ONE*. **11**. 1–14.

Frenette, P. S., Denis, C. V., Weiss, L., Jurk, K., Subbarao, S., Kehrel, B., Hartwig, J. H., Vestweber, D., & Wagner, D. D. (2000). P-selectin glycoprotein ligand 1 (PSGL-1) is expressed on platelets and can mediate platelet-endothelial

interactions in vivo. *Journal of Experimental Medicine*. **191**. 1413–1422.

Fukui, Y., Engler, S., Inoue, S., & De Hostos, E. L. (1999). Architectural dynamics and gene replacement of coronin suggest its role in cytokinesis. *Cell Motility and the Cytoskeleton*. **42**. 204–217.

Gandhi, M., & Goode, B. L. (2008). Coronin: the double-edged sword of actin dynamics. *Subcellular Biochemistry*. **48**. 72–87.

Gao, G., Chen, L., Dong, B., Gu, H., Dong, H., Pan, Y., Gao, Y., & Chen, X. (2009). RhoA effector mDia1 is required for PI 3-kinase-dependent actin remodeling and spreading by thrombin in platelets. *Biochemical and Biophysical Research Communications*. ***385.*** 439–444.

Gardiner, E. E., Arthur, J. F., Berndt, M. C., & Andrews, R. K. (2005). Role of calmodulin in platelet receptor function. *Current Medicinal Chemistry: Cardiovascular and Hematological Agents*. **3**. 283–287.

Gatfield, J., Imke Albrecht, Zanolari, B., Steinmetz, M. O., & Pieters, J. (2005). Association of the Leukocyte Plasma Membrane with the Actin Cytoskeleton through Coiled Coil-mediated Trimeric Coronin 1 Molecules. *Molecular Biology of the Cell*. **16**. 2786–2798.

Geer, L. Y., Marchler-Bauer, A., Geer, R. C., Han, L., He, J., He, S., Liu, C., Shi, W., & Bryant, S. H. (2009). The NCBI BioSystems database. *Nucleic Acids Research*. **38**. 492–496.

Ghalloussi, D., Dhenge, A., & Bergmeier, W. (2019). New insights into cytoskeletal remodeling during platelet production. *Journal of Thrombosis and Haemostasis*. **17**. 1430–1439.

Gibbins, J. M., & Mahaut-Smith, M. P. (2012). Platelets and Megakaryocytes. In *Human Press* (Vol. 3).

Gibbins, Jonathan M. (2004). Platelet adhesion signalling and the regulation of thrombus formation. *Journal of Cell Science*. **117**. 3415–3425.

Gieselmann, R., & Mann, K. (1992). ASP-56, a new actin sequestering protein from pig platelets with homology to CAP, an adenylate cyclase-associated protein from yeast. *FEBS Letters*. **298**. 149–153.

Gloss, A., Rivero, F., Khaire, N., Muller, R., L., Oomis, W. F., Schleicher, M., &

Noegel, A. A. (2003). Villidin, a Novel WD-repeat and Villin-related Protein from Dictyostelium, Is Associated with Membranes and the Cytoskeleton. *Molecular Biology of the Cell*. **14**. 2716–2727.

Goggs, R., Savage, J. S., Mellor, H., & Poole, A. W. (2013). The small GTPase Rif is dispensable for platelet filopodia generation in mice. *PLoS ONE, 8*(1), 1–12.

Goggs, R., Williams, C. M., Mellor, H., & Poole, A. W. (2015). Platelet Rho GTPases – a focus on novel players, roles and relationships. *Biochemical Journal*. **466**. 431–442.

Golebiewska, E. M., & Poole, A. W. (2015). Platelet secretion: From haemostasis to wound healing and beyond. *Blood Reviews*. **29**. 153–162.

Guidetti, G.F., Canobbio, I. and Torti, M. (2015). PI3K/Akt in platelet integrin signaling and implications in thrombosis. *Advances in biological regulation*. **59**. 36-52.

Guo, M., Ehrlicher, A. J., Mahammad, S., Fabich, H., Jensen, M. H., Moore, J. R., Fredberg, J. J., Goldman, R. D., & Weitz, D. A. (2013). The role of vimentin intermediate filaments in cortical and cytoplasmic mechanics. *Biophysical Journal*. **105**. 1562–1568.

Gurniak, C. B., Perlas, E., & Witke, W. (2005). The actin depolymerizing factor n-cofilin is essential for neural tube morphogenesis and neural crest cell migration. *Developmental Biology*. **278**. 231–241.

Gyulkhandanyan, A. V., Mutlu, A., Freedman, J., & Leytin, V. (2013). Selective triggering of platelet apoptosis, platelet activation or both. *British Journal of Haematology*. **161**. 245–254.

Habib, A., Fitzgerald, G. A., & Maclouf, J. (1999). Phosphorylation of the thromboxane receptor α, the predominant isoform expressed in human platelets. *Journal of Biological Chemistry*. **274**. 2645–2651.

Hacker, U., Albrecht, R., & Maniak, M. (1997). Fluid-phase uptake by macropinocytosis in Dictyostelium. *Journal of Cell Science*. **110**. 105–112.

Haglund, C. M., & Welch, M. D. (2011). Pathogens and polymers: Microbe-host interactions illuminate the cytoskeleton. *Journal of Cell Biology*. **195**. 7–17.

Hall, A. (1998). Rho GTPases and the Actin Cytoskeleton. *Science*. **279**. 509–514.

Hall, K. J., Harper, M. T., Gilio, K., Cosemans, J. M., Heemskerk, J. W. M., & Poole, A. W. (2008). Genetic analysis of the role of protein kinase Cθ in platelet function and thrombus formation. *PLoS ONE*. **3**. e3277

Haraldsson, M. K., Louis-Dit-Sully, C. A., Lawson, B. R., Sternik, G., Santiago-Raber, M. L., Gascoigne, N. R. J., Theofilopoulos, A. N., & Kono, D. H. (2008). The Lupus-Related Lmb3 Locus Contains a Disease-Suppressing Coronin-1A Gene Mutation. *Immunity*. **28**. 40–51.

Harper, A. G. S., & Sage, S. O. (2017). Platelet Signalling : Calcium. *Platelets in Thrombotic and Non-Thrombotic Disorders*. **28,** 285–296.

Hartwig, J. H., Barkalow, K., Azim, A., & Italiano, J. (1999). The elegant platelet: Signals controlling actin assembly. *Thrombosis and Haemostasis*. **82**. 392–398.

Heck, O. (2019). Role of cyclase-associated protein 2 in platelet function and description of an inherited macrothrombocytopenia Rolle von cyclase-associated protein 2 PhD Thesis. Julius-Maximilians-Universität Würzburg. Würzburg,

Henn, V., Slupsky, J. R., Gräfe, M., Anagnostopoulos, I., Förster, R., Müller-Berghaus, G., & Kroczek, R. A. (1998). CD40 ligand on activated platelets triggers an inflammatory reaction of endothelial cells. *Nature*. **391**. 591–594.

Holinstat, M., Boutaud, O., Apopa, P.L., V., Esci, J., Bala, M., Oates, J. A., & Hamm, H. . (2011). Protease-Activated Receptor Signaling in Platelets Activates Cytosolic Phospholipase A2α Differently for Cyclooxygenase-1 and 12-Lipoxygenase Catalysis. Arteriosclerosis, Thrombosis, and Vascular Biology. **31**. 435–442.

Horvath, A. R., Muszbek, L., & Kellie, S. (1992). Translocation of pp60c-src to the cytoskeleton during platelet aggregation. *The EMBO Journal*. **11**. 855–861.

Hsu, W. H., Yu, Y. R., Hsu, S. H., Yu, W. C., Chu, Y. H., Chen, Y. J., Chen, C. M., & You, L. R. (2013). The Wilms' tumor suppressor Wt1 regulates Coronin 1B expression in the epicardium. *Experimental Cell Research*. **319**. 1365–1381.

Huang, J., Li, X., Shi, X., Zhu, M., Wang, J., Huang, S., Huang, X., Wang, H., Li, L., Deng, H., Zhou, Y., Mao, J., Long, Z., Ma, Z., Ye, W., Pan, J., Xi, X., & Jin, J. (2019). Platelet integrin αiIbβ3: Signal transduction, regulation, and its

therapeutic targeting. *Journal of Hematology and Oncology*. **12**. 1-22

Huang, P. L. (1999). Neuronal and endothelial nitric oxide synthase gene knockout mice. *Brazilian Journal of Medical and Biological Research*. **32**. 1353–1359.

Hummler, E., Dousse, A., Rieder, A., Stehle, J. C., Rubera, I., Osterheld, M. C., Beermann, F., Frateschi, S., & Charles, R. P. (2013). The Channel-Activating Protease CAP1/Prss8 Is Required for Placental Labyrinth Maturation. *PLoS ONE*. **8**. e55796

Humphries, C. L., Balcer, H. I., D'Agostino, J. L., Winsor, B., Drubin, D. G., Barnes, G., Andrews, B. J., & Goode, B. L. (2002). Direct regulation of Arp2/3 complex activity and function by the actin binding protein coronin. *Journal of Cell Biology*. **159**. 993–1004.

Huntzinger, E., & Izaurralde, E. (2011). Gene silencing by microRNAs: Contributions of translational repression and mRNA decay. *Nature Reviews Genetics*. **12**. 99–110.

Ikeda, S., Cunningham, L. A., Boggess, D., Hobson, C. D., Sundberg, J. P., Naggert, J. K., Smith, R. S., & Nishina, P. M. (2003). Aberrant actin cytoskeleton leads to accelerated proliferation of corneal epithelial cells in mice deficient for destrin (actin depolymerizing factor). *Human Molecular Genetics*. **12**. 1029–1036.

Italiano, J. E., Lecine, P., Shivdasani, R. A., & Hartwig, J. H. (1999). Blood platelets are assembled principally at the ends of proplatelet processes produced by differentiated megakaryocytes. *Journal of Cell Biology*. **147**. 1299–1312.

Italiano, J. E., Patel-Hett, S., & Hartwig, J. H. (2007). Mechanics of proplatelet elaboration. *Journal of Thrombosis and Haemostasis*. **5**. 18–23

Ito, Y., Ohno, K., Morikawa, Y., Tomizawa, A., & Mizuno, M. (2018). Vasodilator-stimulated phosphoprotein (VASP) is not a major mediator of platelet aggregation , thrombogenesis , effect of prasugrel in rats. *Scientific Reports*. **8**. 1-11.

Jang, H. D., Lee, S. E., Yang, J., Lee, H. C., Shin, D., Lee, H., Lee, J., Jin, S., Kim, S., Lee, S. J., You, J., Park, H. W., Nam, K. Y., Lee, S. H., Park, S. W., Kim, J. S., Kim, S. Y., Kwon, Y. W., Kwak, S. H., … Kim, H. S. (2020). Cyclase-associated protein 1 is a binding partner of proprotein convertase

subtilisin/kexin type-9 and is required for the degradation of low-density lipoprotein receptors by proprotein convertase subtilisin/kexin type-9. *European Heart Journal*. **41**. 239–252.

Jansen, S., Collins, A., Golden, L., Sokolova, O., & Goode, B. L. (2014). Structure and mechanism of mouse cyclase-associated protein (CAP1) in regulating actin dynamics. *Journal of Biological Chemistry*. **289**. 30732–30742.

Jarvis, G. E. (2004). Platelet Aggregation: Turbidimetric Measurements. *Methods in Molecular Biology*. **272**. 65–76.

Jarvis, Gavin E. (2004). Platelet Aggregation in Whole Blood. *Methods in Molecular Biology*. **272**. 77–87.

Jayachandran, R., Gumienny, A., Bolinger, B., Khanna, N., Rossi, S. W., Pieters, J., Jayachandran, R., Gumienny, A., Bolinger, B., Ruehl, S., & Lang, M. J. (2019). Disruption of Coronin 1 Signaling in T Cells Promotes Allograft Tolerance while Maintaining Anti-Pathogen Article Disruption of Coronin 1 Signaling in T Cells Promotes Allograft Tolerance while Maintaining Anti-Pathogen Immunity. *Immunity*. **50**. 152–165.

Jayachandran, R., Liu, X., BoseDasgupta, S., M??ller, P., Zhang, C. L., Moshous, D., Studer, V., Schneider, J., Genoud, C., Fossoud, C., Gambino, F., Khelfaoui, M., M??ller, C., Bartholdi, D., Rossez, H., Stiess, M., Houbaert, X., Jaussi, R., Frey, D., … Pieters, J. (2014). Coronin 1 Regulates Cognition and Behavior through Modulation of cAMP/Protein Kinase A Signaling. *PLoS Biology*. **12**. e1001820.

Jayachandran, R., Sundaramurthy, V., Combaluzier, B., Mueller, P., Korf, H., Huygen, K., Miyazaki, T., Albrecht, I., Massner, J., & Pieters, J. (2007). Survival of Mycobacteria in Macrophages Is Mediated by Coronin 1-Dependent Activation of Calcineurin. *Cell*. **130**. 37-50

Johnston-Cox, H. A., & Ravid, K. (2011). Adenosine and blood platelets. *Purinergic Signalling*. **7**. 357–365.

Joshi, P. L. (2017). Effects of resistin on platelet function and its receptor, adenylyl cyclase associated protein 1. P.h.D. thesis, Hull York Medical School.

Joshi, P., Riley, D. R. J., Khalil, J. S., Xiong, H., Ji, W., & Rivero, F. (2018). The

membrane-associated fraction of cyclase associate protein 1 translocates to the cytosol upon platelet stimulation. *Scientific Reports*. **8**. 1–12.

Jung, S. M., & Moroi, M. (1988). Platelet cytoskeletal protein distributions in two Triton-insoluble fractions and how they are affected by stimulants and reagents that modify cytoskeletal protein interactions. *Thrombosis Research*. **88**. 775–787.

Kahr, W. H. A., Pluthero, F. G., Elkadri, A., Warner, N., Drobac, M., Chen, C. H., Lo, R. W., Li, L., Li, R., Li, Q., Thoeni, C., Pan, J., Leung, G., Lara-Corrales, I., Murchie, R., Cutz, E., Laxer, R. M., Upton, J., Roifman, C. M., … Muise, A. M. (2017). Loss of the Arp2/3 complex component ARPC1B causes platelet abnormalities and predisposes to inflammatory disease. *Nature Communications*. **8**. 14816.

Kammerer, R. a, Kostrewa, D., Progias, P., Honnappa, S., Avila, D., Lustig, A., Winkler, F. K., Pieters, J., & Steinmetz, M. O. (2005). A conserved trimerization motif controls the topology of short coiled coils. *Proceedings of the National Academy of Sciences of the United States of America*. **102**. 13891–13896.

Kardos, R., Pozsonyi, K., Nevalainen, E., Lappalainen, P., Nyitrai, M., & Hild, G. (2009). The effects of ADF/cofilin and profilin on the conformation of the ATP-binding cleft of monomeric actin. *Biophysical Journal*. **96**. 2335–2343.

Karpatkin, S., & Charmate, A. (1969). Heterogeneity of human platelets. *Journal of Clinical Investigation*. **48**. 1073–1082.

Kato, K., Kanaji, T., Russell, S., Kunicki, T. J., Furihata, K., Kanaji, S., Marchese, P., Reininger, A., Ruggeri, Z. M., & Ware, J. (2003). The contribution of glycoprotein VI to stable platelet adhesion and thrombus formation illustrated by targeted gene deletion. *Blood*. **102**. 1701–1707.

Khan, S., Zhang, X., Lv, D., Zhang, Q., He, Y., Zhang, P., Liu, X., Thummuri, D., Yuan, Y., Wiegand, J.S. and Pei, J. (2019). A selective BCL-X L PROTAC degrader achieves safe and potent antitumor activity. *Nature medicine*. **25**. 1938-1947.

Klinger, M. H. F., & Jelkmann, W. (2002). Role of blood platelets in infection and inflammation. *Journal of Interferon and Cytokine Research*. **22**. 913–922.

233

Kotila, T., Kogan, K., Enkavi, G., Guo, S., Vattulainen, I., Goode, B. L., & Lappalainen, P. (2018). Structural basis of actin monomer re-charging by cyclase-Associated protein. *Nature Communications*. **9**. 1–12.

Lam, F. W., Vijayan, K. V., & Rumbaut, R. E. (2015). Platelets and their interactions with other immune cells. *Comprehensive Physiology*. **5**. 1265–1280.

Lee, S., Lee, H. C., Kwon, Y. W., Lee, S. E., Cho, Y., Kim, J., Lee, S., Kim, J. Y., Lee, J., Yang, H. M., Mook-Jung, I., Nam, K. Y., Chung, J., Lazar, M. A., & Kim, H. S. (2014). Adenylyl cyclase-associated protein 1 is a receptor for human resistin and mediates inflammatory actions of human monocytes. *Cell Metabolism*. **19**. 484–497.

Lewandrowski, U., Wortelkamp, S., Lohrig, K., Zahedi, R. P., Wolters, D. A., Walter, U., & Sickmann, A. (2009). Platelet membrane proteomics: A novel repository for functional research. *Blood*. **114**. 10–20.

Li, X., Zhong, K., Yin, Z., Hu, J., Wang, W., Li, L., Zhang, H., Zheng, X., Wang, P., & Zhang, Z. (2019). The seven transmembrane domain protein MoRgs7 functions in surface perception and undergoes coronin MoCrn1-dependent endocytosis in complex with Gα subunit MoMagA to promote cAMP signaling and appressorium formation in Magnaporthe oryzae. *PLoS Pathogens*. **15**. 1–28.

Li, Zhenyu, Xi, X., Gu, M., Feil, R., Ye, R. D., Eigenthaler, M., Hofmann, F., & Du, X. (2003). A Stimulatory Role for cGMP-Dependent Protein Kinase in Platelet Activation.. *Cell*. **112**. 77–86.

Li, Zhi, Kim, E. S., & Bearer, E. L. (2002). *Arp2/3 complex is required for actin polymerization during platelet shape change*. **99**. 4466–4474.

Lila, T., & Drubin, D. G. (1997). Evidence for physical and functional interactions among two Saccharomyces cerevisiae SH3 domain proteins, an adenylyl cyclase-associated protein and the actin cytoskeleton. *Molecular Biology of the Cel.* **8**. 367–385.

Linardopoulou, E. V., Parghi, S. S., Friedman, C., Osborn, G. E., Parkhurst, S. M., & Trask, B. J. (2007). Human subtelomeric WASH genes encode a new subclass of the WASP family. *PLoS Genetics*. **3**. 2477–2485.

Lisman, T., Weeterins, C., & de Groot, P. (2005). Thrombosis and Haemostasis

Laboratory, Department of Haematology, University Medical Centre Utrecht, Utrecht, and Institute of Biomembranes, Utrecht University, Utrecht, The Netherlands. *Haemostasis.* **5**. 2504–2517.

Liu, C. Z., Chen, Y., & Sui, S. F. (2006). The identification of a new actin-binding region in p57. *Cell Research.* **16**. 106–112.

Liu, X., Bosedasgupta, S., Jayachandran, R., Studer, V., Rühl, S., Stiess, M., & Pieters, J. (2016). Activation of the cAMP/protein kinase A signalling pathway by coronin 1 is regulated by cyclin-dependent kinase 5 activity. *FEBS Letters.* **590**. 279–287.

Londin, E. R., Hatzimichael, E., Loher, P., Edelstein, L., Shaw, C., Delgrosso, K., Fortina, P., Bray, P. F., McKenzie, S. E., & Rigoutsos, I. (2014). The human platelet: strong transcriptome correlations among individuals associate weakly with the platelet proteome. *Biology Direct.* **9**. 3.

Lopez, J. J., Salido, G. M., Pariente, J. A., & Rosado, J. A. (2008). Thrombin induces activation and translocation of Bid, Bax and Bak to the mitochondria in human platelets. *Journal of Thrombosis and Haemostasis.* **6**. 1780–1788.

Ma, C., Yao, Y., Yue, Q. X., Zhou, X. W., Yang, P. Y., Wu, W. Y., Guan, S. H., Jiang, B. H., Yang, M., Liu, X., & Guo, D. A. (2011). Differential proteomic analysis of platelets suggested possible signal cascades network in platelets treated with Salvianolic acid B. *PLoS ONE.* **6**.. e14692

Makkonen, M., Bertling, E., Chebotareva, N. A., Baump, J., & Lappalainen, P. (2013). Mammalian and malaria parasite cyclase-associated proteins catalyze nucleotide exchange on G-actin through a conserved mechanism. *Journal of Biological Chemistry*. **288**. 984–994.

Maniak, M., Rauchenberger, R., Albrecht, R., Murphy, J., & Gerisch, G. (1995). Coronin involved in phagocytosis: Dynamics of particle-induced relocalization visualized by a green fluorescent protein tag. *Cel.* **83**. 915–924.

Manicassamy, S., Gupta, S., Huang, Z., Molkentin, J. D., Shang, W., & Sun, Z. (2008). Requirement of Calcineurin Aβ for the Survival of Naive T Cells. *The Journal of Immunology.* **180**. 106–112.

McArdle, B., & Hofmann, A. (2013). Coronin Structure and Implications. In *The*

235

Coronin Family of Proteins. **48**. 56–71. Springer, New York, NY.

McCaffery, P. J., & Berridge, M. V. (1986). Expression of the leukocyte functional molecule (LFA-1) on mouse platelets. *Blood.* **67**. 1757–1764.

McCarty, O. J. T., Larson, M. K., Auger, J. M., Kalia, N., Atkinson, B. T., Pearce, A. C., Ruf, S., Henderson, R. B., Tybulewicz, V. L. J., Machesky, L. M., & Watson, S. P. (2005). Rac1 is essential for platelet lamellipodia formation and aggregate stability under flow. *Journal of Biological Chemistry.* **280**. 39474–39484.

McEver, R. P. (2002). Selectins: Lectins that initiate cell adhesion under flow. *Current Opinion in Cell Biology.* **14**. 581–586.

McGrath, J., Roy, P., & Perrin, B. . (2017). Stereocilia morphogenesis and maintenance through regulation of actin stability. *Seminars in Cell & Developmental Biology.* **65**. 88–95.

McKenzie, S. E. (2002). Humanized mouse models of FcR clearance in immune platelet disorders. *Blood Reviews.* **16**. 3–5.

Menna, E., Fossati, G., Scita, G., & Matteoli, M. (2011). From filopodia to synapses: The role of actin-capping and anti-capping proteins. *European Journal of Neuroscience.* **34**. 1655–1662.

Menter, D. G., Tucker, S. C., Kopetz, S., Sood, A. K., Crissman, J. D., & Honn, K. . (2014). Platelets and cancer: A casual or causal relationship: Revisited. *Cancer and Metastasis Reviews.* **33**. 231–269.

Millard, T. H., Sharp, S. J., & Machesky, L. M. (2004). Signalling to actin assembly via the WASP (Wiskott-Aldrich syndrome protein)-family proteins and the Arp2/3 complex. *The Biochemical Journal.* **380**. 1–17.

Mishima, M., & Nishida, E. (1999). Coronin localizes to leading edges and is involved in cell spreading and lamellipodium extension in vertebrate cells. *Journal of Cell Science.* **112**. 2833–2842.

Mitsios, J. V., Prévost, N., Kasirer-Friede, A., Gutierrez, E., Groisman, A., Abrams, C. S., Wang, Y., Litvinov, R. I., Zemljic-Harpf, A., Ross, R. S., & Shattil*, S. J. (2010). What Is Vinculin Needed for in Platelets?. *Journal of Thrombosis and Haemostasis.* **8**. 2294–2304.

Moebiust, J., Zahedi, R. P., Lewandrowski, U., Berger, C., Walter, U., & Sickmann,

A. (2005). The human platelet membrane proteome reveals several new potential membrane proteins. *Molecular and Cellular Proteomics*. **4**. 1754–1761.

Mohun, T., Adams, D. J., Baldock, R., Bhattacharya, S., Copp, A. J., Hemberger, M., Houart, C., Hurles, M. E., Robertson, E., Smith, J. C., Weaver, T., & Weninger, W. (2013). Deciphering the mechanisms of developmental disorders (DMDD): A new programme for phenotyping embryonic lethal mice. *DMM Disease Models and Mechanisms*. **6**. 562–566.

Moore, S. F., Van Den Bosch, M. T. J., Hunter, R. W., Sakamoto, K., Poole, A. W., & Hers, I. (2013a). Dual regulation of glycogen synthase kinase 3 (GSK3)α/β by protein kinase C (PKC)α and Akt promotes thrombin-mediated integrin α∥bβ3 activation and granule secretion in platelets. *Journal of Biological Chemistry*. **288**. 3918–3928.

Morgan, R. O., & Fernandez, M. P. (2008). Molecular phylogeny and evolution of the coronin gene family. *Sub-Cellular Biochemistry*. **48**. 41–55.

Moriyama, K., & Yahara, I. (2002). Human CAP1 is a key factor in the recycling of cofilin and actin for rapid actin turnover. *Journal of Cell Science*. **115**. 1591–1601.

Moshous, D., Martin, E., Carpentier, W., Lim, A., Callebaut, I., Canioni, D., Hauck, F., Majewski, J., Schwartzentruber, J., Nitschke, P., Sirvent, N., Frange, P., Picard, C., Blanche, S., Revy, P., Fischer, A., Latour, S., Jabado, N., & De Villartay, J. P. (2013). Whole-exome sequencing identifies Coronin-1A deficiency in 3 siblings with immunodeficiency and EBV-associated B-cell lymphoproliferation. *Journal of Allergy and Clinical Immunology*. **131**. 1594-1603

Mueller, P., Liu, X., & Pieters, J. (2011). Migration and homeostasis of naive T cells depends on coronin 1-mediated prosurvival signals and not on coronin 1-dependent filamentous actin modulation. *Journal of Immunology*. **186**. 4039–4050.

Mueller, P., Massner, J., Jayachandran, R., Combaluzier, B., Albrecht, I., Gatfield, J., Blum, C., Ceredig, R., Rodewald, H.-R., Rolink, A. G., & Pieters, J. (2008). Regulation of T cell survival through coronin-1-mediated generation of inositol-

1,4,5-trisphosphate and calcium mobilization after T cell receptor triggering. *Nature Immunology*. **9**. 424–431.

Munjas, J., Sopić, M., Spasojević-Kalimanovska, V., Kalimanovska-Oštrić, D., Anđelković, K., & Jelić-Ivanović, Z. (2017). Association of adenylate cyclase-associated protein 1 with coronary artery disease. *European Journal of Clinical Investigation*. **47**. 659–666.

Murata, T., Ushikubi, F., Matsuoka, T., Hirata, M., Yamasaki, A., Sugimoto, Y., Ichikawa, A., Aze, Y., Tanaka, T., Yoshida, N., Ueno, A., Oh-ishi, S., & Narumiya, S. (1997). Altered pain perception and inflammatory response in mice lacking prostacyclin receptor. *Nature*. **388**. 678–682.

Nagy, Z., & Smolenski, A. (2018). Cyclic nucleotide-dependent inhibitory signaling interweaves with activating pathways to determine platelet responses. *Research and Practice in Thrombosis and Haemostasis*. **2**. 558–571.

Nakamura, T., Takeuchi, K., Muraoka, S., Takezoe, H., Takahashi, N., & Mori, N. (1999). A neurally enriched coronin-like protein, ClipinC, is a novel candidate for an actin cytoskeleton-cortical membrane-linking protein. *Journal of Biological Chemistry*. **274**. 13322–13327.

Nal, B., Carroll, P., Mohr, E., Verthuy, C., Da Silva, M. I., Gayet, O., Guo, X. J., He, H. T., Alcover, A., & Ferrier, P. (2004). Coronin-1 expression in T lymphocytes: Insights into protein function during T cell development and activation. *International Immunology*. **16**. 231–240.

Nash, G. F., Turner, L. F., Scully, M. F., & Kakkar, A. K. (2002). Platelets and cancer. *Lancet Oncology*. **3**. 425–430.

Neer, E., & Smith, T. F. (1996). G protein heterodimers: new structure propels new questions. *Cell*. **84**. 175–178.

Nevalainen, E. M., Skwarek-Maruszewska, A., Braun, A., Moser, M., & Lappalainen, P. (2009). Two biochemically distinct and tissue-specific twinfilin isoforms are generated from the mouse Twf2 gene by alternative promoter usage. *Biochemical Journal*. **417**. 593–600.

Ngo, A. T. P., Thierheimer, M. L. D., Babur, Ö., Rocheleau, A. D., Huang, T., Pang, J., Rigg, R. A., Mitrugno, A., Theodorescu, D., Burchard, J., Nan, X., Demir, E.,

McCarty, O. J. T., & Aslan, J. E. (2017). Assessment of roles for the rho-specific guanine nucleotide dissociation inhibitor Ly-GDI in platelet function: A spatial systems approach. *American Journal of Physiology - Cell Physiology*. **312**. C527–C536.

Nieswandt, B., & Watson, S. P. (2003). Platelet-collagen interaction: Is GPVI the central receptor? *Blood*. **102**. 449–461.

Nishida, Y., Shima, F., Sen, H., Tanaka, Y., Yanagihara, C., Yamawaki-Kataoka, Y., Kariya, K. I., & Kataoka, T. (1998). Coiled-coil interaction of N-terminal 36 residues of cyclase-associated protein with adenylyl cyclase is sufficient for its function in Saccharomyces cerevisiae Ras pathway. *Journal of Biological Chemistry*. **273**. 28019–28024.

Norbnop, P., Ingrungruanglert, P., Israsena, N., Suphapeetiporn, K. and Shotelersuk, V. (2020). Generation and characterization of HLA-universal platelets derived from induced pluripotent stem cells. *Scientific Reports*. **10**. 1-9.

Noegel, A. A., Rivero, F., Albrecht, R., Janssen, K. P., Köhler, J., Parent, C. A., & Schleicher, M. (1999). Assessing the role of the ASP56/CAP homologue of Dictyostelium discoideum and the requirements for subcellular localization. *Journal of Cell Science*. **112**. 3195–3203.

Normoyle, K. P. M., & Brieher, W. M. (2012). Cyclase-associated protein (CAP) acts directly on F-actin to accelerate cofilin-mediated actin severing across the range of physiological pH. *Journal of Biological Chemistry*. **287**. 35722–35732.

Nurden, A. T. (2011). Platelets, inflammation and tissue regeneration. *Thrombosis and Haemostasis*. **105**. 13–33.

Ojeda, V., Robles-Valero, J., Barreira, M., & Bustelo, X. R. (2015). The disease-linked Glu-26-Lys mutant version of Coronin 1A exhibits pleiotropic and pathwayspecific signaling defects. *Molecular Biology of the Cell*. **26**. 2895–2912.

Oku, T., Itoh, S., Ishii, R., Suzuki, K., Nauseef, W. M., Toyoshima, S., & Tsuji, T. (2005). Homotypic dimerization of the actin-binding protein p57/coronin-1 mediated by a leucine zipper motif in the C-terminal region. *The Biochemical Journal*. **387**. 325–331.

Oku, T., Itoh, S., Okano, M., Suzuki, A., Suzuki, K., Nakajin, S., Tsuji, T., Nauseef,

W. M., & Toyoshima, S. (2003). Two regions responsible for the actin binding of p57, a mammalian coronin family actin-binding protein. *Biological & Pharmaceutical Bulletin*. **26**. 409–416.

Omary, M. B. (2009). "IF-pathies": a broad spectrum of intermediate filament–associated diseases. *Journal of Clinical Investigation*. **119**. 1756–1762.

Ono, S. (2010). Dynamic regulation of sarcomeric actin filaments in striated muscle. *Cytoskeleton*. **67**. 677–692.

Ono, S. (2013). The role of cyclase-associated protein in regulating actin filament dynamics - more than a monomer-sequestration factor. *Journal of Cell Science*. **126**. 3249–3258.

Ozaki, Y., Suzuki-Inoue, 1, K., & Inoue, O. (2009). Novel Interactions in Platelet Biology: CLEC-2/podoplanin and laminin/GPVI. *Thromb Haemost*, *7*, 191–194.

Page, C., & Pitchford, S. (2013). Neutrophil and platelet complexes and their relevance to neutrophil recruitment and activation. *International Immunopharmacology*. **17**. 1176–1184.

Patel-Hett, S., Wang, H., Begonja, A. J., Thon, J. N., Alden, E. C., Wandersee, N. J., An, X., Mohandas, N., Hartwig, J. H., & Italiano, J. E. (2011). The spectrin-based membrane skeleton stabilizes mouse megakaryocyte membrane systems and is essential for proplatelet and platelet formation. *Blood*. **118**.

Paul, A. S., & Pollard, T. D. (2009). Review of the mechanism of processive actin filament elongation by formins. *Cell Motility and the Cytoskeleton*. **66**. 606–617.

Paul, D. S., Casari, C., Wu, C., Piatt, R., Pasala, S., Campbell, R. A., Poe, K. O., Ghalloussi, D., Lee, R. H., Rotty, J. D., Cooley, B. C., Machlus, K. R., Italiano, J. E., Weyrich, A. S., Bear, J. E., & Bergmeier, W. (2017). Deletion of the Arp2/3 complex in megakaryocytes leads to microthrombocytopenia in mice. *Blood Advances*. **1**. 1398–1408.

Peche, V. S., Holak, T. A., Burgute, B. D., Kosmas, K., Kale, S. P., Wunderlich, F. T., Elhamine, F., Stehle, R., Pfitzer, G., Nohroudi, K., Addicks, K., Stöckigt, F., Schrickel, J. W., Gallinger, J., Schleicher, M., & Noegel, A. A. (2013). Ablation of cyclase-associated protein 2 (CAP2) leads to cardiomyopathy. *Cellular and Molecular Life Sciences*. **70**. 527–543.

Peche, V., Shekar, S., Leichter, M., Korte, H., Schröder, R., Schleicher, M., Holak, T. A., Clemen, C. S., Ramanath-Y., B., Pfitzer, G., Karakesisoglou, I., & Noegel, A. A. (2007). CAP2, cyclase-associated protein 2, is a dual compartment protein. *Cellular and Molecular Life Sciences*. **64**(. 2702–2715.

Peña, E., Padro, T., Molins, B., Vilahur, G., & Badimon, L. (2011). Proteomic signature of thrombin-activated platelets after in vivo nitric oxide-donor treatment: Coordinated inhibition of signaling (phosphatidylinositol 3-kinase-γ, 14-3-3ζ, and growth factor receptor-bound protein 2) and cytoskeleton protein translocati. *Arteriosclerosis, Thrombosis, and Vascular Biology*. **31**. 2560–2569.

Petricevic, M., Biocina, B., Milicic, D., Konosic, S., Svetina, L., Lekić, A., Zdilar, B., Burcar, I., Milosevic, M., Brahimaj, R., Samardzic, J., & Gasparovic, H. (2013). Bleeding risk assessment using whole blood impedance aggregometry and rotational thromboelastometry in patients following cardiac surgery. *Journal of Thrombosis and Thrombolysis*. **36**. 514–526.

Philippeaux, M. M., Vesin, C., Tacchini-Cottier, F., & Piguet, P. F. (1996). Activated human platelets express β2 integrin. *European Journal of Haematology*. **56**. 130–137.

Pick, R., Begandt, D., Stocker, T. J., Salvermoser, M., Thome, S., Böttcher, R. T., Montanez, E., Harrison, U., Forné, I., Khandoga, A. G., Coletti, R., Weckbach, L. T., Brechtefeld, D., Haas, R., Imhof, A., Massberg, S., Sperandio, M., & Walzog, B. (2017). Coronin 1A, a novel player in integrin biology, controls neutrophil trafficking in innate immunity. *Blood*. **130**. 847–858.

Pieters, J., Müller, P., & Jayachandran, R. (2013). On guard: coronin proteins in innate and adaptive immunity. *Nature Reviews. Immunology*. **13**. 510–518.

Piguet, P. F., Vesin, C., & Rochat, A. (2001). Beta2 integrin modulates platelet caspase activation and life span in mice. *European Journal of Cell Biology*. **80**. 171–177.

Pitchford, S. C., Momi, S., Giannini, S., Casali, L., Spina, D., Page, C. P., & Gresele, P. (2005). Platelet P-selectin is required for pulmonary eosinophil and lymphocyte recruitment in a murine model of allergic inflammation. *Blood*. **105**. 2074–2081.

Pollard, T.D., 2016. Actin and actin-binding proteins. *Cold Spring Harbor perspectives in biology*. **8**. 1-17

Pollard, T. D., & Borisy, G. G. (2003). Cellular motility driven by assembly and disassembly of actin filaments. *Cell*. **112**. 453–465.

Pollitt, A. Y., & Insall, R. H. (2009). WASP and SCAR/WAVE proteins: the drivers of actin assembly. *Journal of Cell Science*. **122**. 2575–2578.

Poulter, N. S., Pollitt, A. Y., Davies, A., Malinova, D., Nash, G. B., Hannon, M. J., Pikramenou, Z., Rappoport, J. Z., Hartwig, J. H., Owen, D. M., Thrasher, A. J., Watson, S. P., & Thomas, S. G. (2015). Platelet actin nodules are podosome-like structures dependent on Wiskott-Aldrich syndrome protein and ARP2/3 complex. *Nature Communications*. **6**. 7254.

Poulter, N. S., Staiger, C. J., Rappoport, J. Z., & Franklin-Tong, V. E. (2010). Actin-binding proteins implicated in the formation of the punctate actin foci stimulated by the self-incompatibility response in papaver. *Plant Physiology*. **152**. 1274–

Priya, R., Wee, K., Budnar, S., Gomez, G. A., Yap, A. S., & Michael, M. (2016). Coronin 1B supports RhoA signaling at cell-cell junctions through Myosin II. *Cell Cycle*. **0**. 3033-3-41.

Quinn, S. N., Graves, S. H., Dains-McGahee, C., Friedman, E. M., Hassan, H., Witkowski, P., & Sabbatini, M. E. (2017). Adenylyl cyclase 3/adenylyl cyclase-associated protein 1 (CAP1) complex mediates the anti-migratory effect of forskolin in pancreatic cancer cells. *Molecular Carcinogenesis*. **56**. 1344–1360.

Ranjith, M. P., DivyaRaj, R., Mathew, D., George, B., & Krishnan, M. N. (2016). Mean platelet volume and cardiovascular outcomes in acute myocardial infarction. *Heart Asia*. **8**. 16–20.

Raslan, Z., & Naseem, K. M. (2014). Compartmentalisation of cAMP-dependent signalling in blood platelets: The role of lipid rafts and actin polymerisation. *Platelets*. **26**. 349-357.

Riley, D.R., Khalil, J.S., Naseem, K.M. and Rivero, F. (2020). Biochemical and immunocytochemical characterization of coronins in platelets. *Platelets*, **31***. 913-924.

Riley, D. R. J., Khalil, J. S., Pieters, J., Naseem, K. M. & Rivero, F. (2020). Coronin

1 is required for integrin β2 translocation in platelets. *International Journal of Molecular Sciences*. **21**. 356.

Rivera, J., Lozano, M. L., Navarro-Núñez, L., & Vicente García, V. (2009). Platelet receptors and signaling in the dynamics of thrombus formation. *Haematologica*. **94**. 700–711.

Roberts, W., Michno, A., Aburima, A., & Naseem, K. M. (2009). Nitric oxide inhibits von Willebrand factor-mediated platelet adhesion and spreading through regulation of integrin α IIbβ 3 and myosin light chain. *Journal of Thrombosis and Haemostasis*. **7**. 2106–2115.

Roffers-Agarwal, J., Xanthos, J. B., & Miller, J. R. (2005). Regulation of actin cytoskeleton architecture by Eps8 and Abi1. *BMC Cell Biology*. **6**. 1–15.

Rondina, M. T., Freitag, M., Pluthero, F. G., Kahr, W. H. A., Rowley, J. W., Kraiss, L. W., Franks, Z., Zimmerman, G. A., Weyrich, A. S., & Schwertz, H. (2016). Non-genomic activities of retinoic acid receptor alpha control actin cytoskeletal events in human platelets. *Journal of Thrombosis and Haemostasis*. **14**. 1082–1094.

Rondina, M.T. & Weyrich, A.S., (2012). Targeting phosphodiesterases in anti-platelet therapy. A*ntiplatelet Agents.* 225-238. Springer, Berlin, Heidelberg.

Rosentreter, A., Hofmann, A., Xavier, C. P., Stumpf, M., Noegel, A. A., & Clemen, C. S. (2007). Coronin 3 involvement in F-actin-dependent processes at the cell cortex. *Experimental Cell Research*. **313**. 878–895.

Rottner, K., & Stradal, T. E. B. (2015). How distinct Arp2/3 complex variants regulate actin filament assembly. *Nature Cell Biology*. **18**. 1–3.

Rowley, J. W., Oler, A. J., Tolley, N. D., Hunter, B. N., Low, E. N., Nix, D. a, Yost, C. C., Zimmerman, G. a, & Weyrich, A. S. (2011). Genome wide RNA-seq analysis of human and mouse platelet transcriptomes. *Blood*. **118**. e101-11.

Ruiz, F. A., Lea, C. R., Oldfield, E., & Docampo, R. (2004). Human platelet dense granules contain polyphosphate and are similar to acidocalcisomes of bacteria and unicellular eukaryotes. *Journal of Biological Chemistry*. **279**. 44250–44257.

Rumi-Masantea, J., Rusingab, F. I., Lestera, T. E., Dunlapa, T. B., Williamsc, T. D., Dunkerd, A. K., Weisb, D. D., & Creamera, T. P. (2012). Structural basis for

activation of calcineurin by calmodulin. Journal of Molecular Biology*. **415**. 307–317.

Rybakin, V., & Clemen, C. S. (2005). Coronin proteins as multifunctional regulators of the cytoskeleton and membrane trafficking. *BioEssays*. **27**. 625–632.

Rybakin, V., Stumpf, M., Schulze, A., Majoul, I. V., Noegel, A. A., & Hasse, A. (2004). Coronin 7, the mammalian POD-1 homologue, localizes to the Golgi apparatus. *FEBS Letters*. **573**. 161–167.

Sakariassen, K. S., Bolhuis, P. A., & Sixma, J. J. (1979). Human blood platelet adhesion to artery subendothelium is mediated by factor VIII-Von Willebrand factor bound to the subendothelium. *Nature*. **279**. 636–638).

Sato, H., Muraoka, S., Kusunoki, N., Masuoka, S., Yamada, S., Ogasawara, H., Imai, T., Akasaka, Y., Tochigi, N., Takahashi, H., Tsuchiya, K., Kawai, S., & Nanki, T. (2017). Resistin upregulates chemokine production by fibroblast-like synoviocytes from patients with rheumatoid arthritis. *Arthritis Research and Therapy*. **19**. 6–11.

Schwer, H. D., Lecine, P., Tiwari, S., Italiano, J. E., Hartwig, J. H., & Shivdasani, R. A. (2001). A lineage-restricted and divergent β-tubulin isoform is essential for the biogenesis, structure and function of blood platelets. *Current Biology*. **11**. 579-586.

Shattil, S. J. (1999). Signaling through platelet integrin alpha IIb beta 3: inside-out, outside-in, and sideways. *Thrombosis and Haemostasis*, *82*(2), 318–31825.

Shina, M. C., & Noegel, A. A. (2008). Invertebrate coronins. *Subcellular Biochemistry*. **48**, 88–97.

Shiow, L. R., Paris, K., Akana, M. C., Cyster, J. G., Sorensend, R. U., & Puck, J. M. (2009). Severe Combined Immunodeficiency (SCID) and Attention Deficit Hyperactivity Disorder (ADHD) Associated with a Coronin-1A Mutation and a Chromosome 16p11.2 Deletion. *Clinical immunology*. **131**. 24–30.

Shiow, L. R., Roadcap, D. W., Paris, K., Waston, S. R., Grigorova, I. L., Lebet, T., An, J., Xu, Y., Jenne, C. N., Föger, N., & Cyster, J. G. (2008). The actin regulator coronin-1A is mutated in a thymic egress deficient mouse strain and in a T− B+ NK+ SCID patient. *Nature Immunology*. **9**. 1307–1315.

Siegmund, K., Thuille, N., Posch, N., Fresser, F., & Baier, G. (2015). Novel Protein kinase C θ: Coronin 1A complex in T lymphocytes. *Cell Communication and Signaling*. **13**. 1–8.

Simon, D. I. (2011). Opening the field of integrin biology to "biased agonism." *Circulation Research*. **109**. 1199–1201.

Smolenski, A. (2012). Novel roles of cAMP/cGMP-dependent signaling in platelets. *Journal of Thrombosis and Haemostasis*. **10**. 167–176.

Smyth, S. S., Mcever, R. P., Weyrich, A. S., Morrell, C. N., Hoffman, M. R., Arepally, G. M., French, P. A., Dauerman, H. L., & Becker, R. C. (2009). Platelet functions beyond hemostasis. *Journal of Thrombosis and Haemostasis*. **7**. 1759–1766.

Soulet, C., Gendreau, S., Missy, K., Benard, V., Plantavid, M., & Payrastre, B. (2001). Characterisation of Rac activation in thrombin- and collagen- stimulated human blood platelets. *FEBS Letters*. **507**. 253–258.

Spoerl, Z., Stumpf, M., Noegel, A. A., & Hasse, A. (2002). Oligomerization, F-actin interaction, and membrane association of the ubiquitous mammalian coronin 3 are mediated by its carboxyl terminus. *Journal of Biological Chemistry*. **277**. 48858–48867.

Springer, T. A., Zhu, J., & Xiao, T. (2008). Structural basis for distinctive recognition of fibrinogen γC peptide by the platelet integrin αIIbβ3. *Journal of Cell Biology*. **182**. 791–800.

Stelzer, G., Rosen, N., Plaschkes, I., Zimmerman, S., Twik, M., Fishilevich, S., & Kaplan, S. (2016). The GeneCards suite: from gene data mining to disease genome sequence analyses. *Protocols in Bioinformatics*. **54**. 1–30.

Stocker, T. J., Pircher, Ã. J., Skenderi, Ã. A., Ehrlich, A., Megens, R. T. A., Petzold, T., Zhang, Z., Walzog, B., Weber, A. M. C., Massberg, S., Ishikawa-ankerhold, H., Schulz, Ã. C., & Eberle, C. (2018). The Actin Regulator Coronin-1A Modulates Platelet Shape Change and Consolidates Arterial Thrombosis. *Cellular Haemostasis and Platelets*. **118**. 2098–2111.

Stritt, S., Beck, S., Becker, I. C., Vögtle, T., Hakala, M., Heinze, K. G., Du, X., Bender, M., Braun, A., Lappalainen, P., & Nieswandt, B. (2017). Twinfilin 2a

regulates platelet reactivity and turnover in mice. *Blood*. **130**. 1746–1756.

Subramanian, H., Zahedi, R. P., Sickmann, A., Walter, U., & Gambaryan, S. (2013). Phosphorylation of CalDAG-GEFI by protein kinase A prevents Rap1b activation. Journal of Thrombosis and Haemostasis. **11**. 1574-1582.

Sunahara, R. K., & Insel, P. A. (2016). The molecular pharmacology of G protein signaling then and now: A tribute to alfred G. Gilman. *Molecular Pharmacology*. **89**. 585–592.

Suo, D., Park, J., Young, S., Makita, T., & Deppmann, C. D. (2015). Coronin-1 and Calcium Signaling Governs Sympathetic Final Target Innervation. *Journal of Neuroscience*. **35**. 3893–3902.

Svitkina, T. (2018). The actin cytoskeleton and actin-based motility. *Cold Spring Harbor Perspectives in Biology*. **10**. 1–21.

Swaminathan, K., Müller-Taubenberger, A., Faix, J., Rivero, F., & Noegel, A. A. (2013). A Cdc42- and Rac-interactive binding (CRIB) domain mediates functions of coronin. *Proceedings of the National Academy of Sciences of the United States of America*. **111**. E25-33.

Tang, D. D., & Gerlach, B. D. (2017). The roles and regulation of the actin cytoskeleton, intermediate filaments and microtubules in smooth muscle cell migration. *Respiratory Research*. **18**. 1–12.

Tardieux, I., Liu, X., Poupel, O., Parzy, D., Dehoux, P., & Langsley, G. (1998). A Plasmodium falciparum novel gene encoding a coronin-like protein which associates with actin filaments. *FEBS Letters*. **441**. 251–256.

Tasher, D., & Dalal, I. (2012). The genetic basis of severe combined immunodeficiency and its variants. *The Application of Clinical Genetics*. **5**. 67–80.

Taylor, M. P., Koyuncu, O. O., & Enquist, L. W. (2011). Subversion of the actin cytoskeleton during viral infection. *Nature Reviews. Microbiology*. **9**. 427–439.

Tchang, V. S. Y., Stiess, M., Siegmund, K., Karrer, U., & Pieters, J. (2016). Role for coronin 1 in mouse NK cell function. *Immunobiology*. **222**. 291-300.

Tertyshnikova, S., Yan, X., & Fein, A. (1998). cGMP inhibits IP3-induced Ca2+ release in intact rat megakaryocytes via cGMP- and cAMP-dependent protein

kinases. *Journal of Physiology*. **512**. 89–96.

Thiele, T., Braune, J., Dhople, V., Hammer, E., Scharf, C., Greinacher, A., Volker, U., & Steil, L. (2016). Proteomic profile of platelets during reconstition of platelet counts after apheresis. *Proteomics. Clinical Applications*. **10**. 831–838.

Thomas, S. G., Poulter, N. S., Bem, D., Finney, B., Machesky, L. M., & Watson, S. P. (2016). The actin binding proteins cortactin and HS1 are dispensable for platelet actin nodule and megakaryocyte podosome formation. *Platelets*. **28**. 72-379.

Thome, S., Begandt, B., Pick, R., Salvermoser, M., & Barbara, W. (2018). Intracellular β 2 integrin (CD11/CD18) interacting partners in neutrophil trafficking. *European Journal of Clinical Investigation*. **54**. 2404–2408.

Thon, J. N., & Italiano, J. E. (2012). Platelets: Past, present and future. *Handbook of Experimental Pharmacology*. **210**. 3–22.

Tojkander, S., Gateva, G., & Lappalainen, P. (2012). Actin stress fibers - assembly, dynamics and biological roles. *Journal of Cell Science*. **125**. 1855–1864.

Tonon, G., Luo, X., Greco, N. J., Chen, W., Shi, Y., & Jamieson, G. A. (2002). Weak platelet agonists and U46619 induce apoptosis-like events in platelets, in the absence of phosphatidylserine exposure. *Thrombosis Research*, **107**. 345–350.

Torti, M., Bertoni, A., Canobbio, I., Sinigaglia, F., Lapetina, E. G., & Balduini, C. (1999). Rap1B and Rap2B translocation to the cytoskeleton by von Willebrand factor involves FCγII receptor-mediated protein tyrosine phosphorylation. *Journal of Biological Chemistry*. **274**. 13690-13697.

Tsujita, K., Itoh, T., Kondo, A., Oyama, M., Kozuka-Hata, H., Irino, Y., Hasegawa, J., & Takenawa, T. (2010). Proteome of acidic phospholipid-binding proteins: Spatial and temporal regulation of coronin 1A by phosphoinositides. *Journal of Biological Chemistry*. **285**. 6781–6789.

Uetrecht, A. C., & Bear, J. E. (2006). Coronins: the return of the crown. In *Trends in Cell Biology*. *16*. 421–426).

Uhlén, M., Fagerberg, L., Hallström, B. M., Lindskog, C., Oksvold, P., Mardinoglu, A., Sivertsson, Å., Kampf, C., Sjöstedt, E., Asplund, A., Olsson, I., Edlund, K., Lundberg, E., Navani, S., Szigyarto, C. A., Odeberg, J., Djureinovic, D.,

Takanen, J. O., Hober, S., … Pontén, F. (2015). Tissue-based map of the human proteome. *Science.* **347**. 1260419

van der Meijden, P. E. J., & Heemskerk, J. W. M. (2019). Platelet biology and functions: new concepts and clinical perspectives. *Nature Reviews Cardiolog.* **16**. 166–179.

Vanguri, V. K., Wang, S., Godyna, S., Ranganathan, S., & Liau, G. (2000). Thrombospondin-1 binds to polyhistidine with high affinity and specificity. *The Biochemical Journal.* **347**. 469–473.

Varga-Szabo, D., Pleines, I., & Nieswandt, B. (2008). Cell adhesion mechanisms in platelets. *Arteriosclerosis, Thrombosis, and Vascular Biology.* **28**. 403–413.

Vartiainen, M. K., Mustonen, T., Mattila, P. K., Ojala, P. J., Thesleff, I., Partanen, J., & Lappalainen, P. (2002). The three mouse actin-depolymerizing factor/cofilins evolved to fulfill cell-type-specific requirements for actin dynamics. *Molecular Biology of the Cel.* **13**. 183–194.

Verhoeven, A. J. M., Mommersteeg, M. E., & Akkerman, J.-W. N. (1984). Metabolic energy is required in human platelets at any stage during optical aggregation and secretion. *Biochimica EtBiophvsica Acta.* **800**. 242–250.

Vinet, A. F., Fiedler, T., Studer, V., Froquet, R., Dardel, A., Cosson, P., & Pieters, J. (2014). Initiation of multicellular differentiation in Dictyostelium discoideum is regulated by coronin A. *Molecular Biology of the Cell.* **25**. 688–701.

von Andrian, U. H., Hasslen, S. R., Nelson, R. D., Erlandsen, S. L., & Butcher, E. C. (1995). A central role for microvillous receptor presentation in leukocyte adhesion under flow. *Cell.* **82**. 989–999.

Wagner, A.R., Luan, Q., Liu, S. L., & Nolen, B. J. (2013). WISH/DIP/SPIN90 proteins form a class of Arp2/3 complex activators that function without preformed actin filaments. *Current Biology.* **23**. 1990–1998.

Wang, C., Zhou, G. L., Vedantam, S., Li, P., & Field, J. (2008). Mitochondrial shuttling of CAP1 promotes actin- and cofilin-dependent apoptosis. *Journal of Cell Science.* **121**. 2913–2920.

Wang, Y., Gao, H., Shi, C., Erhardt, P. W., Pavlovsky, A., Soloviev, D. A., Bledzka, K., Ustinov, V., Zhu, L., Qin, J., Munday, A. D., Lopez, J., Plow, E., & Simon, D.

I. (2017). Leukocyte integrin Mac-1 regulates thrombosis via interaction with platelet GPIbα. *Nature Communications*. **8**. 1-16

Wardell, M. R., Reynolds, C. C., Berndt, M. C., Wallace, R. W., & Fox, J. E. B. (1989). Platelet glycoprotein Ib(β) is phosphorylated on serine 166 by cyclic AMP-dependent protein kinase. *Journal of Biological Chemistry*. **264**. 15656–15661.

Watson, S. P., Herbert, J. M. J., & Pollitt, A. Y. (2010). GPVI and CLEC-2 in hemostasis and vascular integrity. *Journal of Thrombosis and Haemostasis*. **8**. 1456–1467.

Welch, & Mullins. (2002). Cellular control of actin nucleation. *Annual Review of Cell and Developmental Biology*. **18**. 247–288.

Westritschnig, K., BoseDasgupta, S., Tchang, V., Siegmund, K., & Pieters, J. (2013). Antigen processing and presentation by dendritic cells is independent of coronin 1. *Molecular Immunology*. **53**. 379–386.

Williamson, R. C., Cowell, C. A. M., Hammond, C. L., Bergen, D. J. M., Roper, J. A., Feng, Y., Rendall, T. C. S., Race, P. R., & Bass, M. D. (2014). Coronin-1C and RCC2 guide mesenchymal migration by trafficking Rac1 and controlling GEF exposure. *Journal of Cell Science*. **127**. 4292–4307.

Williamson, R. C., Cowell, C. a. M., Reville, T., Roper, J. a., Rendall, T. C. S., & Bass, M. D. (2015). Coronin-1C protein and caveolin protein provide constitutive and inducible mechanisms of Rac1 protein trafficking. *Journal of Biological Chemistry*. **290**. 15437-15449.

Witke, W., Sharpe, A. H., Hartwig, J. H., Azuma, T., Stossel, T. P., & Kwiatkowski, D. J. (1995). Hemostatic, inflammatory, and fibroblast responses are blunted in mice lacking gelsolin. *Cell*. **81**. 41–51.

Wolf, B. B., Goldstein, J. C., Stennicke, H. R., Beere, H., Amarante-Mendes, G. P., Salvesen, G. S., & Green, D. R. (1999). Calpain functions in a caspase-independent manner to promote apoptosis-like events during platelet activation. *Blood*. **94**. 1683–1692.

Wolf, E., Kim, P. S., & Berger, B. (1997). MultiCoil: A program for predicting two-and three-stranded coiled coils. *Protein Science*. **6**. 1179–1189.

Woolfson, D. N., & Alber, T. (1995). Predicting oligomerization states of coiled coils. *Protein Science*. **4**. 1596–1607.

Wu, Y., Ai, Z., Yao, K., Cao, L., Du, J., Shi, X., Guo, Z., & Zhang, Y. (2013). CHIR99021 promotes self-renewal of mouse embryonic stem cells by modulation of protein-encoding gene and long intergenic non-coding RNA expression. *Experimental Cell Research*. **319**. 2684–2699.

Xavier, C.-P., Rastetter, R. H., Blömacher, M., Stumpf, M., Himmel, M., Morgan, R. O., Fernandez, M.-P., Wang, C., Osman, A., Miyata, Y., Gjerset, R. a, Eichinger, L., Hofmann, A., Linder, S., Noegel, A. a, & Clemen, C. S. (2012). Phosphorylation of CRN2 by CK2 regulates F-actin and Arp2/3 interaction and inhibits cell migration. *Scientific Reports*. **2**. 1-14

Xue, B., & Robinson, R. C. (2013). Guardians of the actin monomer. *European Journal of Cell Biology*. **92**. 316–332.

Yadav, S., Williamson, J. K., Aronova, M. A., Prince, A. A., Pokrovskaya, I. D., Leapman, R. D., & Storrie, B. (2017). Golgi proteins in circulating human platelets are distributed across non-stacked, scattered structures. *Platelets*. **28**. 400–408.

Yamin, R., & Morgan, K. G. (2012). Deciphering actin cytoskeletal function in the contractile vascular smooth muscle cell. *The Journal of Physiology*. **590**. 4145–4154.

Yan, M, Collins, R. F., Grinstein, S., & Trimble, W. S. (2005). Coronin-1 Function Is Required for Phagosome Formation. *Molecular Biology of the Cell*. **16**. 3077–3087.

Yan, Ming, Di Ciano-Oliveira, C., Grinstein, S., & Trimble, W. S. (2007). Coronin function is required for chemotaxis and phagocytosis in human neutrophils. *Journal of Immunology.* **178**. 5769–5778.

Zeiler, M., Moser, M., & Mann, M. (2014). Copy number analysis of the murine platelet proteome spanning the complete abundance range. *Molecular & Cellular Proteomics : MCP*. **13**. 3435–3445.

Zelicof, A., Protopopov, V., David, D., Lin, X. Y., Lustgarten, V., & Gerst, J. E. (1996). Two separate functions are encoded by the carboxyl-terminal domains

of the yeast cyclase-associated protein and its mammalian homologs. Dimerization and actin binding. *Journal of Biological Chemistry*. **271**. 18243–18252.

Zhang, H., Ghai, P., Wu, H., Wang, C., Field, J., & Zhou, G. L. (2013). Mammalian adenylyl cyclase-associated protein 1 (CAP1) regulates cofilin function, the actin cytoskeleton, and cell adhesion. *Journal of Biological Chemistry*. **288**. 20966–20977.

Zhang, H., Ramsey, A., Xiao, Y., Karki, U., Xie, J. Y., Xu, J., Kelly, T., Ono, S., & Zhou, G.-L. (2020). Dynamic Phosphorylation and Dephosphorylation of Cyclase-Associated Protein 1 by Antagonistic Signaling through Cyclin-Dependent Kinase 5 and cAMP Are Critical for the Protein Functions in Actin Filament Disassembly and Cell Adhesion. *Molecular and Cellular Biology*. **40**. 1–24.

Zhang, M., Yan, L., Wang, G. J., & Jin, R. (2019). Resistin effects on pancreatic cancer progression and chemoresistance are mediated through its receptors CAP1 and TLR4. *Journal of Cellular Physiology*. **234**. 9457–9466.

Zhou, G. L., Zhang, H., Wu, H., Ghai, P., & Field, J. (2014). Phosphorylation of the cytoskeletal protein CAP1 controls its association with cofilin and actin. *Journal of Cell Science*. **127**. 5052–5065.

Zimmerman, G. a, & Weyrich, A. S. (2008). Signal-Dependent Protein Synthesis by Activated Platelets. *Arteriosclerosis & Thrombosis*. **28**. 17–24

Zuidscherwoude, M., Green, H. L. H., & Thomas, S. G. (2019). Formin proteins in megakaryocytes and platelets: regulation of actin and microtubule dynamics. *Platelets*. **30**. 23–30.

8 Appendix

8.1 Additional experimental data

8.1.1 Coronin 2 associates with the Triton X-100 insoluble pellet

This study previously summarised how human platelets were stimulated by thrombin in a time course, lysed, subjected to a of the Triton X-100 insoluble fractionation and probed with SDS-PAGE/WB (**Figure 3.2.4**). The membranes were also probed with coronin 2, however the signal was weak and the protein was degraded so the data was not considered strong enough for the main text. Coronin 2 demonstrated a comparable trend over the time course of thrombin (**Appendix 8.1.1A**) or collagen (**Appendix 8.1.1B**) to coronin 1 and 3. However coronin 2 only reached statistical significance at 120 and 180 seconds for thrombin and 30 and 120 seconds for collagen. This may be due to the relative low power (3) and high experimental deviation (**Appendix 8.1.1A & B**). More experimental repeats would likely yield different statistical significances. This indicates that coronins 1, 2 and 3 are F-actin associated in human platelets.
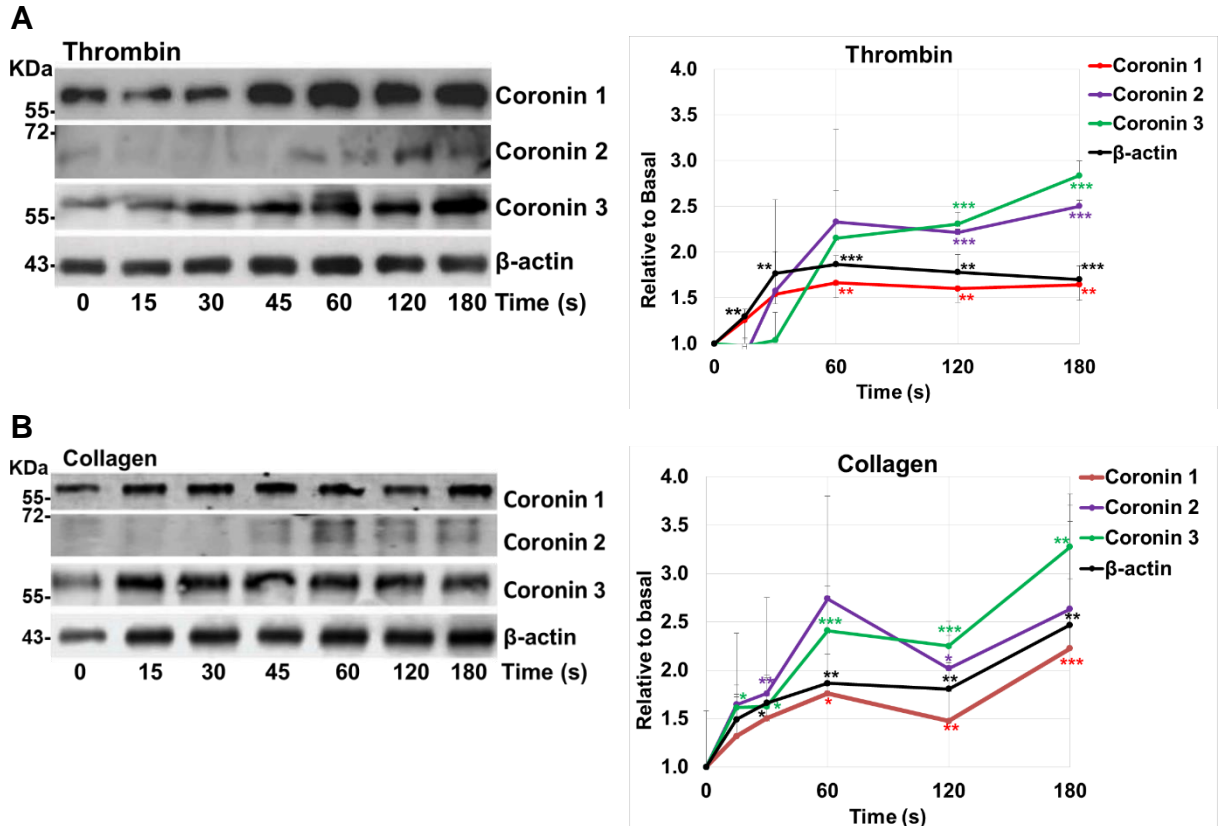
Appendix 8.1.1 – Coronin 2 association with the Triton X-100 insoluble pellet in human platelets.
Experiment performed as in **Figure 3.2.**. Probing for coronin 2 was performed on the same membrane as with coronin 1 and 3 for thrombin (**A**) and collagen (**B**) treatments.

8.1.2 Human platelet aggregation dose responses

Human platelets were subjected to aggregation prior to experiments including membrane/cytosol fractionation and Triton X-100 insoluble pellet fractionation, to titrate agonists and to ensure strong aggregation responses occurred with (**Appendix 8.1.2A**) thrombin and collagen (**Appendix 8.1.2B**). 0.1 U/ml thrombin and 50 µg/ml collagen were the highest doses which achieved 83% (**Figure 8.1.2A)** or 92 % aggregation, respectively at 5 minutes (**Appendix 8.1.2A & B**). A detailed titration of murine platelets in aggregation is provided in **Section 4.2.7**. This indicates the dose that should be a strong agonist for experiments across this thesis including fractionations.
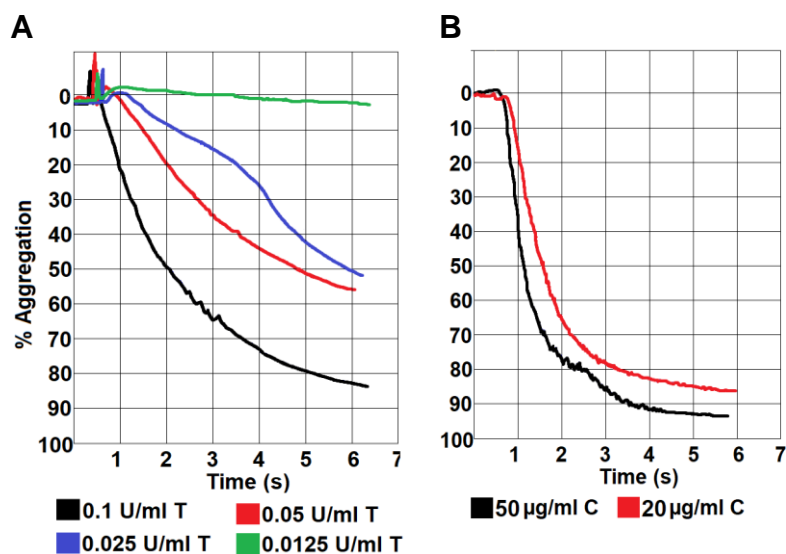
Appendix 8.1.2 – Human platelet aggregation dose response.
245 µl of washed human platelets at 3×10^8 ml^{-1} were subjected to aggregation for over 5 minutes with stirring at 1000 RPM at 37°C in a Chrono-log aggregometer (Chronolog Instrument 490 + 4) by the addition of 5 µl of thrombin (**A**) or collagen (**B**), resulting in the final concentrations indicated. T = thrombin, C = collagen.

8.1.3 Presence of coronins 1, 2 , 3 and 7 in human and mouse platelets

The most sensitive studies of the presence of coronin mRNA and proteins in platelets were summarised in **Figure** & **Figure** . Several additional, less sensitive, proteomic and transcriptomic studies have also found coronins in platelets. The presence of at least 3 members of the coronin family have been detected in platelets. A study which identified just over 1000 proteins in human platelets found coronin 1, 2 and 3 in the platelet proteome (Thiele *et al*. 2016, suppl 2). A more comprehensive and sensitive study which found around 4000 proteins in human platelets found coronin 1, 2, 3 and also 7 in platelets (Burkhart *et al*. 2012 suppl 3) (**Appendix 8.1.3**) The Plateletweb database states that coronin 1, 2 and 3 have been detected in platelets but not 4, 5, 6 or 7 (Boyanova, *et al*. 2011). Coronin 1 is the most abundant protein in human platelets, followed closely by coronin 3, coronin 2 is less abundant and coronin 7 demonstrates a relatively extremely low abundance (Burkhart, *et al*. 2012, suppl 3). The data for murine platelets is more

254

limited. A study of the murine platelet proteome found 17,100 copies per cell of coronin 1, 3200 copies per cell of coronin 2, 3000 copies per cell of coronin 3 and 700 copies per cell of coronin 7 (Zeiler *et al.*, 2014). To summarise the proteomic data, it appears that coronin proteins 1, 2 and 3 are abundant in platelets, levels of coronin 7 are very low and 4, 5 and 6 have never been found in platelets. These findings are summarised in **Appendix 8.1.3**.

A transcriptomics study which found over 5000 transcripts in human platelets found transcripts for coronin 1, 2 and 3 in platelets. This study also determined there is only a weak correlation between transcripts and the proteome in platelets (Londin, *et al.* 2014) (**Appendix 8.1.3**). However transcript abundance does not necessarily correlate with protein abundance or even presence.

A transcriptomics study which analysed both mouse and human platelets examined reads per kilobase of exon model per million mapped reads (RPKM). The study in human platelets found the transcripts abundance order was coronin 3, 1 and 2 (all high), followed by coronin 7 (lower), coronins 4 and 5 (extremely low levels) and no transcripts for coronin 6. In mice the order of abundance of transcripts was coronin 2, 3, 1 (high) followed by 7 (lower) then coronins 6, 4 (extremely low) with no transcripts for coronin 5 (Rowley *et al.*, 2011) (**Appendix 8.1.3**).

Appendix 8.1.3 – Presence of different coronin proteins/transcripts in human and mouse platelets.

Protein	Organism	Type	Method	Abundance	Reference
Coronin 1	Human	**Protein**	LC-ESI-MS/MS and 2D-DIGE	Present	(Thiele *et al.*, 2016)
	Human	**Protein**	Quantitative mass spectrometry	23,400 copies per cell	(Burkhart *et al.*, 2012)
	Human	**Protein**	Mass Spectrometry	17100 copies per cell	(Zeiler *et al.*, 2014)
	Human	Transcript	PCR of total RNA	Present	(Londin, *et al.*

255

			(transcript)		2014)
	Human	Transcript	RNA-seq	16.07 RPKM	(Rowley *et al.*, 2011)
	Mouse	Transcript	RNA-seq	1.61 RPKM	(Rowley *et al.*, 2011)
Coronin 2	Human	**Protein**	LC-ESI-MS/MS and 2D-DIGE	Present	(Thiele *et al.*, 2016)
	Human	**Protein**	Quantitative mass spectrometry	6,900 copies per cell	(Burkhart *et al.*, 2012)
	Human	**Protein**	Mass Spectrometry	3200 copies per cell	(Zeiler *et al.*, 2014)
	Human	Transcript	PCR of total RNA (transcript)	Present	(Londin, *et al.* 2014)
	Human	Transcript	RNA-seq	11.79 RPKM	(Rowley *et al.*, 2011)
	Mouse	Transcript	RNA-seq	41.18 RPKM	(Rowley *et al.*, 2011)
Coronin 3	Human	**Protein**	LC-ESI-MS/MS and 2D-DIGE	23,300 copies per cell	(Thiele *et al.*, 2016)
	Human	**Protein**	Quantitative mass spectrometry	Present	(Burkhart *et al.*, 2012)
	Human	**Protein**	Mass Spectrometry	3000 copies per cell	(Zeiler *et al.*, 2014)
	Human	Transcript	PCR of total RNA (transcript)	Present	(Londin, *et al.* 2014)
	Human	Transcript	RNA-seq	73.46 RPKM	(Rowley *et al.*, 2011)
	Mouse	Transcript	RNA-seq	21.31 RPKM	(Rowley *et al.*, 2011)
Coronin 4	Human	Transcript	RNA-seq	0.01 RPKM	(Rowley *et al.*, 2011)
	Mouse	Transcript	RNA-seq	0.01 RPKM	(Rowley *et al.*, 2011)
Coronin 5	Human	Transcript	RNA-seq	0.02 RPKM	(Rowley *et al.*, 2011)

Coronin 6	Mouse	Transcript	RNA-seq	0.07 RPKM	(Rowley *et al.*, 2011)
Coronin 7	Human	**Protein**	Quantitative mass spectrometry	760 copies per cell	(Burkhart *et al.*, 2012)
	Human	**Protein**	Mass Spectrometry	700 copies per cell	(Zeiler *et al.*, 2014)
	Human	Transcript	RNA-seq	1.70 RPKM	(Rowley *et al.*, 2011)
	Mouse	Transcript	RNA-seq	0.71 RPKM	(Rowley *et al.*, 2011)

8.1.4 Platelet apoptosis

During apoptosis, CAP1 has been reported to rapidly translocate to the mitochondria independently of caspase activation (C. Wang *et al.*, 2008). Platelets have a short lifespan and undergo apoptosis over time. The calcium ionophore or treatment with a high dose of thrombin has been reported to induce apoptosis in platelets (Gyulkhandanyan *et al.*, 2013). Platelets also undergo apoptosis over time and a marker of this is a breakdown product of gelsolin (Tonon et al., 2002; Wolf et al., 1999). Treatment with thrombin or the calcium ionophore has been reported to cause platelet apoptosis, determined by membrane potential depolarisation (Gyulkhandanyan *et al.*, 2013). With a view to investigating CAP1 localisation on platelets undergoing apoptosis, controls to confirm platelet apoptosis were performed. Platelets were lysed immediately after isolation or left for 28 hours at 37°C or treated with 0.1 to 5 U/ml thrombin for 15 minutes at 37°C or with 10 µM of calcium ionophore A23187 for 15 minutes at 37°C. A band showing a breakdown product of gelsolin at ~50 KDa was present in the platelets which were left for 28 hours which is not in the control platelets (**Appendix 7.1.4 A**), indicating that apoptosis had occurred. However, probing for gelsolin could not detect breakdown products after thrombin (**Appendix 8.1.4B**) or calcium ionophore treatment (**Appendix 8.1.4C**), so the occurrence of apoptosis was inconclusive

257
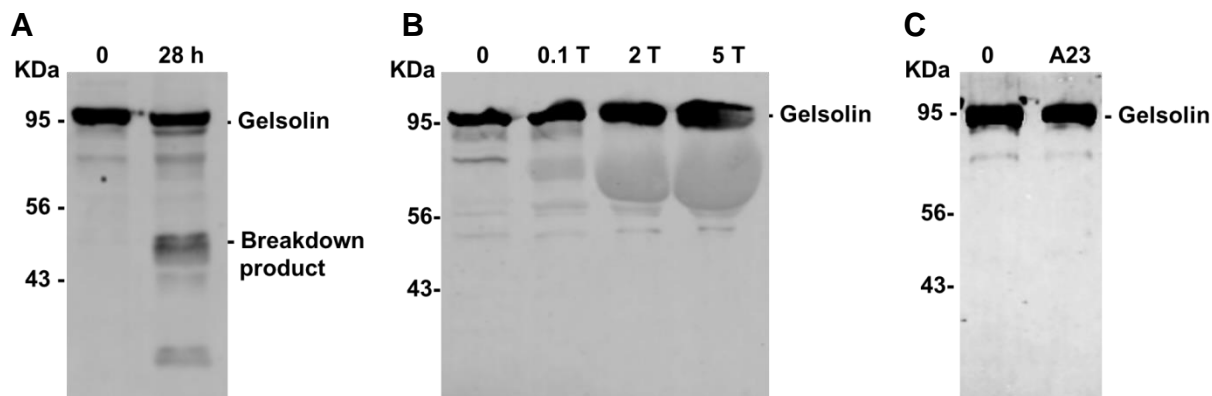
Appendix 8.1.4 - Platelet apoptosis.
Platelets were produced and either immediately lysed with Laemmli buffer or left for 28 hours at 37°C, or treated with 0.1, 2 or 5 U/ml thrombin for 15 minutes at 37°C. or treated with 10 µm A23187 for 15 minutes at 37°C, then lysed. Lysates were subjected to SDS-PAGE/WB and probed for gelsolin. The full length gelsolin is present near the 95 KDa marker and the breakdown product is visible in the 28 hour sample at around 50 KDa.

8.1.5 WBC-platelet interaction: blood lysis and fixing controls for FACS

Cells can be visualised on FACS by their size as forward scatter (FSC) and granularity as side scatter (SSC), with WBCs being the largest and most granulated, followed by RBCs, then platelets. It should be noted that in human WBCs subjected to FACS, the granulocytes appear as the largest and granulated, followed by monocytes then lymphocytes. However, murine WBCs do not demonstrate distinct populations on FSC and SSC alone and appear as a dispersed cluster of cells, some larger than RBCs and some overlapping.

Integrin β2, with CD11 forms LFA-1 and can bind to ICAM-1 on WBCs (Thome *et al.*, 2018). Coronin 1 was found to be required for β2 integrin translocation in platelets with a view to determining if platelet-WBC intercations are impaired in *Coro1A*$^{-/-}$ platelets, lysis and fixing control were performed on murine blood. In unfixed and unlysed blood, the platelets, RBCs and WBCs can be identified with platelets the smallest and least granulated and WBCs being the largest and most granulated. RBCs are in the middle and overlap with WBCs (**Appendix 8.1.5A**). Upon treatment, the blood would need to be fixed and the RBCs removed before analysis. 5x BD fix/lyse buffer destroyed the RBCs,

258

generating cellular debris which obscured the WBCs and it also destroyed the majority of the WBCs, likely due to the high methanol content (**Appendix 8.1.5B**). High yield fix/lyse buffer lysed the RBCs and the debris was much smaller and the WBCs were intact (**Appendix 8.1.5C**). 10x BD fix/lyse buffer destroyed the RBCs and generated cellular debris which obscured the WBCs (**Appendix 8.1.5D**).

The WBC populations stained very intensely for CD45 before and after fixation and lysis (data not shown). The platelet population stained intensely for GPVI (data not shown), however they could only be stained in blood that was not fixed or lysed as this process resulted in the platelet population becoming obscured by cellular debris (**Appendix 8.1.5B** - **D**). Subsequent experiments attempted to analyse the platelet-WBC binding but were not continued due to unsatisfactory reproducibility, inability of antibodies and peptides to block undesirable platelet-WBC interactions and time constraints.
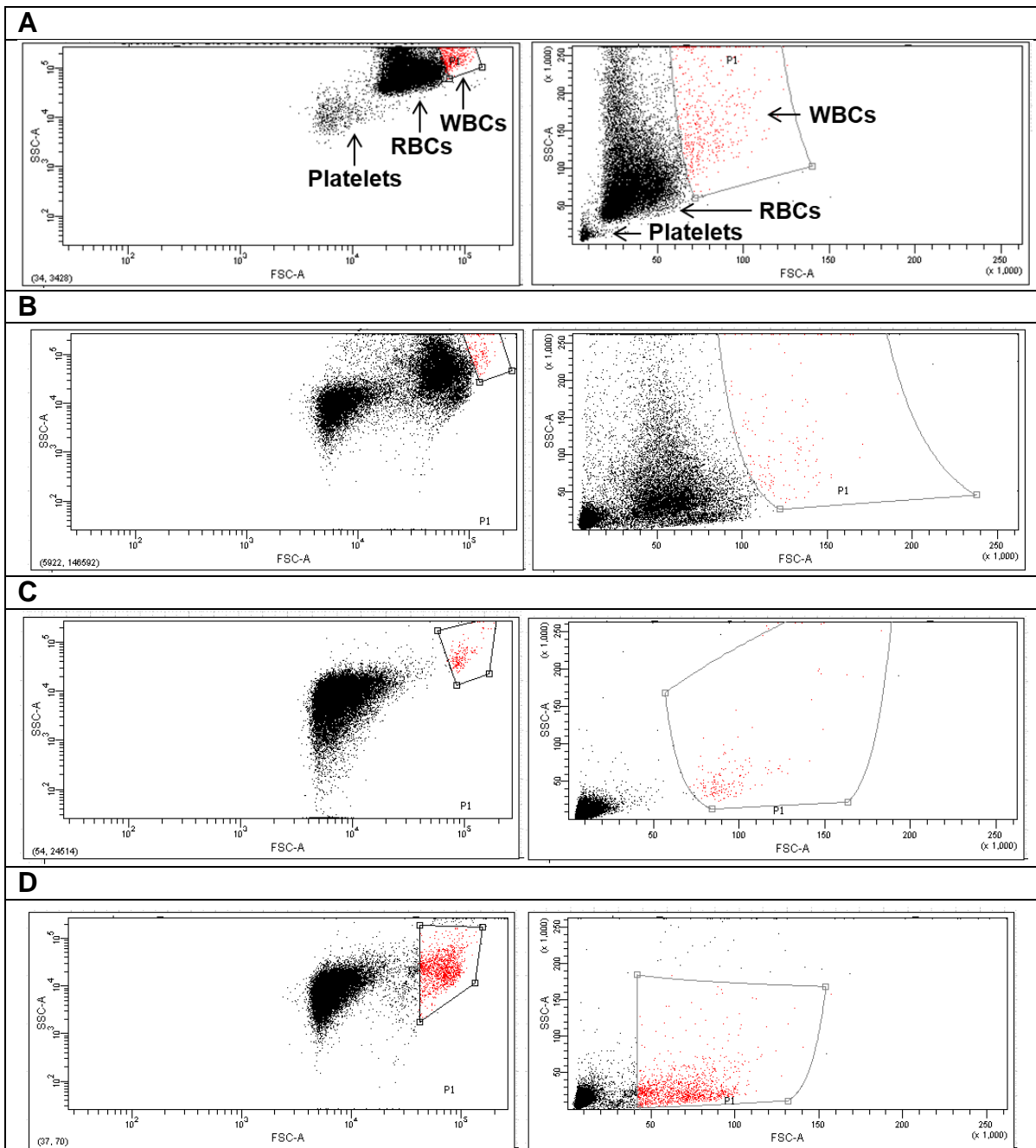
Appendix 8.1.5 - FACS blood lysis and fixing controls.
Left FSC not logged, right FSC logged. **A**) Murine blood with no fixing or lysis. The platelets are in the bottom left and the WBCs are in the top right (red) with the RBCs in the middle overlapping with WBCs. **B**) 5x BD fix/lyse buffer. **C**) High yield fix/lyse buffer. **D**) BD 10x fix/lyse buffer. P1 represents the WBCs. 300 V FSC, 325 V SSC. Threshold 5000. The number of events counted is not consistent in each graph.

8.1.6 Calcium measurements on Flexstation

Coronin 1 is involved in calcium/calcineurin signaling and is required for survival in T cells (Mueller *et al.*, 2008). An experiment to measure the calcium content over platelets over a time course was optimised, with a view to testing *Coro1A*$^{-/-}$ platelets. Platelets were incubated in either CaCl$_2$ calcium or a negative control of EGTA in the dark with 2 µM Fluo-3 for 1 hour. They were subjected to 2 injections, one at 30 and one at 930 seconds – first with thrombin (to a final concentration of 0.1 U/ml) or a negative control of MTB followed by a second injection of either a calcium ionophore (to a final concentration of 10 µM A23187 or a negative control of MTB. The platelets incubated in calcium and treated with thrombin demonstrated a peak which was not present in the other samples, demonstrating it was caused by thrombin and calcium and not by displacement. The two samples incubated with calcium then injected with A23187 demonstrated a peak whereas the other 4 samples did not, demonstrating the peak is due to calcium levels and not displacement (**Appendix 8.1.6**). The conditions could not be optimised with murine platelets due to their different behavior as well as resources and time constraints.
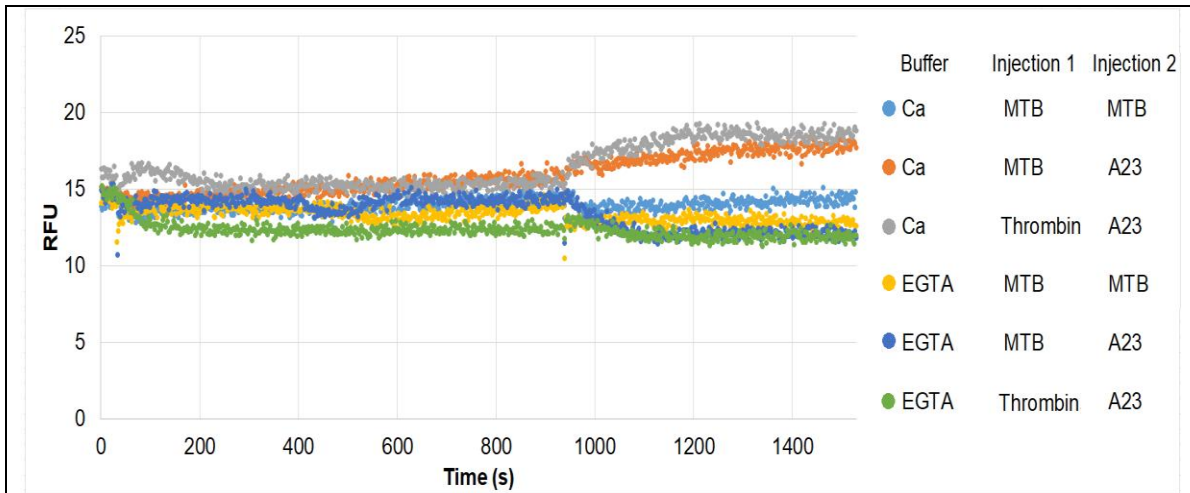
Appendix 8.1.6 - Time course of calcium measurements in human platelets.
Platelets were incubated in either 2 mM calcium or a negative control of 4 mM EGTA. They were subjected to 2 injections, one at 30 and one at 930 seconds – first with 0.1 U/ml thrombin or a negative control of MTB followed by a second injection of either a calcium ionophore or a negative control of MTB.

8.2 Research papers

8.2.1 Biochemical and immunocytochemical characterization of coronins in platelets

Taylor & Francis
Taylor & Francis Group

Check for updates

Biochemical and immunocytochemical characterization of coronins in platelets

David R. J. Riley[1*], Jawad S. Khalil[1,2*], Khalid M. Naseem[3], & Francisco Rivero [1]

[1]Centre for Atherothrombosis and Metabolic Disease, Hull York Medical School, Faculty of Health Sciences, University of Hull, Hull, UK, [2]School of Physiology, Pharmacology and Neuroscience, Faculty of Life Sciences, University of Bristol, Bristol, UK, and [3]Leeds Institute for Cardiovascular and Metabolic Medicine, University of Leeds, Leeds, UK

Abstract

Rapid reorganization of the actin cytoskeleton in response to receptor-mediated signaling cascades allows platelets to transition from a discoid shape to a flat spread shape upon adhesion to damaged vessel walls. Coronins are conserved regulators of the actin cytoskeleton turnover but they also participate in signaling events. To gain a better picture of their functions in platelets we have undertaken a biochemical and immuno-cytochemical investigation with a focus on Coro1. We found that class I coronins Coro1, 2 and 3 are abundant in human and mouse platelets whereas little Coro7 can be detected. Coro1 is mainly cytosolic, but a significant amount associates with membranes in an actin-independent manner and does not translocate from or to the membrane fraction upon exposure to thrombin, collagen or prostacyclin. Coro1 rapidly translocates to the Triton insoluble cytoskeleton upon platelet stimulation with thrombin or collagen. Coro1, 2 and 3 show a diffuse cytoplasmic localization with discontinuous accumulation at the cell cortex and actin nodules of human platelets, where all three coronins colocalize. Our data are consistent with a role of coronins as integrators of extracellular signals with actin remodeling and suggests a high extent of functional overlap among class I coronins in platelets.

Introduction

Platelets are anucleate fragments of megakaryocytes that play pivotal roles in hemostasis, thrombosis, wound healing and immunological processes. Platelets display a remarkable morphological plasticity. While in circulation they have a characteristic discoid shape, but are capable of undergoing profound changes upon adhesion to damaged blood vessel walls, transitioning to a spherical shape that extends filopodia and lamellipodia as the cell spreads and flattens [1]. This process is accompanied by secretion of granules and activation of integrins that support and consolidate the formation of a platelet aggregate. Remodeling of the cytoskeleton, formed by a network of actin filaments and a marginal ring of microtubules and associated proteins constitutes a crucial aspect of platelet function and is the result of multiple exquisitely integrated signaling cascades [2]. A plethora of proteins with various biochemical activities is responsible for the dynamics of actin remodeling during platelet activation,

including actin nucleators like formins and the Arp2/3 complex and their regulators (WAVE, WASP), monomeric actin-binding proteins like profilin, β-thymosin and the cyclase-associated protein (CAP) and others like gelsolin, cofilin, and coronins [3–5].

Coronins constitute a family of conserved regulators of the actin cytoskeleton turnover. The defining architectural element of this family is the WD40 repeat that folds in a β-propeller structure and characteristically participates in protein–protein interactions [6]. The β-propeller is flanked by short highly conserved extensions. The C-terminal extension is followed by a variable unique region and a coiled-coil domain, and the latter involved in oligomerization [7,8]. Mammals express seven coronins that have been grouped into three classes [9,10]. Among class I coronins (Coro1, 2, 3 and 6), Coro1 is the most widely studied for its role in coordinating actin dynamics through modulation of Arp2/3 complex and cofilin function [11]. Coro1 also plays less well-understood roles in NADPH oxidase complex regulation, calcium release, vesicle trafficking and apoptosis [12–15]. Class I coronins localize at the leading edge of migrating cells and to phagosomes in neutrophils [7,15,16]. Class II coronins (Coro4 and 5) are involved in focal adhesion turnover, reorganization of the cytoskeleton and cell migration [17,18]. The class III coronin (Coro7) has an unusual structure, as it consists of two coronin blocks in tandem and lacks a coiled-coil region. This atypical coronin plays a role in Golgi morphology maintenance and does not appear to participate in actin-related processes [19].

While coronins have been widely investigated in a variety of cell types, very little is known about these proteins in platelets. A recent report investigating the role of Coro1 in platelet

---

*Equal contribution

Color versions of one or more of the figures in the article can be found online at **www.tandfonline.com/iplt**.

Correspondence: Francisco Rivero, Centre for Atherothrombosis and Metabolic Disease, Hull York Medical School, Faculty of Health Sciences, University of Hull, Hull HU6 7RX UK. E-mail: francisco. rivero@hyms.ac.uk

264

function using a knockout mouse model revealed impaired agonist-induced actin polymerization and cofilin phosphoregulation and altered thrombus formation in vivo as salient phenotypes, in the absence of an overt hemostasis defect in vivo [5]. This mild phenotype suggests a complex picture, with class I coronins potentially sharing roles extensively in platelets.

We have undertaken a biochemical and immunocytochemical investigation as an approach toward a clearer picture of the functions of coronins in platelets. We show that class I coronins are abundant in human and mouse platelets whereas little Coro7 can be detected. Coro1 is mainly cytosolic, but a significant amount associates with membranes in an actin-independent manner and does not translocate from or to the membrane fraction upon platelet stimulation. In immunocytochemistry studies, Coro1, 2 and 3 show a diffuse cytoplasmic localization with accumulation at the cell cortex and actin nodules, where all three coronins colocalize. Our study strengthens the view of complex redundancy among coronins in platelets, an aspect to take into consideration in future functional studies.

Materials and Methods

Reagents

Primary antibodies against following proteins were used: Coro1 (ab56820 and ab72212), Coro2 (ab99407), CAP1 (ab133655), β-actin (ab20272) from Abcam (Cambridge, UK); Coro3 (K6-444 hybridoma supernatant) [7], Coro7 (K37-142-1 hybridoma supernatant) [20]; CD36 (H-300 sc-9154), Syk (4D10 sc-1240), β3-integrin (HC93 sc-14009) and Gαs (sc-823) from Santa Cruz Biotechnology (Heidelberg, Germany); cofilin (D3F9 #5175), profilin-1 (#3237), phosphor-VASP (Ser157) (#3111) and phosphor-MLC (Ser19) (#3671) from Cell Signaling Technology (Leiden, The Netherlands); α-tubulin (05–829) and GAPDH (6C5-CB1001) from Calbiochem/Merck (Watford, UK); p34-Arc/ARPC2 (07–227) from Millipore/Merck; vinculin (SAB4200080) from Sigma/Merck; Myc, mouse monoclonal 9E10 (kind gift of Angelika A. Noegel, University of Cologne, Germany). Specificity of antibodies raised against Coro1, Coro2 and Coro3 was tested on recombinantly expressed proteins in HEK 293T cell lysates (Supplemental Figure 1)

Secondary antibodies Alexa Fluor 568- or 488-conjugated anti-mouse and anti-rabbit immunoglobulins (Molecular Probes, Thermo Fisher Scientific, Altrincham, UK) were used for immunofluorescence. Peroxidase-conjugated anti-mouse and anti-rabbit immunoglobulins (Merck) or IRDye 680 or IRDye 800 anti-mouse and anti-rabbit immunoglobulins (LI-COR Biosciences, Lincoln, USA) were used for Western blot.

Human fibrinogen was from Enzyme Research (Swansea, UK), collagen (Kollagenreagens Horm) was from Takeda (Osaka, Japan), latrunculin B was from Enzo Life Sciences (Exeter, UK), nocodazole and CK-666 were from Tocris Bioscience (Abingdon, UK). PGI2 was from Cayman Chemical (Michigan, USA). Thrombin, FITC or TRITC-conjugated phalloidin were from Merck. Alexa Fluor 680-conjugated phalloidin was from Thermo Fisher Scientific. Other reagents were from Merck unless otherwise indicated.

Human Platelet Preparation

Human blood was taken from drug-free volunteers by clean venepuncture into acid citrate dextrose (ACD) (29.9 mM trisodium citrate, 113.8 mM glucose, 72.6 mM NaCl and 2.9 mM citric acid, pH 6.4). Platelet-rich plasma (PRP) was obtained by centrifugation of whole blood at $190 \times g$ for 15 min at room temperature. Platelets were isolated from PRP by centrifugation at $800 \times g$ for 12 min in the presence of 6 mM citric acid. Platelets were washed in pH 6.5 buffer (0.036 M citric acid, 0.01 M EDTA, 0.005 M glucose, 0.005 M KCl, 0.09 M NaCl) and centrifuged at $800 \times g$ for 12 min. Sedimented platelets were resuspended in modified Tyrode's buffer (150 mM NaCl, 5 mM HEPES, 0.55 mM NaH_2PO_4, 7 mM $NaHCO_3$, 2.7 mM KCl, 0.5 mM $MgCl_2$, and 5.6 mM glucose, pH 7.4) and maintained at 37°C for 30 min prior to experiments. The study was approved by the Hull York Medical School Research Ethics Committee and all research was performed in accordance with relevant guidelines and regulations. Informed consent was obtained from all blood donors.

Mouse Platelet Preparation

Blood was taken by cardiac puncture into ACD, centrifuged at $100 \times g$ for 5 min and the PRP was collected in a separate tube. Modified Tyrode's buffer was added to the blood and the procedure repeated to increase the platelet yield. The platelets were then pelleted at $800 \times g$ for 6 min, resuspended in modified Tyrode's buffer and maintained at 37°C for 30 min prior to experiments.

Platelet Fractionation

Washed platelet suspensions (5×10^8 platelets/ml), either untreated or treated with various substances for the appropriate time, were mixed with an equal volume of fractionation buffer (320 mM sucrose, 4 mM HEPES, 0.5 mM Na_3VO_4, pH 7.4) supplemented with phosphatase and protease inhibitor cocktail. Latrunculin B (LatB) was used at 20 μM for 20 min to depolymerize F-actin prior to lysis. Samples were subjected to five freeze-thaw cycles in liquid nitrogen. Intact platelets were removed by centrifugation at $1,000 \times g$ for 5 min at 4°C and fractionation was done by centrifugation at $100,000 \times g$ for 60 min at 4°C. The fractions were normalized by volume and analyzed by Western blot.

Detergent-Insoluble Pellet Extraction

Washed platelet suspensions (1×10^9 platelets/ml) were lysed in an equal volume of Triton X-100 containing lysis buffer (2% Triton X-100, 10 mM Tris-HCl, 10 mM EGTA, pH 7.4) supplemented with protease inhibitors. Lysates were spun at $15,600 \times g$ for 20 min (low speed) or $100,000 \times g$ for 1 h (high speed) to separate the detergent soluble fraction from the detergent-insoluble pellet. The fractions were normalized by volume, resolved on 10% SDS-PAGE and analyzed by Western blot.

Immunoprecipitation

Platelets (1×10^9/ml) were lysed with one volume of lysis buffer (20 mM HEPES, 30 mM NaCl, 0.3 mM EDTA, 2% n-dodecyl β-D-maltoside, 0.5 mM DTT, pH 7.4) supplemented with protease inhibitors for 30 min on ice. Two hundred to five hundred micrograms per milliliter of protein lysate were incubated overnight with gentle rotation at 4°C with 1 μg of specific antibody or same species control immunoglobulin. Twenty microliters of pre-equilibrated protein G Sepharose beads were added to lysate-antibody mixture and incubated at 4°C for 1 h. After several washing steps with TBS-T (20 mM Tris-HCl, 150 mM NaCl, 0.1% Tween 20, pH 7.4) the beads were resuspended in 2× Laemmli buffer and immunocomplexes analyzed by Western blot.

Western Blot

Proteins were resolved by SDS-polyacrylamide gel electrophoresis (PAGE) and blotted onto polyvinylidene difluoride (PVDF) membrane. The membrane was incubated with the relevant primary antibody and either the corresponding peroxidase-conjugated secondary antibody followed by enhanced chemiluminescence detection (Pierce, Thermo Fisher Scientific Inc.) or the corresponding fluorochrome-labeled secondary antibody and visualized and quantified with an LI-COR Odyssey CLx Imaging System (LI-COR Biosciences, Lincoln, USA).
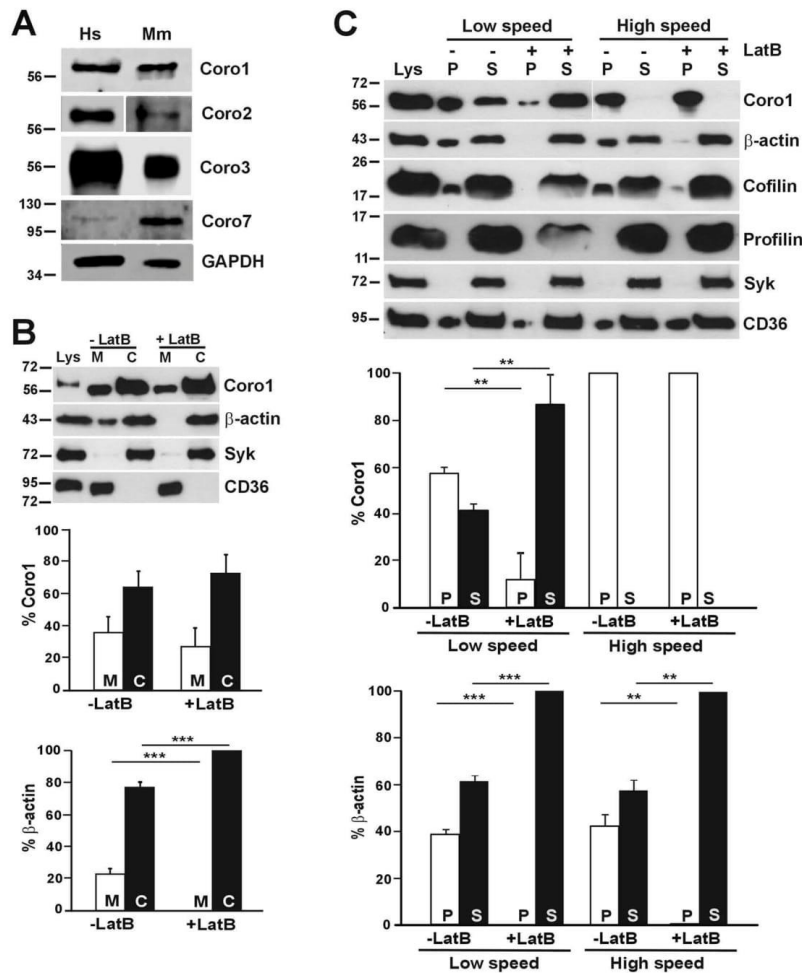
Figure 1. Coronins present in human and mouse platelets and subcellular distribution of human Coro1. (A) Western blot of human and mouse platelet lysates. Twenty micrograms of protein were resolved by 10% SDS-PAGE, blotted onto PVDF membrane and probed with antibodies for the indicated proteins. The mouse Coro2 blot corresponds to a higher exposure than the human one. The Coro7 blot was enhanced to make the human protein apparent (see Supplemental Figure 2 for details). GAPDH was used as a loading control. (B) Subcellular fractionation. Human platelets were lysed by freeze-thaw in liquid nitrogen and spun at $100,000 \times g$ for 1 h to separate membrane (M) and cytosolic (C) fractions. The fractions were normalized by volume and resolved by 12% SDS-PAGE, blotted onto PVDF membrane and probed with antibodies for the indicated proteins. CD36 was used as a membrane marker and Syk as a cytosolic marker in resting platelets. Latrunculin B (LatB; 20 μM, 20 min) was used to depolymerize F-actin prior to lysis. Coro1 and actin distribution were quantified by densitometry and expressed as a percentage relative to the respective totals (M + C). (C) Association of Coro1 to actin in the detergent-insoluble pellet. Human platelets (8×10^8/ml) were lysed in the presence of 1% Triton X-100 and lysates spun at low speed ($15,600 \times g$) for 20 min and high speed ($100,000 \times g$) for 1 h. Supernatant (S) and pellet (P) fractions were normalized by volume and resolved by 12% SDS-PAGE, blotted onto PVDF membrane and probed with antibodies for the indicated proteins. LatB (20 μM, 20 min) was used to depolymerize F-actin prior to lysis. Coro1 and actin distribution in pellet and supernatant were quantified by densitometry and expressed as a percentage of the respective total (P + S). Data of B and C represent mean ± SD of three independent experiments. **$P < .01$, ***$P < .001$ vs LatB-treated, Student's t-test.

Immunostaining and Microscopy

Washed platelets in suspension were fixed with an equal volume of ice-cold 4% paraformaldehyde (PFA) in PBS or, for tubulin staining, 3% PFA in 16 mM PIPES, 0.2 mM MgCl$_2$, 0.2 mM EGTA, pH 6.8 and spun at $350 \times g$ for 10 min on poly-L-lysine (0.01% in PBS)

coated coverslips. For adhesion studies, coverslips were coated overnight at 4°C with 100 μg/ml fibrinogen or collagen and blocked with heat-denatured fatty-acid-free bovine serum albumin for 1 h before the experiment. Washed platelets were allowed to spread for 45 min at 37°C, then fixed with 4% PFA. Fixed platelets were permeabilized
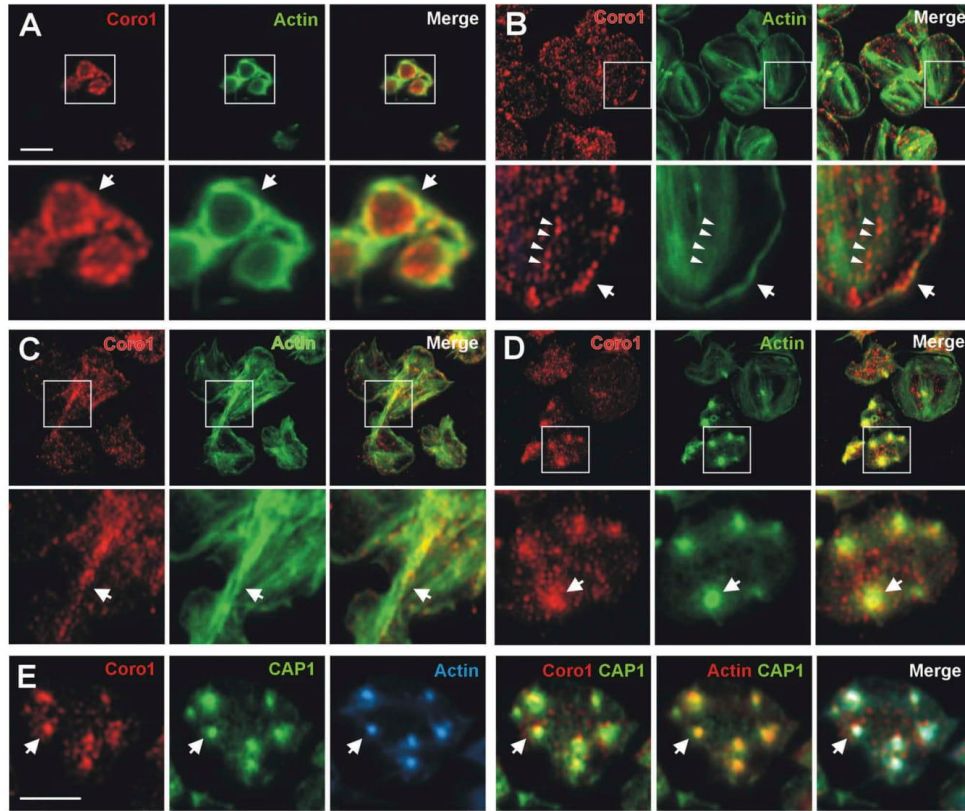
Figure 2. Subcellular localization of Coro1. Human platelets were fixed in suspension with paraformaldehyde and spun on poly-L-lysine coated coverslips (A) or were allowed to spread on 100 µg/ml fibrinogen (B, D) or collagen (C) coated coverslips and fixed with paraformaldehyde. For A, B, C and D cells were immunostained with an anti-Coro1 antibody followed by an Alexa568-coupled secondary antibody (red) and counterstained with FITC-phalloidin for filamentous actin (green). For E platelets were treated with 100 nM PGI2 at 37°C 5 min prior to fixation in order to increase the proportion of cells displaying actin nodules. Platelets were then immunostained with anti-Coro1 and anti-CAP1 antibodies followed by Alexa568 and Alexa488-coupled secondary antibodies, respectively (red and green), and counterstained with Alexa680-phalloidin for filamentous actin (blue). Actin color has been changed to red in the double staining panel with CAP1 for better visualization. Images were acquired with a fluorescence microscope equipped with a structured illumination attachment and deconvolved. Magnified regions are indicated with a square. Arrows point at regions of interest: cell cortex (A, B), actin filaments (C), actin nodules (D, E). Arrowheads in B point at Coro1 along stress fibers. Scale bars 5 µm. The scale bar on A applies to B, C, and D.

with 0.3% Triton® X-100 in PBS for 5 min and stained for 1 h at room temperature with the indicated primary antibodies followed the corresponding secondary antibodies and/or fluorescently labeled phalloidin diluted in PBG (0.5% BSA, 0.05% fish gelatin in PBS). Platelets were imaged by fluorescence microscopy using a Zeiss ApoTome.2 equipped with AxioCam 506 and Zeiss Plan-Apochromat 63×/1.4 and 100×/1.4 oil immersion objectives. Images were processed with Zeiss Zen software.

Statistical Analysis

Experimental data were analyzed by GraphPad Prism v6.0 (La Jolla, CA, USA). Data are presented as means ± standard error of the mean (SEM) or standard deviation (SD) of at least three independent experiments. Normality was assessed by the Shapiro-Wilk test. Differences between groups were assessed using the Student's t-test, Mann-Whitney U-test, Wilcoxon test,

analysis of variance (ANOVA) or Kruskal-Wallis test and statistical significance taken at $p \leq 0.05$.

Results

Platelets Express at Least Four Coronins

Proteomics and transcriptomics studies indicate that both human and mouse platelets express Coro1, 2, 3 and 7, while other coronins are practically undetectable (Supplemental Table 1 and 2). To demonstrate the presence of coronins in platelets we resolved human and mouse platelet lysates by SDS-PAGE, followed by western blot with a panel of antibodies specific for various coronins (see Supplemental Figure 1 for antibody specificity). Coro1, 2 and 3 appeared as single bands with apparent molecular weights of or above 56 kDa whereas Coro7 appeared as a single band of 100 kDa (Figure 1A). While Coro1, 2 and 3 appear relatively abundant, Coro 7 is expressed at much lower levels in both human and mouse platelets. In this study

267

we will mainly focus on human Coro1 as a paradigm of class I coronins, but will also address Coro3 and Coro2 is some assays and will verify if our findings apply to mouse coronins.

Subcellular Distribution of Coro1

To investigate the distribution of Coro1 we carried out a simple subcellular fractionation in human platelets. Resting platelets were lysed in an isotonic sucrose solution and cytosol and membrane fractions separated by ultracentrifugation and analyzed by immunoblot. As shown in Figure 1B, most of Coro1 (64%) was recovered in the cytosolic fraction and the rest associated with the membrane fraction. The blot was reprobed for β-actin and 77% of the actin was cytosolic and the rest membrane-associated. Since Coro1 is an actin-binding protein, we further investigated whether this membrane association is mediated by actin. Resting platelets were treated with 20 μM latrunculin B (LatB) to depolymerize F-actin prior to subcellular fractionation. As expected, under these conditions almost all actin was recovered in the cytosolic fraction. There was no statistically significant difference in Coro1 association to the membrane fraction in the absence ($35.7 \pm 9.6\%$) or presence ($27.1 \pm 11.7\%$) of LatB, indicating that the association of Coro1 to platelet membranes is independent of its association with actin. In these experiments, probing for the cytosolic marker in resting platelets spleen tyrosine kinase (Syk) and the membrane marker CD36 confirmed that each fractionation was free from cross-contamination.

We next characterized the association of Coro1 to the actin cytoskeleton. Resting human platelets were lysed in the presence of Triton X-100 and separated into soluble (containing G-actin) and insoluble (containing F-actin) fractions by centrifugation at low and high speeds followed by immunoblot analysis of the fractions (Figure 1C)[21]. Under these conditions, actin is distributed as approximately 60% soluble and 40% insoluble. At low speed, almost 60% of Coro1 was present in the Triton X-100 insoluble pellet, which contains large crosslinked actin filaments. Treatment with LatB, which efficiently depolymerized actin filaments, solubilized most of the Coro1, indicating that Coro1 in the LS pellet is predominantly associated with F-actin.

At high speed nearly all the Coro1 was recovered in the Triton X-100 insoluble pellet, which contains short actin filaments, even upon treatment with LatB, indicating that the association of Coro1 to the HS pellet is independent of an association with short actin filaments. We investigated the behavior of profilin and cofilin, two proteins involved in actin filament turnover. Profilin was recovered in the supernatants at both LS and HS, consistent with its role as monomeric actin-binding protein. Cofilin, which interacts with F-actin in addition to G-actin, was observed in HS and LS pellets and was removed from the LS pellet upon actin depolymerization, but not completely from the HS pellet. Coro1, as well as part of cofilin, may be associated with membranes or membrane proteins independently of actin, as suggested by the presence of a fraction of the membrane protein and lipid rafts component CD36 [22]. Syk was used as Triton X-100 soluble fraction marker to confirm that isolation of cytoskeleton fraction was clean.

To verify whether mouse Coro1 behaves similarly to human Coro1, we carried out subcellular and Triton-X100 fractionations as above and observed a similar distribution in membrane and cytosol fractions as well as in Triton-X100 supernatant and pellet fractions of mouse platelets (Supplemental Figure 3A, B).

Localization of Coronins in Platelets

We used immunostaining and fluorescence microscopy to study the distribution of Coro1, 2 and 3 in human and mouse platelets. In resting platelets in suspension, which are predominantly discoid, the distribution of Coro1 is punctate, very often accumulating at the cell cortex, where it colocalizes with F-actin (Figure 2A). In platelets spread on fibrinogen Coro1 displays a predominantly punctate diffuse distribution, with frequent instances of discontinuous accumulation in cortical regions, where the protein co-localizes with F-actin (Figure 2B, arrows). Under these conditions, Coro1 does not display a striking pattern of association to stress fibers, although in some cases puncta appear to align with stress fibers (Figure 2B, arrowheads). Platelets spread on collagen fibers extend more broadly and present more prominent stress fibers. Under these conditions we often see Coro1 accumulating along with thick actin cables in a discontinuous manner (Figure 2C). Coro1 conspicuously accumulates at actin nodules (Figure 2D), where it colocalizes with CAP1, which we have described previously as a component of actin nodules (4). Both Coro1 and CAP1 display a broad pattern of accumulation compared to the sharper pattern of F-actin (Figure 2E).

Coronins have been proposed as organizers of the actin, microtubule and intermediate filament systems [23]. We investigated the effect of disrupting the actin or microtubule cytoskeletons on Coro1 localization in platelets in suspension (Figure 3). LatB treatment resulted in almost complete disappearance of filamentous actin and loss of Coro1 cortical accumulation while the microtubule ring was intact. By contrast, treatment with the microtubule depolymerizing drug nocodazole resulted in the dispersal of the microtubule ring but intact cortical accumulation of Coro1 and actin. This indicates that Coro1 accumulation at the platelet cortex is primarily dependent on F-actin.

Coro2 and Coro3 display patterns of localization very similar to Coro1. In platelets, in suspension, both proteins show a punctate pattern, often enriched at the cell cortex and colocalizing with F-actin (Figure 4A, D). When spread on fibrinogen the pattern of localization of Coro2 and Coro3 was relatively uniformly dotty, with frequent discontinuous accumulation at the cell cortex (Figure 4B, E). This pattern of cortical enrichment was less apparent with Coro2, which in general gave an overall weaker staining than Coro3. Both coronins also accumulated and colocalized with F-actin at actin nodules (Figure 4C, F). Taking into account the weaker staining of Coro2, its accumulation at actin nodules appeared relatively more intense than that of Coro3.

In mouse platelets spread on fibrinogen the localization of Coro1, 2 and 3 resembled that of the respective human counterpart, with a predominantly punctate pattern and frequent discontinuous accumulation and colocalization with F-actin at the cortex (Supplemental Figure 3C).

Class I Coronins Co-immunoprecipitate and Colocalize in Platelets

Coro1 has been reported to interact with the Gαs subunit of heterotrimeric G proteins and stimulate the cAMP/PKA pathway in murine excitatory neurons and loss of Coro1 results in neurobehavioral defects [24]. To explore whether this interaction reproduces in platelets we performed immunoprecipitation experiments in human platelet lysates and found that Coro1 is able to co-immunoprecipitate Gαs (Figure 5A, upper panel). Upon co-immunoprecipitation of Coro2, Gαs was also retrieved in the immunocomplexes along with Coro3 (Figure 5A, lower panel). In support of Gαs forming complexes with coronins, we immunostained platelets in suspension for Coro1 and Gαs. Coro1 showed the characteristic discontinuous cortical accumulation, whereas the distribution of Gαs was punctate and uniform. We observed, however, instances of co-localization of both proteins at the cell cortex (Figure 5B). In these experiments, ARPC2, a subunit of the Arp2/3 complex, was found in the immunocomplexes and partially colocalizing with Coro1 at the cell cortex of spread platelets, compatible with the already reported interaction
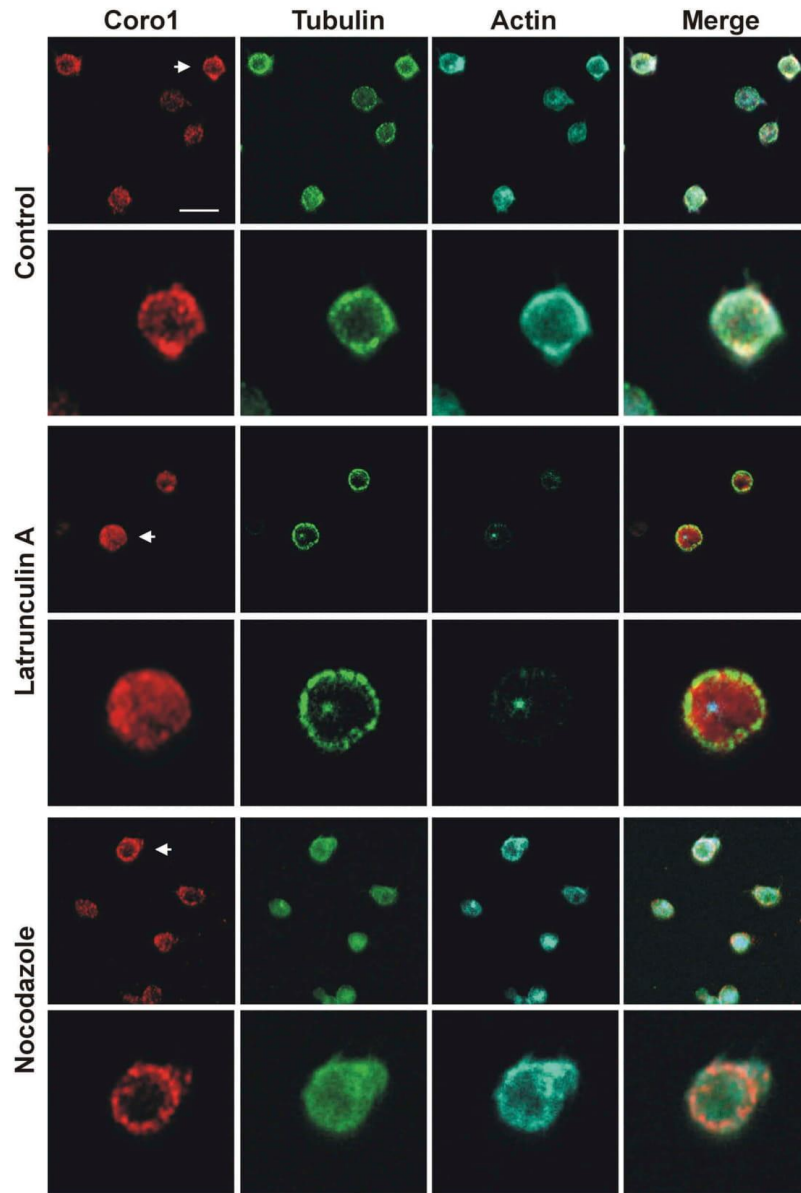
Figure 3. Subcellular localization of Coro1 upon disruption of the actin and tubulin cytoskeletons. Human platelets were incubated with 3 μM LatB or 10 μM nocodazole for 30 min, fixed in suspension with paraformaldehyde and spun on poly-L-lysine coated coverslips. Cells were immunostained with anti-Coro1 and anti-tubulin antibodies followed by Alexa568 and Alexa488-coupled secondary antibodies, respectively (red and green), and counter-stained with Alexa680-phalloidin for filamentous actin (blue). Images were acquired with a fluorescence microscope equipped with a structured illumination attachment and deconvolved. Arrows indicate the magnified cell shown in the second row of each treatment. Scale bar 5 μm.

of the Arp2/3 complex with class I coronins (Figure 5B) [25–27]. To further investigate this colocalization we studied the effect of inhibiting the Arp2/3 complex on Coro1 localization (Supplemental Figure 4). We treated platelets with the Arp2/3 complex inhibitor CK-666 at a range of concentrations spanning three orders of magnitude (0.5, 5 and 50 μM), stimulated them with thrombin and allowed them to spread on fibrinogen for 45 min. Without thrombin stimulation, most untreated platelets

269
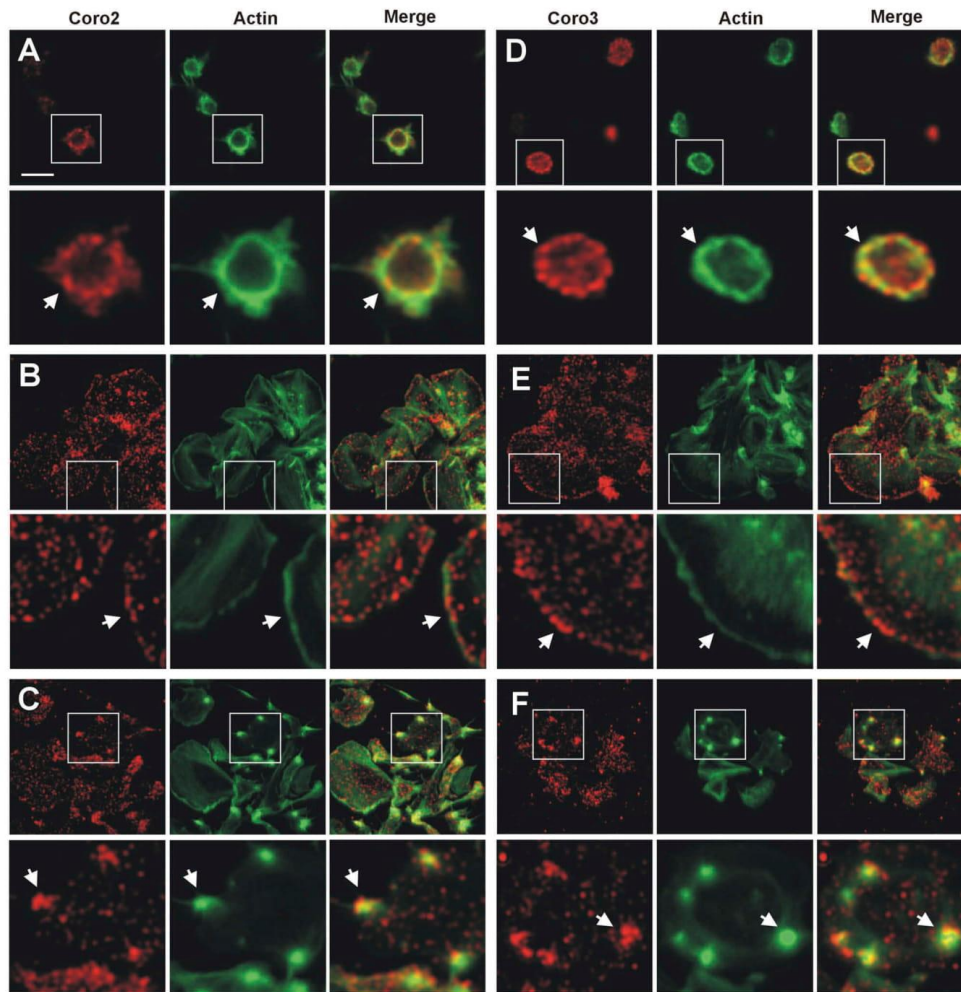
Figure 4. Subcellular localization of Coro2 and 3. Human platelets were fixed in suspension with paraformaldehyde and spun on poly-L-lysine coated coverslips (A, D) or were allowed to spread on 100 µg/ml fibrinogen coated coverslips (B, E, C, F) and fixed with paraformaldehyde. Cells were immunostained with an anti-Coro2 or Coro3 antibody followed by an Alexa568-coupled secondary antibody (red) and counterstained with FITC-phalloidin for filamentous actin (green). Images were acquired with a fluorescence microscope equipped with a structured illumination attachment and deconvolved. Magnified regions are indicated with a square. Arrows point at regions of interest: cell cortex (A, B, D, E), actin nodules (C, F). Scale bar 5 µm.

adopted a spiky morphology with numerous actin nodules but responded to thrombin with an extended round morphology and clear enrichment of ARPC2 at the cortex, with Coro1 often accumulating at the cortex too. The lower concentration of CK-666 had little effect on ARPC2 and Coro1 localization. Increasing concentrations of the inhibitor resulted in a high proportion of non-spread round platelets in the absence of thrombin stimulation, however the cells responded to thrombin. While 5 µM CK-666 still resulted in round well-spread platelets, with 50 µM CK-666 most platelets adopted an irregular shape with a few filopods, consistent with the inhibited formation of lamellipodia [28]. The cortical accumulation of ARPC2 persisted upon treatment with

CK-666, consistent with the fact that CK-666 stabilizes the inactive state of the Arp2/3 complex, but does not prevent its binding to actin filaments [29], however Coro1 cortical accumulation was largely lost.

The similar patterns of subcellular localization of all three class I coronins suggest that they might be performing similar functions and may co-localize and participate in complexes with each other. In fact, as indicated above, Coro2 and Coro3 co-immunoprecipitate. To investigate the extent of co-localization of the three-class I coronins in platelets we performed a combination of double stainings (Figure 5C). These studies revealed that while all three coronins accumulate at the cell
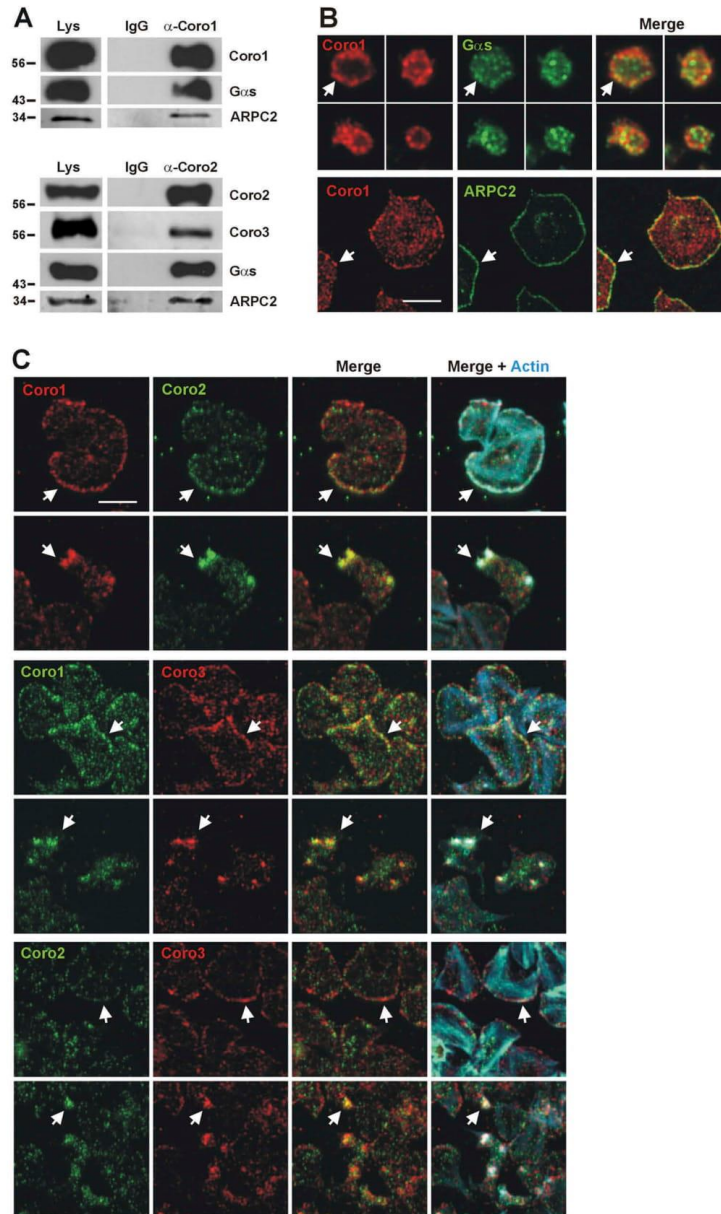
Figure 5. Coronins exist in complexes with each other and with Gαs and the Arp2/3 complex. (A) Human platelet lysates were subject to immunoprecipitation with Coro1 or Coro2-specific antibodies. The same species of the total immunoglobulin G (IgG) was used as a control. Protein complexes were examined by Western blot for the presence of the indicated proteins. (B) Colocalization of Coro1 with Gαs and ARPC2. For Gαs platelets were fixed in suspension with paraformaldehyde and spun on poly-L-lysine coated coverslips. For ARPC2 platelets were allowed to spread on 100 μg/ml fibrinogen coated coverslips and fixed with paraformaldehyde. Cells were immunostained with anti-Coro1 and anti-ARPC2 or anti-Gαs antibody followed by Alexa568 or Alexa488-coupled secondary antibodies, respectively (red and green). Images were acquired with a fluorescence microscope equipped with a structured illumination attachment and deconvolved. Arrows point at regions of apparent colocalization. Scale bar 5 μm. (C) Coronins colocalize with each other. Platelets were allowed to spread on 100 μg/ml fibrinogen coated coverslips, fixed with paraformaldehyde, immunostained with the indicated coronin antibodies followed by Alexa568 or Alexa488-coupled secondary antibodies, respectively (red and green), and counterstained with Alexa680-phalloidin for filamentous actin (blue). Images were acquired as in (B). Arrows point at regions of interest: cell cortex (upper panels), actin nodules (lower panels). Scale bar 5 μm.

cortex, some extent of co-localization was apparent in all combinations, although in the case of Coro1 and Coro3 colocalization seemed clearer. A clear pattern of colocalization was observed in actin nodules in every combination of coronin immunostainings.

Translocation of Coronins upon Platelet Stimulation

Stimulation with strong agonists typically provokes a rapid increase in actin polymerization that can be monitored on time by analyzing the amount of actin in the LS detergent-insoluble pellet. Both upon thrombin and collagen stimulation the proportion of actin in the LS pellet rapidly increased to a twofold peak at 60 s and remained elevated afterward (Figure 6). We explored the effect of those agonists in the association of Coro1 and 3 to the LS pellet. Platelets were stimulated with 0.1 U/ml thrombin or 50 μg/ml collagen and the reaction was stopped with lysis buffer at various time points up to 3 min. We observed a statistically significant time-dependent increase in the proportion of both Coro1 and 3 in the LS pellet that roughly paralleled that of actin (Figure 6). In mouse platelets both actin and Coro1 behaved similarly to their human counterparts in response to thrombin and collagen, although Coro1 appeared to peak earlier (at 15 s) (Supplemental Figure 3D).

As shown above, one-third of Coro1 is membrane associated. To investigate whether exposure to various stimuli would affect this pattern of distribution we treated platelets in suspension with 0.1 U/ml thrombin, 50 μg/ml collagen or 100 nM PGI2 and subjected them to subcellular fractionation followed by Western blot analysis. We did not observe any significant change in the proportion of Coro1 or Coro3 upon any of the treatments (Figure 7).

Discussion

In this study, we present immunological evidence of the presence of members of the coronin family in human and mouse platelets. We show that class I coronins Coro1, 2 and 3 are abundant in platelets from both species, whereas expression of Coro7 is comparatively very low. Our results are in very broad agreement with data from proteomics and transcriptomic studies (Supplemental Table 1 and 2), with the caveat that western immunoblot results are not suitable for quantitative comparisons due to the fact that all the antibodies we have used were raised against fragments of human coronins; therefore, we expect them to have different affinities for the corresponding mouse protein. In addition, the affinities of the antibodies are also expected to vary among the different coronins of the same species.

At 53,600 copies per platelet, class I coronins taken together are among the most abundant proteins in human platelets [30], and appear to be approximately 2.5 times more abundant in mouse

platelets [31]. Coro2 exists in less copies per platelet than Coro1 and 3 in both human and mouse, which might explain the weaker signal we usually observe in immunostainings for this coronin. While Coro1 and 3 are present in similar copy numbers in human platelets, Coro1 is considerably more abundant than Coro3 in mouse platelets [30,31]. Interestingly, proteomics and transcriptomics studies reveal a lack of correlation of protein and transcript levels: Coro3 mRNAs are present at considerably high levels in human platelets, whereas Coro1 mRNAs are present at very low levels in mouse platelets [32].

Coro7 is the least abundant coronin in platelets, with an estimated 760 and 3571 copies in human and mouse platelets, respectively [30]. Our western blot data clearly reflect this difference in abundance between species. Some proteomics and transcriptomics studies fail to identify Coro7, probably due to technical limitations [33,34], or to expression lying below the cutoff set for a gene to be included in the list of expressed genes [35,36]. A significant proportion of Coro7 associates with Golgi membranes [19,20]. Usually, very little Golgi is present in mature platelets, explaining the relatively very low abundance of this isoform, which we speculate might have a role in platelet maturation by regulating Golgi-related processes. Based on transcriptomics studies, Coro4, 5 and 6 do not appear to be expressed to significant levels in human and mouse platelets and consequently remain undetectable in proteomics studies (Supplemental Table 1 and 2).

In platelets, approximately 36% of Coro1 is recovered in the membrane fraction and this association is independent of the actin cytoskeleton, as indicated by its persistence after LatB treatment. This is in broad agreement with a study in J774 macrophages, where Gatfield et al. found 20% of Coro1 associated with membranes [8]. Also, 40% of Coro3 had previously been found associated with membranes [7]. We are not aware of any study that formally addresses the subcellular distribution of Coro2, but this coronin is required for endosome fission, therefore some extent of membrane association is expected [37]. Membrane association has been reported for the *Plasmodium falciparum* homolog too [38,39], and therefore seems to be a common feature of coronins. Several mechanisms might account for the membrane association of coronins, most notably their ability to directly bind PI(4,5)P2 [39,40], but interactions with other membrane-associated proteins are also likely to contribute, for example, Rac1 and Gαs with Coro1 and Rab27a with Coro3 [24,41,42]. None of the stimuli we have tested in platelets produces a noticeable translocation of Coro1 or 3 between the membrane fraction and the cytosol, suggesting that either translocation is not required for coronin function or the amount that translocates is below the levels detectable with our techniques.
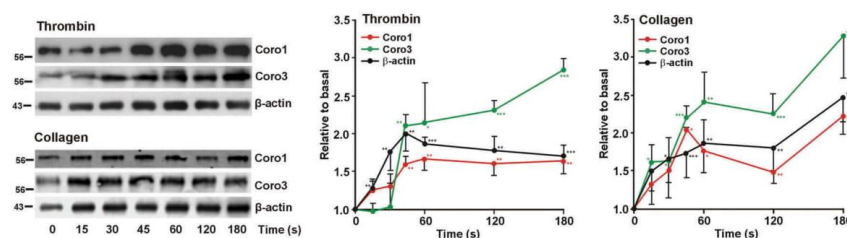
Figure 6. Dynamics of Coro1 along with F-actin in the Triton X-100 insoluble pellet of platelets stimulated with thrombin or collagen. Washed human platelets were stimulated with thrombin (0.1 U/ml) or collagen (50 μg/ml) at the indicated time points and lysed immediately in 1% Triton X-100 lysis buffer. Triton insoluble pellets were prepared by low-speed centrifugation (15,600 × g for 15 at 4°C), run on SDS-PAGE and subjected to Western blot analysis with anti-Coro1, Coro3 and β-actin antibodies. Densitometry values are expressed as means ± SEM of 3–7 experiments *$P < .05$, **$P < .01$, ***$P < .001$ relative to basal, student's t-test.
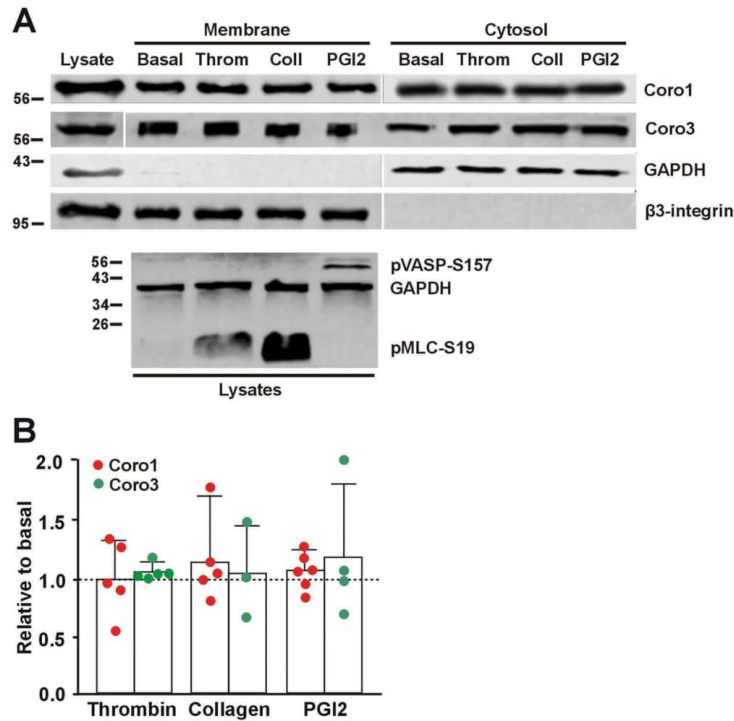
Figure 7. Coronins do not translocate upon platelet stimulation. (A) Washed human platelets (8×10^8/ml) were treated with 1 mM EGTA, 10 nM indomethacin and 2 U/ml apyrase for 20 min at 37°C to prevent aggregation. They were then treated with 0.1 U/ml thrombin, 50 μg/ml collagen or 100 nM PGI2 for 1 min at 37°C prior to lysis and subcellular fractionation. Fractions were normalized by volume and resolved on 12% SDS-PAGE, blotted onto PVDF membrane and probed with antibodies for Coro1 and Coro3. Integrin β3 was used as a membrane marker and GAPDH as a cytosolic marker. The phosphoproteins pMLC-S19 and pVASP-S157 were used as markers of the effects of thrombin/collagen and PGI2, respectively, and GAPDH as a loading control. (B) Membrane-associated Coro1 and Coro3 upon stimulation were quantified by densitometry, normalized to integrin β3 and expressed relative to the respective coronin in the basal membrane fraction. Data represent the mean ± SEM of 3–6 independent experiments. No statistically significant differences were found relative to basal for any coronin using Mann-Whitney U and Kruskal-Wallis tests.

Sixty percent of the Coro1 fractionates in the LS detergent-insoluble pellet of platelets, predominantly associated with F-actin. A similar behavior has been described for this coronin in J774 macrophages [8]. The proportion of Coro1 in the LS pellet increases rapidly upon stimulation with strong agonists and Coro3 shows a comparable behavior, consistent with the role of class I coronins in actin filament remodeling in platelets. By contrast, virtually all the Coro1 was recovered in the HS pellet of platelets and this association was not disrupted by LatB, indicating that it is independent of actin. This may represent Coro1 associated with membrane-containing structures like lipid rafts, along with a fraction of cofilin. Coro3 too has been reported as abundant in the HS pellet of HaCat cells, from where it is partially extracted in the presence of LatB [26].

Coro1, 2 and 3 display a similar localization in human platelets, with a diffuse punctate cytoplasmic localization and a discontinuous enrichment at the cortex of both suspended and spread platelets, where it co-localizes with F-actin and, in the latter, the Arp2/3 complex. This pattern is similar to the reported localization of Coro1 in macrophages and lymphocytes, [8,13,43,44] as well as in unicellular organisms like *Dictyostelium discoideum, Trichomonas vaginalis* and *Plasmodium falciparum* [39,45,46], but Coro1 is also recruited at phagosomes in macrophages and neutrophils [27,43]. Coro2 and 3 have been shown to display a diffuse cytosolic

localization with enrichment at peripheral protrusions in a variety of cells, like DRG neurons, lung endothelial cells, fibroblasts, HEK cells, oligodendrocytes, HaCat cells, and Pop10 hepatocarcinoma cells [7,25,26,47–49]. The accumulation of Coro1 at the cell cortex seems to be dependent on the activity of the Arp2/3 complex and is evident only in spread platelets morphologically compatible with the presence of lamellipods. We observed Coro1 localizing in a discontinuous pattern at stress fibers, more clearly in platelets spread on collagen, a matrix protein that usually leads to the formation of more robust actin cables compared to fibrinogen. Localization of class I coronins at stress fibers has been very seldom reported and might indicate sites of active remodeling under specific circumstances [23]. Mouse class I coronins showed a pattern of predominantly diffused cytoplasmic distribution with some cortical accumulation, similar to their human counterparts and in agreement with a recent report that addressed the immunolocalization of Coro1 in mouse platelets [5].

A localization of class I coronins in actin nodules has not been reported before. These podosome-related structures consist of a core rich in actin and Arp2/3 complex core surrounded by a ring rich in focal adhesion molecules like talin and vinculin [50]. They are usually visible during early adhesion and spreading [51]. We have recently shown that CAP1, a protein involved in recycling of actin

monomers, is also a component of the actin nodule ring [4], therefore we speculate that coronins too might contribute to the actin filament turnover of these highly dynamic structures.

Class I coronins are reported to exist as homo-oligomers and there is no evidence for the formation of hetero-oligomers [7,8,25]. The colocalization of class I coronins to the same structures in platelets suggests that they might be part of large complexes containing more than one isoform, as demonstrated by the ability of Coro2 to co-immunoprecipitate Coro3. This is in contrast to the report of Cai et al. (2005) that failed to observe a co-immunoprecipitation of Coro2 with any other coronin in a fibroblast cell line [25], however large-scale interactome studies have identified class I coronins as part of the same complexes [52,53].

In summary, we provide evidence that class I coronins are abundant cytoskeleton regulators in platelets, where they may play roles in organizing the cortical cytoskeleton upon adhesion and spreading, consistent with the emerging role of coronins as integrators of extracellular signals with actin remodeling. The fact that class I coronins co-localize and different isoforms might participate in the same complex strongly suggests a high extent of functional overlap and would explain the mild phenotype of platelets lacking Coro1 [5]. Functional overlap is expected to occur in most white blood cell types, where all three class I coronins appear to be expressed simultaneously (Supplemental Figure 5). Further studies on animal models lacking one or more class I coronins will be required to elucidate the unique and shared roles of these proteins in platelet function.

Disclosure statement

Khalid M. Naseem is an editorial board member of *Platelets*.

ORCID

Francisco Rivero http://orcid.org/0000-0001-5435-6991

References

1. Ghoshal K, Bhattacharyya M. Overview of platelet physiology: its hemostatic and nonhemostatic role in disease pathogenesis. Sci World J 2014;2014:1–16. doi: 10.1155/2014/781857
2. Hartwig JH. The platelet cytoskeleton. In: Michelson AD, editor. Platelets. London: Academic Press; 2013. p. 145–168.
3. Falet H. Anatomy of the platelet cytoskeleton. In: Graesele P, Kleinman NS, Lopez JA, Page CP, editors. Platelets in thrombotic and non-thrombotic disorders. Berlin: Springer; 2017. p. 139–156.
4. Joshi P, Riley DRJ, Khalil JS, Xiong H, Ji W, Rivero F. The membrane-associated fraction of cyclase associate protein 1 translocates to the cytosol upon platelet stimulation. Sci Rep 2018;8:10804. doi: 10.1038/s41598-018-29151-w
5. Stocker T, Pircher J, Skenderi A, Ehrlich A, Eberle C, Megens R, Petzold T, Zhang Z, Walzog B, Müller-Taubenberger A, et al. The actin regulator coronin-1A modulates platelet shape change and

6. Jain BP, Pandey S. WD40 repeat proteins: signalling scaffold with diverse functions. Protein J 2018;37:391–406. doi: 10.1007/s10930-018-9785-7
7. Spoerl Z, Stumpf M, Noegel AA, Hasse A. Oligomerization, F-actin interaction, and membrane association of the ubiquitous mammalian coronin 3 are mediated by its carboxyl terminus. J Biol Chem 2002;277:48858–48867. doi: 10.1074/jbc.M205136200
8. Gatfield J, Albrecht I, Zanolari B, Steinmetz MO, Pieters J. Association of the leukocyte plasma membrane with the actin cytoskeleton through coiled coil-mediated trimeric coronin 1 molecules. Mol Biol Cell 2005;16:2786–2798. doi: 10.1091/mbc.e05-01-0042
9. Chan KT, Creed SJ, Bear JE. Unraveling the enigma: progress towards understanding the coronin family of actin regulators. Trends Cell Biol 2011;21:481–488. doi: 10.1016/j.tcb.2011.04.004
10. Martorella M, Barford K, Winckler B, Deppmann C. Emergent role of coronin-1a in neuronal signaling. Vitam Horm 2017;104:113–131.
11. Cai L, Marshall TW, Uetrecht AC, Schafer DA, James E. Coronin 1B coordinates Arp2/3 complex and Cofilin activities at the leading edge. Cell 2007;128:915–929. doi: 10.1016/j.cell.2007.01.031
12. Galletta BJ, Chuang DY, Cooper JA. Distinct roles for Arp2/3 regulators in actin assembly and endocytosis. PLoS Biol 2008;6: e1. doi: 10.1371/journal.pbio.0060001
13. Combaluzier B, Mueller P, Massner J, Finke D, Pieters J. Coronin 1 is essential for IgM-mediated Ca^{2+} mobilization in B cells but dispensable for the generation of immune responses in vivo. J Immunol 2009;182:1954–1961. doi: 10.4049/jimmunol.0801811
14. Moriceau S, Kantari C, Mocek J, Davezac N, Gabillet J, Guerrera IC, Brouillardf F, Tondelier D, Sermet-Gauzdelus I, Danel C, et al. Coronin-1 is associated with neutrophil survival and is cleaved during apoptosis: potential implication in neutrophils from cystic fibrosis patients. J Immunol 2009;182:7254–7263. doi: 10.4049/jimmunol.0803312
15. Grogan A, Reeves E, Keep N, Wientjes F, Totty NF, Burlingame AL, Hsuan JJ, Segal AW. Cytosolic phox proteins interact with and regulate the assembly of coronin in neutrophils. J Cell Sci 1997;110:3071–3081.
16. Cai L, Makhov AM, Schafer DA, Bear JE. Coronin 1B antagonizes Cortactin and remodels Arp2/3- containing actin branches in lamellipodia. Cell 2008;134:828–842. doi: 10.1016/j.cell.2008.06.054
17. Marshall TW, Aloor HL, Bear JE. Coronin 2A regulates a subset of focal-adhesion-turnover events through the cofilin pathway. J Cell Sci 2009;122:3061–3069. doi: 10.1242/jcs.051482
18. Nakamura T, Takeuchi K, Muraoka S, Hirakota T, Takahashi N, Mori N. A neurally enriched coronin-like protein, clipinC, is a novel candidate for an actin cytoskeleton-cortical membrane-linking protein. J Biol Chem 1999;274:13322–13327. doi: 10.1074/jbc.274.19.13322
19. Rybakin V, Gounko NV, Späte K, Höning S, Majoul IV, Duden R, Noegel AA. Crn7 interacts with AP-1 and is required for the maintenance of Golgi morphology and protein export from the Golgi. J Biol Chem 2006;281:31070–31078. doi: 10.1074/jbc.M604680200
20. Rybakin V, Stumpf M, Schulze A, Majoul IV, Noegel AA, Hasse A. Coronin 7, the mammalian POD-1 homologue, localizes to the Golgi apparatus. FEBS Lett 2004;573:161–167. doi: 10.1016/j.febslet.2004.07.066
21. Fox JEB, Reynolds CC, Boyles JK. Studying the platelet cytoskeleton in Triton X-100 lysates. Methods Enzym 1992;215:42–58.
22. Zeng Y, Tao N, Chung K-N, Heuser JE, Lublin DM. Endocytosis of oxidized low density lipoprotein through scavenger receptor CD36 utilizes a lipid raft pathway that does not require caveolin-1. J Biol Chem 2003;278:45931–45936. doi: 10.1074/jbc.M307722200
23. Behrens J, Solga R, Ziemann A, Rastetter RH, Berwanger C, Herrmann H, Noegel AA, Clemen CS. Coronin 1C-free primary mouse fibroblasts exhibit robust rearrangements in the orientation of actin filaments, microtubules and intermediate filaments. Eur J Cell Biol 2016;95:239–251. doi: 10.1016/j.ejcb.2016.04.004
24. Jayachandran R, Liu X, Bosedasgupta S, Müller P, Zhang C-L, Moshous D, Studer V, Schneider J, Genoud C, Fossoud C, et al. Coronin 1 regulates cognition and behavior through modulation of

cAMP/protein kinase A signaling. PLoS Biol 2014;12:e1001820. doi: 10.1371/journal.pbio.1001820

25. Cai L, Holoweckyj N, Schaller MD, Bear JE. Phosphorylation of coronin 1B by protein kinase C regulates interaction with Arp2/3 and cell motility. J Biol Chem 2005;280:31913–31923. doi: 10.1074/jbc.M504146200

26. Rosentreter A, Hofmann A, Xavier C-P, Stumpf M, Noegel AA, Clemen CS. Coronin 3 involvement in F-actin-dependent processes at the cell cortex. Exp Cell Res 2007;313:878–895. doi: 10.1016/j.yexcr.2006.12.015

27. Yan M, Di Ciano-Oliveira C, Grinstein S, Trimble WS. Coronin function is required for chemotaxis and phagocytosis in human neutrophils. J Immunol 2007;178:5769–5778. doi: 10.4049/jimmunol.178.9.5769

28. Severin S, Gaits-Iacovoni F, Allart S, Gratacap M-P, Payrastre B. A confocal-based morphometric analysis shows a functional crosstalk between the actin filament system and microtubules in thrombin-stimulated platelets. J Thromb Haemost 2013;11:183–186. doi: 10.1111/jth.12053

29. Hetrick B, Han MS, Helgeson LA, Nolen BJ. Small molecules CK-666 and CK-869 inhibit Arp2/3 complex by blocking an activating conformational change. Chem Biol 2013;20:701–712. doi: 10.1016/j.chembiol.2013.03.019

30. Burkhart JM, Vaudel M, Gambaryan S, Radau S, Walter U, Martens L, Geiger J, Sickman A, Zahedi RP. The first comprehensive and quantitative analysis of human platelet protein composition allows the comparative analysis of structural and functional pathways. Blood 2012;120:e73–82. doi: 10.1182/blood-2012-04-416594

31. Zeiler M, Moser M, Mann M. Copy number analysis of the murine platelet proteome spanning the complete abundance range. Mol Cell Proteomics 2014;13:3435–3445. doi: 10.1074/mcp.M114.038513

32. Rowley JW, Oler AJ, Tolley ND, Hunter BN, Low EN, Nix DA, Yost CC, Zimmerman GA, Weyrich AS. Genome wide RNA-seq analysis of human and mouse platelet transcriptomes. Blood 2011;118:e101–111. doi: 10.1182/blood-2011-03-339705

33. Thiele T, Braune J, Dhople V, Hammer E, Scharf C, Greinacher A, Völker U, Steil L. Proteomic profile of platelets during reconstitution of platelet counts after apheresis. Proteomics - Clin Appl 2016;10:831–838. doi: 10.1002/prca.v10.8

34. Qureshi AH, Chaoji V, Maiguel D, Faridi MH, Barth CJ, Salem SM, Singhal M, Stoub D, Krastins B, Ogihara M, et al. Proteomic and phospho-proteomic profile of human platelets in basal, resting state: insights into integrin signaling. PLoS One 2009;4:e7627. doi: 10.1371/journal.pone.0007627

35. Osman A, Hitzler WE, Ameur A, Provost P, Schubert M. Differential expression analysis by RNA-seq reveals perturbations in the platelet mRNA transcriptome triggered by pathogen reduction systems. PLoS One 2015;10:1–17. doi: 10.1371/journal.pone.0133070

36. Londin ER, Hatzimichael E, Loher P, Edelstein L, Shaw C, Delgrosso K, Fortina P, Bray PF, McKenzie SE, Rigoutsos I. The human platelet: strong transcriptome correlations among individuals associate weakly with the platelet proteome. Biol Direct 2014;9:3. doi: 10.1186/1745-6150-9-3

37. Hoyer MJ, Chitwood PJ, Ebmeier CC, Striepen JF, Qi RZ, Old WM, Voeltz GK. A novel class of ER membrane proteins regulates ER-associated endosome fission. Cell 2018;175:1–12. doi: 10.1016/j.cell.2018.08.030

38. Tardieux I, Liu X, Poupel O, Parzy D, Dehoux P, Langsley G. A *Plasmodium falciparum* novel gene encoding a coronin-like protein which associates with actin filaments. FEBS Lett 1998;441:251–256. doi: 10.1016/S0014-5793(98)01557-9

39. Olshina MA, Angrisano F, Marapana DS, Riglar DT, Bane K, Wong W, Catimel B, Yin M-X, Holmes AB, Frischknecht F, et al. *Plasmodium falciparum* coronin organizes arrays of parallel actin

filaments potentially guiding directional motility in invasive malaria parasites. Malar J 2015;14:280. doi: 10.1186/s12936-015-0801-5

40. Tsujita K, Itoh T, Kondo A, Oyama M, Kozuka-Hata H, Irino Y, Hasegawa J, Takenawa T. Proteome of acidic phospholipid-binding proteins: spatial and temporal regulation of Coronin 1A by phosphoinositides. J Biol Chem 2010;285:6781–6789. doi: 10.1074/jbc.M109.057018

41. Castro-Castro A, Ojeda V, Barreira M, Sauzeau V, Navarro-Lérida I, Muriel O, Couceiro JR, Pimentel-Muíños FX, Del Pozo MA, Bustelo JR. Coronin 1A promotes a cytoskeletal-based feedback loop that facilitates Rac1 translocation and activation. Embo J 2011;30:3913–3927. doi: 10.1038/emboj.2011.310

42. Kimura T, Taniguchi S, Niki I. Actin assembly controlled by GDP-Rab27a is essential for endocytosis of the insulin secretory membrane. Arch Biochem Biophys 2010;496:33–37. doi: 10.1016/j.abb.2010.01.017

43. Ferrari G, Langen H, Naito M, Pieters J. A coat protein on phagosomes involved in the intracellular survival of mycobacteria. Cell 1999;97:435–447. doi: 10.1016/S0092-8674(00)80754-0

44. Nal B, Carrol P, Mohr E, Verthuy C, Da Silva M-I, Gayet O, Guo XJ, He H-T, Alcover A, Ferrier P. Coronin-1 expression in T lymphocytes: insights into protein function during T cell development and activation. Int Immunol 2004;16:231–240. doi: 10.1093/intimm/dxh022

45. de Hostos E, Bradtke B, Lottspeich F, Guggenheim R, Gerisch G. Coronin, an actin binding protein of *Dictyostelium discoideum* localized to cell surface projections, has sequence similarities to G protein b subunits. Embo J 1991;10:4097–4104. doi: 10.1002/j.1460-2075.1991.tb04986.x

46. Bricheux G, Coffe G, Bayle D, Brugerolle G. Characterization, cloning and immunolocalization of a coronin homologue in *Trichomonas vaginalis*. Eur J Cell Biol 2000;79:413–422. doi: 10.1078/0171-9335-00065

47. Di Giovanni S, De Biase A, Yakovlev A, Finn T, Beers J, Hoffman EP, Faden AI. *In vivo* and *in vitro* characterization of novel neuronal plasticity factors identified following spinal cord injury. J Biol Chem 2005;280:2084–2091. doi: 10.1074/jbc.M411975200

48. Usatyuk PV, Burns M, Mohan V, Pendyala S, He D, Ebenezer DL, Harijith A, Fu P, Huang LS, Bear JE, et al. Coronin 1B regulates S1P-induced human lung endothelial cell chemotaxis: role of PLD2, protein kinase C and Rac1 signal transduction. PLoS One 2013;8: e63007. doi: 10.1371/journal.pone.0063007

49. Hasse A, Rosentreter A, Spoerl Z, Stumpf M, Noegel AA, Clemen CS. Coronin 3 and its role in murine brain morphogenesis. Eur J Neurosci 2005;21:1155–1168. doi: 10.1111/ejn.2005.21.issue-5

50. Poulter NS, Pollitt AY, Davies A, Malinova D, Nash GB, Hannon MJ, Pikramenou Z, Rappoport JZ, Hartwig JH, Owen DM, et al. Platelet actin nodules are podosome-like structures dependent on Wiskott-Aldrich syndrome protein and ARP2/3 complex. Nat Commun 2015;6:7254. doi: 10.1038/ncomms8254

51. Calaminus SDJ, Thomas S, McCarty OJT, Machesky LM, Watson SP. Identification of a novel, actin-rich structure, the actin nodule, in the early stages of platelet spreading. J Thromb Haemost 2008;6:1944–1952. doi: 10.1111/jth.2008.6.issue-11

52. Huttlin EL, Ting L, Bruckner RJ, Gebreab F, Gygi MP, Szpyt J, Tam S, Zarraga G, Colby G, Baltier K, et al. The BioPlex network: A systematic exploration of the human interactome. Cell 2015;162:425–440. doi: 10.1016/j.cell.2015.06.043

53. Huttlin EL, Bruckner RJ, Paulo JA, Cannon JR, Ting L, Baltier K, Colby G, Gebreab F, Gygi MP, Parzen H, et al. Architecture of the human interactome defines protein communities and disease networks. Nature 2017;545:505–509. doi: 10.1038/nature22366

Supplemental Table 1. Presence of coronins in human platelets based on proteomics and transcriptomics studies. For transcriptomics only selected studies that use RNA-seq have been considered. LC-ESI-MS/MS, liquid chromatography electrospray ionization tandem mass spectrometry; 2D-DIGE, two-dimensional differential in gel electrophoresis. Expression levels have been collated or calculated from the supplemental tables of the referenced studies.

Study	Type	Method	Population	Coro1 CORO1A	Coro2 CORO1B	Coro3 CORO1C	Coro4 CORO2A	Coro5 CORO2B	Coro6 CORO6	Coro7 CORO7
(Thiele et al., 2016)	Protein	LC-ESI-MS/MS and 2D-DIGE	1 healthy male donor upon apheresis	+	+	+	-	-	-	-
(Burkhart et al., 2012) a	Protein	Quantitative LC-MS/MS	4 healthy donors	23,400	6,900	23,300	-	-	-	760
(Qureshi et al., 2009)	Protein	LC-MS/MS	5 healthy donors + 5 PRP samples from blood bank	+	+	+	-	-	-	-
(Osman, Hitzler, Ameur, Provost, & Schubert, 2015) b	Transcript	RNA-seq	20 platelet concentrates (4 conditions plus control, 4 samples each)	65	352	115,687	-	-	-	-
(Londin, et al. 2014) c	Transcript	RNA-seq	10 healthy male donors	4.72×10^{-4}	9.02×10^{-4}	13.80×10^{-4}	-	-	-	-
(Bray et al., 2013) d	Transcript	RNA-seq	4 healthy donors	-10.20	-10.50	-4.21	-15.23	-	-	-12.98
(Rowley et al., 2011) e	Transcript	RNA-seq	1 female and 1 male healthy donors	16.07	11.79	73.46	0.01	0.02	0.00	1.70

a. Data are average copies per cell.
b. Cutoff: $\geq 1/10,000$ of β-actin ($ACTB$) expression. Data was corrected for fold expression upon experimental condition relative to control and averaged for all four experimental conditions. Average β-actin's expression was 306,795.
c. Cutoff: expressed within 13 PCR cycles of $ACTB$ ($\geq 1/10,000$ of β-actin's expression) in all ten individuals studied. Average β-actin expression in this study was 0.906.
d. Cutoff: transcripts with an estimated abundance that was 2^{-10} times that of β-actin, and whose absolute ratio value was 2× between two preparations. Data is average of expression of all transcripts per sample. Values are $\log_2$(normalized expression to β-actin). Number of transcripts: $CORO1A$ (1), $CORO1B$ (2), $CORO1C$ (5), $CORO2A$ (2), $CORO7$ (3). For coro4 expression was detected in (and averaged from) 2 out of 4 samples.
e. Data are reads per kilobase of exon model per million mapped reads.

276

Supplemental Table 2. Presence of coronins in mouse platelets based on proteomics and transcriptomics studies. LC- MS/MS, liquid chromatography tandem mass spectrometry. Expression levels have been collated from the supplemental tables of the referenced studies.

Study	Type	Method	Samples	Coro1 *Coro1a*	Coro2 *Coro1b*	Coro3 *Coro1c*	Coro4 *Coro2a*	Coro5 *Coro2b*	Coro6 *Coro6*	Coro7 *Coro7*
(Zeiler, et al., 2014) a	Protein	Quantitative LC-MS/MS	3 mice + ultra-purified pool	87,469	18,955	29,555	-	-	-	3571
(Rowley et al., 2011) b	Transcript	RNA-seq	1 female pool and 1 male pool	1.61	41.18	21.31	0.01	0.00	0.07	0.71

a. Data are average copies per cell.
b. Data are reads per kilobase of exon model per million mapped reads.

References to proteomics and transcriptomics studies

Bray PF, McKenzie SE, Edelstein LC, Nagalla S, Delgrosso K, Ertel A, Kupper J, Jing Y, Londin E, Loher P, Chen H-W, Fortina P, Rigoutsos I. The complex transcriptional landscape of the anucleate human platelet. BMC Genomics. 2013;14:1. doi: 10.1186/1471-2164-14-1.

Burkhart JM, Vaudel M, Gambaryan S, Radau S, Walter U, Martens L, Martens L, Geiger J, Sickmann A, Zahedi RP. The first comprehensive and quantitative analysis of human platelet protein composition allows the comparative analysis of structural and functional pathways. Blood. 2012;120:e73-82. doi: 10.1182/blood-2012-04-416594.

Londin ER, Hatzimichael E, Loher P, Edelstein L, Shaw C, Delgrosso K, Fortina P, Bray PF, McKenzie SE, Rigoutsos I. The human platelet: strong transcriptome correlations among individuals associate weakly with the platelet proteome. Biology Direct. 2014;9, 3. doi: 10.1186/1745-6150-9-3.

Osman A, Hitzler WE, Ameur A, Provost P, Schubert M. Differential expression analysis by RNA-seq reveals perturbations in the platelet mRNA transcriptome triggered by pathogen reduction systems. PLoS ONE. 2015;10:1–17. doi: 10.1371/journal.pone.0133070.

Qureshi AH, Chaoji V, Maiguel D, Faridi MH, Barth CJ, Salem SM, Singhal M, Stoub D, Krastins B, Ogihara M, Zaki MJ, Gupta V. Proteomic and phospho-proteomic profile of human platelets in basal, resting state: insights into integrin signaling. PloS ONE. 2009;4:e7627. doi: 10.1371/journal.pone.0007627.

Rowley JW, Oler AJ, Tolley ND, Hunter BN, Low EN, Nix DA, Yost CC, Zimmerman GA, Weyrich AS. Genome wide RNA-seq analysis of human and mouse platelet transcriptomes. Blood. 2011;118:e101-11. doi: 10.1182/blood-2011-03-339705.

Thiele T, Braune J, Dhople V, Hammer E, Scharf C, Greinacher A, Völker U, Steil L. Proteomic profile of platelets during reconstitution of platelet counts after apheresis. Proteomics Clin Appl. 2016;10:831–838. doi: 10.1002/prca.201500134.

Zeiler M, Moser M, Mann M. Copy number analysis of the murine platelet proteome spanning the complete abundance range. Mol Cell Proteomics. 2014;13:3435–3445. doi: 10.1074/mcp.M114.038513.

277

A. Human coronins

B. Mouse coronins

Myc   Coro1 (Rb)   Coro1 (Mm)   Coro2   Coro3
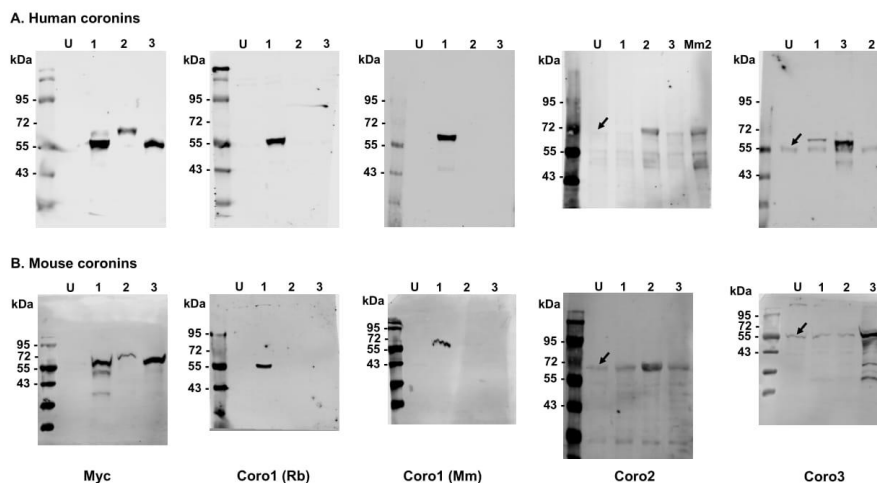
Supplemental Figure 1. Specificity of coronin antibodies used in this study. HEK 293T cells were transfected with plasmids encoding human (A) and mouse (B) Coro1, 2 and 3 fused to a Myc tag. After 18 h cells were lysed and 15 (A) or 20 μg (B) of lysate were analyzed by Western blot with antibodies for the indicated proteins. U, untransfected cells. 1, 2 and 3 refer to the respective coronin. Mm2 refers to mouse Coro2 on a blot with human coronins. Note that the lanes for Coro2 and 3 on the right-most human coronin blot are swapped. Coro2 and Coro3 antibodies detect the respective endogenous proteins in HEK 293T cells (arrows).

Materials and methods for Supplemental Figure 1. The antibodies used were: Myc, mouse monoclonal 9E10 (kind gift of Angelika A. Noegel, University of Cologne, Germany); Coro1(Rb), rabbit polyclonal ab72212 (Abcam); Coro1(Mm) mouse monoclonal ab56820 (Abcam); Coro2 ab99407; Coro3, mouse monoclonal K6-444 (Spoerl et al., J. Biol. Chem 277:48858-48867, 2002). Plasmids encoding mouse Coro2 and 3 as N-terminal myc fusions were purchased from Sino Biological (Beijing, China). Complementary DNAs encoding human Coro1, 2 and 3 (kindly provided by Christoph Clemen, University of Bochum, Germany) and mouse Coro1 were amplified using Q5 high fidelity polymerase (New England Biolabs, Hitchin, UK) and cloned into the EcoRI/KpnI sites of pCMV-myc. All plasmids were verified by sequencing. HEK 293T cells were cultivated at 37°C in a humidified incubator supplied with 5% CO_2. The cells were grown in Dulbecco's modified Eagle's medium (4.5 g/l glucose) (Merck) enriched with 10% fetal bovine serum (FBS) (Biochrom AG, Berlin, Germany), 2 mM glutamine (Merck), 1 mM sodium pyruvate (Merck), 100 U/ml penicillin, and 100 μg/ml streptomycin (PAA Laboratories GmbH, Pasching, Austria). Cells were transiently transfected using Lipofectamine 2000 (Invitrogen, ThermoFisher Scientific) according to the manufacturer's instructions and cultivated for 18 h. Transfected cells were lysed with 50 mM Tris–HCl, pH 8.0, 150 mM NaCl, 1% Triton® X-100 and protease inhibitors for 30 min. Cell debris was removed by centrifugation at 10,000×g at 4 °C for 10 min. The clarified lysate was resolved by SDS-PAGE and blotted onto PVDF.

278
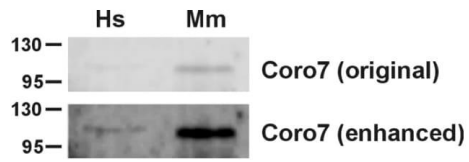
Supplemental Figure 2. Enhancement of Coro7 blot (Fig. 1A). The enhanced image was obtained with ImageJ by setting the minimum and maximum intensity values at 178 and 225 respectively, equivalent to linearly decreasing the brightness and increasing the contrast.

279
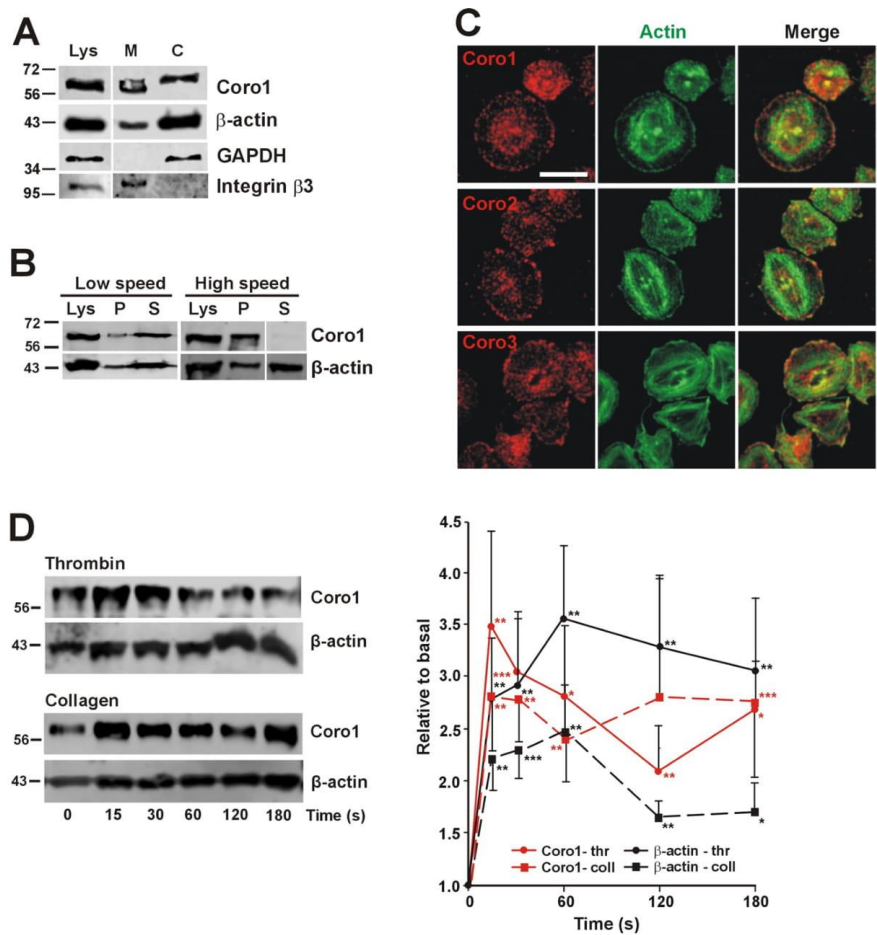
Supplemental Figure 3. Features of mouse coronins. (**A**) Subcellular fractionation of mouse platelets. Platelets were processed as in Fig. 1B. Integrin β3 was used as membrane marker and GAPDH as a cytosolic marker. (**B**) Association of Coro1 to actin in the detergent insoluble pellet of mouse platelets. Platelets were processed as in Fig. 1C. (**C**) Subcellular localization of mouse class I coronins. Mouse platelets were stimulated with 0.1 U/ml thrombin, allowed to spread on 100 μg/ml fibrinogen coated coverslips and fixed with paraformaldehyde. Cells were immunostained with the indicated coronin antibody followed by an Alexa568-coupled secondary antibody (red) and counterstained with FITC-phalloidin for filamentous actin (green). Images were acquired with a fluorescence microscope equipped with a structured illumination attachment and deconvolved. Scale bar 5 μm. (**D**) Dynamics of Coro1 along with F-actin in the Triton X-100 insoluble pellet of mouse platelets stimulated with thrombin or collagen. Washed mouse platelets were stimulated and processed as in Fig. 5A. Blots were quantified by densitometry and expressed as relative to the basal (unstimulated) platelets (time zero). The values are expressed as means ± SEM of 6-7 experiments. *P< 0.05, **P < 0.01, ***P < 0.001 relative to basal, Student's t test.
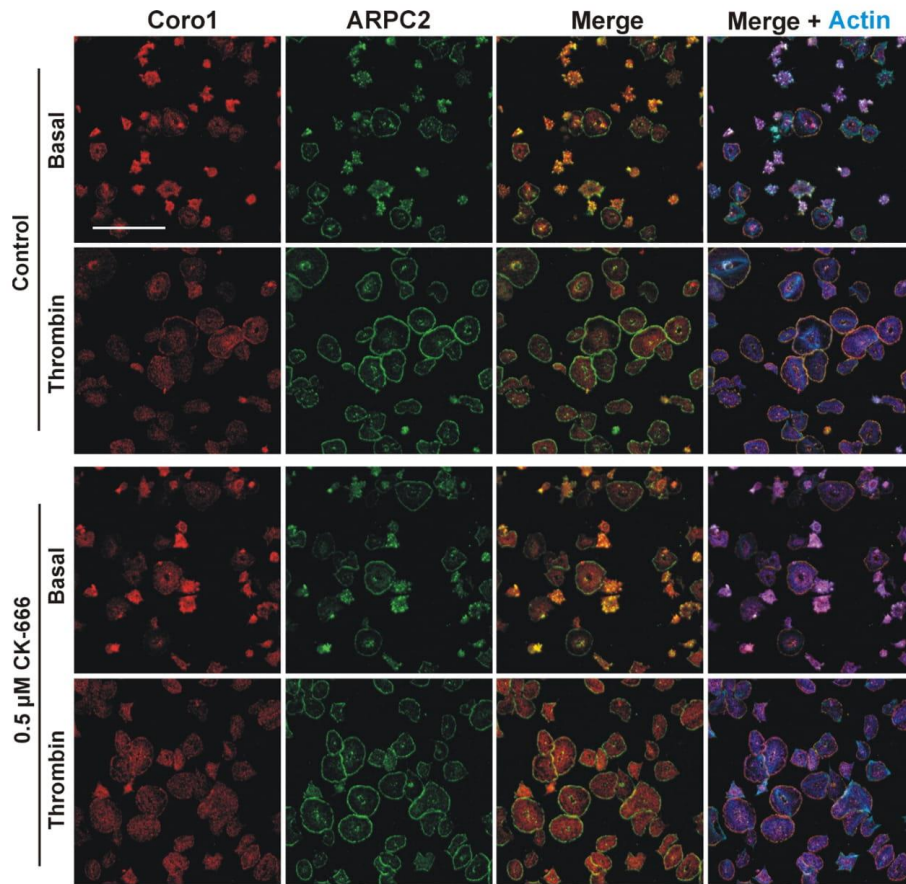
Supplemental Figure 4 (Continued on next page). Effect of the Arp2/3 complex inhibitor CK-666 on Coro1 localization. Human platelets were incubated with the indicated concentrations of CK-666 for 30 min, stimulated with 0.1 U/ml thrombin, immediately allowed to spread on 100 μg/ml fibrinogen coated coverslips and fixed after 45 min with paraformaldehyde. Cells were immunostained with anti-Coro1 and anti-ARPC2 antibodies, respectively (red and green) and counterstained with Alexa680-phalloidin for filamentous actin (blue). Images were acquired with a fluorescence microscope equipped with a structured illumination attachment and deconvolved. Scale bar 5 μm.

Supplemental Figure 4 (Continuation).

Supplemental Figure 5. Estimated protein expression of class I coronins in human tissues based on integrated proteomics data. Taken from GeneCards (genecards.com), where details on data sources and normalization can be found.
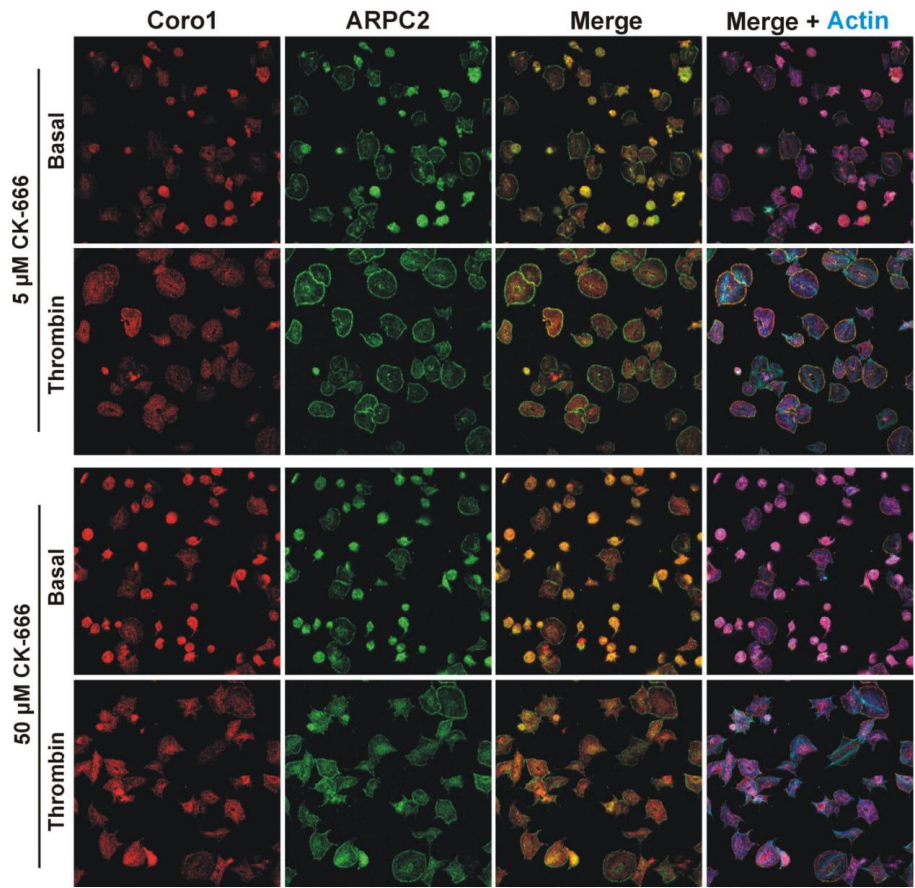
8.2.2 Coronin 1 is required for integrin β2 translocation in platelets

Article

Coronin 1 Is Required for Integrin β2 Translocation in Platelets

David R. J. Riley [1]**, Jawad S. Khalil** [1,2]**, Jean Pieters** [3]**, Khalid M. Naseem** [4] **and Francisco Rivero** [1,]*

[1] Centre for Atherothrombosis and Metabolic Disease, Hull York Medical School, Faculty of Health Sciences, University of Hull, Hull HU6 7RX, UK; David.riley@hyms.ac.uk (D.R.J.R.); jawad.khalil@bristol.ac.uk (J.S.K.)
[2] School of Physiology, Pharmacology and Neuroscience, Faculty of Life Sciences, University of Bristol, Bristol BS8 1TD, UK
[3] Biozentrum, University of Basel, CH-4056 Basel, Switzerland; jean.pieters@unibas.ch
[4] Leeds Institute for Cardiovascular and Metabolic Medicine, University of Leeds, Leeds LS2 9NL, UK; k.naseem@leeds.ac.uk
* Correspondence: Francisco.rivero@hyms.ac.uk; Tel.: +44-1482-644-633

check for updates

Abstract: Remodeling of the actin cytoskeleton is one of the critical events that allows platelets to undergo morphological and functional changes in response to receptor-mediated signaling cascades. Coronins are a family of evolutionarily conserved proteins implicated in the regulation of the actin cytoskeleton, represented by the abundant coronins 1, 2, and 3 and the less abundant coronin 7 in platelets, but their functions in these cells are poorly understood. A recent report revealed impaired agonist-induced actin polymerization and cofilin phosphoregulation and altered thrombus formation in vivo as salient phenotypes in the absence of an overt hemostasis defect in vivo in a knockout mouse model of coronin 1. Here we show that the absence of coronin 1 is associated with impaired translocation of integrin β2 to the platelet surface upon stimulation with thrombin while morphological and functional alterations, including defects in Arp2/3 complex localization and cAMP-dependent signaling, are absent. Our results suggest a large extent of functional overlap among coronins 1, 2, and 3 in platelets, while aspects like integrin β2 translocation are specifically or predominantly dependent on coronin 1.

Keywords: actin; Arp2/3 complex; cAMP; coronin 1; integrin β2; platelets; thrombin; collagen; prostacyclin

1. Introduction

Vascular injury leads to exposure of prothrombotic extracellular matrix proteins, which facilitates the entrapment and activation of platelets through specialized receptors. These interactions contribute to stable adhesion of platelets by generating intracellular signals that lead to shape change, secretion of granules, and activation of integrins. Activation of integrins facilitates the binding of the plasma protein fibrinogen, which subsequently supports platelet aggregation and clot formation, rapidly consolidated by secreted soluble agonists [1]. While this process is critical to hemostatic protection of the vasculature after injury, the rupture of atherosclerotic plaques drives uncontrolled platelet activation that leads to arterial thrombosis and clinical events such as myocardial infarction and stroke.

Platelet activation is the result of multiple integrated signaling cascades that ultimately drive remodeling of the platelet cytoskeleton and sustain the morphological changes required for adhesion, spreading, aggregation, and secretion at the sites of vascular damage [2]. The cytoskeleton is also the target of inhibitory signaling pathways regulated by cyclic nucleotides that balance the activating

pathways and prevent thrombus formation [3]. Coronins are a family of evolutionarily conserved regulators of the actin cytoskeleton turnover represented by seven members in mammals They have been grouped into three classes based on phylogenetic and functional criteria [4,5]. Class I includes Coronins 1, 2, 3, and 6 (also called 1A, 1B, 1C, and 1D) that associate with the actin cytoskeleton, localize at the leading edge of migrating cells, and participate in various signaling processes. Class II includes Coro4 and 5 (also called 2A and 2B), involved in focal adhesion turnover, reorganization of the cytoskeleton, and cell migration. The class III coronin (Coro7) has an unusual structure and plays a role in Golgi morphology maintenance. We have reported that class I coronins coronin 1, 2, and 3 are abundant in both human and mouse platelets, whereas coronin 7 is also present in human and mouse platelets in very low amounts and class II coronins are apparently absent [6].

Coronin 1 (coronin-1A or Coro1, also known as P57 or Tryptophan Aspartate containing COat protein (TACO)) [7,8] participates in the modulation of a number of processes through protein–protein interactions. For example, it modulates cyclic adenosine monophosphate (cAMP) signaling in neurons through interaction with the $G\alpha s$ subunit of heterotrimeric G proteins [9], neutrophil adhesion through interaction with the cytoplasmic tail of integrin $\beta2$ [10], and the activity of the small GTPase Rac1 [11]. Coro1 also participates in a number of other cellular processes including NADPH oxidase complex regulation, calcium signaling, vesicle trafficking, and apoptosis [12–16].

Coro1 is abundantly expressed in cells of the hematopoietic lineage, where it is essential for the survival of naïve T cells [16–19], but little is known about its role in platelets. We have shown that Coro1 is mainly a cytosolic protein, but a significant amount associates to membranes in an actin-independent manner. It rapidly translocates to the detergent-insoluble cytoskeleton upon platelet stimulation with thrombin or collagen. Along with Coro2 and 3, it accumulates at the cell cortex and actin nodules [6]. Stocker et al. reported the absence of an overt hemostasis defect in vivo in a knockout mouse model of Coro1. Detailed examination revealed impaired agonist-induced actin polymerization and cofilin phosphoregulation and altered thrombus formation in vivo as salient phenotypes [20]. Here we extend Stocker et al. report by an in-depth characterization of platelet function exploring additional aspects. Our data show that the absence of Coro1 is associated with impaired translocation of integrin $\beta2$ to the platelet surface upon stimulation with thrombin but otherwise does not result in noticeable morphological and functional alterations, including Arp2/3 complex localization and cAMP-dependent signaling. This mild phenotype suggests a complex picture in which class I coronins might share roles extensively in platelets.

2. Results

2.1. Absence of Coro1 Is Not Compensated by Increased Coro3

To gain insight into the roles of Coro1 in platelet function, we undertook the characterization of a previously described *Coro1a* knockout (KO) model [15]. We confirmed the absence of the protein in platelet lysates of homozygous KO mice by Western blot analysis and observed that heterozygous mouse platelets expressed approximately half of the amount of the protein present in wild type (WT) mouse platelets (Figure 1A). Coro1 KO mice have been reported to exhibit unaffected hematological parameters, including platelet counts, indicating that hematopoiesis is not affected [17,20]. The size of Coro1 KO platelets was comparable to that of WT platelets as estimated from the forward light scatter in flow cytometry experiments ($p = 0.8164$, Student's t-test) (Figure 1B).
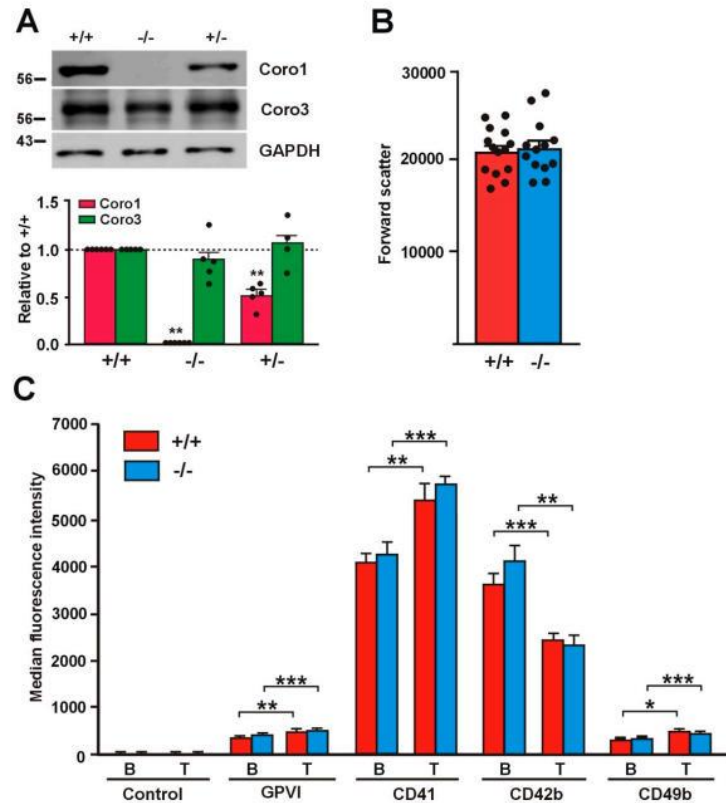
Figure 1. Relative size and receptor expression in *Coro1a* deficient platelets. (**A**) Absence of Coro1 in *Coro1a* deficient platelets and no obvious compensation by Coro3. Platelet lysates were resolved by SDS-PAGE, blotted and probed with specific antibodies for the indicated proteins. GAPDH was used for normalization. Data represent mean ± standard error of the mean (SEM) of 4–6 independent experiments. ** $p < 0.01$; Mann–Whitney U-test. Full blots are shown in Supplemental Figure S1; (**B**) Relative size of *Coro1a* deficient platelets. Mean platelet volume was estimated in platelet-rich plasma (PRP) by mean forward light scatter area using flow cytometry. Data represent mean ± SEM of 13–14 independent experiments. No statistically significant differences were found, Student's *t*-test; (**C**) Surface receptor expression in *Coro1a* deficient platelets. Platelet surface receptors were determined in PRP by flow cytometry both in basal conditions (B) and upon stimulation with 0.1 U/mL thrombin for 20 min at 37 °C (T). Data represent mean ± SEM of 7–16 independent experiments. * $p < 0.05$; ** $p < 0.01$; *** $p < 0.001$; paired Student's *t*-test between basal and stimulated conditions. No statistically significant differences were found between wild type and knockout, nonpaired Student's *t*-test.

2.2. Receptor Expression Is Not Affected in Coro1 Deficient Platelets

We assessed the expression of characteristic surface platelet receptors (GPVI, CD41, CD42b, and CD49b) by flow cytometry both in unstimulated and in thrombin-stimulated platelets. Thrombin stimulation caused a significant increase in the expression of GPVI, CD41 (integrin αIIb), and CD49b (integrin α2) (20–40%) and a significant decrease in the expression of CD42b (GP1b) (32–43%), the latter

287

due to cleavage and internalization of the GP1b/IX/V complex [21]. Both basal and thrombin-stimulated receptor expression levels were comparable in Coro1 WT and KO platelets (Figure 1C).

2.3. Translocation of Integrin β2 Is Impaired in the Absence of Coro1

Coro1 interacts with the cytoplasmic tail of integrin β2 and regulates its function in neutrophils [10]. Although less abundant than integrins β1 and β3, integrin β2 (CD18) is expressed in murine platelets [22–25] and has also been described in human platelets, where expression increases upon thrombin stimulation [26]. This prompted us to investigate whether Coro1 deficiency would have an effect on this integrin. We used flow cytometry to assess the levels of expression of CD18 both in resting and in thrombin stimulated platelets and observed that in resting platelets the levels of CD18 were higher, although statistically not significant, in WT platelets (940 ± 70 median fluorescence intensity) than in KO platelets (783 ± 51; $p = 0.1016$). However, upon thrombin stimulation expression increased significantly in WT platelets to 1562 ± 158 ($p = 0.0032$ relative to basal) but only modestly in KO platelets (to 986 ± 110; $p = 0.0915$ relative to basal, $p = 0.0123$ relative to WT) (Figure 2A,B). The impaired translocation of CD18 in KO platelets can be visualized in immunostained platelets (Figure 2C).

Integrin β2 main ligand is intercellular adhesion molecule-1 (ICAM-1), a glycoprotein expressed in endothelial cells and leukocytes. We used fluorescence microscopy to investigate the effect of Coro1 absence on platelet adhesion and spreading on surfaces coated with 5 mg/mL native BSA, a surrogate method of assessing binding to ICAM-1, both basally and upon stimulation with 0.1 U/mL thrombin [27,28]. On average, similar numbers of WT and KO resting platelets adhered to coverslips (116.7 ± 14.0 and 120.8 ± 7.1, respectively). Resting platelets of both strains attached to the BSA-coated surface but most did not appear to spread, presenting a round morphology and covering a small area (approximately 9 μm^2) (Figure 2D–F). Thrombin stimulation prior to seeding resulted in more than twice the numbers of adhering platelets (280.3 ± 17.2 in WT vs. 276.9 ± 24.0 in KO). Most stimulated platelets presented a well spread round morphology with stress fibers, although some had a spiky morphology, and covered an area of approximately 21 μm^2. No obvious differences were apparent in cell area between WT and KO platelets (Figure 2D–F). To investigate whether stimulation with lower thrombin doses would reveal any subtle difference in spreading between WT and KO platelets, we performed a set of experiments basally and upon stimulation with 0.05 and 0.025 U/mL thrombin. We observed that both doses resulted in numbers of adhering platelets similar to those obtained with 0.1 U/mL: 309.3 ± 16.8 in the WT vs. 282.0 ± 13.7 in the KO with 0.05 U/mL and 296.3 ± 22.4 in the WT vs. 320.8 ± 38.9 in the KO with 0.025 U/mL. The areas of the spread platelets were also in a range similar (20–21 μm^2) to those observed with 0.1 U/mL thrombin. This indicates that low thrombin doses (0.025 U/mL) are sufficient to elicit full spreading on native BSA and Coro1 is dispensable for this response.
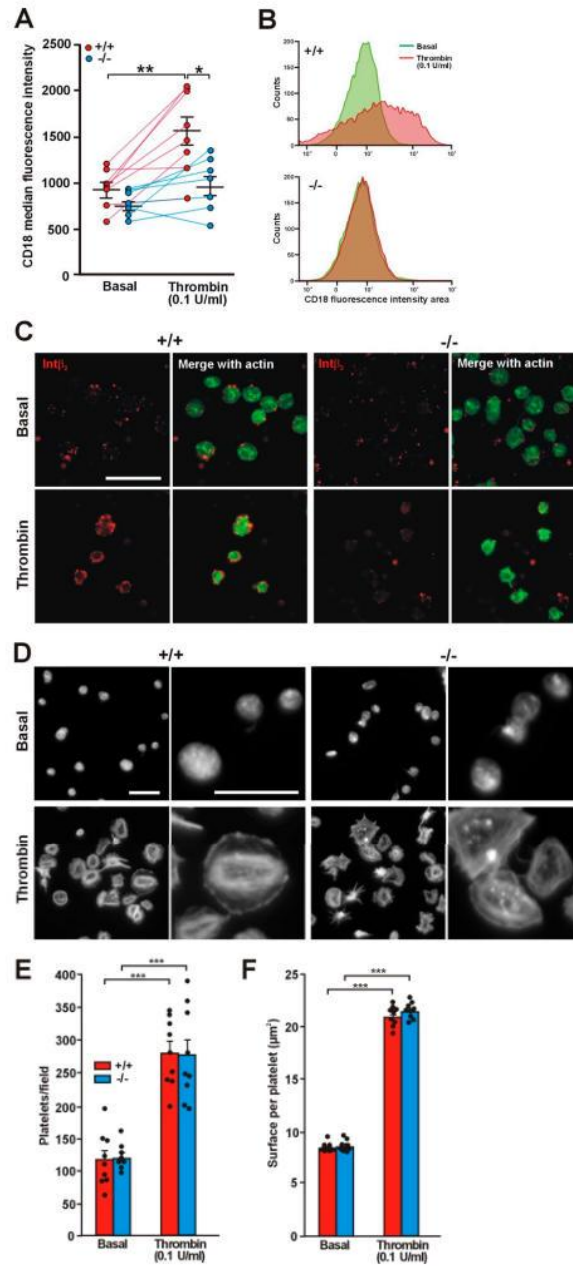
Figure 2. Impaired translocation of integrin β2 in *Coro1a* deficient platelets. (**A**) Platelet surface integrin β2 (CD18) was determined in PRP by flow cytometry both in basal conditions and upon stimulation

289

with 0.1 U/mL thrombin for 20 min at 37 °C. Individual data and the mean ± SEM of 7–8 independent experiments are shown. * $p < 0.05$; ** $p < 0.01$; paired Student's *t*-test between basal and stimulated conditions. Nonpaired Student's *t*-test between wild type (WT) and knockout (KO); (**B**) Representative flow cytometry data of platelet surface CD18 distribution in basal conditions and upon thrombin stimulation; (**C**) Washed platelets were stimulated in suspension with 0.1 U/mL thrombin, fixed with 4% paraformaldehyde (PFA) and spun on poly-L-lysine coated coverslips. The permeabilization step was omitted and the cells were stained with an anti-integrin β2 antibody followed by an Alexa568-coupled secondary antibody (red) and counterstained with fluorescein isothiocyanate (FITC)-phalloidin for filamentous actin (green). Images were acquired with a fluorescence microscope equipped with a structured illumination attachment and deconvolved. Scale bar represents 10 μm; (**D**) Adhesion of Coro1 KO and WT platelets to native bovine serum albumin (BSA). Washed platelets were stimulated with 0.1 U/mL thrombin and immediately allowed to attach to glass coverslips coated with 5 mg/mL of native BSA. Adherent platelets were fixed with 4% PFA, permeabilized with 0.3% Triton X-100, and stained with tetramethylrhodamine isothiocyanate (TRITC)-phalloidin. Images of random areas were acquired with a fluorescence microscope. Examples of platelets at two magnifications are shown. Scale bars represent 10 μm; (**E**) Number of platelets adhering to BSA. 5 fields each 31,560 μm^2 from 9 independent experiments were scored per condition. Data represent mean ± SEM. Number of platelets was significantly higher upon thrombin stimulation (** $p < 0.01$, paired Student's *t*-test). No significant differences were found between WT and KO platelets both resting and stimulated (unpaired Student's *t*-test); (**F**) Surface coverage per platelet calculated by thresholding using ImageJ. Data represent mean ± SEM from 9 independent experiments and 600–1200 platelets per condition for each experiment. Platelet surface was significantly higher upon thrombin stimulation (*** $p < 0.001$, paired Student's *t*-test). No significant differences were found between WT and KO platelets, both resting and stimulated (unpaired Student's *t*-test).

2.4. Effect of Coro1 Deficiency on Integrin αIIbβ3 Activation and Granule Secretion

We assessed the potential effects of Coro1 deficiency on integrin αIIbβ3 activation with the activation state-specific antibody JON/A by flow cytometry. Stimulation with a wide range of agonists (thrombin, collagen-related peptide (CRP), as well as adenosine diphosphate (ADP) and the thromboxane analog U46619 alone or in combination) caused activation of αIIbβ3, in the case of thrombin and CRP in a dose-dependent manner (Figure 3A). However, we were not able to detect any significant differences in JON/A levels between Coro1 KO and WT platelets, indicating that Coro1 is dispensable for αIIbβ3 activation.

We next explored whether Coro1 KO platelets have a defect in granule secretion. To monitor alpha and dense granule secretion, we induced P-selectin and CD63 expression, respectively, by the same agonists as in the αIIbβ3 activation experiment. In both cases, thrombin produced a clear dose–response effect, CRP had little effect and ADP and U46619 had a synergistic effect in both WT and KO platelets (Figure 3B,C). None of the conditions tested revealed any statistically significant difference between both populations, suggesting that Coro1 is dispensable for granule secretion.
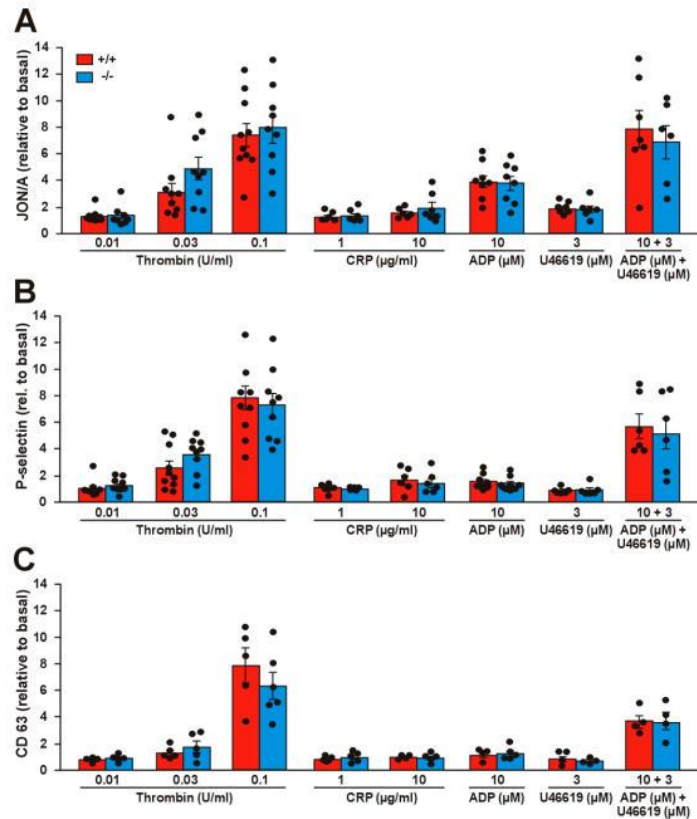
Figure 3. Integrin activation and secretion in *Coro1a* deficient platelets. Integrin activation (**A**), P-selectin exposure (**B**), and CD63 exposure (**C**) were determined in PRP upon stimulation with the indicated doses of agonists for 20 min at 37 °C and subsequent flow cytometry analysis. The data (median fluorescence intensity) represent the mean ± SEM of 5–9 independent experiments expressed relative to basal (unstimulated) platelets. No statistically significant differences were found between WT and KO, Student's *t*-test.

2.5. Effect of Coro1 Deficiency on Platelet Aggregation and Spreading

A functioning actin cytoskeleton remodeling is critical for platelet aggregation and for adhesion and spreading on extracellular matrix proteins. We next investigated the implications of Coro1 deficiency for those processes. Stocker et al. reported subtle defects in aggregation induced by low doses of collagen using impedance-based aggregometry on whole blood [20]. We applied light transmission aggregometry on washed platelets using a range of doses of thrombin (0.0125–0.1 U/mL), collagen (1–10 µg/mL), and CRP (3–10 µg/mL). All three agonists elicited, as expected, a dose-dependent aggregation response, which was comparable in both WT and KO platelets at all doses (Figure 4). The aggregation velocity, calculated as the slope of the aggregation curve, was also dose-dependent for all three agonists. We only observed a statistically significant alteration in the response to high-dose thrombin, with KO platelets showing a marginally higher percentage of aggregation (91.7 vs. 82.4, $p = 0.0420$) and a moderately higher velocity (3.29 vs. 4.30, $p = 0.0137$, Student's *t*-test) compared

291

to WT platelets. We did not observe any statistically significant difference between WT and KO platelets at any dose of collagen or CRP.
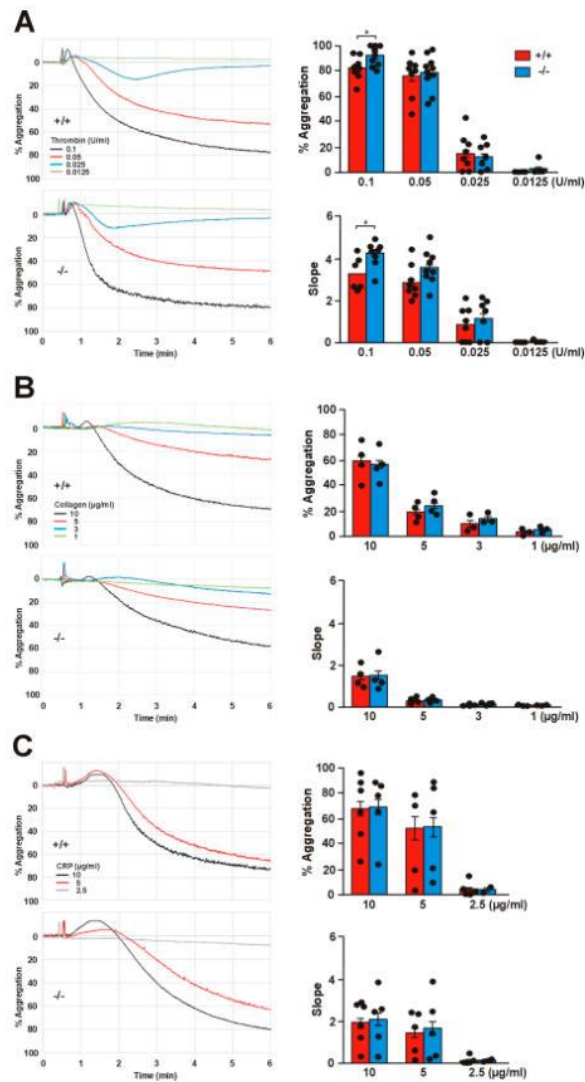
Figure 4. Aggregation in *Coro1a* deficient platelets. Washed platelets (2.0×10^8 platelets/mL) were stimulated with the indicated doses of thrombin (**A**), collagen (**B**), or collagen-related peptide (CRP) (**C**) and aggregation was recorded for 6 min in a Chrono-Log aggregometer. Representative traces are shown on the left. Bar diagrams show percentage of maximum aggregation within 5 min of stimulation and slope as calculated from the linear part of the aggregation trace. Data are mean ± SEM of 4–10 independent experiments. * $p < 0.05$, Student's *t*-test for thrombin; no significant differences were found with collagen and CRP, Mann–Whitney U-test.

The effect of Coro1 absence on platelet adhesion and spreading was further investigated on surfaces coated with collagen (100 µg/mL) or fibrinogen (100 µg/mL) by fluorescence microscopy. On average, slightly more platelets per observation field adhered on fibrinogen; however, there were no statistically significant differences in the numbers of platelets adhering to either surface between the WT and the KO platelets (60.4 ± 4.5 vs. 61.4 ± 5.1 on fibrinogen and 48.3 ± 4.6 vs. 52.3 ± 7.4 on collagen) (Figure 5A, B). Irrespective of genotype, platelets covered a slightly larger surface on collagen (13.43 ± 1.07 µm^2 in the WT vs. 15.83 ± 0.85 µm^2 in the KO) than on fibrinogen (10.75 ± 0.74 µm^2 in the WT vs. 11.89 ± 0.71 µm^2 in the KO) (Figure 5C). Characteristically, on fibrinogen, most platelets showed abundant filopods and actin nodules whereas on collagen most displayed stress fibers, however, no differences in the morphology were apparent between WT and KO platelets in any of the matrices.
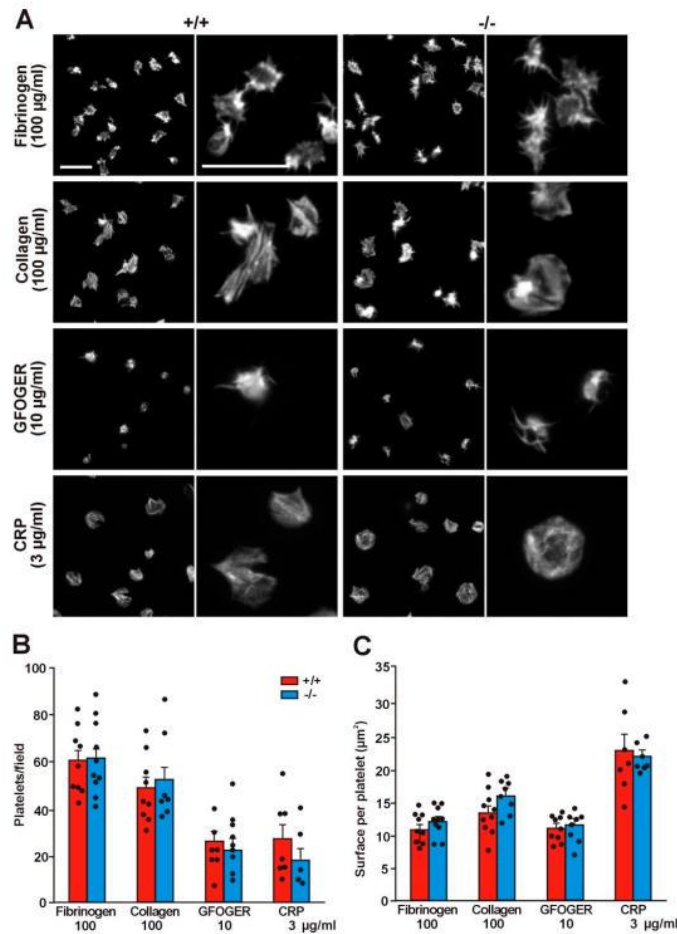
Figure 5. Absence of Coro1 does not impair platelet spreading. (**A**) Adhesion of washed platelets to glass coverslips coated with the indicated concentration of collagen, fibrinogen, Gly-Phe-Hyp-Gly-Glu-Arg (GFOGER), or CRP. Adherent platelets were fixed with 4% PFA, permeabilized with 0.3% Triton X-100,

and stained with TRITC-phalloidin. Images were acquired with a fluorescence microscope equipped with a structured illumination attachment and deconvolved. Examples of platelets at two magnifications are shown. Scale bars represent 10 μm; (**B**) Number of platelets adhering to the indicated concentrations of collagen, fibrinogen, GFOGER, or CRP. 5 fields each 12,500 μm^2 from 5–10 independent experiments were scored per condition. Data represent mean ± SEM. No significant differences were found between WT and KO platelets for any condition (Mann-Whitney U-test); (**C**) Surface coverage per platelet calculated by thresholding using ImageJ. Data represent mean ± SEM from 5–10 independent experiments and 250–1000 platelets per condition for each experiment. No significant differences were found between WT and KO platelets for any condition (Mann–Whitney U-test).

We investigated any subtle effect of Coro1 ablation on adhesion to specific collagen receptors using coverslips coated with peptides that discriminate between receptors, Gly-Phe-Hyp-Gly-Glu-Arg (GFOGER) (for α2β1 integrin), or CRP (for GPVI). Approximately 50% less platelets adhered on GFOGER and CRP compared to collagen and the trend was similar in both WT and KO platelets (Figure 5B). Surface coverage was lower on GFOGER (10.98 ± 0.62 μm^2 in the WT vs. 11.43 ± 0.81 μm^2 in the KO) and higher on CRP (22.92 ± 2.24 μm^2 in the WT vs. KO 21.96 ± 0.77 μm^2 in the KO) compared to collagen (Figure 5C). On CRP, platelets morphologically resembled the ones on collagen, whereas on GFOGER they were discoid and spiky. Again, there were neither statistically significant differences in surface coverage between WT and KO platelets nor noticeable morphological differences in collagen receptor-specific matrices.

2.6. Coro1 Is Dispensable for Arp2/3 Complex Localization

We have shown that in platelets Coro1 co-immunoprecipitates and colocalizes with components of the Arp2/3 complex and that the activity of the complex is necessary for extension of lamellipodia and accumulation of Coro1 at the cell cortex of spreading platelets [6]. We used Coro1 deficient platelets to address whether Coro1 is necessary for Arp2/3 complex localization by allowing them to spread on fibrinogen upon activation with 0.1 U/mL thrombin (Figure 6A). Virtually all unstimulated platelets spread on fibrinogen and showed abundant filopods and actin nodules. In those platelets, the Arp2/3 component ARPC2 (p34-Arc, component of the Arp2/3 complex) displayed a diffuse distribution and some accumulation at actin nodules. Upon thrombin stimulation, approximately 92% of platelets adopted a well spread circular shape with stress fibers and neat accumulation of actin and ARPC2 at the cell cortex. These patterns of platelet morphology and ARPC2 distribution were indistinguishable in both WT and KO platelets (Figure 6B), indicating that Coro1 is dispensable for Arp2/3 localization and lamellipodia formation upon platelet stimulation. Using the same approach, we explored whether activation of the Arp2/3 complex is required for spreading and for cortical localization of ARPC2 upon thrombin stimulation (Figure 6A). We treated wild type and Coro1 deficient platelets with the Arp2/3 complex inhibitor CK666 (50 μM) prior to stimulation with thrombin and seeding. While still capable of adhering to fibrinogen, virtually all unstimulated platelets remained discoid with inconspicuous ARPC2 distribution. Upon thrombin stimulation, approximately 80% of platelets remained discoid, whereas the rest spread, however, their morphology was irregular, their F-actin staining was weaker compared to untreated platelets, and ARPC2 was almost never found at the cell cortex. This shows that activation of the Arp2/3 complex is required for its cortical localization and for efficient spreading, irrespective of the presence of coronin 1.
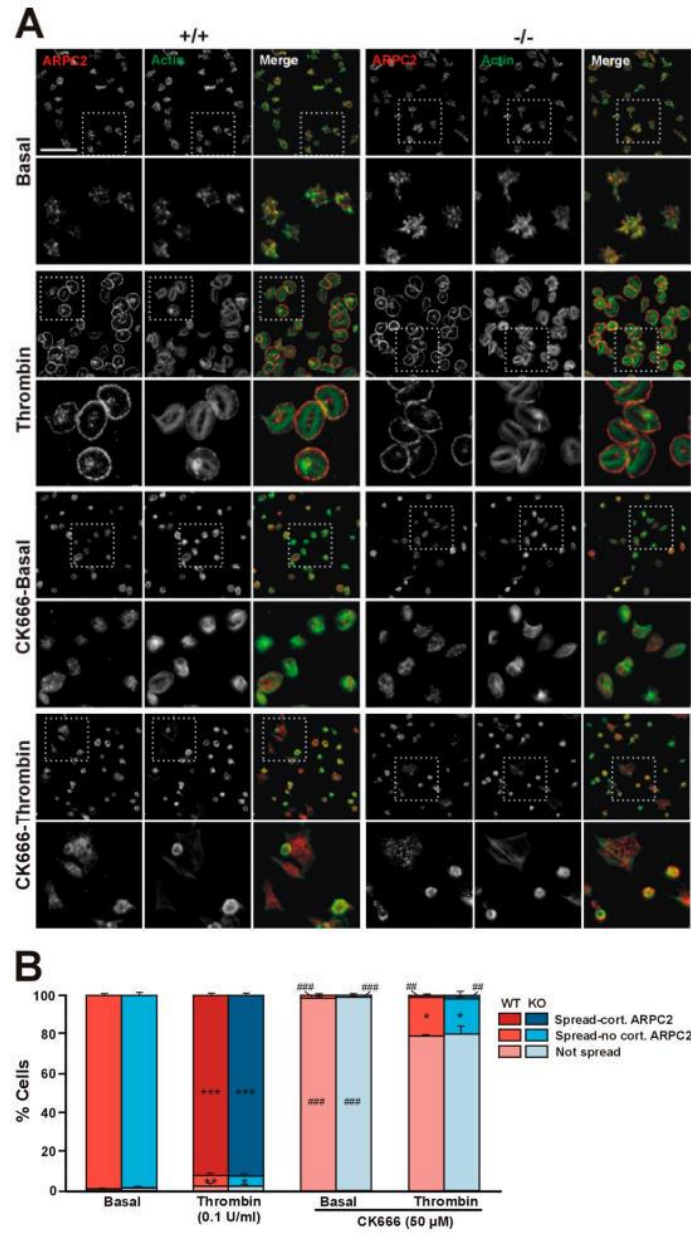
Figure 6. Coro1 is dispensable for Arp2/3 complex localization. (**A**) Localization of ARPC2 in resting and thrombin-stimulated platelets. Washed platelets were stimulated with 0.1 U/mL thrombin and immediately allowed to attach to glass coverslips coated with 100 μg/mL of fibrinogen. A population

295

of platelets was treated with the Arp2/3 complex inhibitor CK666 (50 µM) for 30 min at 37 °C prior to thrombin stimulation. Adherent platelets were fixed with 4% PFA, permeabilized with 0.3% Triton X-100, stained with an anti-ARPC2 antibody followed by an Alexa568-coupled secondary antibody (red) and counterstained with FITC-phalloidin for filamentous actin (green). Images were acquired with a fluorescence microscope equipped with a structured illumination attachment and deconvolved. Examples of platelets at two magnifications are shown. Boxes mark the enlarged regions. Scale bar represents 25 µm; boxes are 27 × 27 µm; (**B**) Platelet morphology. Platelets were assigned to one of three classes based on spreading and ARPC2 distribution (cortical or not). 5 fields each 36,670 µm^2 from 4 independent experiments were scored per condition. Data are shown as percentage of platelets of each class and represent mean ± SEM. * $p < 0.05$, ** $p < 0.01$, *** $p < 0.001$ relative to the corresponding basal condition. ## $p < 0.01$, ### $p < 0.001$ relative to platelets not treated with CK666 of the same condition. Symbols are placed inside their corresponding bars. No significant differences were found between WT and KO platelets for any condition (Kruskal–Wallis test).

2.7. Absence of Coro1 Does Not Affect cAMP Signaling

Jayachandran et al. have shown that Coro1 interacts with Gαs and modulates the cAMP signaling pathway in neurons and T cells [9,29]. In platelets the cAMP pathway can be triggered by exposure to prostacyclin (PGI2), whose receptor is coupled to heterotrimeric G proteins containing the Gαs subunit, resulting in dampening of the ability to respond to thrombin stimulation. We have shown that in platelets Coro1 is able to immunoprecipitate and colocalize with Gαs [6], prompting us to investigate the functionality of the cAMP pathway in Coro1 deficient platelets. We monitored the activity of the cAMP pathway by detection of vasodilator-stimulated phosphoprotein (VASP) phosphorylation at Ser157. Treatment with a low (5 nM) and a high (100 nM) dose of PGI2 resulted in a dose-dependent increase in the amount of pVASP-S157 in both WT and KO platelets. No statistically significant differences were observed between both genotypes (Figure 7A). We used flow cytometry to quantify the effect of PGI2 on thrombin-stimulated integrin αIIbβ3 activation and granule secretion. Platelets were pretreated with 100 nM PGI2 prior to stimulation with 0.1 U/mL thrombin. As already shown in Figure 3, stimulation with thrombin caused activation of integrin β3 as well as P-selectin and CD63 expression, whereas PGI2 itself did not elicit any response. Treatment with 100 nM PGI2 prior to thrombin stimulation completely abolished those responses both in WT and KO platelets (Figure 7B). Collectively, our results indicate that Coro1 is dispensable for Gαs-dependent modulation of the cAMP pathway in platelets.

2.8. Absence of Coro1 Does Not Impair Hemostasis

To evaluate the influence of *Coro1a* deletion on hemostasis, we examined tail bleeding (Figure 8). Both Coro1 KO and WT animals showed a comparable average bleeding time (1.99 ± 0.19 min in the KO vs. 1.71 ± 0.20 min in the WT). In these experiments, two WT and two KO mice out of 15 per genotype re-bled within one minute of cessation of bleeding.
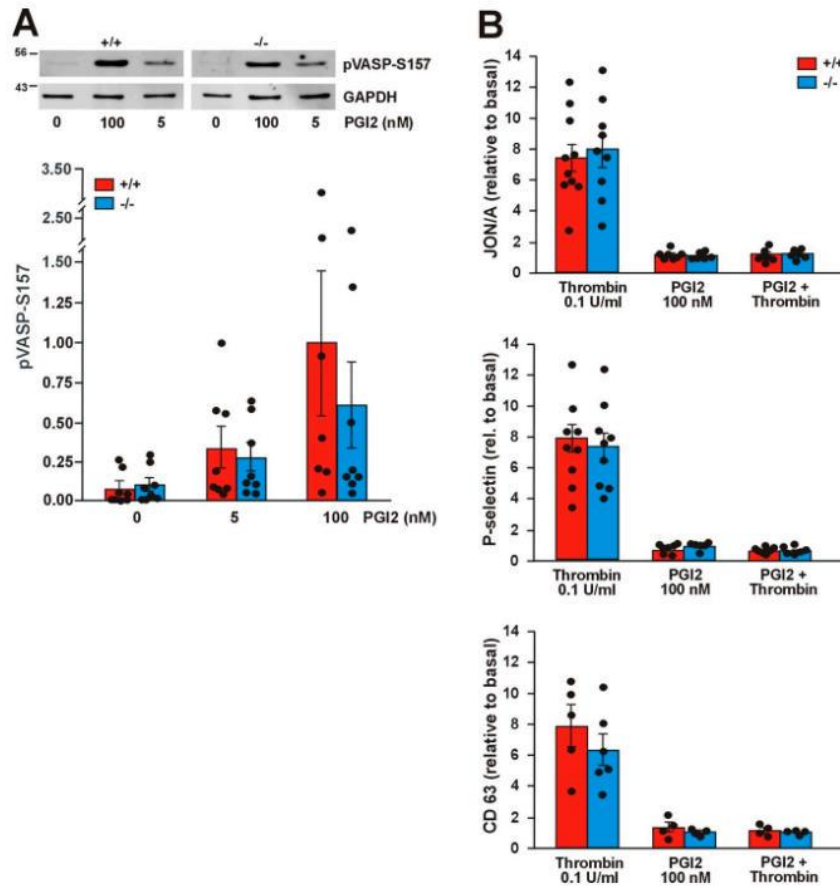
Figure 7. The cAMP pathway is not affected in *Coro1a* deficient platelets. (**A**) Phosphorylation of vasodilator-stimulated phosphoprotein (VASP) upon prostacyclin (PGI2) stimulation for 5 min at the indicated doses. Platelet lysates were resolved by SDS-PAGE, blotted, and probed with specific antibodies for pVASP-Ser157. GAPDH was used for normalization. Representative blots and bar diagrams showing mean ± SEM of 7 independent experiments. Full blots are shown in Supplemental Figure S2; (**B**) Integrin activation, P-selectin exposure, and CD63 exposure upon stimulation with thrombin prior to PGI2. Platelets in PRP were treated with 100 nM PGI2 for 5 min prior to stimulation with 0.1 U/mL thrombin and subsequently analyzed by flow cytometry. This set of experiments was carried out simultaneously with the ones presented in Figure 3. The data (median fluorescence intensity) are expressed relative to basal (unstimulated) platelets. The data represent the mean ± SEM of 4–9 independent experiments. No significant differences were found between WT and KO in any of the assays (Student's *t*-test or Mann–Whitney U-test).
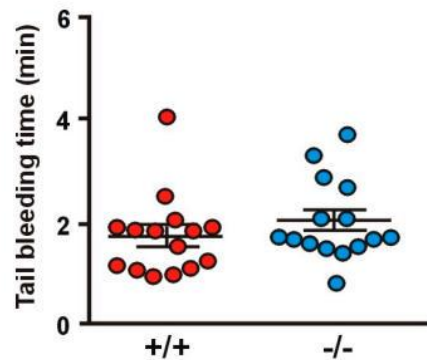
Figure 8. Tail bleeding time. Tests were performed by cutting off 2 mm of the tail tip and immediately placing the tail in PBS at 37 °C. The time until hemostasis was recorded for up to 10 min and re-bleeding monitored for 60 s beyond hemostasis. Data represent mean ± SEM of 15 animals. No significant differences were found between WT and KO (Student's *t*-test).

3. Discussion

The availability of animal models has significantly contributed to elucidate the roles in platelet function of cytoskeleton proteins, which usually cannot be targeted pharmacologically [30]. Here we present a functional characterization of Coro1, an abundant class I coronin, in a KO mouse model. The salient phenotype of Coro1 deficient platelets is the impaired translocation of integrin β2 to the cell surface upon thrombin stimulation, in the absence of any alteration in a range of morphological and functional tests. Our study broadly confirms a recent report by Stocker et al. and explores aspects not covered there [20]. However, we failed to observe some of the mild defects reported by Stocker et al., namely increased relative platelet size and adhesion receptor expression, decreased platelet spreading area upon stimulation with thrombin or collagen, and decreased velocity of aggregation in response to low-dose collagen [20]. These divergent outcomes could be tracked back to methodological differences, size of experimental populations, and statistical analysis. For example, Stocker et al. used an impedance-based method on whole blood to study aggregometry, whereas we used light transmission aggregometry on washed platelets. Impedance-based aggregometry on whole blood captures responses that depend on interactions with leukocytes and red blood cells and is, therefore, closer to the physiological situation, however, it is considered insensitive to low levels of platelet activation. Light transmission aggregometry, by contrast, requires more manipulations but takes platelets at face value, without the influence of variations in hematocrit and cellular content [31,32]. The different methods might have influenced platelet reactivity, causing opposite outcomes, although the differences between WT and KO were always small.

While translocation and activation of integrin αIIbβ3 were not affected in the Coro1 KO platelets, we observed impaired translocation of integrin β2 by deletion of Coro1, suggesting that Coro1 is specifically implicated in the regulation of this integrin in platelets. Integrin β2, a component of lymphocyte function-associated antigen 1 (LFA-1) when associated with integrin αL, is one of the 6 integrins expressed in mouse platelets and the fourth most abundant [25]. β2 integrins are important for polymorphonuclear neutrophil adhesion to the endothelium and subsequent events, like extravasation [33]. Coro1 is critical for these processes because it interacts with the cytoplasmic tail of integrin β2 and regulates the accumulation of activated integrin in focal zones of adherent cells [10]. In platelets, LFA-1 has not been extensively investigated. Platelets from mice deficient in integrin β2 are characterized by a shorter lifespan, reduced adhesion to the endothelium in response to tumor necrosis factor (TNF), and caspase activation [24]. Stocker et al. reported a normal lifespan of Coro1 deficient

platelets, suggesting that this coronin is not the only protein responsible for the regulation of integrin β2 [20]. Similarly, we did not observe any defective adhesion and spreading on an ICAM-1 surrogate matrix, suggesting that Coro1 deficient platelets retain sufficient binding capacity through LFA-1 and/or other mechanisms. In line with this observation, Stocker et al. reported unaffected accumulation of neutrophils within arterial thrombi in Coro1 deficient platelets [20]. However, the role of integrin β2 in platelet–leukocyte interaction is difficult to dissect due to concurrent and more prevalent mechanisms mediating those interactions [34] and to the fact that the interactions mediated by LFA-1 and ICAM family molecules are reciprocal: both are present simultaneously in platelets and leukocytes. A rigorous attempt at exploring this aspect would require the generation of a platelet-specific Coro1 knockout model combined with platelet-specific deletion of ICAM-2, the adhesion molecule isoform present in the platelet membrane [25].

Jayachandran et al. have uncovered the role of Coro1 in modulating the cAMP signaling pathway in excitatory neurons, where deficiency of the protein resulted in the loss of excitatory synapses and a range of neurobehavioral disabilities [9]. Coro1 interacts with Gαs in a stimulus-dependent manner, leading to increased cAMP production [9]. Moreover, the association of Coro1 with Gαs is regulated by cyclin-dependent kinase 5 (CDK5)-mediated phosphorylation of Coro1 on two particular threonine residues [35]. Furthermore, Coro1 regulates cAMP signaling in T cells [29] whereas the homolog in *Dictyostelium discoideum* regulates cAMP-dependent initiation of multicellular aggregation [36] and the homolog in the fungus *Magnaporthe oryzae* interacts with a Gαs subunit to regulate cAMP production and pathogenicity [37]. In platelets, Gαs activation and subsequent cAMP production are coupled to binding of PGI2 to its G protein-coupled receptor. Although Coro1 is able to co-immunoprecipitate Gαs in platelets [6], absence of Coro1 does not appear to be detrimental to the production of cAMP, as demonstrated by the ability of Coro1 deficient platelets to phosphorylate VASP and block the effects of thrombin stimulation when exposed to PGI2. The role of Coro1 in cAMP regulation is, however, complex. In T cells depletion of Coro1 results in reduced production of cAMP, however, cAMP levels are increased due to a compensatory decrease in phosphodiesterase 4 (PDE4) levels [29]. Further research would be needed to clarify whether Coro1 regulates the cAMP pathway in platelets and, if so, through which molecular mechanisms. PDE4 is absent [38] but CDK5 is present both in human and mouse platelets [25,39], although the role of the latter in platelets has not been addressed so far. In addition, we have reported the presence of Coro2 and Coro3 in immunocomplexes with Gαs [6], suggesting that these two class I coronins may compensate for the absence of Coro1 for regulation of the cAMP pathway. Functional compensation by other class I coronins might also explain the retained ability of the Arp2/3 complex to accumulate at the cell cortex and enable the formation of lamellipodia and consequently spreading. We have shown that Coro2 and 3 can be found in immunocomplexes with ARPC2 and accumulate at the cell cortex of spread platelets [6].

In summary, we propose that class I coronins display a large extent of functional overlap in platelets. This would explain the absence of a strong phenotype in most platelet functional assays while aspects like integrin β2 translocation reported by us and the formation of F-actin and cofilin dephosphorylation in response to agonists reported by others [20] are specifically or more strongly dependent on Coro1 function. This is not uncommon among components of the actin cytoskeleton, where examples abound [30]. Thus, disruption of the Arp2/3 complex regulators cortactin and its homolog HS1 does not cause any noticeable alteration in platelet function, indicating that their roles might be fulfilled by other proteins [40]. Similarly, disruption of the formin mDia results in no major platelet phenotype, pointing at functional compensation by other formins present in platelets [41]. Future studies toward the elucidation of coronin function in platelets will, therefore, require the generation of mouse models lacking two or three class I coronins in order to arrive at a complete picture of the shared and unique roles of these proteins.

4. Materials and Methods

4.1. Reagents

Primary antibodies against following proteins were used: Coro1 (ab56820 and ab72212), β-actin (ab20272) from Abcam (Cambridge, UK); Coro3 (K6-444 hybridoma supernatant) [42]; β3-integrin (HC93 sc-14009) and Gαs (sc-823) from Santa Cruz Biotechnology (Heidelberg, Germany); phosphor-VASP(Ser157) (#3111) from Cell Signaling Technology (Leiden, The Netherlands); GAPDH (6C5-CB1001) from Calbiochem/Merck (Watford, UK); p34-Arc/ARPC2 (07-227) from Millipore/Merck. Secondary antibodies Alexa Fluor 568-conjugated anti-rat or anti-rabbit immunoglobulins (Molecular Probes, Thermo Fisher Scientific, Altrincham, UK) were used for immunofluorescence. IRDye 680 or IRDye 800 anti-mouse and anti-rabbit immunoglobulins (LI-COR Biosciences, Lincoln, NE, USA) were used for Western blot. Human fibrinogen was from Enzyme Research (Swansea, UK), collagen (Kollagenreagens Horm) was from Takeda (Osaka, Japan), and PGI2 was from Cayman Chemical (Ann Arbor, MI, USA). Phosflow Lyse/Fix Buffer and P-selectin were from BD Biosciences (Oxford, UK). Gly-Phe-Hyp-Gly-Glu-Arg (GFOGER) and collagen-related peptide (CRP) were from Cambridge University (Cambridge, UK). U46619 was from Enzo (Exeter, UK). CK666 was from Tocris Bioscience (Abingdon, UK). Thrombin, ADP and FITC, or TRITC-conjugated phalloidin were from Merck (Dorset, UK). Other reagents were from Merck unless otherwise indicated.

4.2. Experimental Animals

C57Bl/6 mice with a homozygous targeting of the *Coro1a* gene have been previously described [15] and are available from The Jackson Laboratory (JAX stock no. 030203). The animals were kept in the animal facility of the University of Hull using standard conditions. All animal work was performed in accordance with UK Home Office regulations, UK Animals (Scientific Procedures) Act of 1986, under the Home Office project license no. PPL 70/8253 (2 January 2015). Age-matched WT littermates were used as controls in all experiments. Twelve to twenty-week-old animals were used for experiments.

4.3. Mouse Platelet Preparation

Blood was taken by cardiac puncture into acid citrate dextrose (ACD) (29.9 mM trisodium citrate, 113.8 mM glucose, 72.6 mM NaCl, and 2.9 mM citric acid, pH 6.4) or sodium citrate (109 mM tri-sodium citrate pH 7.4) and centrifuged at $100 \times g$ for 5 min. The platelet-rich plasma (PRP) was collected in a separate tube, modified Tyrode's buffer was added to the pellet, and the procedure repeated to increase the platelet yield. For washed platelet preparation, the PRP was pelleted at $800 \times g$ for 6 min and platelets resuspended in modified Tyrode's buffer and allowed to rest for 30 min at 37 °C prior to experiments.

4.4. Western Blot

Lysates were prepared from washed platelet suspensions by mixing with one volume of 2× Laemmli buffer. Proteins were resolved by SDS-polyacrylamide gel electrophoresis (PAGE) and blotted onto polyvinylidene difluoride (PVDF) membrane. The membrane was incubated with the relevant primary antibody and the corresponding fluorochrome-labeled secondary antibody and visualized and quantified with an LI-COR Odyssey CLx Imaging System (LI-COR Biosciences).

4.5. Flow Cytometry

PRP was prepared in sodium citrate and stimulated with thrombin (in the presence of 10 μM Gly-Pro-Arg-Pro-NH$_2$), CRP, ADP, or U46619 for 20 min at 37 °C in the presence of FITC-conjugated anti-P-selectin (BD Biosciences), PE-conjugated JON/A (Emfret, Würzburg, Germany) and APC/Cy7-conjugated anti-CD63 (Biolegend) antibodies. Platelets were subsequently fixed and

300

analyzed by fluorescence-activated cell sorting (FACS) using an LSRFortessa cell analyzer (BD Biosciences) and FlowJo software.

For receptor expression studies, PRP was incubated with FITC-conjugated antibodies directed against surface membrane glycoproteins GP1b (CD42b), GPVI, integrin $\alpha2$ (CD49b) (Emfret, Eibelstadt, Germany), integrin αIIb (CD41) (BD Biosciences, Oxford, UK), or PE-conjugated antibodies against integrin $\beta2$ (CD18) (Biolegend). Receptor expression was also studied upon stimulation with 0.1 U/mL thrombin for 20 min at 37 °C in the presence of 10 μM Gly-Pro-Arg-Pro-NH$_2$. Platelets were subsequently analyzed by FACS.

4.6. Aggregation, Spreading, and Immunostaining

Platelet aggregation in response to agonists was recorded in washed platelets under constant stirring conditions (1000 rpm) for 7 min at 37 °C using light transmission aggregometry with a CHRONO-LOG 490 aggregometer (CHRONO-LOG, Havertown, PA, USA). Washed platelets in suspension were fixed with an equal volume of ice-cold 4% paraformaldehyde (PFA) and spun at $350\times g$ for 10 min on poly-L-lysine (0.01% in PBS) coated coverslips. Platelets were stained for 1 h at room temperature with the indicated primary antibodies followed by the corresponding secondary antibodies and fluorescently labeled phalloidin diluted in PBG (0.5% bovine serum albumin (BSA), 0.05% fish gelatin in PBS). For adhesion studies, coverslips were coated overnight at 4 °C with fibrinogen, collagen, CRP, or GFOGER in PBS at the concentrations indicated and blocked with 5 mg/mL heat-denatured fatty acid free BSA for 1 h before the experiment. For adhesion on native BSA, coverslips were coated overnight at 4 °C with 5 mg/mL fatty acid free BSA in 0.05 M sodium bicarbonate buffer pH 9 [27]. Washed platelets were allowed to spread for 45 min at 37 °C, fixed with 4% PFA for 10 min, permeabilized with 0.3% Triton X-100 for 5 min, and stained as described above for platelets in suspension. Platelets were imaged by fluorescence microscopy using a Zeiss ApoTome.2 equipped with an AxioCam 506 and Zeiss Plan-Apochromat 63× and 100× NA 1.4 objectives. Platelets were manually counted, and the surface coverage area was analyzed by thresholding using ImageJ.

4.7. Tail Bleeding Assay

Mice were anesthetized with 50 mg/kg ketamine and 1 mg/kg medetomidine. The tail was cut off at 2 mm from the tip and immediately immersed in 37 °C PBS. Bleeding time between the cut and cessation of bleeding for at least one minute was monitored by visual inspection until hemostasis for up to 10 min.

4.8. Statistical Analysis

Experimental data were analyzed by GraphPad Prism v6.0 (La Jolla, CA, USA). Data are presented as mean ± standard error of the mean (SEM) of at least 4 independent experiments. Normality was assessed by the Shapiro–Wilk test. Differences between groups were assessed using the appropriate parametric or nonparametric test and statistical significance was taken at $p \leq 0.05$.

Abbreviations

ACD	acid citrate dextrose
ADP	adenosine diphosphate
ARPC2	p34-Arc, component of the Arp2/3 complex
BSA	bovine serum albumin
cAMP	cyclic adenosine monophosphate
CDK5	cyclin-dependent kinase 5
CDx	cluster of differentiation x
CRP	collagen related peptide
FACS	fluorescence-activated cell sorting
FITC	fluorescein isothiocyanate
GEFOGER	Gly-Phe-Hyp-Gly-Glu-Arg
ICAM-1	intercellular adhesion molecule 1
KO	knockout
LFA-1	lymphocyte function-associated antigen 1
PAGE	polyacrylamide gel electrophoresis
PBS	phosphate buffered saline
PDE4	phosphodiesterase 4
PFA	paraformaldehyde
PGI2	prostacyclin
PRP	platelet-rich plasma
SEM	standard error of the mean
TNF	tumor necrosis factor
TRITC	tetramethylrhodamine isothiocyanate
VASP	vasodilator-stimulated phosphoprotein
WT	wild type

References

1. Tomaiuolo, M.; Brass, L.F.; Stalker, T.J. Regulation of platelet activation and coagulation and its role in vascular injury and arterial thrombosis. *Interv. Cardiol. Clin.* **2017**, *6*, 1–12. [CrossRef] [PubMed]

2. Hartwig, J.H. The platelet cytoskeleton. In *Platelets*, 3rd ed.; Michelson, A.D., Ed.; Academic Press: London, UK, 2013; pp. 145–168.

3. Smolenski, A. Novel roles of cAMP/cGMP-dependent signaling in platelets. *J. Thromb. Haemost.* **2012**, *10*, 167–176. [CrossRef] [PubMed]

4. Chan, K.T.; Creed, S.J.; Bear, J.E. Unraveling the enigma: Progress towards understanding the coronin family of actin regulators. *Trends Cell Biol.* **2011**, *21*, 481–488. [CrossRef] [PubMed]

5. Pieters, J.; Muller, P.; Jayachandran, R. On guard: Coronin proteins in innate and adaptive immunity. *Nat. Rev. Immunol.* **2013**, *13*, 23765056. [CrossRef] [PubMed]

6. Riley, D.R.J.; Khalil, J.S.; Naseem, K.M.; Rivero, F. Biochemical and immunocytochemical characterization of coronins in platelets. *Platelets* **2019**, *4*, 1–12. [CrossRef]

7. Suzuki, K.K.; Nishihata, J.; Arai, Y.; Honma, N.; Yamamoto, K.; Irimura, T.; Toyoshima, S. Molecular cloning of a novel actin-binding protein, p57, with a WD repeat and a leucine zipper motif. *FEBS Lett.* **1995**, *364*, 283–288. [CrossRef]

8. Ferrari, G.; Langen, H.; Naito, M.; Pieters, J. A coat protein on phagosomes involved in the intracellular survival of mycobacteria. *Cell* **1999**, *97*, 435–447. [CrossRef]

9. Jayachandran, R.; Liu, X.; Bosedasgupta, S.; Müller, P.; Zhang, C.-L.; Moshous, D.; Studer, V.; Schneider, J.; Genoud, C.; Fossoud, C.; et al. Coronin 1 regulates cognition and behavior through modulation of cAMP/protein kinase A signaling. *PLoS Biol.* **2014**, *12*, e1001820. [CrossRef]

10. Pick, R.; Begandt, D.; Stocker, T.J.; Salvermoser, M.; Thome, S.; Böttcher, R.T.; Montanez, E.; Harrison, U.; Forné, I.; Khandoga, A.G.; et al. Coronin 1A, a novel player in integrin biology, controls neutrophil trafficking in innate immunity. *Blood* **2017**, *130*, 847–858. [CrossRef]

11. Ojeda, V.; Castro-Castro, A.; Bustelo, X.R. Coronin1 proteins dictate Rac1 intracellular dynamics and cytoskeletal output. *Mol. Cell. Biol.* **2014**, *34*, 3388–3406. [CrossRef]

12. Combaluzier, B.; Mueller, P.; Massner, J.; Finke, D.; Pieters, J. Coronin 1 is essential for IgM-mediated Ca^{2+} mobilization in B cells but dispensable for the generation of immune responses in vivo. *J. Immunol.* **2009**, *182*, 1954–1961. [CrossRef] [PubMed]

13. Grogan, A.; Reeves, E.; Keep, N.; Wientjes, F.; Totty, N.F.; Burlingame, A.L.; Hsuan, J.J.; Segal, A.W. Cytosolic phox proteins interact with and regulate the assembly of coronin in neutrophils. *J. Cell Sci.* **1997**, *110*, 3071–3081. [PubMed]

14. Moriceau, S.; Kantari, C.; Mocek, J.; Davezac, N.; Gabillet, J.; Guerrera, I.C.; Brouillard, F.; Tondelier, D.; Sermet-Gaudelus, I.; Danel, C.; et al. Coronin-1 is associated with neutrophil survival and is cleaved during apoptosis: Potential implication in neutrophils from cystic fibrosis patients. *J. Immunol.* **2009**, *182*, 7254–7263. [CrossRef] [PubMed]

15. Jayachandran, R.; Sundaramurthy, V.; Combaluzier, B.; Mueller, P.; Korf, H.; Huygen, K.; Miyazaki, T.; Albrecht, I.; Massner, J.; Pieters, J. Survival of mycobacteria in macrophages is mediated by coronin 1-dependent activation of calcineurin. *Cell* **2007**, *130*, 37–50. [CrossRef] [PubMed]

16. Mueller, P.; Massner, J.; Jayachandran, R.; Combaluzier, B.; Albrecht, I.; Gatfield, J.; Blum, C.; Ceredig, R.; Rodewald, H.R.; Rolink, A.G.; et al. Regulation of T cell survival through coronin-1-mediated generation of inositol-1,4,5-trisphosphate and calcium mobilization after T cell receptor triggering. *Nat. Immunol.* **2008**, *9*, 424–431. [CrossRef] [PubMed]

17. Föger, N.; Rangell, L.; Danilenko, D.M.; Chan, A.C. Requirement for coronin 1 in T lymphocyte trafficking and cellular homeostasis. *Science* **2006**, *313*, 839–842. [CrossRef]

18. Shiow, L.R.; Roadcap, D.W.; Paris, K.; Watson, S.R.; Grigorova, I.L.; Lebet, T.; An, J.; Xu, Y.; Jenne, C.N.; Föger, N.; et al. The actin regulator coronin 1A is mutant in a thymic egress-deficient mouse strain and in a patient with severe combined immunodeficiency. *Nat. Immunol.* **2008**, *9*, 1307–1315. [CrossRef]

19. Haraldsson, M.K.; Louis-Dit-Sully, C.A.; Lawson, B.R.; Gascoigne, N.R.J.; Argyrios, N.; Kono, D.H. The lupus-related Lmb3 locus contains a disease-suppressing Coronin-1A gene mutation. *Immunity* **2009**, *28*, 40–51. [CrossRef]

20. Stocker, T.; Pircher, J.; Skenderi, A.; Ehrlich, A.; Eberle, C.; Megens, R.; Petzold, T.; Zhang, Z.; Walzog, B.; Müller-Taubenberger, A.; et al. The actin regulator coronin-1A modulates platelet shape change and consolidates arterial thrombosis. *Thromb. Haemost.* **2018**, *118*, 2098–2111. [CrossRef]

21. Michelson, A.; Barnard, M.; Hechtman, H.; MacGregor, H.; Connolly, R.; Loscalzo, J.; Valeri, C. In vivo tracking of platelets: Circulating degranulated platelets rapidly lose surface P-selectin but continue to circulate and function. *Proc. Natl. Acad. Sci. USA* **1996**, *93*, 11877–11882. [CrossRef]

22. Piguet, P.F.; Vesin, C.; Ryser, J.E.; Senaldi, G.; Grau, G.E.; Tacchini-Cottier, F. An effector role for platelets in systemic and local lipopolysaccharide—Induced toxicity in mice, mediated by a CD11a- and CD54-dependent interaction with endothelium. *Infect. Immun.* **1993**, *61*, 4182–4187. [CrossRef] [PubMed]

23. Guo, J.; Piguet, P.F. Stimulation of thrombocytopoiesis decreases platelet beta2 but not beta1 or beta3 integrins. *Br. J. Haematol.* **1998**, *100*, 712–719. [CrossRef] [PubMed]

24. Piguet, P.F.; Vesin, C.; Rochat, A. Beta2 integrin modulates platelet caspase activation and life span in mice. *Eur. J. Cell Biol.* **2001**, *80*, 171–177. [CrossRef] [PubMed]

25. Zeiler, M.; Moser, M.; Mann, M. Copy number analysis of the murine platelet proteome spanning the complete abundance range. *Mol. Cell. Proteom.* **2014**, *13*, 3435–3445. [CrossRef]

26. Philippeaux, M.M.; Vesin, C.; Tacchini-Cottier, F.; Piguet, P.F. Activated human platelets express β2 integrin. *Eur. J. Haematol.* **2009**, *56*, 130–137. [CrossRef]

27. Zhu, X.; Subbaraman, R.; Sano, H.; Jacobs, B.; Sano, A.; Boetticher, E.; Muñoz, N.M.; Leff, A.R. A surrogate method for assessment of β2-integrin-dependent adhesion of human eosinophils to ICAM-1. *J. Immunol. Methods* **2000**, *240*, 157–164. [CrossRef]

28. Liu, J.; Muñoz, N.M.; Meliton, A.Y.; Zhu, X.; Lambertino, A.T.; Xu, C.; Myo, S.; Myou, S.; Boetticher, E.; Johnson, M.; et al. β2-Integrin adhesion caused by eotaxin but not IL-5 is blocked by PDE-4 inhibition and β2-adrenoceptor activation in human eosinophils. *Pulm. Pharmacol. Ther.* **2004**, *17*, 73–79. [CrossRef]

29. Jayachandran, R.; Gumienny, A.; Bolinger, B.; Ruehl, S.; Lang, M.J.; Fucile, G.; Mazumder, S.; Tchang, V.; Woischnig, A.-K.; Stiess, M.; et al. Disruption of coronin 1 signaling in T cells promotes allograft tolerance while maintaining anti-pathogen immunity. *Immunity* **2019**, *50*, 152–165. [CrossRef]

30. Falet, H. Anatomy of the platelet cytoskeleton. In *Platelets in Thrombotic and Non-Thrombotic Disorders*; Graesele, P., Kleiman, N.S., Lopez, J.A., Page, C.P., Eds.; Springer: Berlin, Germany, 2017; pp. 139–156.

31. Jarvis, G.E. Platelet aggregation: Turbidimetric measurements. *Methods Mol. Biol.* **2004**, *272*, 65–76.

32. Jarvis, G.E. Platelet aggregation in whole blood: Impedance and particle counting methods. *Methods Mol. Biol.* **2004**, *272*, 77–87.

33. Fagerholm, S.C.; Guenther, C.; Asens, M.L.; Savinko, T.; Uotila, L.M. Beta2-Integins and interacting proteins in leukocyte trafficking, immune supression, and immunodeficiency disease. *Front. Immunol.* **2019**, *10*, 1–10. [CrossRef] [PubMed]

34. Cerletti, C.; de Gaetano, G.; Lorenzet, R. Platelet-leukocyte interactions: Multiple links between inflammation, blood coagulation and vascular risk. *Mediterr. J. Hematol. Infect. Dis.* **2010**, *2*, e2010023. [CrossRef] [PubMed]

35. Liu, X.; Bosedasgupta, S.; Jayachandran, R.; Studer, V.; Rühl, S.; Stiess, M.; Pieters, J. Activation of the cAMP/protein kinase A signalling pathway by coronin 1 is regulated by cyclin-dependent kinase 5 activity. *FEBS Lett.* **2016**, *590*, 279–287. [CrossRef] [PubMed]

36. Vinet, A.F.; Fiedler, T.; Studer, V.; Froquet, R.; Dardel, A.; Cosson, P.; Pieters, J. Initiation of multicellular differentiation in *Dictyostelium discoideum* is regulated by coronin A. *Mol. Biol. Cell* **2014**, *25*, 688–701. [CrossRef] [PubMed]

37. Li, X.; Zhong, K.; Yin, Z.; Hu, J.; Wang, W.; Li, L.; Zhang, H.; Zheng, X.; Wang, P.; Zhang, Z. The seven transmembrane domain protein MoRgs7 functions in surface perception and undergoes coronin MoCrn1-dependent endocytosis in complex with Gα subunit MoMagA to promote cAMP signaling and appressorium formation in *Magnaporthe oryzae*. *PLoS Pathog.* **2019**, *15*, e1007382. [CrossRef] [PubMed]

38. Rondina, M.T.; Weyrich, A.S. Targeting phosphodiesterases in anti-platelet therapy. *Handb. Exp. Pharmacol.* **2012**, *210*, 225–238.

39. Burkhart, J.M.; Vaudel, M.; Gambaryan, S.; Radau, S.; Walter, U.; Martens, L.; Geiger, J.; Sickmann, A.; Zahedi, R.P. The first comprehensive and quantitative analysis of human platelet protein composition allows the comparative analysis of structural and functional pathways. *Blood* **2012**, *120*, e73–e82. [CrossRef]

40. Thomas, S.G.; Poulter, N.S.; Bem, D.; Finney, B.; Machesky, L.M.; Watson, S.P. The actin binding proteins cortactin and HS1 are dispensable for platelet actin nodule and megakaryocyte podosome formation. *Platelets* **2017**, *28*, 372–379. [CrossRef]

41. Zuidscherwoude, M.; Green, H.L.H.; Thomas, S.G. Formin proteins in megakaryocytes and platelets: Regulation of actin and microtubule dynamics. *Platelets* **2019**, *30*, 23–30. [CrossRef]

42. Spoerl, Z.; Stumpf, M.; Noegel, A.A.; Hasse, A. Oligomerization, F-actin interaction, and membrane association of the ubiquitous mammalian coronin 3 are mediated by its carboxyl terminus. *J. Biol. Chem.* **2002**, *277*, 48858–48867. [CrossRef]
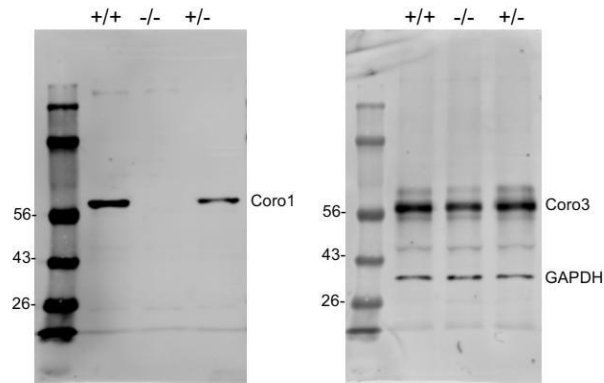
Supplemental Figure 1. Full length blots corresponding to Figure 1A.
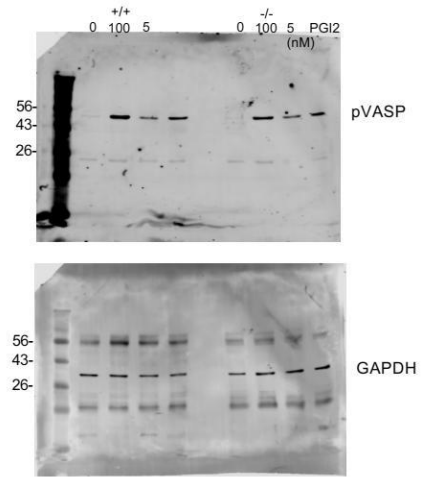
Supplemental Figure 2. Full length blots corresponding to Figure 7A. The fourth lane of each genotype corresponds to an experimental condition not included in the article.

305

8.2.3 The membrane-associated fraction of cyclase associate protein 1 translocates to the cytosol upon platelet stimulation

SCIENTIFIC REPRTS

The membrane-associated fraction of cyclase associate protein 1 translocates to the cytosol upon platelet stimulation

Pooja Joshi[1,2], David R. J. Riley[2], Jawad S. Khalil[2], Huajiang Xiong[3], Wei Ji[1,2] & Francisco Rivero[2]

Platelets undergo profound shape changes upon adhesion to damaged blood vessel walls that are mediated by reorganisation of the actin cytoskeleton in response to receptor-mediated signalling cascades. The highly conserved 56 kDa multidomain cyclase associated protein 1 (CAP1) works in concert with cofilin and profilin to modulate actin filament turnover by facilitating cofilin-mediated actin filament severing and depolymerisation and catalysing profilin-mediated regeneration of actin monomers for reutilisation in growing filaments. CAP1 is abundant in platelets but its roles remain unexplored. We report that in suspended platelets CAP1 localises predominantly at the cell cortex whereas in spread platelets it is uniformly distributed in the cytoplasm, with enrichment at the cell cortex and the periphery of actin nodules. Upon subcellular fractionation most CAP1 was found cytosolic but part associated to the membrane fraction in an actin-independent manner. Interestingly, upon stimulation with thrombin a significant proportion of the membrane-associated CAP1 translocates to the cytosol. This relocalisation was prevented by prior treatment with PGI2 or the nitric oxide donor GSNO, or by inhibition of GSK3. Our results place CAP1 at a crossroad of signalling pathways that control platelet activation by contributing to actin remodelling at the cell cortex and actin nodules during platelet spreading.

Platelets in circulation adopt a discoid shape that is maintained thanks to a highly organised cytoskeleton that includes a peripheral microtubule coil, a network of cross-linked actin filaments that fill the cytoplasmic space and, connected to this, a cortical spectrin-based skeleton associated to the plasma membrane[1]. Platelets undergo profound shape changes when they adhere to the damaged blood vessel wall, first becoming spherical, and then producing filopodia and actin nodules that progress to lamellipodia and stress fibres as the cell spreads and flattens[2]. These changes in platelet morphology are mediated by reorganisation of the actin cytoskeleton in response to multiple receptor-mediated signalling cascades[3]. Platelet activation is accompanied by a rapid increase in the amount of actin assembled into filaments[4]. Numerous proteins with various biochemical activities participate in the dynamics of actin remodelling, including the Arp2/3 complex and their regulators (WAVE, WASP), formins, gelsolin, cofilin, coronin and monomeric actin binding proteins like profilin, β-thymosin and the cyclase associated protein (CAP)[5,6].

The highly conserved CAP is a 56 kDa multidomain protein that works in concert with cofilin and profilin to modulate actin filament turnover[7]. The C-terminal half harbours two actin-binding domains (a WH2 domain followed by a β-sheet domain) and two proline-rich regions that recruit profilin. This part of CAP competitively displaces cofilin from ADP-actin monomers and catalyses nucleotide exchange by profilin. The N-terminal half enhances cofilin-mediated severing and depolymerisation of actin filaments and is required for hexamerisation[8,9].

Consistent with that important role in actin turnover, lack of CAP affects cell morphology, polarity, motility and endocytosis, as shown in studies in mammalian cells and various organisms (reviewed in[7]). In mammals two CAP isoforms exist, the ubiquitously expressed CAP1 and the tissue-restricted CAP2, expressed mainly in brain,

[1]School of Life Science and Technology, Changchun University of Science and Technology, Changchun, Jilin, China. [2]Centre for Atherothrombosis and Metabolic Disease, Hull York Medical School, Faculty of Health Sciences, University of Hull, Hull, UK. [3]Department of Biochemistry, University of Oxford, Oxford, UK. Pooja Joshi and David R. J. Riley contributed equally to this work. Correspondence and requests for materials should be addressed to W.J. (email: jiweicust@163.com) or F.R. (email: francisco.rivero@hyms.ac.uk)

heart, skeletal muscle, skin and testis[10,11]. CAP1 is a predominantly cytosolic protein, although a small fraction has been found associated to membranes[12]. It usually shows a diffuse cytoplasmic localisation and accumulates in dynamic actin structures at the cell cortex where it co-localises with cofilin[13-15]. Silencing of CAP1 results in accumulation of thick and less dynamic stress fibres, formation of cofilin aggregates and alterations of cell morphology, motility and adhesion, the latter through interaction with talin and focal adhesion kinase (FAK)[15,16]. Additionally mammalian CAP1 has been shown to be a proapoptotic protein[17]. Whilst no mouse knockout model for CAP1 has been described, CAP2 deficient mice show reduced postnatal viability and a series of cardiac and neural morphofunctional defects[18,19]. Primary cells isolated from CAP2 deficient mice display alterations in the formation of protrusions and in actin turnover[20,21].

Given the central role of actin remodelling for platelet function a deep knowledge of its regulation is warranted. Although CAP1 is an important regulator of the actin turnover and, incidentally, the first mammalian CAP orthologue was first isolated from pig platelet lysates[22] no reports investigate this protein in platelets. Here we show that CAP1 is an abundant protein in human platelets. CAP1 is mainly cytosolic, but a significant amount associates to membranes in an actin-independent manner and translocates to the cytosol upon stimulation with thrombin. In immunocytochemistry studies CAP1 shows a diffuse cytoplasmic localisation with accumulation at the cell cortex, filopodia and actin nodules. Our study paves the way for further studies towards establishing the role of CAP1 in platelet actin dynamics and platelet function.

Methods

Reagents.   Primary antibodies against following proteins were used: CAP1 (Abcam ab133655), CD36 (Santa Cruz H-300 sc-9154), Syk (Santa Cruz 4D10 sc-1240), GAPDH (Calbiochem 6C5-CB1001), β-actin (Abcam ab20272), β3-integrin (Santa Cruz HC93 sc-14009), cofilin (Cell Signaling Technology D3F9 #5175), profilin-1 (Cell Signaling Technology #3237), and vinculin (Sigma SAB4200080). Secondary antibodies Alexa Fluor 568- or 488-conjugated anti-mouse and anti-rabbit immunoglobulins (Molecular Probes, Invitrogen Life Technologies Ltd.) were used for immunofluorescence. Peroxidase-conjugated anti-mouse and anti-rabbit immunoglobulins (Sigma-Aldrich Co. Ltd.) or IRDye 680 or IRDye 800 anti-mouse and anti-rabbit immunoglobulins (LI-COR Biosciences, Lincoln, USA) were used for Western blot.

Human fibrinogen was from Enzyme Research (Swansea, UK), collagen (Kollagenreagens Horm) was from Takeda (Osaka, Japan), recombinant human resistin (450-19) was from PeproTech (London, UK), latrunculin B and GSNO were from Enzo Life Sciences (Exeter, UK). PGI2 was from Cayman Chemical (Michigan, USA). Glycogen synthase kinase 3 (GSK3) inhibitor CHIR99021 was from Abcam. Other reagents were from Sigma-Aldrich unless otherwise indicated.

Platelet preparation.   Human blood was taken from drug-free volunteers by clean venepuncture into acid citrate dextrose (ACD) (29.9 mM sodium citrate, 113.8 mM glucose, 72.6 mM NaCl and 2.9 mM citric acid, pH 6.4). Platelet-rich plasma (PRP) was obtained by centrifugation of whole blood at $200 \times g$ for 15 minutes. Platelets were isolated from PRP by centrifugation at $800 \times g$ for 12 minutes in the presence of 6 mM citric acid. Platelets were washed in low pH buffer (0.036 mM citric acid, 0.01 mM EDTA, 0.005 mM glucose, 0.05 mM KCl, 0.09 mM NaCl) and centrifuged at $800 \times g$ for 12 minutes. Sedimented platelets were resuspended in modified Tyrode's buffer (150 mM NaCl, 5 mM HEPES, 0.55 mM NaH$_2$PO$_4$, 7 mM NaHCO$_3$, 2.7 mM KCl, 0.5 mM MgCl$_2$, and 5.6 mM glucose, pH 7.3) and maintained at 37 °C for 45 minutes prior to experiments. The study was approved by the Hull York Medical School Research Ethics Committee and all research was performed in accordance with relevant guidelines and regulations. Informed consent was obtained from all blood donors.

Platelet fractionation.   Washed platelet suspensions (5×10^8 platelets/ml), either untreated or treated with various substances for the appropriate time, were mixed with an equal volume of fractionation buffer (320 mM sucrose, 4 mM HEPES, 0.5 mM Na$_3$VO$_4$, pH 7.4) supplemented with phosphatase and protease inhibitor cocktail. Latrunculin B (LatB) was used at 20 μM for 20 min to depolymerise F-actin prior to lysis. Samples were subjected to 5 freeze-thaw cycles in liquid nitrogen. Intact platelets were removed by centrifugation at $1,000 \times g$ for 5 minutes at 4 °C before centrifugation at $100,000 \times g$ for 60 minutes at 4 °C. Cytosol and membrane fractions were normalised by volume and analysed by Western blot.

Detergent insoluble pellet extraction.   Washed platelet suspensions (1×10^9 platelets/ml) were lysed in an equal volume of Triton X-100 containing lysis buffer (2% Triton X-100, 10 mM Tris-HCl, 10 mM EGTA) supplemented with protease inhibitors. Lysates were spun at $15,600 \times g$ for 20 minutes (low speed) or $100,000 \times g$ for 1 hour (high speed) to separate the detergent soluble fraction from the detergent insoluble pellet. The fractions were normalised by volume, resolved on 12% SDS-PAGE and analysed by Western blot.

Western blot.   Proteins were resolved by SDS-polyacrylamide gel electrophoresis (PAGE) and blotted onto polyvinylidene difluoride (PVDF) membrane. The membrane was incubated with the relevant primary antibody and either the corresponding peroxidase-conjugated secondary antibody followed by enhanced chemiluminiscence detection (Pierce, Thermo Fisher Scientific Inc.) or the corresponding fluorochrome–labelled secondary antibody and visualised and quantified with a LI-COR Odyssey CLx Imaging System (LI-COR Biosciences, Lincoln, USA).

Immunostaining and microscopy.   Washed platelets in suspension were fixed with an equal volume of ice-cold 4% paraformaldehyde and spun at $3,500 \times g$ for 10 minutes on poly-L-lysine (0.01% in PBS) coated coverslips. Alternatively washed platelets were allowed to adhere and spread for 45 minutes on coverslips pre-coated with fibrinogen (100 μg/ml) overnight and blocked with 0.5% bovine serum albumin (BSA) prior to fixing with 4% paraformaldehyde. Cells were permeabilised with 0.3% Triton® X-100 in PBS for 5 min, and subsequently

308

incubated in PBG (0.5% BSA, 0.05% fish gelatine in PBS) for 30 min at room temperature. Primary and secondary antibodies were diluted in PBG and applied for intervals of 1 h. Cells were washed with PBG several times between each incubation step. F-actin was stained with FITC or TRITC-labelled phalloidin (Sigma-Aldrich Co. Ltd.) or blue CytoPainter (Abcam). The coverslips were mounted on object slides using gelvatol or ProLong Diamond antifade mountant (ThermoFisher Scientific) as embedding media. Coverslips were imaged using a Zeiss ApoTome.2 equipped with an AxioCam 506 and a Zeiss Plan-Apochromat $100\times/1.4$ objective. Images were processed with Zeiss Zen software.

Statistical analysis. Data are presented as average ± standard deviation (SD) or standard error of the mean (SEM). Normality was tested and statistics were performed using appropriate non-parametric or parametric tests in Graph Pad Prism V6. P values less than 0.05 were considered significant. The data that support the findings of this study are available from the corresponding author upon reasonable request.

Results

CAP1 is abundant in platelets. CAP1 is an abundant actin-binding protein ubiquitously expressed in human tissues. To demonstrate the presence of CAP1 in human platelets we resolved platelet lysates along with lysates from various cell lines by SDS-PAGE, blotted and probed with a CAP1-specific polyclonal antibody. CAP1 appeared as a single band with an apparent molecular weight above 56 kDa (Fig. 1A). The antibody we used throughout this study (rabbit monoclonal ab133655) proved specific for human CAP1 but we have demonstrated the presence of CAP1 also in murine platelets using a different antibody (not shown).

To investigate the distribution of CAP1 in platelets we carried out a simple subcellular fractionation. Resting platelets were lysed in an isotonic sucrose solution and cytosol and membrane fractions separated by ultracentrifugation. As shown in Fig. 1B, most of CAP1 (77%) is cytosolic and the rest associates with the membrane fraction. The membrane marker CD36 and the cytosolic marker in resting platelets Syk confirmed that each fraction was free from cross-contamination. Since CAP1 is an actin-binding protein, we further investigated whether this membrane association is mediated by actin. Resting platelets were treated with 20 µM latrunculin B (LatB) to depolymerise F-actin prior to subcellular fractionation. There was no statistically significant difference (Mann-Whitney test) in CAP1 association to the membrane fraction in the absence (22%) or presence (23%) of LatB, indicating that the association of CAP1 to platelet membranes is independent of its association with actin.

To characterise the association of CAP1 to the actin cytoskeleton, resting platelets were lysed in the presence of Triton X-100 and separated into soluble and insoluble fractions by centrifugation at low and high speeds[23] (Fig. 1C). We observed that CAP1 was not present in the low speed (LS) detergent insoluble pellet, where crosslinked actin filaments and associated proteins sediment, but was recovered in the detergent soluble fraction. At high speed (HS) most CAP1 was soluble, but approximately 17% was found in the detergent insoluble pellet. Notably, no significant difference (Mann-Whitney test) in the amount of CAP1 was observed in the HS pellet when the actin cytoskeleton was depolymerised with LatB prior to centrifugation, indicating that the association of CAP1 to the detergent insoluble pellet is independent of an association to actin.

Because cofilin and profilin function in concert with CAP1, we investigated their behaviour as well. Profilin was recovered in the supernatants at both LS and HS, consistent with its role as monomeric actin binding protein. Cofilin, which interacts with F-actin in addition to G-actin, was observed in HS and LS pellets. It was removed from the LS pellet upon actin depolymerisation, but behaved similarly to CAP1 in the HS pellet. The HS pellet may contain lipid rafts, as suggested by the presence of a fraction of the membrane protein CD36[24], indicating that the CAP1 and cofilin in the HS pellet are associated to membranes or membrane proteins.

Localisation of CAP1 in platelets. We studied the distribution of CAP1 in both suspended and spread platelets by immunostaining and fluorescence microscopy. Resting platelets in suspension have a predominantly discoid shape. In these cells the distribution of CAP1 is predominantly cortical, with a significant proportion of diffuse cytoplasmic staining. CAP1 co-localises with F-actin mainly in cortical regions (Fig. 2A).

In platelets spread on fibrinogen-coated coverslips some CAP1 appears distributed diffusely in the cytoplasm, with conspicuous accumulations in the cortical regions (Fig. 2B), filopodia (Fig. 2C) and actin nodules (Fig. 2D), where it colocalises with F-actin. CAP1-F-actin colocalisation is also observed in central areas, where the platelet granulomere is expected (Fig. 2B). CAP1 is apparently absent from stress fibres. In actin nodules CAP1 displays a broad distribution circling the sharper F-actin staining (Fig. 2D). A co-immunostaining with vinculin, an adhesion protein that localises at actin nodules[25], showed a clear colocalisation of CAP1 and vinculin at the periphery of the nodules (Fig. 2E).

To visualise the actin-independent association of a fraction of CAP1 to the cell cortex we treated spread cells with the actin-depolymerising drug latrunculin A. This drug caused rounding and retraction of platelets along with fragmentation of stress fibres and weak diffuse phalloidin staining. CAP1 appeared diffusely distributed all over the cell, making the identification of any cortical accumulation impossible (Supplementary Fig. 2).

CAP1 translocates away from the cell cortex upon platelet stimulation. Thrombin is a potent platelet activator and causes cytoskeletal changes through G-protein coupled receptors PAR1 and PAR4, leading to shape change, aggregation and spreading[26]. To visualise any effect of thrombin stimulation on CAP1 localisation platelets were spread on immobilised fibrinogen prior to stimulation with 0.1 U/mL thrombin for increasing durations before fixation and immunostaining (Fig. 3A). This dose of thrombin was shown to cause the maximum aggregation response in preliminary experiments. In spread platelets CAP1 shows the characteristic subcellular distribution described above (Fig. 2), with 70% cells displaying a predominantly cortical accumulation and 18% showing no particular cortical enrichment (Fig. 3B). Upon thrombin stimulation cortical CAP1 appeared to increasingly disperse with time, so that at 30 seconds the proportion of cells with cortical CAP1 was down to

309
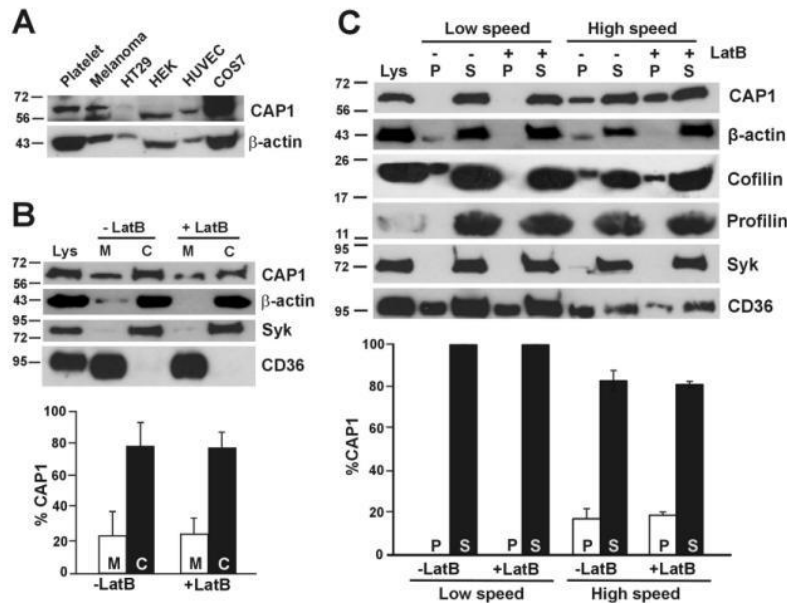
Figure 1. Subcellular distribution of CAP1 in platelets. (**A**) Specificity of anti-CAP1 antibody. Platelet and cell line lysates (30 μg total protein) were resolved by 12% SDS-PAGE, blotted onto PVDF membrane and probed with an antibody for CAP1. The blots were probed for β-actin as a loading control. HT29, human colorectal cancer cell line; HEK, human embryonic kidney 293 cell line; HUVEC, human umbilical vein endothelial cell; COS7, fibroblast-like tissue from monkey kidney tissue. (**B**) Subcellular fractionation. Platelets were lysed by freeze-thaw in liquid nitrogen and spun at $100,000 \times g$ for 1 hour to separate membrane (M) and cytosolic (C) fractions. The fractions were normalised by volume and resolved by 12% SDS-PAGE, blotted onto PVDF membrane and probed with antibodies for the indicated proteins. CD36 was used as membrane marker and Syk as a cytosolic marker in resting platelets. Latrunculin B (LatB; 20 μM, 20 min) was used to depolymerise F-actin prior to lysis. CAP1 distribution was quantified by densitometry and expressed as percentage relative to the total (M + C) CAP1 in the lysate. Data represent mean ± SD of three independent experiments. (**C**) Association of CAP1 to actin in detergent insoluble pellet. Platelets (8×10^8/mL platelets) were lysed in the presence of 1% TX-100 and lysates spun at low speed ($15,600 \times g$) for 20 min and high speed ($100,000 \times g$) for 1 hour. Supernatant (S) and pellet (P) were normalised by volume and resolved by 12% SDS-PAGE, blotted onto PVDF membrane and probed with antibodies for the indicated proteins. LatB (20 μM, 20 min) was used to depolymerise F-actin prior to lysis. CAP1 concentration in pellet and supernatant were quantified by densitometry as percent of total (P + S). Data represent mean ± SD of three independent experiments. Full-length blots are presented in Supplementary Fig. 1.

43%, similar to the proportion of cells with diffuse CAP1 (46%). After 3 minutes CAP1 had partially reverted to the cortex. In these experiments between 11 and 23% of the cells were excluded as they failed to spread, showing a too bright signal to appreciate any clear CAP1 distribution.

In several cell lines CAP1 has been reported to translocate to the outer mitochondrial membrane and promote apoptosis independently of caspase activation[17]. Out attempts to visualise a similar behaviour in platelets were hampered by the small size of these cells in suspension.

To characterise the behaviour of CAP1 biochemically we stimulated platelets in suspension with 0.1 U/mL thrombin and subjected them to fractionation into membranes and cytosol followed by Western blot analysis (Fig. 4A). A significant reduction in the amount of CAP1 associated to the membrane fraction was observed after 30 seconds of thrombin stimulation. The proportion of membrane-associated CAP1 decreased to as low as 30% of the proportion in resting platelets and persisted for at least 3 minutes. The proportion of actin associated to the membrane fraction did not show apparent changes upon thrombin stimulation, confirming that the behaviour of CAP1 is independent of its association with actin.

We next explored the effect of thrombin in the association of CAP1 to the HS detergent insoluble pellet. Platelets were stimulated with 0.1 U/mL thrombin and the reaction was stopped with lysis buffer at various time points up to 5 minutes. HS pellets were subjected to Western blot analysis (Fig. 4B). We observed a statistically significant time dependent decrease in the proportion of CAP1 in the HS pellet down to 40% of the proportion in
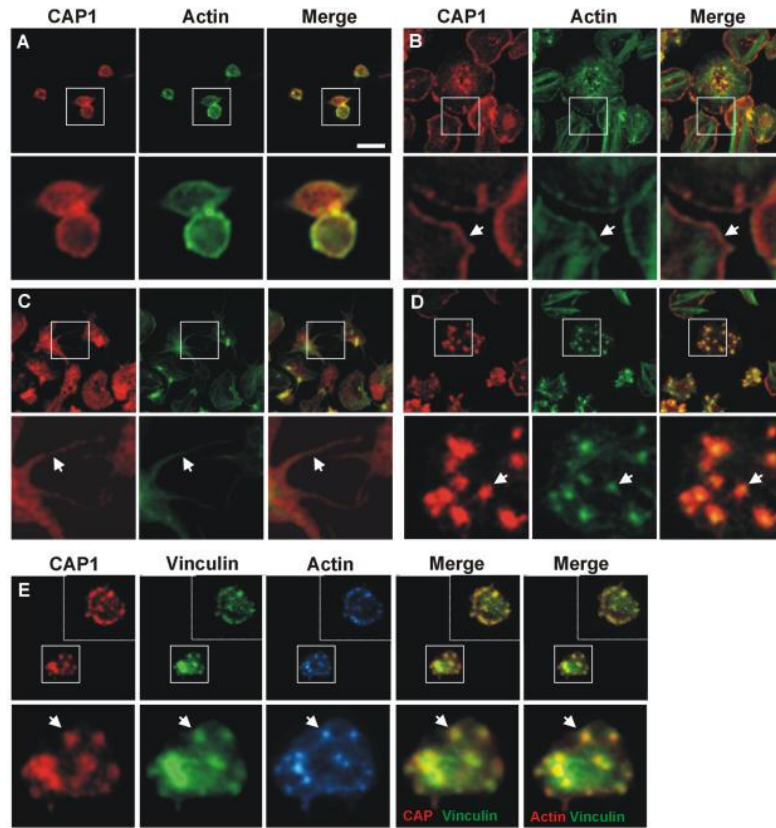
Figure 2. Subcellular localisation of CAP1. Platelets were fixed in suspension with paraformaldehyde and spun on poly-L-lysine coated coverslips (**A**) or were allowed to spread on fibrinogen coated coverslips and fixed with paraformaldehyde (**B–E**). For (**A–D**) cells were immunostained with an anti-CAP1 antibody followed by an Alexa568-coupled secondary antibody (red) and counterstained with FITC-phalloidin for filamentous actin (green). For E platelets were treated with 100 nM PGI2 5 minutes prior to fixation in order to increase the proportion of cells displaying actin nodules[30]. Platelets were then immunostained with anti-CAP1 and anti-vinculin antibodies followed by Alexa568 or Alexa488-coupled secondary antibodies, respectively (red and green), and counterstained with blue CytoPainter for filamentous actin (blue). Actin colour has been changed to red in the double staining merge panel for better visualisation. Optical sections were acquired with a fluorescence microscope equipped with a structured illumination attachment. Sections were 230 nm apart. Shown is a maximum intensity projection image after deconvolution and single planes of the region are indicated with a square. Arrows point at regions of interest: cell cortex (**B**), filopodia (**C**) and actin nodules (**D,E**). Scale bar 5 μm.

resting platelets. The proportion of actin in the HS pellet only showed a very modest increase in the first minute upon thrombin stimulation that did not reach statistical significance. By contrast, as expected, the proportion of actin in the LS pellet rapidly increased upon thrombin stimulation, reached a 1.7 fold peak at 60 seconds and remained elevated afterwards. Again, the behaviour of CAP1 was independent of its association with actin.

To demonstrate that the effects of thrombin on CAP1 re-distribution are primarily due to the agonist and not to secondary mediators we assessed CAP1 localisation in the presence of the thromboxane A2 synthesis inhibitor indomethacin and the ADP degrading enzyme apyrase. Platelets were treated with 10 μM indomethacin and 1 U/ml apyrase for 20 minutes prior to stimulation with two doses of thrombin for one minute and extraction of high speed detergent insoluble pellets (Fig. 4C). We observed a significant dose-dependent translocation of CAP1 from the high speed pellet, with approximately 60% remaining in the pellet with 0.1 U/ml thrombin and 20–35%

311
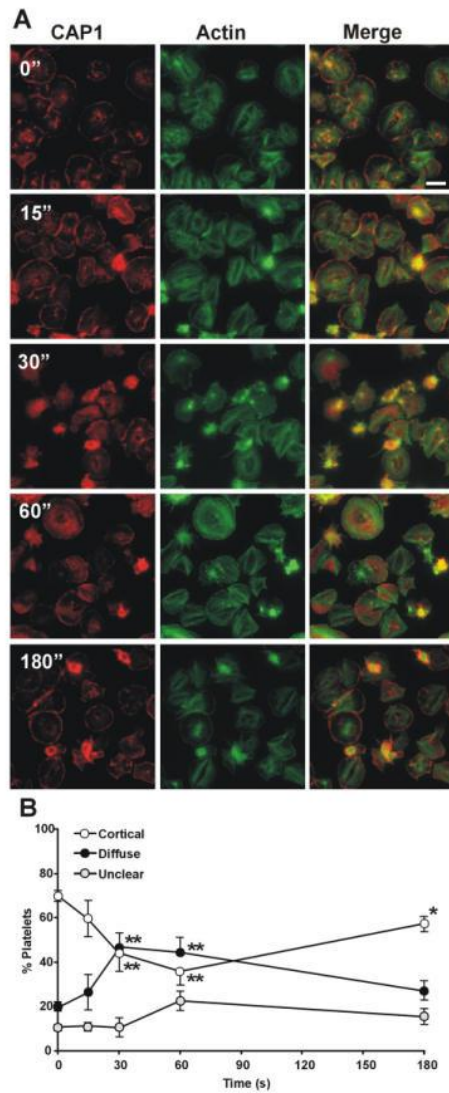
Figure 3. CAP1 relocalises upon thrombin stimulation. (**A**) Platelets were allowed to spread on fibrinogen-coated coverslips and then stimulated with 0.1 U/mL thrombin for the indicated times, fixed with paraformaldehyde and immunostained with an anti-CAP1 antibody followed by an Alexa568-coupled secondary antibody (red) and counterstained with FITC-phalloidin for filamentous actin (green). Images were acquired with a fluorescence microscope equipped with a structured illumination attachment. Scale bar 5 µm. (**B**) Quantification of the pattern of CAP1 distribution upon thrombin stimulation. The proportions of cells with predominantly cortical or diffuse distribution of CAP1 in images like the ones shown in A were calculated from three independent experiments each performed in duplicate coverslips. At least 1000 cells per time point in each experiment were scored. Unclear refers to cells that were not sufficiently enough spread to make a judgment. Data are average ± SEM of four or five independent experiments. *$p \leq 0.05$, **$p \leq 0.01$, relative to 0 s, Mann-Whitney test.

312
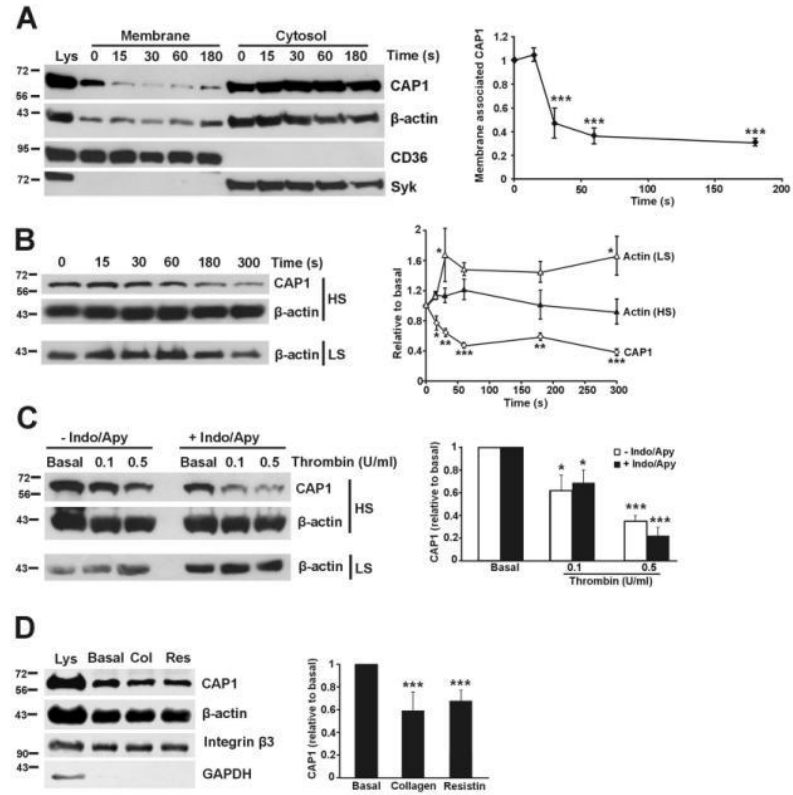
Figure 4. Translocation of CAP1 upon agonist stimulation. (**A**) Reduced membrane-associated CAP1 upon thrombin stimulation. Platelets $(8 \times 10^8/\text{mL})$ were treated with 0.1 U/mL thrombin in the presence of 1 mM EGTA to prevent aggregation for the indicated times prior to lysis and fractionation. Fractions were normalised by volume and resolved on 12% SDS-PAGE, blotted onto PVDF membrane and probed with antibodies for the indicated proteins. CD36, membrane marker; Syk, cytosolic marker. Membrane-associated CAP1 was quantified by densitometry, normalised to CD36 and expressed relative to CAP1 in the 0 s membrane fraction. Data represent mean ± SEM of four independent experiments. (**B**) CAP1 moves away from the high speed (HS) detergent insoluble pellet of thrombin stimulated platelets. Platelets $(8 \times 10^8/\text{mL})$ were stimulated with 0.1 U/mL thrombin prior to lysis in Triton X-100 containing buffer and spun at high speed $(100,000 \times g)$ for 1 hour. Only pellets of HS samples were resolved on 12% SDS-PAGE gel, blotted onto PVDF membrane and probed with antibodies for CAP1 and β-actin. CAP1 was quantified by densitometry, normalised to β-actin and expressed relative to the 0 s pellet fraction. The low speed (LS) $(15,600 \times g)$ pellet shows the typical increase in actin upon thrombin stimulation. Data represent mean ± SEM of four independent experiments. (**C**) Effect of indomethacin and apyrase on the response of CAP1 in the HS detergent insoluble pellet upon thrombin stimulation. The experiment was performed as in (**B**) in the presence or absence of indomethacin $(10\,\mu\text{M})$ and apyrase (1 U/mL) using the indicated thrombin doses for 1 min. Blots of HS pellets were probed with antibodies for CAP1 and β-actin. The experiment was repeated with centrifugation at low speed (LS) to show the effect of thrombin on actin. CAP1 was quantified by densitometry, normalised to β-actin and expressed relative to the basal pellet fraction. Data represent mean ± SEM of three independent experiments. (**D**) Effect of collagen and resistin on the amount of membrane-associated CAP1. The experiment was performed as in (**A**) using 10 µg/mL collagen for 3 min or 200 ng/mL resistin for 15 min. Only the membrane fractions were analysed. Integrin β3 was used as membrane marker and for normalisation. Data represent mean ± SEM of 4 to 6 independent experiments. For all panels *$p \leq 0.05$, **$p \leq 0.01$, ***$p \leq 0.001$ relative to 0 s or basal. Mann-Whitney test was used for non-parametric data and t-tests were used for parametric data with a Bonferroni correction where appropriate. Full-length blots are presented in Supplementary Fig. 3.

313

with 0.5 U/ml thrombin. Both thrombin doses also caused, as expected, an increase in the amount of actin in the low speed pellet. The presence of indomethacin and apyrase did not cause any significant alteration in CAP1 behaviour, indicating that the effect of thrombin is not mediated by secondary mediators.

We next sought to investigate whether the changes in the distribution of CAP1 we saw with thrombin are specific to this agonist. Collagen is one of the key platelet agonists and acts mainly through the GPVI receptor[27]. A collagen concentration of 10 μg/mL, which resulted in maximal aggregation, was used for stimulation followed by subcellular fractionation. We observed that collagen stimulation caused a significant translocation of approximately 40% of CAP1 away from the membrane fraction (Fig. 4D).

Lee et al.[12] proposed that CAP1 is a receptor for resistin, mediating its role in inflammation. Subsequent studies have found an association of resistin and CAP1 with conditions like coronary artery disease and rheumatoid arthritis[28,29]. Sato et al.[29] in particular have shown that resistin contributes to the pathogenesis of rheumatoid arthritis by increasing the production of specific chemokines by fibroblast-like synoviocytes in a CAP1 dependent manner. We have observed that resistin pre-treatment causes an attenuation of platelet aggregation in response to low doses of thrombin (manuscript in preparation). These observations prompted us to investigate the effects of resistin treatment on CAP1 distribution. Platelets were treated with 200 ng/mL resistin for 30 minutes, which we have determined to cause the maximum inhibition of platelet aggregation, followed by subcellular fractionation (Fig. 4D). Upon those conditions we noticed a significant translocation of approximately 35% of CAP1 away from the membrane fraction, suggesting that some of the effects of resistin on platelets may be mediated by CAP1.

Inhibitory signalling pathways and GSK3 inhibition prevent CAP1 translocation.

Platelets in circulation are continually subject to the effects of inhibitory agents produced by the endothelial cells, namely prostacyclin (PGI2) and nitric oxide, which provoke increases in cAMP and cGMP respectively, and prevent spontaneous platelet activation. We speculated that increased cyclic nucleotide levels would prevent the thrombin-stimulated translocation of CAP1. To test this hypothesis we treated spread platelets with 100 nM PGI2 for 5 minutes or 10 μM S-nitrosoglutathione (GSNO), a nitric oxide donor, for 20 minutes prior to stimulation with 0.1 U/mL thrombin for 30 seconds (Fig. 5A). PGI2 caused a reduction of the proportion of cells with stress fibres and increased abundance of actin nodules, and this effect was less conspicuous with GSNO, as previously described[30,31]. Neither PGI2 nor GSNO per se altered the proportion of cells with predominantly cortical CAP1 distribution (about 70%) (Fig. 5B), however both prevented the effect of thrombin stimulation, which in control cells caused a reduction of the proportion of cells with cortical CAP1 to 56% and a concomitant almost two-fold increase in the proportion of cells with absent cortical CAP1 from 21% to 39%.

Zhou et al.[32] have uncovered a phosphorylation-dependent cycle mediated by GSK3 and other kinases that regulates CAP1 association with cofilin and actin and, notably, also its subcellular localisation. More specifically, in pancreatic cells inhibition of GSK prevented CAP1 enrichment at leading edges and cortical areas. Platelets express predominantly the beta isoform of GSK3, which is tonically active in resting cells[33], and external stimuli like thrombin cause phosphorylation and inhibition of this kinase. To investigate whether the effect of GSK3 on CAP1 localisation is conserved in platelets we first treated spread platelets with the GSK3 inhibitor CHIR99021 (2 μM) for up to 10 minutes and scored the proportions of cells with predominantly cortical or diffuse CAP1 localisation at various time points. These experiments did not reveal any significant deviation from the results obtained in control platelets (Supplementary Fig. 4). We next investigated whether inhibition of GSK3 would have an effect on thrombin-stimulated translocation of CAP1. We treated spread platelets with 2 μM CHIR99021 for 10 minutes prior to stimulation with 0.1 U/mL thrombin for 30 seconds (Fig. 5A) and observed that GSK3 inhibition prevented CAP1 translocation upon thrombin stimulation (Fig. 5B). Our results suggest that GSK activity has little influence on CAP1 localisation in resting platelets, but is required for CAP1 translocation upon agonist stimulation.

Discussion

We present immunological evidence of the presence of CAP1 in human platelets, where it appears to be abundant. Proteomics studies place CAP1 among the top 100 most abundant proteins in platelets[34,35]. Burkhart et al.[35] estimate the abundance of CAP1 in 41,700 copies per platelet, approximately one copy per 600 actin monomers. This indicates that CAP1 is unlikely to be an important actin monomer sequestering protein in platelets in vivo, an activity that would require equimolar concentrations of CAP1 and G-actin. In sub-stoichiometric amounts relative to G-actin like the ones in platelets, CAP1 would be expected to accelerate the addition of actin monomers to barbed ends[14]. Based on proteomics and transcriptomics studies CAP2 does not appear to be expressed in human platelets and is expressed at very low levels in murine platelets, where CAP1 is also abundant[35–37].

Although CAP is usually described as a cytosolic protein, in platelets approximately 25% associates with membranes and this association is independent of the actin cytoskeleton. In support of our findings, proteomics studies of enriched platelet plasma membranes clearly identify CAP1[38,39]. Notably, these studies also identify cofilin and profilin in the plasma membrane proteome. Interestingly, the study of Moebius et al.[38] identified CAP1 after applying a purification protocol that significantly reduced the amount of cytoskeleton proteins prior to analysis. This is in agreement with our data showing that CAP1 remains in the membrane fraction after disassembly of the actin cytoskeleton by LatB. An association of a small proportion of CAP1 with the membrane fraction has been reported in the human monocytic leukemia cell line THP-1 and is likely to represent a common feature of CAP[12].

As expected for a G-actin binding protein, CAP1 does not fractionate in the LS detergent insoluble pellet. A significant proportion does however fractionate in the HS pellet. Again, this association was not disrupted by LatB, indicating that it is independent of actin. The fraction in the HS pellet may correspond to CAP1 associated to membrane-containing structures, probably lipid rafts. Consistent with this, CAP1 has been identified in lipid rafts extracted from mouse brain[40].

314
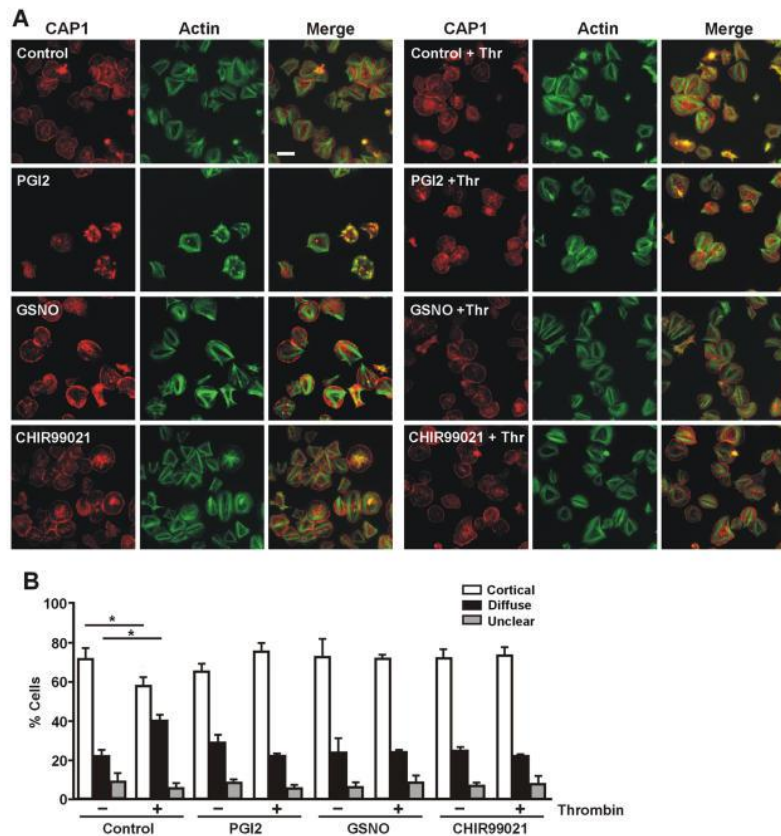
Figure 5. Effects of PGI2, GSNO and GSK3 inhibition on CAP1 relocalisation upon thrombin stimulation. Platelets were allowed to spread on fibrinogen-coated coverslips and then treated with 100 nM PGI2 for 5 minutes, 10 μM GSNO for 20 minutes or 2 μM CHIR99021 for 10 minutes prior to stimulation with 0.1 U/mL thrombin for 30 seconds. Platelets were fixed with paraformaldehyde and immunostained with an anti-CAP1 antibody followed by an Alexa568-coupled secondary antibody (red) and counterstained with FITC-phalloidin for filamentous actin (green). Images were acquired with a fluorescence microscope equipped with a structured illumination attachment. Scale bar 5 μm. (**B**) Quantification of the pattern of CAP1 distribution before (−) and after (+) thrombin stimulation. The proportions of cells with predominantly cortical or diffuse distribution of CAP1 in images like the ones shown in A were calculated from 2 to 5 independent experiments each performed in duplicate coverslips. At least 1000 cells per condition in each experiment were scored. Unclear refers to cells that were not sufficiently enough spread to make a judgment. Data are average ± SEM. *p ≤ 0.05 relative to the respective population not stimulated with thrombin, Mann Whitney test.

CAP1 displays a conspicuous enrichment at the cortex of both suspended and spread platelets, where it co-localises with F-actin, although this enrichment is more apparent in spread platelets. Similarly, in several mammalian cell lines, as well as in the social amoeba *Dictyostelium discoideum*, CAP1 displays predominantly a diffuse cytoplasmic localisation, but it also accumulates at actin-rich membrane ruffles and lamellipodia[13–16,32,41]. We did not detect CAP1 in stress fibres, in agreement with reports of a small fraction of CAP1 in stress fibres in a few cell lines only, suggesting that an interaction of CAP1 with F-actin is most likely transitory, possibly dependent on its association to cofilin[13–15]. CAP1 localisation in central areas of the spread platelet suggests a role for this protein in vesicle trafficking events associated with degranulation, a process that requires F-actin disassembly[42].

We report for the first time an accumulation of CAP1 in actin nodules, podosome-related structures visible during early adhesion and spreading[2]. They consist of an actin and Arp2/3 complex core devoid of integrins and surrounded by a ring rich in focal adhesion molecules like talin and vinculin[25]. Interestingly, in HeLa cells CAP1

315

co-immunoprecipitates focal adhesion kinase (FAK) and talin and appears to interact directly with talin[16]. We observe an accumulation of CAP1 in the ring structure, where we speculate it would be recruited by an interaction with talin. We propose that CAP1 may contribute to the actin turnover of these highly dynamic structures through its actin filament depolymerising and monomer regeneration activities.

Intrigued by the association of CAP1 to the platelet membrane fraction (most likely corresponding to the plasma membrane, as we were unable to distinguish any immunolocalisation pattern that suggests a particular organelle) we sought to visualise changes in CAP1 distribution upon stimulation with the strong agonist thrombin. We observed a fast translocation of CAP1 away from the cell cortex of spread platelets that is mirrored by a depletion of the protein from the membrane fraction and from the HS pellet in platelets in suspension. As we have determined that the HS pellet contains CAP1 in an actin-independent manner, the translocated CAP1 must correspond to membrane-associated CAP1. Moreover, CAP1 translocation parallels the course of actin polymerisation, suggesting that both events are linked to common signalling pathways. We have no explanation to the fact that CAP1 seems to revert to the cortex of spread platelets three minutes after stimulation while translocation persists in platelets in suspension.

Collagen stimulation also provoked CAP1 translocation from the membrane to the cytosol fraction, suggesting that this phenomenon is triggered by a common signalling step downstream of the respective receptors for thrombin and collagen. Similarly, signals downstream of both cAMP and cGMP prevent CAP1 translocation. It is well known that the respective cyclic nucleotide dependent kinases PKA and PKG both share numerous substrates and prevent platelet activation by diverse agonists[43]. A fraction of CAP1 may be associated to one or more membrane receptors or associated proteins but at this moment we ignore the functional relevance of this putative association. Lee et al.[12] have proposed recently that CAP1 is a receptor for the adipokine resistin in monocytic cells, where it mediates the inflammatory response by promoting an increase of cAMP levels. While it is debatable how circulating resistin may interact directly with CAP1, which is not exposed to the cell outside, we observed that exposure of platelets to resistin provoked a comparable translocation of CAP1 to the cytosol. This is in contrast with the effect of resistin reported on a leukemia cell line[12]. Resistin may have effects on platelets different from the ones it elicits in other cell lines that would be worth investigating.

Quinn et al.[44] have recently reported that CAP1 co-immunoprecipitates several adenylyl cyclase (AC) isoforms (at least AC1, 3, 4 and 7) in pancreatic cancer cells and forms an AC3/CAP1/G-actin complex upon stimulation with forskolin that inhibits cell motility. Human platelets express mainly the transmembrane AC6, but also AC3 and AC5 and possibly AC7 and AC9 based on transcriptomics and proteomics studies[35,36]. We were unable to immunoprecipitate AC6 from platelet lysates due to unsatisfactory antibody performance and possibly also low abundance (estimated in 2500 copies per platelet). Should an interaction of CAP1 with ACs in platelets reproduce, we hypothesise that a fraction of CAP1 may be associated to these enzymes at the plasma membrane, contributing to their action and therefore to their inhibitory effects. Stimulation with agonists like thrombin and collagen would disrupt that interaction, shifting the balance towards platelet activation.

The mechanisms controlling CAP1 localisation and translocation are poorly understood. Phosphorylation appears to play a role in pancreatic cancer cells, where CAP1 is a substrate of GSK3 and inhibition of this enzyme resulted in abolished enrichment at leading edges[32]. We did not observe a similar effect in platelets treated with CHIR99021, however inhibition of GSK3 prevented CAP1 translocation to the cytosol in response to thrombin, indicating that although GSK activity is not required basally, it is upon thrombin stimulation. The exact mechanism requires further clarification, as thrombin activation has been shown to inhibit GSK3 in platelets[33]. In fact phosphorylation by GSK3 appears not to be the only regulator of CAP1 translocation because a non-phosphorylatable CAP1 mutant (S307A/S309A) also shows lack of cortical enrichment upon GSK3 inhibition in pancreatic cancer cells[32].

In summary, we provide evidence that CAP1 is an abundant cytoskeleton regulator in platelets, where it may play roles at the cell cortex and actin nodules during platelet spreading. A fraction of CAP1 remains associated to the membrane in an actin-independent manner and translocates to the cytosol in response to agonists, placing it at a crossroad of the signalling pathways that control platelet activation. Verification of those roles in platelets will require studies in an appropriate animal model lacking CAP1.

References

1. Falet, H. In *Platelets in thrombotic and non-thrombotic disorders* (eds Gresele, P., Kleiman, N. S., López, J. A. & Page, C. P.) 139–156 (Springer International Publishing, 2017).
2. Calaminus, S. D. J., Thomas, S., McCarty, O. J. T., Machesky, L. M. & Watson, S. P. Identification of a novel, actin-rich structure, the actin nodule, in the early stages of platelet spreading. *J. Thromb. Haemost.* 6, 1944–1952 (2008).
3. Hartwig, J., Barkalow, K., Azim, A. & Italiano, J. E. The elegant platelet: signals controlling actin assembly. *Thromb Haemost* 82, 392–398 (1999).
4. Lind, S. E., Janmey, P. A., Chaponnier, C., Herbert, T.-J. & Stossel, T. P. Reversible binding of actin to gelsolin and profilin in human platelet extracts. *J. Cell Biol.* 105, 833–842 (1987).
5. Xue, B. & Robinson, R. C. Guardians of the actin monomer. *Eur. J. Cell Biol.* 92, 316–332 (2013).
6. Siton-Mendelson, O. & Bernheim-Groswasser, A. Functional actin networks under construction: the cooperative action of actin nucleation and elongation factors. *Trends Biochem. Sci.* 42, 413–430 (2017).
7. Ono, S. The role of cyclase-associated protein in regulating actin filament dynamics – more than a monomer- sequestration factor. *J. Cell Sci.* 126, 3249–3258 (2013).
8. Balcer, H. I. et al. Coordinated regulation of actin filament turnover by a high-molecular-weight Srv2/CAP complex, cofilin, profilin, and Aip1. *Curr. Biol.* 13, 2159–2169 (2003).
9. Chaudhry, F. et al. Srv2/cyclase-associated protein forms hexameric shurikens that directly catalyze actin filament severing by cofilin. *Mol. Biol. Cell* 24, 31–41 (2013).
10. Yu, G., Swiston, J. & Young, D. Comparison of human CAP and CAP2, homologs of the yeast adenylyl cyclase-associated proteins. *J. Cell Sci.* 107, 1671–1678 (1994).
11. Peche, V. et al. CAP2, cyclase-associated protein 2, is a dual compartment protein. *Cell Mol Life Sci* 64, 2702–2715 (2007).

12. Lee, S. *et al.* Adenylyl cyclase-associated protein 1 is a receptor for human resistin and mediates inflammatory actions of human monocytes. *Cell Metab.* **19**, 484–97 (2014).
13. Freeman, N. L. & Field, J. Mammalian homolog of the yeast cyclase associated protein, CAP/Srv2p, regulates actin filament assembly. *Cell Motil Cytoskelet.* **45**, 106–120 (2000).
14. Moriyama, K. & Yahara, I. Human CAP1 is a key factor in the recycling of cofilin and actin for rapid actin turnover. *J Cell Sci* **115**, 1591–1601 (2002).
15. Bertling, E. *et al.* Cyclase-associatedprotein1 (CAP1) promotes cofilin-induced actin dynamics in mammalian nonmuscle cells. *Mol Biol Cell* **15**, 2324–2334 (2004).
16. Zhang, H. *et al.* Mammalian adenylyl cyclase-associated protein 1 (CAP1) regulates cofilin function, the actin cytoskeleton, and cell adhesion. *J. Biol. Chem.* **288**, 20966–77 (2013).
17. Wang, C., Zhou, G.-L., Vedantam, S., Li, P. & Field, J. Mitochondrial shuttling of CAP1 promotes actin- and cofilin-dependent apoptosis. *J. Cell Sci.* **121**, 2913–2920 (2008).
18. Peche, V. S. *et al.* Ablation of cyclase-associated protein 2 (CAP2) leads to cardiomyopathy. *Cell Mol Life Sci* **70**, 527–543 (2012).
19. Field, J. *et al.* CAP2 in cardiac conduction, sudden cardiac death and eye development. *Sci. Rep.* **5**, 17256 (2015).
20. Kumar, A. *et al.* Neuronal Actin Dynamics, Spine Density and Neuronal Dendritic Complexity Are Regulated by CAP2. *Front. Cell. Neurosci.* **10**, 1–17 (2016).
21. Kosmas, K. *et al.* CAP2 is a regulator of the actin cytoskeleton and its absence changes infiltration of inflammatory cells and contraction of wounds. *Eur. J. Cell Biol.* **94**, 32–45 (2015).
22. Gieselmann, R. & Mann, K. ASP-56, a new actin sequestering protein from pig platelets with homology to CAP, an adenylate cyclase-associated protein from yeast. *FEBS Lett* **298**, 149–153 (1992).
23. Fox, J. E. B., Reynolds, C. C. & Boyles, J. K. Studying the platelet cytoskeleton in Triton X-100 lysates. *Methods Enzym.* **215**, 42–58 (1992).
24. Zeng, Y., Tao, N., Chung, K.-N., Heuser, J. E. & Lublin, D. M. Endocytosis of oxidized low density lipoprotein through scavenger receptor CD36 utilizes a lipid raft pathway that does not require caveolin-1. *J. Biol. Chem.* **278**, 45931–45936 (2003).
25. Poulter, N. S. & Thomas, S. G. Cytoskeletal regulation of platelet formation: Coordination of F-actin and microtubules. *Int. J. Biochem. Cell Biol.* **66**, 69–74 (2015).
26. Coughlin, S. Thrombin signalling and protease-activated receptors. *Nature* **407**, 258–264 (2000).
27. Nieswandt, B. *et al.* Glycoprotein VI but not α2β1 integrin is essential for platelet interaction with collagen. *EMBO J.* **20**, 2120–2130 (2001).
28. Munjas, J. *et al.* Association of adenylate cyclase-associated protein 1 with coronary artery disease. *Eur. J. Clin. Invest.* **47**, 659–666 (2017).
29. Sato, H. *et al.* Resistin upregulates chemokine production by fibroblast-like synoviocytes from patients with rheumatoid arthritis. *Arthritis Res. Ther.* **19**, 6–11 (2017).
30. Yusuf, M. Z. *et al.* Prostacyclin reverses platelet stress fibre formation causing platelet aggregate instability. *Sci. Rep.* **7**, 5582 (2017).
31. Atkinson, L. *et al.* Reversal of stress fibre formation by nitric oxide mediated RhoA inhibition leads to reduction in the height of preformed thrombi. *Sci. Rep.* **8**, 3032 (2018).
32. Zhou, G.-L., Zhang, H., Wu, H., Ghai, P. & Field, J. Phosphorylation of the cytoskeletal protein CAP1 controls its association with cofilin and actin. *J. Cell Sci.* **127**, 5052–5065 (2014).
33. Moore, S. F. *et al.* Dual regulation of glycogen synthase kinase 3 (GSK3)α/β by protein kinase C (PKC)α and Akt promotes thrombin-mediated integrin αIIbβ3 activation and granule secretion in platelets. *J. Biol. Chem.* **288**, 3918–3928 (2013).
34. Qureshi, A. H. *et al.* Proteomic and phospho-proteomic profile of human platelets in basal, resting state: insights into integrin signaling. *PLoS One* **4**, e7627 (2009).
35. Burkhart, J. M. *et al.* The first comprehensive and quantitative analysis of human platelet protein composition allows the comparative analysis of structural and functional pathways. *Blood* **120**, e73–82 (2012).
36. Rowley, J. W. *et al.* Genome wide RNA-seq analysis of human and mouse platelet transcriptomes. *Blood* **118**, e101–11 (2011).
37. Zeiler, M., Moser, M. & Mann, M. Copy number analysis of the murine platelet proteome spanning the complete abundance range. *Mol Cell Proteomics* **13**, 3435–3445 (2014).
38. Moebius, J. *et al.* The human platelet membrane proteome reveals several new potential membrane proteins. *Mol. Cell. Proteomics* **4**, 1754–1761 (2005).
39. Lewandrowski, U. *et al.* Platelet membrane proteomics: a novel repository for functional research. *Blood* **114**, e10–e19 (2009).
40. Chadwick, W., Brenneman, R., Martin, B. & Maudsley, S. Complex and multidimensional lipid raft alterations in a murine model of Alzheimer's disease. *Int. J. Alzheim. Dis.* **2010**, 604792 (2010).
41. Noegel, A. A. *et al.* Assessing the role of the ASP56/CAP homologue of Dictyostelium discoideum and the requirements for subcellular localization. *J Cell Sci* **3203**, 3195–3203 (1999).
42. Flaumenhaft, R. *et al.* The actin cytoskeleton differentially regulates platelet alpha-granule and dense-granule secretion. *Blood* **105**, 3879–87 (2005).
43. Smolenski, A. Novel roles of cAMP/cGMP-dependent signaling in platelets. *J. Thromb. Haemost.* **10**, 167–176 (2012).
44. Quinn, S. N. *et al.* Adenylyl cyclase 3/adenylyl cyclase-associated protein 1 (CAP1) complex mediates the anti-migratory effect of forskolin in pancreatic cancer cells. *Mol. Carcinog.* **56**, 1344–1360 (2017).

Acknowledgements

Author Contributions

P.J., W.J. and D.R.J.R. performed experiments and analyzed data; J.S.K. and H.X. performed experiments; F.R. designed the research and wrote the manuscript. All authors reviewed the manuscript.

Additional Information

Supplementary information accompanies this paper at https://doi.org/10.1038/s41598-018-29151-w.

Competing Interests: The authors declare no competing interests.

Publisher's note: Springer Nature remains neutral with regard to jurisdictional claims in published maps and institutional affiliations.

317

318

Supplementary Figures

The membrane-associated fraction of cyclase associate protein 1 translocates to the cytosol upon platelet stimulation

Pooja Joshi, David Riley, Jawad S. Khalil, Huajiang Xiong, Wei Ji and Francisco Rivero
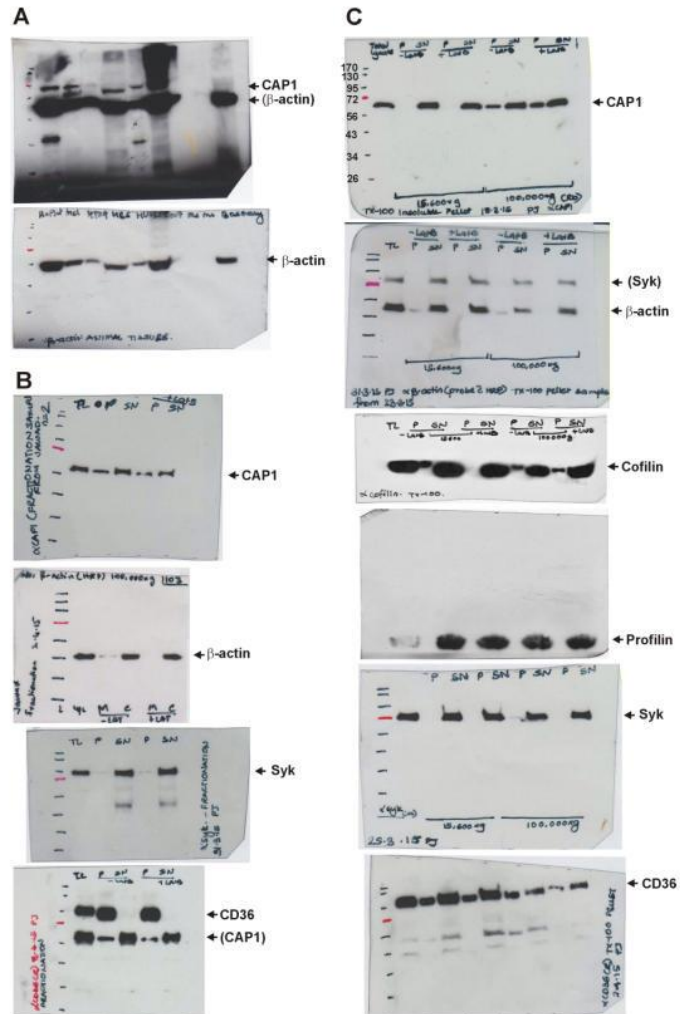
Supplementary Figure 1. Full-length blots corresponding to Figure 1. The blots have been arranged in the same order as they appear in the figure. Note that some blots have been re-probed to visualise a second protein, in which case the first protein (in brackets) may appear over or underexposed. The first blot of panel C displays the band sizes of the protein ladder as an example. For cofilin the lower third of the membrane was cut and used for probing.

319
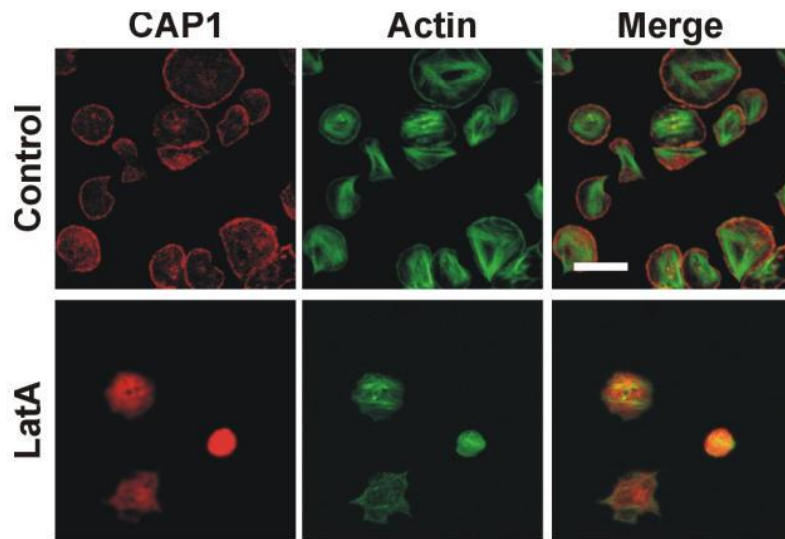
Supplementary Figure 2. Effect of latrunculin A on CAP1 distribution. Platelets were allowed to spread on fibrinogen-coated coverslips and then treated with 3 µM latrunculin A for 30 minutes. Platelets were fixed with paraformaldehyde and immunostained with an anti-CAP1 antibody followed by an Alexa568-coupled secondary antibody (red) and counterstained with CytoPainter for filamentous actin (colour changed to green). Images were acquired with a fluorescence microscope equipped with a structured illumination attachment. Scale bar 10 µm.

Supplementary Figure S3. Full-length blots corresponding to Figure 4. The blots have been arranged in the same order as they appear in the figure. Note that some blots have been re-probed to visualise further proteins, in which case the previous proteins (in brackets) may appear over or underexposed. The first blot of panels C and D each displays the band sizes of the protein ladder as an example.

A

CAP1 | Actin | Merge

0'

1'

2'

4'

10'

Supplementary Figure 4. Effect of GSK3 inhibition on CAP1 and actin distribution. (A) Platelets were allowed to spread on fibrinogen-coated coverslips and then treated with 2 μM CHIR99021 for the indicated times. Platelets were fixed with paraformaldehyde and immunostained with an anti-CAP1 antibody followed by an Alexa568-coupled secondary antibody (red) and counterstained with FITC-phalloidin for filamentous actin (green). Images were acquired with a fluorescence microscope equipped with a structured illumination attachment. Scale bar 5 μm. (B) Quantification of the pattern of CAP1 distribution. The proportions of cells with predominantly cortical or diffuse distribution of CAP1 in images like the ones shown in A were calculated from 2 to 5 independent experiments each performed in duplicate coverslips. At least 1000 cells per condition in each experiment were scored. Unclear refers to cells that were not sufficiently enough spread to make a judgment. Data are average ± SEM. No significant differences relative to the respective population not stimulated with thrombin, Mann-Whitney test.

B